



Immunoregulatory Roles of CD48 in Autoimmunity and Tolerance

Citation

McArdel, Shannon. 2015. Immunoregulatory Roles of CD48 in Autoimmunity and Tolerance. Doctoral dissertation, Harvard University, Graduate School of Arts & Sciences.

Permanent link

<http://nrs.harvard.edu/urn-3:HUL.InstRepos:17467326>

Terms of Use

This article was downloaded from Harvard University's DASH repository, and is made available under the terms and conditions applicable to Other Posted Material, as set forth at <http://nrs.harvard.edu/urn-3:HUL.InstRepos:dash.current.terms-of-use#LAA>

Share Your Story

The Harvard community has made this article openly available.
Please share how this access benefits you. [Submit a story](#).

[Accessibility](#)

Immunoregulatory roles of CD48 in autoimmunity and tolerance

A dissertation presented

by

Shannon Leah McArdel

to

The Division of Medical Sciences

in partial fulfillment of the requirements

for the degree of

Doctor of Philosophy

in the subject of

Immunology

Harvard University

Cambridge, Massachusetts

April 2015

© 2015 Shannon Leah McArdel

All rights reserved.

Immunoregulatory roles of CD48 in autoimmunity and tolerance**Abstract**

CD48 is an adhesion and costimulatory molecule expressed constitutively on nearly all hematopoietic cells. Via interactions with its ligand CD2, it contributes to synapse organization between T cells and APCs, and can enhance TCR signaling; via interactions with its higher affinity ligand CD244, CD48 mediates interactions with T cells and NK cells. In addition to its roles in T cell activation and NK-mediated lysis, CD48 deficiency is associated with development of spontaneous lupus-like disease on a mixed 129 and B6 genetic background, but not on a mixed 129 and Balb/c background. Despite these cellular and clinical observations, the mechanisms by which CD48 might contribute to autoimmunity and tolerance in vivo were not well defined. In this thesis we examined the immunoregulatory roles of CD48 in spontaneous and induced models of autoimmune disease, using CD48 deficient mouse strains and anti-CD48 antibodies. We found that CD48 deficiency did not precipitate spontaneous lupus-like disease in mice on a pure B6 background, but resulted in a spontaneous increase in lymphocyte activation within both young and aged mice. This implicated neighboring immunoreceptor genes in development of lupus-like disease. CD48 deficient mice had modestly attenuated disease in a mouse model of multiple sclerosis, experimental autoimmune encephalomyelitis (EAE), including reduced severity and accelerated resolution. At the peak of disease, CNS-infiltrating CD4⁺ T cells in CD48 deficient mice produced less GM-CSF, a cytokine that contributes to encephalitogenicity of T cells in EAE. When we examined CD48 expression in wild type mice during EAE, we found that CD48 expression was increased on activated CD4⁺ T cells, and that CD48⁺⁺ CD4⁺ T cells were enriched for GM-CSF, IL-17A and IFN γ -producing cells. Administration of anti-CD48 antibody during EAE in wild type mice dramatically reduced the number of these cytokine-producing cells, and could significantly attenuate or even prevent disease. Anti-CD48-mediated attenuation of EAE was partially dependent on Fc receptors, suggesting a mechanism of depletion of activated CD48⁺⁺ CD4⁺ T effectors. Collectively, our data support a critical role for CD48 in regulating the generation of activated lymphocytes and suggest that CD48 may be used to identify pathogenic self-reactive T cells in autoimmune disease.

Table of Contents

Part I: Immunoregulatory roles of CD48 in autoimmunity and tolerance.....	1
1. Introduction.....	2
2. Materials and Methods.....	28
3. Susceptibility of CD48 ^{-/-} [B6] mice to spontaneous and induced lupus-like disease.....	35
i. Results.....	35
ii. Discussion.....	46
4. Susceptibility of CD48 ^{-/-} [B6] mice to an induced model of autoimmunity, experimental autoimmune encephalomyelitis.....	52
i. Results.....	52
ii. Discussion.....	68
5. Mechanisms of action of an anti-CD48 monoclonal antibody in attenuation of experimental autoimmune encephalomyelitis.....	78
i. Results.....	78
ii. Discussion.....	116
Part II: Immunologic regulation of IgG glycosylation.....	135
6. Introduction.....	136
7. Materials and Methods.....	141
8. Hypogalactosylation of IgG in the K/BxN model of inflammatory arthritis.....	142
i. Results.....	145
ii. Discussion.....	157
Part III: General Discussion.....	160
Part IV: Bibliography.....	164

Acknowledgements

First and foremost, I would like to thank Dr. Arlene Sharpe for giving me the opportunity to learn and work in her lab. She adopted me when I was an orphan, showed exceptional patience during times of difficulty, and offered warm encouragement at all times. During the writing of this thesis, she provided invaluable reviews, revisions, and suggestions. I am also especially indebted to Dr. Dan Brown. He has been a thoughtful and entertaining mentor, teaching me how to think on my feet when things are not going according to plan and how to recover from would-be disasters—both incredibly valuable life skills. I would also like to thank: Dr. Peter Sage, Dr. Alison Paterson, and Dr. Loise Francisco for exceptional guidance, both technical and intellectual, and willingness to share their expertise; Vikram Junega, Cat Tan, Jernej Godec, Dr. Katie McGuire, Dr. Frank Schildberg and Marty LaFleur for helping to make the Sharpe lab the fun and encouraging place that it is; Sarah Hillman, for bringing her outstanding organization skills and personable nature to lab every day, and for helping to ensure that meetings and birthday celebrations happened at their appointed times; Justin Trombley, Susie Kim, Xiaohui He, Baolin Chang, Huiping Zhang, Caroline Armet, Flor Gonzalez, and Rob Ortega for generous technical support in the Sharpe Lab; and past Sharpe Lab members for their friendly support.

For the teaching and encouragement during the first portion of my graduate studies, I would like to thank Dr. David Lee, Dr. Eric Boilard, Dr. Altan Ercan, Dr. Peter Nigrovic and Kate Larabee Tuttle. In particular, Dr. David Lee encouraged me to appreciate the value of the latter components of “Ready, Aim, Fire.”

I would also like to thank the members of my dissertation advisory committee, Dr. Mike Carroll, Dr. Shiv Pillai, Dr. Kai Wucherpennig and Dr. Diane Mathis, for sharing their time and knowledge on a semi-regular basis; my dissertation examination committee, Dr. Eric Huseby, Dr. Cox Terhorst, and Dr. George Tsokos, for volunteering their time and effort to support my training; and Susan Perkins for her remarkable organization and coordination of the Immunology Program.

Lastly, I would like to thank my family for their emotional support; and I would especially like to thank Richard Pasek for being such a great friend over the past six years, and for encouraging me in both academic and scientific outreach projects.

Attributions

Studies of spontaneous and induced lupus in the CD48^{-/-} [B6.129] and CD48^{-/-} [B6] strains were performed in collaboration with Dr. Dan Brown. Data in Figures 3.1 and 3.2A-B are from experiments performed by Dr. Dan Brown, and are included for completeness.

CNS processing for histology was performed by the Rodent Histopathology Core at Dana Farber and Harvard Cancer Center. CNS lesions were enumerated by Dr. Ray Sobel of Stanford University.

Cell sorting was performed by John Sullivan and Chad Araneo of the Microbiology and Immunobiology Flow Cytometry Facility at Harvard Medical School.

The NanoString analysis was performed under the kind guidance of Youjin Lee, in the lab of Vijay Kuchroo at Harvard Medical School.

Anti-CD48 F(ab')₂ was generated from whole IgG by Mohan Brahmandam at the Dana Farber Monoclonal Antibody Core.

Figure 6.1B is adapted from Mimura Y, Jefferis R, Mimura-Kimura Y, Abrahams J, Rudd PM. (2008) Glycosylation of therapeutic IgGs. Unpublished book chapter, shared by personal communication.

For the study of IgG glycosylation, described in Part II, many serum samples and clinical data were provided by generous collaborators: Dr. Eric Boilard of the David Lee lab; Dr. Haochu Huang at the University of Chicago; Dr. Joyce Wu of the Dr. Christophe Benoist and Dr. Diane Mathis lab at Harvard Medical School; and Dr. Bryce Binstadt at the University of Minnesota.

Great ideas were generously provided by members of the Sharpe Lab, in the Department of Microbiology and Immunobiology at Harvard Medical School.

This work is dedicated to my mother
for her enduring strength, even when it left her.

Part I

Immunoregulatory roles of CD48 in autoimmunity and tolerance

Chapter 1: Introduction

CD48 (SLAMF2, BLAST-1) is a cell surface molecule expressed on most immune cells, with described roles in cell adhesion and costimulation. Initially discovered as a molecule highly upregulated on blasting B cells during Epstein-Barr virus (Thorley-Lawson and Poodry 1982), CD48 has since been characterized as a member of the signaling lymphocyte activation molecule family (SLAMF), a subgroup of the CD2 superfamily of immunoglobulin domain-containing proteins (Davis and van der Merwe 1996), with genes found on chromosome 1 in both mice and humans (Staunton et al. 1989; Wong et al. 1990). The SLAMF locus has been linked to autoimmune susceptibility in both mice and humans, and the numerous surface proteins encoded in this region have been of interest for their roles in immune cell function (Calpe et al. 2008; Cannons, Tangye, and Schwartzberg 2011). Although understanding of the function of the SLAMF molecules continues to grow rapidly, interpretation of data has been complicated by the polymorphic nature of these genes and the mixed genetic backgrounds that sometimes resulted during generation of the initial SLAM family knockout mice (Keszei et al. 2011). To eliminate potentially confounding factors due to polymorphisms in the SLAMF locus, we have used a CD48^{-/-} mouse generated in a B6 ES cell, and kept on the B6 background to bring clarity to the roles of CD48 in immune function, and to shed additional light on the potential of the CD48 pathway as a target of therapy for diseases of immune dysfunction.

The SLAM family and autoimmunity

Overview of the SLAM family

The SLAM family includes nine cell surface molecules: CD150 (SLAM, SLAMF1), CD48 (SLAMF2, BLAST-1), Ly9 (SLAMF3, CD229), CD244 (SLAMF4, 2B4), CD84 (SLAMF5), Ly108 (SLAMF6, known as NTB-A in humans), CRACC (SLAMF7, CD319), BLAME (SLAMF8), and CD84H (SLAMF9, SF2001). CD244 is a high affinity ligand for CD48 (Brown et al. 1998), the ligands for SLAMF 8 and 9 are unknown (Kingsbury et al. 2001; Fraser et al. 2002; Fennelly et al. 2001; Zhang et al. 2001), and the remaining SLAM receptors are all self-ligands (Martin et al. 2001; Flaig, Stark, and Watzl 2004; Cao et al. 2006; Falco et al. 2004; Kumaresan et al. 2002; Mavaddat et al. 2000; Punnonen et al. 1997; Romero et al. 2005; Yan et al. 2007). These receptors each have unique expression patterns on immune cells, and participate in diverse aspects of

immune function including costimulation, cytokine production, and cytotoxicity (Calpe et al. 2008; Cannons, Tangye, and Schwartzberg 2011). All but CD48, SLAMF8 and SLAMF9 contain one or more immunoreceptor tyrosine-based switch motifs (ITSM), which allow them to signal via the intracellular adaptors SAP and/or EAT-2 (SLAM-associated protein and EWS-Fli1-activated transcript-2, respectively) (Sayos et al. 1998; Morra et al. 2001; Shlapatska et al. 2001; Li et al. 1999; Poy et al. 1999). CD48, as discussed below, is GPI-linked, while SLAMF8 and SLAMF9 do not have any tyrosine motifs in their intracellular domains (Kingsbury et al. 2001; Fraser et al. 2002; Fennelly et al. 2001; Zhang et al. 2001).

The SLAMF locus on mouse chromosome 1

The SLAM family genes are located on chromosome 1, within a region that has been linked to spontaneous lupus-like disease in mice. This region was initially identified for its ability to precipitate lupus-like disease in B6 mice when crossed to the lupus-prone NZM2410 mouse (Morel et al. 1994; Mohan et al. 1998). B6 mice with the 'Sle1' segment of chromosome 1 from NZM2410 mice develop glomerulonephritis and anti-nuclear antibodies (Mohan et al. 1998; Morel et al. 2001). Extensive characterization of the Sle1 region revealed multiple loci that independently contribute to lupus-like disease on the B6 background (Morel et al. 2001). The 'Sle1b' subregion was shown to have the strongest link to humoral autoimmunity, and contains the SLAM family genes (Morel et al. 2001; Wandstrat et al. 2004). Because the SLAM family was already implicated in immune function, these were the strongest candidates for disease susceptibility in this region.

To better understand the mechanisms involved in the loss of tolerance to chromatin and generation of anti-nuclear antibodies, Croker et al. combined each of the Sle1a, Sle1b and Sle1c alleles with Y autoimmunity accelerator (Yaa) or Faslpr mutations. They found that Yaa mutations could accelerate lupus in mice with the Sle1b allele only, but not in mice with Sle1a or Sle1c alone. This suggests that Sle1b and Yaa are involved in the same pathway that can lead to humoral autoimmunity (Croker, Gilkeson, and Morel 2003). In contrast, the lpr mutation could accelerate lupus with any one of the three Sle1 subloci, but caused most severe disease in combination with Sle1a. This suggests that Sle1a and lpr are part of the same pathway that can lead to antinuclear antibodies and glomerulonephritis (Croker, Gilkeson, and Morel 2003).

Further examination of the Sle1b region associated polymorphisms in the SLAM family genes with lupus susceptibility. At least two haplotypes of the SLAM family region were found in inbred mouse strains, one in B6 strains and a second in NZW, Balb/c, 129 and NOD strains. Notably, the Sle1b-derived SLAM family haplotype causes autoimmunity only in B6 strains, and not in strains with the second SLAM haplotype, indicating that epistatic interactions with other portions of the B6 genome are required for autoimmunity (Wandstrat et al. 2004).

This identification of multiple SLAM family haplotypes, and their effects on autoimmunity, were critical for reevaluation of contemporary studies using SLAM family gene knockout mice. Many knockout strains were made by gene targeting in 129-derived embryonic stem (ES) cells, and then backcrossing onto the desired background—Balb/c, B6, etc. For SLAM family gene knockouts backcrossed onto B6, this meant a mixed genetic background in a known polymorphic region with known autoimmune linkage. The CD48^{-/-} mouse was one such example.

CD48^{-/-} mouse strains and spontaneous autoimmunity

CD48^{-/-} mouse strains were generated by gene targeting in J1 129 embryonic stem cells, and then backcrossing to either B6 or Balb/c backgrounds (Gonzalez-Cabrero et al. 1999). The CD48^{-/-} [B6.129] was found to develop spontaneous anti-DNA autoantibodies and severe glomerulonephritis with aging (Keszei et al. 2011). The kinetics and severity of disease were more severe than that seen in the B6.Sle1b mouse. In contrast, the CD150^{-/-} [B6.129] mouse, which had been made using the same 129 ES cell, was found to develop only mild disease and thus supported an interpretation that disease in CD48^{-/-} [129.B6] mice was due to absence of CD48. However, neither the CD48^{-/-} [Balb/c.129] nor CD150^{-/-} [Balb/c.129] strains had any evidence of anti-DNA autoantibodies or glomerulonephritis. These observations suggested to the authors that the primary effect of CD48 or CD150 deficiency on the lupus-like disease in CD48^{-/-} [B6.129] and CD150^{-/-} [B6.129] strains was due to epistatic interaction of the 129-derived genes with the B6 background. However, the enhanced severity of disease in the CD48^{-/-} [B6.129] mice compared to CD150^{-/-} [B6.129] mice suggested that CD48 deficiency might enhance disease pathology. Moreover, there were data supporting altered T cell responses in vivo in CD48^{-/-} [Balb/c.129] mice compared to WT Balb/c mice, where there were no confounding factors due

to an autoimmune-prone background (Keszei et al. 2011). Collectively, this suggested that CD48 might have a role in regulating T cell autoimmunity and tolerance.

Further characterization of glomerulonephritis in the CD48^{-/-} [B6.129] strain supported a role for CD48 in modulating autoimmunity mediated by the interactions of the B6 genetic background with the CD48 gene knockout locus (Koh et al. 2011). B6 congenic mice that carry a region of the 129 DNA on chromosome 1 that is nearly identical to that contained in CD48^{-/-}[B6.129] mice, were described to have autoantibodies, but no glomerulonephritis (Carlucci et al. 2007). The additional disease severity characterized by Koh et al. suggested that CD48 deficiency had a critical role in promoting development of glomerulonephritis (Koh et al. 2011).

These observations are important to consider when interpreting data generated with these CD48 deficient mice, as both the absence of CD48 and the epistatic interactions of the 129-derived genes with the B6 genetic background have been shown to have consequences for the immune system. It may not be clear which genetic difference is the primary or contributing cause to altered phenotypes, in publications using this CD48^{-/-} [B6.129] strain.

CD48 structure and expression

CD48 structure

Like other CD2 family members of the immunoglobulin superfamily, CD48 contains an IgV-like domain and a C2-like domain, with cysteine residues that allow a disulfide bond in the C2-like domain (Staunton et al. 1989). A single polymorphism in the IgV domain of CD48 was identified in a study of 10 inbred laboratory mouse strains; only B6 mice differed in residue 68, having an asparagine instead of aspartate. This correlates with the two SLAM family haplotypes observed in laboratory strains, as well. Examination of two inbred strains derived from wild mice indicated additional polymorphisms, suggesting that CD48 may be polymorphic in natural populations (Cabrero, Freeman, and Reiser 1998). A wider analysis of SLAM haplotypes in 48 *Mus* species and subspecies revealed substantial polymorphisms in wild mouse populations; however, the aim of this study was to correlate evolution of polymorphisms with autoimmune susceptibility, and did not directly examine the functional effects of alternative protein sequences (Limaye et al. 2008).

CD48 is unique among the SLAM family receptors, in that it is GPI-linked and contains no intracellular motifs (Staunton et al. 1989; Yokoyama et al. 1991). Like other GPI-linked proteins, CD48 is associated with lipid rafts on the cell surface (Stefanova and Horejsi 1991). It can also be detected in a soluble form in the serum and plasma of humans, and is elevated during EBV infection, arthritis, and in lymphoproliferative disorders (Smith et al. 1997). It is not known how the soluble form of CD48 is generated physiologically, but GPI-linked molecules are susceptible to cleavage by phospholipases, such as phospholipase C and phospholipase D (Low and Saltiel 1988; Metz et al. 1994). Two splice variants of CD48 have been detected in humans: one contains 2 exons and encodes isoform 1, the other contains 4 exons and differs in the 3' UTR and coding region, and has a unique C-terminus (Jostins et al. 2012).

CD48 expression

CD48 was initially identified by its high expression on Epstein-Barr virus (EBV)-infected B cells (Thorley-Lawson and Poodry 1982), which appears to be due to the action of an EBV-derived protein acting on a positive element in the CD48 gene (Klaman and Thorley-Lawson 1995). However, further characterization of CD48 revealed that it was expressed on nearly all hematopoietic cells at steady state including B cells, T cells and dendritic cells (Yokoyama et al. 1991; Kato et al. 1992; Baorto et al. 1997).

In mice, the only hematopoietic cell populations that distinctly lack CD48 expression are hematopoietic stem cells (HSC) and multipotent progenitors (MPPs), and this has been used as a means to help distinguish these progenitors from other bone marrow populations. HSCs can be highly purified as CD150⁺CD244⁻CD48⁻, while MPP are CD244⁺CD150⁻CD48⁻, and most lineage-restricted progenitors are CD48⁺ (Kiel et al. 2005). These SLAMF markers were also sufficient to purify HSCs from mouse fetal liver (Kim et al. 2006). In humans and rhesus macaque however, differential CD150 and CD48 surface expression are not sufficient to enrich for HSCs among CD34⁺ blood cells (Larochelle et al. 2011).

CD48 expression can be upregulated by interferon (IFN) alpha/beta and IFN gamma (IFN γ) on human peripheral blood mononuclear cells (PBMCs), including CD3⁺, CD14⁺ and CD19⁺ cells (Tissot et al. 1997). Increased CD48 expression on monocytes and lymphocytes has been detected in patients with viral and

bacterial infections (Katsuura et al. 1998). Soluble CD48 also is increased in the serum of patients with EBV infection, leukemia and arthritis (Smith et al. 1997).

During allergic responses or after IL-3 exposure, CD48 expression on eosinophils has been shown to increase (Munitz et al. 2007; Munitz et al. 2006). During bacterial infection CD48 expression increases on both eosinophils and mast cells (Rocha-de-Souza et al. 2008).

CD48 RNA expression in various mouse immune cell populations was characterized as part of the ImmGen project. CD4⁺ Tregs (CD4⁺ CD3⁺ CD25⁺ CD19⁻) were among the cells with the highest CD48 expression. CD48 transcripts also appear to be high in developing thymocytes and thymus-resident DCs. In neutrophils, CD48 transcripts are extremely low (Davis and Hamilton 2008).

CD48 function: ligand interactions with CD2, CD244 and FimH

CD48 has two binding partners in both mice and humans, CD2 and CD244 (Kaplan et al. 1993; Arulanandam et al. 1993; Brown et al. 1998; Latchman, McKay, and Reiser 1998). In mice, CD48 is the exclusive ligand for CD2, whereas in humans CD2 also binds to CD58 (Dustin et al. 1987). The affinity of mouse CD48 for CD2 is $\sim 90 \mu\text{M}$ (Davis and van der Merwe 1996), while the affinity of CD48 for CD244 is higher, with a $K_d \sim 16 \mu\text{M}$ (Brown et al. 1998). Both CD48 and CD2 are widely expressed on murine immune cells, whereas CD244 is restricted to NK cells, some memory CD8⁺ T cells, $\gamma\delta$ T cells, iELs, monocytes and granulocytes (Garni-Wagner et al. 1993; Schuhmachers et al. 1995; Kubota 2002; Elishmereni et al. 2013; Calpe et al. 2008; Cannons, Tangye, and Schwartzberg 2011). In humans, CD244 expression is also observed on eosinophils, basophils and mast cells (Romero et al. 2004). Thus, the interactions that predominate *in vivo* can depend on both the receptor pairs present and their different affinities. Notably, in insect cells transfected with murine CD2 or CD48, CD2 co-expression in CD48⁺ cells was shown to augment CD48 interactions with CD2⁺ cells, suggesting that CD48 and CD2 can interact *in cis* to influence *trans* interactions (Kaplan et al. 1993).

CD48 can also bind to the lectin FimH on E.coli, and has been shown to be a receptor for detection and endocytosis of bacteria by macrophages and mast cells (Baorto et al. 1997; Shin, Gao, and Abraham 2000; Moller et al. 2013).

The CD48:CD2 interaction has been largely studied in T:APC interactions. The CD48:CD244 interaction has been largely studied in NK:target interactions, where CD244 engagement has been described to lead to either stimulatory or inhibitory effects on NK cytotoxicity, depending on the context. The functional effects of both interactions are described below.

CD48:CD2 interactions in T cell activation: adhesion and signaling

The role of CD48 in T cell activation has been studied both from the side of the T cell and the APC, using a number of methods including crosslinking, blocking, transfection, and knockout. Molecular mechanisms have been inferred from these results, and also directly probed using coimmunoprecipitation assays.

The ability of CD48 to act as a costimulatory molecule on T cells was first observed by using anti-CD48 mAbs to either cross-link or block this molecule during stimulation. Soluble anti-CD48 or anti-CD2, plus secondary antibody, was not capable of inducing proliferation of splenic T cells. However, cross-linking anti-CD48 or anti-CD2 could augment proliferation induced by cross-linking anti-CD3. In contrast, blocking CD2 or CD48 on splenocytes during PHA stimulation reduced proliferation, while these antibodies did not alter proliferation induced by ConA (Kato et al. 1992). This data suggested that signaling into a T cell through either CD2 or CD48 could enhance T cell activation

Due to its GPI linkage, CD48 localizes to lipid raft domains in the cell membrane (Staunton et al. 1989; Stefanova and Horejsi 1991). Lipid rafts are enriched for both signal transduction molecules and actin cytoskeletal components (Harder and Simons 1997). In human T cells, the GPI-linked proteins CD59, CD55 and CD48 were found to associate with the Src family protein-tyrosine kinase Lck, and crosslinking these GPI-anchored molecules resulted in Lck phosphorylation (Stefanova et al. 1991). CD48 crosslinking on human T cells was also shown to cause intracellular Ca⁺⁺ flux, in a cholesterol-dependent mechanism (Stulnig et al.

1997). Thus, CD48 is associated with intracellular signaling molecules and has the capacity to influence signaling cascades.

CD48 costimulation of T cells was later shown to enhance IL-2 production and TCR signaling in a mouse T cell line, using either CD2-expressing APCs or soluble anti-CD48 and anti-CD3 plus secondary antibodies. Compared to CD3 stimulation alone, CD48 costimulation increased phosphorylation of both Lck and the TCR zeta chain and led to association of the phosphorylated zeta chain with the cytoskeleton, in a manner dependent on intact lipid rafts. Using coimmunoprecipitation assays, CD48 was found to physically interact with Lck (Moran and Miceli 1998). This supported a role for CD48 on T cells to contribute to TCR signaling and T cell activation, by its localization to lipid rafts and interaction with Lck.

Further molecular characterization of CD48 signaling was done in human T cell lines, separately analyzing the roles of CD2 and CD48 in early T cell signaling. Drbal et al. found that CD48 became immobilized in the immune synapse of anti-CD3-stimulated T cells, while other GPI-linked proteins like CD59 did not (Drbal et al. 2007). Muhammad et al. then showed that CD2 was required for CD48 to associate with the TCR and CD3, and that lateral interactions between CD2 and CD48 contribute to T cell activation: CD48 can recruit LAT to the TCR when CD2 is also present on the T cell. CD2 was required for CD48 to associate with the TCR, and CD48 was required for LAT association with the TCR (Muhammad et al. 2009). These results propose a model where GPI-linked CD48 interacts in *cis* with CD2 to efficiently bring Lck and LAT to the TCR/CD3 complex, and thus facilitate TCR signaling. When either CD2 or CD48 are lacking from the T cell, there is a reduction in LAT recruitment to the TCR, LAT phosphorylation, calcium flux, and IL-2 production (Muhammad et al. 2009).

A role for CD48 on the APC, to enhance T cell activation, has also been described. Latchman et al. found that CD48, expressed along with the MHC class II molecule IA^d on CHO cells, enhanced DO11.10 T cell proliferation and IL-2 production compared to CHO cells with IA^d alone. This effect was comparable to that obtained by using CHO cells with I-Ad and B7-1, suggesting that CD48 was a strong costimulator. The CD48:CD2 interactions increased adhesiveness, as assessed by a T cell-APC conjugates assay, and the authors

proposed that increased adhesion could be responsible for the increased stimulatory effect (Latchman, McKay, and Reiser 1998). These data complement earlier reports, supporting a role for CD48 in contributing to T cell activation whether it was expressed on the T cell or the APC.

The function of CD48 as an adhesion molecule on APCs has also been examined from a structural perspective. CD48:CD2 interactions were shown to contribute to adhesion between an APC and T cell, stabilize the immune synapse, and set the intermembrane spacing around the TCR to facilitate optimal TCR:MHC interactions (Milstein et al. 2008). By creating mutant forms of CD48 with additional IgV regions, Milstein et al. could examine the importance of the height of CD48 to its role in immune synapse organization. Increasing the size of CD48 on the APC resulted in reduced T cell proliferation and abnormal synapse formation: CD2 clusters on the T cell were biased towards peripheral regions of the synapse instead of the center of the synapse, and overall CD2-TCR colocalization was reduced (Milstein et al. 2008). These studies highlight how both the size of CD48 and its specificity for CD2 can contribute to its function on APCs as both an adhesion and costimulatory molecule.

Studies with the CD48^{-/-} [B6.129] mouse further confirmed the contribution of CD48 to T cell activation from both the T cell and APC. CD48^{-/-} T cells had reduced proliferative potential when stimulated with either WT or CD48^{-/-} APCs, and the CD48^{-/-} APCs were less stimulatory than WT APCs to WT T cells (Gonzalez-Cabrero et al. 1999). This was apparent in alloreactions between B6 and Balb/c splenocytes, but was most dramatic with CD48^{-/-} responders to irradiated Balb/c stimulators. Further investigation showed that purified CD4⁺ T cells had impaired proliferation in response to ConA or anti-CD3 plus PMA, but not to ionomycin plus PMA, supporting a positive role for CD48 in TCR signaling (Gonzalez-Cabrero et al. 1999). Although lymphocytes from knockout mice do not always replicate results using transfection and antibody blocking systems, these results did align with prior investigations.

A role for CD48 on both T cells and macrophages was demonstrated in a model of experimental colitis, using adoptive transfer of CD45RB^{hi} cells into Balb.c.Rag^{-/-} recipients. CD48^{-/-} [Balb.c.129] T cells failed to induce disease in CD48^{-/-} Rag^{-/-} recipients, although CD48 present on either the donor T cells or in the recipient was sufficient to restore disease. The absence of CD48 on either the APC or the T cell reduced IL-2 production in

vitro, but this effect was most dramatic when CD48 was absent on both the T cell and the APC. CD48^{-/-} peritoneal macrophages were less stimulatory to WT T cells in vitro, and produced less TNF α and IL-12 after in vitro stimulation with LPS compared to WT peritoneal macrophages. Attenuated colitis could also be recapitulated by treatment with anti-CD48 antibody, although whether the mechanism of action was blocking, depleting, or a combination of factors was not examined. Collectively, these data suggested that CD48 contributed to colitis from both the T cell and the APC side (Abadia-Molina et al. 2006). The phenotype of CD48^{-/-} macrophages in vitro suggests a potential cell intrinsic role for CD48 on innate immune cells in responding directly to bacterial components such as LPS.

CD48 as a ligand for CD244 on NK cells and CTLs

As the exclusive binding partner of CD244, CD48 can influence signaling through the immune tyrosine switch motive (ITSM)-containing CD244. In mice, CD244 is expressed on NK cells, $\gamma\delta$ T cells, some CD8⁺ T cells, resting monocytes, eosinophils and basophils (Mathew et al. 1993; Schuhmachers et al. 1995; Kubota 2002; Elishmereni et al. 2013). CD244 has been most extensively studied for its influence on cytotoxicity and activation. On NK cells, CD244 has been described as both an activating and inhibitory receptor, either promoting or inhibiting target lysis (Garni-Wagner et al. 1993; Schatzle et al. 1999; Lee et al. 2004; Vaidya et al. 2005; Chlewicki et al. 2008). One factor in mouse NK cells is the relative expression of two different isoforms of CD244: the long form was found to be inhibitory, while the short form was found to be stimulatory (Schatzle et al. 1999). Stimulation was also shown to be dependent on the density of CD244 on the cell surface, the degree of crosslinking, and the amount of the signaling molecule SAP: high surface expression, strong crosslinking and low levels of SAP were associated with inhibitory effects (Chlewicki et al. 2008). Some studies also suggest that signaling through EAT-2 promotes inhibitory effects, whereas signaling via SAP-Fyn promote activation and target lysis (Veillette 2010). This mechanism is supported by studies of NK cells lacking SAP or Fyn, which show defects in lysis of CD48⁺ targets (Bloch-Queyrat et al. 2005). However, signaling through EAT-2 was also shown to result in positive signals involving phospholipase C (Clarkson and Brown 2009). Thus, while it appears that CD244 can influence NK cell cytotoxicity through multiple independent factors, the molecular mechanism is not yet fully elucidated. Furthermore, it was shown that CD2

on NK cells could compete with CD244 for binding to CD48 on target cells, providing additional influences on NK activation (Clarkson and Brown 2009).

The role of CD244 is not always dependent on CD48 expression on the target cell, however. On CD8+ T effector cells, it was shown that CD48 expression on neighboring CTLs was sufficient to enhance CD244-mediated cytotoxicity, independent of CD48 expression on target cells (Lee et al. 2003). CD244-CD48 interactions between NK cells were also shown to prevent NK cell fratricide, further supporting a role for this receptor-ligand pair in the activation of effector cells, prior to target recognition (Taniguchi, Guzior, and Kumar 2007). In one example of crosstalk between NK and CTL, Waggoner et al. found that the CD244^{-/-} mouse was more susceptible to LCMV infection due to enhanced NK-mediated lysis of activated CD44⁺ CD8⁺ T effectors, at early stages of infection. Preferential killing of activated, but not naïve, CD8⁺ T cells prevented effective virus clearance (Waggoner et al. 2010).

These data have important implications for CD244 function during T cell exhaustion, as well. CD244 is highly expressed on the dysfunctional CD8⁺ cells in chronic infection and cancer models (Blackburn et al. 2009). A functional role for CD244 on CD8⁺ memory T cells has also been described. CD244 was shown to be critical for limiting persistence of CD8⁺ memory cells during chronic viral infection, but had no role in persistence or function of naïve CD8⁺ T cells (West et al. 2011).

Anti-CD48 has been described to alter NK cells *in vivo*, increasing CD69 and CD244 surface expression, and inducing cytokine production (Sinha et al. 2010; Yuan, Guo, and Thet 2013). Additionally, anti-CD48 altered the distribution of IgG subtypes produced by B cells after stimulation with the T-independent antigen, NP-Ficoll. This effect was only partially NK-cell dependent, suggesting that anti-CD48 could directly affect both NK cells and B cells *in vivo*, in a model that is independent of T cell help (Yuan, Guo, and Thet 2013).

As a ligand for FimH on bacteria

The bacterial lectin FimH can bind CD48 via the mannose sugar residues in its GPI linkage (Baorto et al. 1997). On mast cells, FimH binding to CD48 can trigger the mast cell TNF α response (Malaviya et al. 1999) or

phagocytosis (Shin, Gao, and Abraham 2000). On macrophages, FimH binding to CD48 leads to an opsonin-free mechanism for phagocytosis of bacteria. This involves formation of caveolae in cholesterol-rich domains of the cell membrane, and facilitates entry of the microbe into macrophages (Baorto et al. 1997; Moller et al. 2013). This mechanism may be particularly relevant for phagocytosis of FimH+ bacteria that have not yet been opsonized, but have adhered to tissue surfaces (Moller et al. 2013).

The ability of FimH to bind to CD48 also has implications for bacterial invasion of human brain microvascular endothelial cells (HBMEC), during E coli K1 infections. FimH binding to cultured HBMECs provides adhesion for E coli K1, and induces cellular changes in the endothelial cells to facilitate bacterial invasion. CD48 was identified on these HBMECs as the putative receptor for FimH in this scenario (Khan et al. 2007).

CD48 function in models of immunity

CD48 on granulocytes, in allergy and asthma

A role for CD48 in innate immune cell activation has been described on both human and mouse cells. Munitz et al. found that CD48 expression was increased on eosinophils from patients with atopic asthma, and also on eosinophils from mice after allergen challenge (Munitz et al. 2006). They also provide evidence for a functional role of CD48 on these cells. Crosslinking CD48 on cultured eosinophils, using plates coated with anti-mouse F(ab')₂ plus anti-CD48 mAb, resulted in degranulation. Human eosinophils also express CD244 and SAP, and crosslinking CD244 results in production of eosinophil peroxidase, IFN γ and IL4 (Munitz et al. 2005).

In a model of allergic airway inflammation, in vivo treatment with anti-CD48 antibody one day before antigen challenge dramatically reduced inflammation, while anti-CD2 had only a mild effect and anti-CD244 had no effect. Anti-CD48 reduced lung cell infiltration, cytokines, and histological signs of inflammation. The authors did not observe depletion of lymphocytes in the spleen, or alterations to eosinophils in the bone marrow, but did see reduced eosinophils in the bronchoalveolar lavage fluid (Munitz et al. 2007). Although CD48 expression was shown to increase on lymphocytes, macrophages and NK cells in the lung as well, the effect of anti-CD48 on the number of these cells in the lung was not described.

CD48 expression can increase on human cord blood-derived mast cells, along with Toll-like receptor (TLR) 2 expression, after infection with *Staphylococcus aureus* in vitro. Blocking CD48 with an anti-CD48 antibody reduced the inflammatory response of these cells (Rocha-de-Souza et al. 2008).

CD48 appears to be involved in eosinophil detection of *S. aureus*. Eosinophils can be stimulated by *S. aureus* to degranulate, and produce IL-8 and IL-10; this can be blocked with an anti-CD48 antibody and does not occur in eosinophils from CD48^{-/-} [B6.129] mice. In a model of peritonitis induced by intraperitoneal injection of Staphylococcal toxin B (SEB), CD48^{-/-} [B6.129] mice had reduced numbers of eosinophils and granulocytes in peritoneal lavage fluid, but no reduction in lymphocytes, when compared to WT mice (Minai-Fleminger et al. 2014). CD48 and CD244 were shown to mediate interactions between mast cells and eosinophils in vitro, allowing eosinophils to costimulate IgE-mediated activation of mast cells (Elishmereni et al. 2013). These data indicate that CD48 can contribute to bacterial sensing, granulocyte activation and immune cell cross-talk in circumstances of allergy or *S.aureus* infection.

Human neutrophils were reported to be stimulated by cross-linking CD48 with an anti-CD48 antibody plus a secondary antibody, although the main aim of this study was to characterize the signaling potential of another GPI-anchored molecule, CD59, during activation of the membrane attack complex of complement.

Crosslinking of CD59, or any of the other GPI-linked molecules examined including CD48, was sufficient to induce intracellular Ca⁺⁺ flux as measured by an intracellular Ca⁺⁺-sensitive dye (Morgan et al. 1993). In mice, however, CD48 mRNA expression in neutrophils is extremely low (Davis and Hamilton 2008), and CD48 function on mouse neutrophils is not yet clear.

CD48 and graft rejection

CD2 is recognized as a strong target for allogeneic responses, and anti-CD2 antibody therapies have been used alone or in combination with other immune suppressants to facilitate graft survival in numerous mouse models (Qin et al. 1994; Chavin, Lau, and Bromberg 1992). Being the only ligand for CD2 in the mouse, CD48 was investigated for its role in graft rejection, as well. Early studies showed that anti-CD48 in vivo could augment the effects of anti-CD2 in prolonging allograft survival (Qin et al. 1994). Anti-CD2 plus anti-CD48 allowed

indefinite cardiac allograft survival, while either antibody alone had milder effects on graft survival (Qin et al. 1994), and anti-CD244 did not enhance the effects of either anti-CD2 or anti-CD48 (Bai et al. 2002). While the combined antibodies were drastically more effective than either antibody alone, this study revealed that anti-CD48 alone could have an effect on both CD4+ and CD8+ T cell responses.

Although targeting CD48 alone has not been an ideal method to promote graft survival, it is being explored in combination therapies. For example, anti-CD48 in combination with anti-LFA1 and FTY720 has been shown to enable survival of embryonic pig pancreatic tissue transplanted into mice (Tchorsh-Yutsis et al. 2009).

CD48 and T cell effector functions

The anti-CD48 antibody has been used both *in vivo* and *in vitro* to distinguish the role of CD48 during priming and effector phases of an immune response. Anti-CD48 treatment *in vivo* was found to limit CTL priming and contact-sensitivity reactions. For CTL responses, anti-CD48 was most effective when given at the time of priming, whereas for CD4+ T cell responses anti-CD48 was most effective during the effector phase. *In vivo* administration could also limit responses to *in vitro* alloantigen stimulation (Chavin et al. 1994). Combined with *in vitro* studies, these data suggest that anti-CD48 could limit priming of CTLs but not target lysis, and could limit effector functions of CD4+ T cells such as proliferation and IL-2 secretion (Qin et al. 1994; Chavin et al. 1994).

Other *in vitro* studies have implicated CD2:CD48 interactions during both T cell priming and effector responses. Anti-CD2 or anti-CD48 mAb reduced IL-2R α expression, IL-2 and IFN γ production, and target lysis by anti-CD3-stimulated bulk T cells. Notably, the reduced target lysis could be rescued by addition of IL-2 (Musgrave, Watson, and Hoskin 2003). The authors suggest that the mechanism regulating the effects of CD48:CD2 costimulation may be similar to that induced by CD28 costimulation, stabilizing IL-2 mRNA (Musgrave et al. 2004).

CD48 in hematopoiesis

CD48 is not expressed on the surface of HSCs or MPPs, but it is found on other lineage-restricted progenitors and nearly all mature hematopoietic cells (Kiel et al. 2005). A role for CD48 in hematopoiesis was first

suggested in studies using an anti-CD48 antibody to prevent graft-versus-host disease (GVHD). Following sublethal irradiation and allogeneic bone marrow transplantation (BMT), combined use of anti-CD48 plus anti-CD2 effectively prevented GVHD. However, it also prevented recovery of the hematopoietic compartment. Anti-CD48 was found to be capable of preventing reconstitution after congenic BMT, as well, and led to reduced CD48 surface expression on cells in the bone marrow. In non-irradiated mice, anti-CD48 treatment also reduced CD48 surface expression in the spleen and bone marrow, but did not deplete cells. The authors concluded that anti-CD48 treatment altered expression of CD48 in the bone marrow, and that CD48 expression here is critical for hematopoietic recovery after sublethal irradiation (Blazar et al. 1998).

Hematopoiesis has also been studied in the CD48^{-/-} [B6.129] mouse, which was found to have a dysregulated hematopoietic stem cell compartment and a propensity towards follicular B cell-type lymphomas. Boles et al. observed a change in the distribution of monocyte and lymphocyte precursors in the bone marrow of CD48^{-/-} mice, and also a reduced proliferative capacity for CD48^{-/-} HSCs. Aged mice had an increased incidence of lymphoma, which correlated with upregulated Pak1 activity in CD19⁺ tumor cells but not in CD19⁺ cells from the spleen (Boles et al. 2011). Whether this phenotype of altered hematopoiesis and increased incidence of tumors occurs in CD48^{-/-} [Balb/c.129] or a pure B6 CD48^{-/-} remains to be shown.

CD48 and CD58 in human disease

Although CD48 is the only known ligand for mouse CD2, in humans the high affinity ligand for CD2 is CD58 (LFA3), while CD48 is a lower affinity binding partner (Dustin et al. 1987; Sandrin et al. 1993). Both CD48 and CD58 have been of interest for their linkage or role in human disease states.

Genome-wide association scans identified CD58 as a risk locus in multiple sclerosis (MS). Investigation of a potential mechanism found that the protective allele resulted in increased CD58 mRNA in PBMCs (De Jager et al. 2009; International Multiple Sclerosis Genetics et al. 2007). CD58 expression was also found to increase during remissions in MS patients (Arthur et al. 2008; De Jager et al. 2009). De Jager et al. propose that the protective allele for CD58 results in increased expression and thus increased engagement of CD2, which can increase Foxp3 expression. Improved functionality of Tregs would then correlate with disease remission.

Interestingly, a separate study examining the effects of anti-VLA-4 mAb therapy (natalizumab) in MS patients found that treatment was associated with an increase in activated cells in the peripheral blood, including an increase in CD58+ and CCR5+ CD8+ T cells. These authors hypothesized that anti-VLA-4 mAb sequestered effector cells in the blood (Kivisakk et al. 2009).

An alternative method of analysis of GWAS data sought to identify nodes of interacting proteins, based on susceptibility genes—a protein-interaction-network-based pathway analysis. CD48 was among a small group of high confidence candidates identified by this analysis, which the authors believe should be further investigated (International Multiple Sclerosis Genetics 2013).

One recent study examined association of CD58 polymorphisms with neuromyelitis optica (NMO, also known as Devic's disease), a demyelinating disease that primarily affects the optic nerve and spinal cord. Two haplotypes and four alleles showed an association with NMO, by TaqMan analysis, but no functional studies were performed (Kim et al. 2014).

CD48 has been of interest in the study of viral infections and some cancers, as the counter-receptor for CD244 on NK and CD8+ T cells. One group observed that CD48 and NTB-A (SLAMF6) were downregulated on HIV-infected T cell blasts, which could potentially limit the ability of NK and CD8+ T cells to lyse infected target cells (Ward et al. 2007). In human cells, CD244:CD48 interactions have been shown to either enhance or inhibit cytotoxicity of NK and CD8+ T cells, depending on the context (Waggoner and Kumar 2012). Another group found that CD244 expression on virus-specific CD8+ T cells decreased after simultaneous TCR and CD244 signaling, suggesting that CD48 engagement could influence CD244 expression (Pacheco et al. 2013).

Perhaps most famously, CD48 expression increases on B cells during Epstein Barr Virus (EBV) infection (Yokoyama et al. 1991). This infection is particularly dangerous for patients with X-linked lymphoproliferative syndrome 1 (XLP-1), a disease resulting from mutation of the SH2D1A gene that encodes the signaling molecule SAP (Sayos et al. 1998). Patients with this disease cannot control EBV infection, and NK cells from these patients are unable to kill EBV+ B cells (Parolini et al. 2000; Purtilo, Cassel, and Yang 1974). This

appears to be due to a lack of activation of SAP-deficient NK cells, upon engagement of CD48+ targets (Parolini et al. 2000). A more recent publication examined cells from female carriers of the XLP-1 mutation who, due to random X chromosome inactivation, have both SAP(+) and SAP(-) cells. They found that all EBV-specific CD8+ T cells in these individuals were SAP(+), whereas CD8+ T cells specific for other viruses, such as cytomegalovirus or flu, were a mixture of SAP(+) and SAP(-). Closer inspection revealed that CD8+ T cells required SAP in order to recognize antigen on B cells, but did not require SAP to recognize antigen on other cell types, and this was dependent on both CD244 and NTB-A expression. The authors suggest that these observations may partially explain why XLP-1 patients are particularly susceptible to EBV and EBV-induced lymphomas (Palendira et al. 2011). Relatedly, Meazza et al. found that EBV+ B cells do not express ligands for the activating NK receptors DNAM-1 and NKG2a, rendering target lysis particularly sensitive to signaling through CD244 (Meazza et al. 2014).

Understanding the unique roles for CD48 and its binding partners, in different types of immune cell interactions, may continue to offer insight into disease pathogenesis and potential therapeutic interventions.

Experimental autoimmune encephalomyelitis as a model for multiple sclerosis

Multiple sclerosis (MS) is a demyelinating disease of the CNS that appears to have both immune and neurodegenerative components, and results in progressive loss of motor and sensory function (Compston and Coles 2002). Its estimated median prevalence is 30 out of 100,000 individuals worldwide, and it affects twice as many women as it does men (World Health Organization 2008). In addition to studying patients and clinical samples, many research groups contribute to knowledge of MS and autoimmune disease by using the experimental autoimmune encephalomyelitis (EAE) disease model. EAE has many similarities to MS and is used to study autoimmunity, CNS inflammation, and potential treatments for MS. Several drugs currently available to treat MS were first studied in EAE, including Natalizumab (anti- α 4 integrin antibody, Tysabri), Glatiramer acetate (semi-random peptide, Copaxone), and FTY720 (small molecule inhibitor of S1P-1 receptor, Fingolimod). However, there are also treatments that have ameliorated EAE that have not worked in MS, either due to lack of efficacy or toxic side effects. Although not a perfect model for the human disease, there are different models of EAE that have unique benefits.

EAE models in mouse strains

EAE in mice typically manifests as ascending paralysis, starting with loss of tail strength and progressing to affect the hind limbs and then forelimbs. This is considered “classical” EAE. Some strains or modes of induction result in a “non-classical” form of EAE, characterized by ataxia, head tilt, spinning or spasticity (Greer et al. 1996; Muller, Pender, and Greer 2000, 2005; Abromson-Leeman et al. 2004; Kroenke, Chensue, and Segal 2010; Batoulis et al. 2011). Histologically, these two types of EAE correlate with infiltration and inflammation focused in the spinal cord in classical EAE, or the brainstem and cerebellum in atypical EAE (Abromson-Leeman et al. 2004; Kroenke, Chensue, and Segal 2010). The combination of clinical and histological evaluation can thus provide insight into mechanisms of disease pathogenesis.

EAE can be induced in mice by immunization with certain CNS-derived proteins, or by adoptive transfer of activated T cells that are specific for particular CNS-derived peptides. Different peptides have been found, experimentally, to be potent at inducing EAE in different mouse strains. Furthermore, the clinical course of EAE varies in different strains and with different methods of induction. For instance, SJL/J mice are susceptible to EAE induced by immunization with a peptide from the myelin protein proteolipid protein, and develop a relapsing-remitting disease that has similarities to relapsing-remitting MS (Tuohy et al. 1989). In contrast, B6 mice are susceptible to immunization with a peptide from myelin oligodendrocyte glycoprotein (MOG), MOG[35-55], and generally develop a chronic disease (Mendel, Kerlero de Rosbo, and Ben-Nun 1995), although varying the dose of antigen and adjuvants can also produce a relapsing-remitting form of EAE (Berard et al. 2010).

Adoptive transfer of activated, myelin-specific CD4⁺ T cells can also induce EAE. One tool that has been extremely useful for the study of CD4⁺ T cells in EAE in B6 mice, is the 2D2 TCR Tg mouse strain. These mice have transgenic TCR alpha and beta chains that are specific for MOG[35-55] peptide presented in IA^b MHCII molecules (Bettelli et al. 2003). These provide a source of MOG-specific CD4⁺ T cells that have the potential to be manipulated, transferred to recipient mice, and then specifically tracked in vivo or ex vivo. 2D2 TCR Tg mice develop spontaneous EAE at a very low frequency. However, when 2D2 mice were crossed to mice with the MOG-specific knock-in B cell receptor IgHMOG, 60% of offspring developed spontaneous and

severe Devic-like disease with lesions restricted to the optic nerve and spinal cord (Bettelli et al. 2006). Thus, the 2D2 mouse has numerous uses in the study of EAE and CNS autoimmunity.

Priming and activation of CD4+ T cells in EAE

CD4+ T cells have been the primary effectors studied in EAE pathogenesis. Early studies using CD4+ T cell-depleting antibodies revealed that CD4+ T cells were important for development of EAE (Kennedy et al. 1987; Whitham et al. 1996). In addition, TCR transgenic mice with MOG-specific CD4+ T cells develop spontaneous EAE, and are more susceptible to peptide-induced EAE (Adlard et al. 1999; Bettelli et al. 2003; Waldner et al. 2000; Pollinger et al. 2009). Some myelin-specific CD8+ T cells can also induce disease (see below), but the predominant use of specific MHCII-restricted peptides or encephalitogenic CD4+ TCR Tg populations has honed the focus of many studies on the role of CD4+ T cells and their activation by MHCII+ APCs.

In addition to requiring initial T cell activation, EAE also requires MHCII-mediated antigen presentation in the CNS during the effector phase of disease (Tompkins et al. 2002). Costimulatory and coinhibitory molecules on CD4+ T cells and APCs thus have the potential to influence EAE during both the priming and effector phases. For example, B7.1^{-/-}B7.2^{-/-} mice, which lack all CD28:B7 costimulation, are resistant to MOG-induced EAE and are also resistant to EAE induced by adoptive transfer of an activated, MOG-specific cell line. CD28^{-/-} mice, which specifically lack the costimulatory signal from B7 molecules, are also resistant to MOG-induced EAE (Chang et al. 1999). However, this can be overcome by *in vivo* blocking of CTLA-4, indicating that elimination of coinhibitory signals is sufficient to restore T cell activation (Chitnis et al. 2001). The CD28:B7:CTLA-4 pathway reveals the sensitivity of CD4+ T cells to stimulatory and inhibitory inputs that are antigen-nonspecific, and suggests the relevance of these molecules as targets of therapy.

Not all costimulatory molecules have the same effect during initiation and effector phases of EAE. For instance, blocking ICOS during T cell priming results in increased Th1 differentiation and IFN γ production, and enhanced EAE severity. In contrast, blocking ICOS during the effector phase limits IFN γ production by splenocytes, chemokine expression in the CNS, and infiltration of lymphocytes into the CNS (Rottman et al. 2001).

Similarly, adhesion molecules such as LFA-1 can have multiple roles in promoting T cell conjugation to APCs, as well as facilitating rolling or firm adhesion to endothelial cells during T cell migration to inflamed tissues (Springer and Dustin 2012). Thus, the relative importance of a molecule to T cell priming, Treg expansion, and tissue homing, can influence the outcome of disease in mice in which that molecule is absent or is transiently blocked. These are critical considerations when evaluating the relevance for disease treatment, as opposed to etiology.

Because costimulatory molecules have the potential to affect both T effectors and Tregs, they can influence the activation and differentiation of T effectors, as well as the proportion of Tregs. The PD-1:PD-L1 pathway has critical roles in limiting activation of autoreactive T cells, as well as promoting development of Tregs (Francisco, Sage, and Sharpe 2010). Together, these roles can influence the size of the T effector population and thus the likelihood and severity of EAE. Indeed, antibody blockade of PD-1 during EAE results in increased T cell proliferation, activation and cytokine production, and enhanced disease severity (Salama et al. 2003).

The cytokine milieu influencing CD4+ T cell differentiation can also influence the course of EAE. Through in vitro differentiation studies, Jager et al. showed that Th1, Th9 and Th17 polarized 2D2 CD4+ T cells were all capable of inducing EAE, albeit with different clinical outcomes, while Th2 polarized 2D2 CD4+ T cells were not capable of inducing EAE (Jager et al. 2009). Thus, the cytokines present during activation and differentiation of the CD4+ T cell can influence the course of EAE.

Effector cytokine production in the CNS

Myelin-specific T cells with a Th1 phenotype are capable of inducing EAE, and IFN γ and TNF α are found in the CNS during EAE (Sriram et al. 1982; Merrill et al. 1992; Ando et al. 1989; Baron et al. 1993). Although neither IFN γ , nor the critical Th1-polarizing cytokine IL-12, are required for EAE (Ferber et al. 1996; Becher, Durell, and Noelle 2002; Gran et al. 2002), IFN γ can shape the course of disease. Using adoptive transfer models, Lees et al. showed that IFN γ production by T cells and IFN γ sensing by the CNS influence the location

of CNS invasion. In the absence of either of these (using either IFN γ ^{-/-} T cells or IFN γ R^{-/-} recipients), adoptively transferred Th1 cells could infiltrate the brainstem and cerebellum but were significantly reduced in the spinal cord (Lees et al. 2008).

Myelin-specific T cells with Th17 polarization are also capable of inducing EAE (Langrish et al. 2005; Jager et al. 2009). In contrast to IL-12, the Th17-stabilizing cytokine IL-23 was found to be critical for EAE (Cua et al. 2003; Becher, Durell, and Noelle 2003), and neutralizing IL-17 can attenuate EAE while neutralizing IFN γ does not (Park et al. 2005; Langrish et al. 2005). However, the results from lacking or neutralizing effector cytokines can be difficult to interpret, since these may play multiple roles during disease. For example, IFN γ also plays a critical role in suppressing activated CD4⁺ T cells during EAE (Willenborg et al. 1996; Krakowski and Owens 1996; Chu, Wittmer, and Dalton 2000), and can induce expression of the co-inhibitory molecule PD-L1 on macrophages and antigen presenting cells (Loke and Allison 2003). Thus cytokines can contribute inflammatory and anti-inflammatory roles in different locations and at different times during the immune response.

Several studies have shown how these two cytokine-producing effectors can differentially affect the course of disease. O'Connor et al. found that IFN γ production was required for entry of Th17 cells into the uninflamed CNS (O'Connor et al. 2008). Kroenke et al. found that the histological, cellular and molecular features of Th1-induced EAE differed from those of Th17-induced EAE (Kroenke, Chensue, and Segal 2010). Stromnes et al. similarly found that the Th1:Th17 ratio of CD4⁺ T cells influenced the location of infiltration. Infiltration of the brain and spinal cord meninges, and the spinal cord parenchyma was not correlated with a specific Th1:Th17 ratio, while accumulation of cells in the brain parenchyma only occurred when Th17 outnumbered Th1 (Stromnes et al. 2008). Th17-induced EAE often shows a higher incidence of 'non-classical' clinical symptoms such as ataxia, head tilt, and spinning (Jager et al. 2009).

In contrast to Th1 and Th17 cells, Th2-polarized cells do not induce EAE, and the cytokines IL-4 and IL-5 are not substantial in the CNS during EAE (Merrill et al. 1992; Baron et al. 1993; Jager et al. 2009). Although neither IFN γ nor IL-17 are required for EAE, the Th17 effector cytokine GM-CSF was found to be both

necessary and sufficient to induce neuroinflammation: in the absence of IFN γ and IL-17, GM-CSF-producing Th could induce EAE, while GM-CSF-deficient Th could not induce disease (Ponomarev et al. 2007; Codarri et al. 2011; El-Behi et al. 2011). GM-CSF production by Th17 cells promotes IL-23 production by APCs, thus creating a positive-feedback loop for inflammation.

CD4+ T cell migration in EAE

Homing molecules, including adhesion molecules and chemokines, have been found to play crucial roles in the development of EAE and have been key targets of therapy. The small molecule FTY720 inhibits T cell egress from the lymph node, and was found to attenuate EAE in both rats and mice (Matloubian et al. 2004; Fujino et al. 2003; Webb et al. 2004). Blocking α 4 integrin (CD49d, a subunit of the heterodimer VLA-4) on T cells, the ligand for VCAM-1 on endothelial cells in CNS capillaries, was initially found to prevent EAE if administered prior to disease onset (Brocke et al. 1999; Theien et al. 2001). Further studies of VLA-4 revealed that this molecule was critical for Th1 CD4+ T effectors to enter the spinal cord during EAE, but that Th17 cells could enter the brain independent of VLA-4 and instead relied on LFA-1 (Rothhammer et al. 2011). Notably, in mice lacking α 4-integrin specifically in Foxp3+ cells, Tregs were capable of entering the CNS using LFA-1 (Glatigny et al. 2015). CD44 was also shown to contribute to CD4+ T cell entry to the CNS, while CD62L was dispensable (Brocke et al. 1999).

Chemokines and chemokine receptors also influence EAE, as they can provide signals to recruit lymphocytes into the CNS. CCR6 was shown to be important for entry of Th17 cells into the choroid plexus (Reboldi et al. 2009). CX₃CR1 was found to be critical for NK cell homing to the inflamed CNS during EAE (Hao et al. 2010). CCL2 (also known as MCP-1) is a chemokine that can attract CCR2+ macrophages, memory T cells, and DCs. It is expressed by epithelial cells of the blood brain barrier, and is upregulated during CNS inflammation (Williams, Holman, and Klein 2014). Although numerous chemokines are found in the CNS during EAE, studies with various chemokine or chemokine receptor deficient mice have revealed that individual chemokines are not always crucial for disease, suggesting overlapping or compensatory roles.

Antigen presenting cells in the CNS during EAE

Although initial CD4+ T cell priming in the MOG/CFA immunization model of EAE occurs in the periphery, T cells must reencounter their cognate antigen in the CNS, in the context of MHCII, in order to initiate disease. In the uninflamed CNS, the only MHCII-expressing cells are microglia and vessel-associated dendritic cells (McMahon et al. 2005; Greter et al. 2005). MHCII expression on CD11c+ DCs alone was shown to be sufficient for induction of EAE, suggesting that antigen presentation by microglia is not required for induction of disease (Greter et al. 2005). However, microglia can contribute to disease progression, and have been demonstrated to upregulate MHCII, as well as costimulatory molecules like CD80 and CD86 (Sedgwick et al. 1998; Aloisi 2001; McMahon et al. 2005; Bechmann et al. 2001; Becher, Bechmann, and Greter 2006). In addition, EAE requires de novo antigen processing and presentation by APCs in the CNS, supporting an important role for CNS APCs in controlling the progression of disease (Tompkins et al. 2002). Thus, a combination of peripheral, CNS-resident, and migratory APC populations can contribute to the pathogenesis of EAE.

Contribution of other lymphocytes to EAE pathogenesis

CD4+ T cells, and their activation by MHCII+ APCs, are widely studied in EAE pathogenesis. However, they are not the only cell type capable of inducing or influencing disease, as CD8+ T cells, B cells and NK cells have been shown to contribute to EAE as well.

CD8+ T cells have been reported to both ameliorate and exacerbate EAE, likely reflecting the many subsets of CD8+ T cells and their unique roles at different phases of the immune response. Adoptive transfer of certain myelin-specific CD8+ T cells lines are capable of inducing EAE (Huseby et al. 2001; Sun et al. 2001). CD8+ T cells were shown to respond to MOG[37-46] peptide after immunization with MOG[35-55] (Ford and Evavold 2005). However, other groups have found that myelin-specific CD8+ T cells could not induce disease (York et al. 2010), or instead have regulatory roles in EAE. For example, CD8^{-/-} MHCII^{-/-} mice have enhanced CNS tissue destruction (Linker et al. 2005), and depleting CD8+ T cells before disease induction exacerbates disease (Montero et al. 2004). Jiang et al found that CD8+ T cells were required for protecting MBP-immunized mice from a second induction of EAE, but were not required for recovery from the first induction of EAE (Jiang,

Zhang, and Pernis 1992). A recent study found that MOG-specific CD8+ T cells attenuated EAE in a perforin-dependent manner (Ortega et al. 2013). Regulatory CD8+ T cells can attenuate EAE after recognizing peptide in Qa-1 on CD4+ T cells (Lu et al. 2008). The mechanisms of suppression by CD8+ Tregs are being further defined, and involve perforin, IFN γ and TFG β (Chen et al. 2009; Beeston et al. 2010). These studies reflect the many roles that CD8+ T cells can play in EAE, whether at different times or in different locations or by different subsets. Notably, CD8+ T cells are prevalent in CNS lesions from MS patients (Friese and Fugger 2009). Thus, developing optimal EAE models in which to study CD8+ T cells will be critical to our understanding of the pathogenic and regulatory roles they play in CNS inflammation (Huseby et al. 2012).

Although not required for peptide-induced EAE, B cells are required for EAE induced by whole MOG protein (Wolf et al. 1996; Hjelmstrom et al. 1998; Lyons et al. 1999), and have been shown to be capable of contributing to EAE in numerous ways. B cell deficient mice had attenuated EAE compared to WT mice (Svensson et al. 2002); anti-MOG antibodies are capable of enhancing EAE in rats (Linnington et al. 1988); and B cells contribute to formation of ectopic germinal centers in the CNS (Gommerman et al. 2003; Magliozzi et al. 2004). Protective roles for B cells have also been described, such as their ability to bias CD4+ T cells towards Th2 differentiation (Pistoia 1997), and produce anti-inflammatory IL-10 (Fillatreau et al. 2002). Matsushita et al. found that IL-10-producing regulatory B cells could inhibit EAE initiation, but had little effect after disease progression. In contrast, B cell depletion during ongoing EAE attenuated disease (Matsushita et al. 2008). Notably, mice containing both transgenic anti-MOG IgH and MOG-specific TCR genes develop spontaneous disease at higher frequency and with different pathology than mice containing only MOG-specific transgenic TCR (Bettelli et al. 2003; Bettelli et al. 2006). Thus, B cells can influence EAE by their functions as APCs, by cytokines they produce (IL-10) or by antibody production, and different subsets may be important during different phases of disease (McLaughlin and Wucherpfennig 2008). Anti-CD20 mAb is an approved treatment for MS, further supporting the relevance of B cell subsets in CNS autoimmunity.

NK cells have also been implicated in EAE, although their roles are less well defined and some contradictory reports about their contribution to EAE have not yet been resolved. Depletion of NK cells starting before EAE induction was shown to enhance disease severity, increase CD4+ T cell proliferation and increase production of

Th1 cytokines (Zhang et al. 1997). Other groups have found that NK depletion at early time points (prior to disease onset) results in attenuation of EAE (Winkler-Pickett et al. 2008; Dungan et al. 2014). This may be due to opposing effects during priming and effector phases of EAE. NK cells have been shown to contribute to Th1 differentiation in lymphoid organs, and to promote Th1-dependent EAE (Shi et al. 2000; Martin-Fontecha et al. 2004; Laouar et al. 2005). However, they also have the potential to migrate to the CNS and influence inflammation during EAE. The chemokine receptor CX3CR1 was found to be important for NK cell migration to the CNS during EAE, but not to the liver during cytomegalovirus infection. Mice deficient in CX3CR1 had more severe EAE than WT mice, and reduced NK cells in the CNS (Huang et al. 2006). Further studies suggested that this was due to action of NK cells in the CNS, inhibiting production of Th17-promoting cytokines by microglia (Hao et al. 2010). However, another group found that CX3CR1^{-/-} mice have more DCs in the CNS during EAE, which could also contribute to the phenotype of exacerbated EAE (Garcia et al. 2013). Thus, NK cells also appear to be able to influence EAE in different ways, at different times and places.

These data indicate that numerous cell types are involved in EAE pathogenesis, and can be influenced to alter the outcome of disease. Further studies in both mice and humans are needed to better understand how each player contributes to overall disease progression and resolution, and which might be best suited as targets of therapeutic intervention.

CD48 and EAE

To date, no published studies have examined CD48 in EAE. Anti-CD2 antibodies were capable of suppressing EAE in the Lewis rat model of EAE. The anti-CD2 antibody OX34 could prevent or significantly attenuate EAE induced by immunization with MBP in CFA, when given two days before immunization or when administered at the onset of clinical disease. OX34 could also block EAE induced by adoptive transfer of an activated encephalitogenic T cell line, when given on the day of cell transfer and four days later. Treatment with OX34 involved a decrease in circulating T cells, and downmodulation of CD2 surface expression, but maintenance of T cell response to antigen *ex vivo* (Jung, Toyka, and Hartung 1995). Another study by the same group found that OX34 caused immediate depletion of CD4⁺ T cells in naïve rats (Hoffmann et al. 1997), raising the possibility that depletion could be responsible for protection from EAE. Alternatively, Sido et al.

proposed that OX34 provides a suppressive signal to T cells rather than blocking a CD2:CD48 interaction (Sido et al. 1997). Thus, it is not clear whether the effects of OX34 on rat EAE can provide any information on the role of CD48 in this model.

Immunoregulatory roles of CD48 in autoimmunity and tolerance

In Part I of this thesis, we examine the roles of CD48 in the context of autoimmunity, including spontaneous and induced models of lupus-like disease, as well as EAE. Using novel mouse strains and a previously-described antibody, we characterize several roles for CD48 in lymphocyte activation, homeostasis and survival in both naïve animals and circumstances of immune pathology.

Chapter 2: Materials and Methods

Mice. 6-12 week old mice were used for all experiments, except as noted for ageing experiments. For EAE experiments, mice were 8-12 weeks old. WT C57BL/6, Rag1^{-/-}, TCR α ^{-/-} and B6(C)-H2-Ab1bm12/KhEgJ (BM12) mice were purchased from The Jackson Laboratory (Bar Harbor, ME). Il2r γ c^{-/-}Rag2^{-/-} mice were purchased from Taconic Biosciences (Hudson, New York). CD48^{-/-} [B6.129] (Gonzalez-Cabrero et al. 1999), CD48^{-/-} [B6.129]+Tg, CD48^{-/-} [B6], CD244^{-/-} (Brown et al. 2011), and 2D2 TCR Tg (Bettelli et al. 2003) mice were maintained in our animal facility. 145F9.BACTg.CD48^{-/-} [B6.129] mice were generously provided by Dr. Cox Terhorst of Beth Israel Deaconess Medical Center and Harvard Medical School. Fc ϵ r1 γ ^{-/-} mice were generously provided by Dr. Tanya Mayadas of Harvard Medical School. CD48^{-/-}Rag^{-/-}, CD48^{-/-}TCR α ^{-/-} and CD48^{-/-}2D2 mice were generated in our laboratory. All mice were housed in a specific pathogen free animal facility, and used in accordance with the Harvard Medical School Standing Committee on Animals and National Institutes of Health animal healthcare guidelines. Animal protocols were approved by the Harvard Medical School Standing Committee on Animals.

CD4 T cell isolation. Spleens and lymph nodes were dissected from donor mice, and mechanically dissociated through a filter. Red blood cells were lysed with ACK (Lonza). Cells were resuspended in staining buffer (PBS with 1% FBS and 2mM EDTA), and stained with CD4 MACS beads (L3T4, Miltenyi) for 15 minutes at 4°C, washed, then run over a MACS column. Eluted cells were counted, washed, and used for downstream purposes. In some cases, as noted in text, cells were further purified by flow cytometry. In this case, cells were stained with directly conjugated antibodies against CD4, CD8 α , B220, and CD11c, and sorted on a FACS Aria (BD, Franklin Lakes, NJ) for CD4⁺ CD8 α ⁻B220⁻CD11c⁻ cells.

Chronic GVHD model of lupus. CD4⁺ T cells were isolated from the spleens of WT, CD48^{-/-} or bm12 mice, using MACS columns. 7-10x10⁶ CD4⁺ T cells were injected intraperitoneally (i.p.) in 200 μ l. Mice were sacrificed at day 7, 10 or 14 after cell transfer. Blood was collected for analysis of serum antibodies by ELISA. Spleens were collected and weighed, then analyzed by flow cytometry.

Flow cytometry. All antibodies for flow cytometry were purchased from BioLegend, BD Biosciences, or eBiosciences. For cell surface staining, antibodies were diluted 1:200 in staining buffer and applied to cells for 20 minutes at room temperature or at 4°C. For intracellular staining, cells were fixed and permeabilized with the eBiosciences Foxp3 staining kit. Antibodies included those against CD2 (RM2-5), CD3 (145-2C11), CD4 (RM4-5), CD8 α (53-67), CD11b (M1/70), CD11c (N418), CD19 (6D5), CD25 (PC61), CD44 (IM7), CD45 (30-F11), CD48 (HM48-1), CD49b (DX5), CD49d (R1-2), CD62L (MEL-14), CD69 (H1.2F3), CD90.1 (OX-7), CD90.2 (30-H12), CD138 (281-2), CD244 (2B4), B220 (RA3-6B2), Foxp3 (FJK-16s), $\gamma\delta$ TCR (GL3), GL7 (GL7), GM-CSF (MP1-22E9), I-A/I-E (M5/114.15.2), ICOS (C398.4A), IFN γ (XMG1.2), IL-2 (JES6-5H4), IL-10 (JES5-16E3), IL-17Av(TC11-18H10.1), Ki67 (B56), Lag3 (C9B7W), LFA-1 (H155-78), NK1.1 (PK136), and Hamster IgG (Poly4055). Samples were collected on a FACSCalibur (BD Biosciences) or LSRII (BD Biosciences), and analysis was performed using FlowJo software (FlowJo LLC).

Assays for apoptosis. For assessment of active caspases by flow cytometry, cells were incubated with 0.5 μ l fluorescein-Z-VAD-FMK (CaspGlow kit, eBioscience) per 100 μ l cell media (RPMI), for 1hr at 37°C. For assessment of apoptosis, cells were incubated with AnnV-APC (BioLegend) in AnnV staining buffer (BD Pharmingen) along with cell surface markers and 7AAD (Biolegend) to exclude dead cells.

IgG ELISA. Serum was collected for analysis of anti-dsDNA and anti-chromatin antibodies. For dsDNA ELISA, 96-well Immunolon Plate 1B (Dynerx) were first irradiated with UV light overnight. To prepare dsDNA, calf thymus DNA (Sigma) was diluted in pre-warmed PBS (Gibco) to 2 μ g/mL, the 0.5 μ l of Mung Bean Nuclease (40U/ μ l, New England Biolabs) was added and incubated at 37°C for one minute, then brought to room temperature. Plates were coated with 50 μ l/well of this dsDNA preparation, and incubated for 1hr at room temperature. Plates were washed 3 times with ELISA wash buffer (0.1% Tween (American Bioanalytical) in PBS), using an ELX405 plate washer (BioTek Instruments, Inc). Plates were blocked with 100 μ l/well of 1% BSA (Sigma-Aldrich) in ELISA wash buffer, for 1hr at room temperature, followed by 3 washes with ELISA wash buffer. Serum samples were diluted at 1:50, 1:150, and 1:350 in blocking buffer (1% BSA), then added to plates at 50 μ l of sample/well. A standard curve was generated by 1:2 serial dilution of control serum from aged MLR/LPR mice, where 1:100 dilution represents 100 reference units. After 1hr of incubation at room

temperature, plates were washed 3 times, then incubated with alkaline-phosphatase conjugated anti-mouse IgG (Southern Biotech) diluted at 1:1000, for 1hr at room temperature. Plates were washed 3 times. The alkaline phosphatase substrate CIP (Sigma-Aldrich) was prepared by dissolving 2 pellets in 9mL of water plus 1mL of 10x DEA buffer (Sigma-Aldrich). 100 μ l of substrate solution was added to each well, and allowed to develop. Plates were read at 405nm.

For anti-chromatin ELISA, 96-well Immunolon Plate 1B (Dynex) were first coated with 100 μ g/mL methylated BSA (Sigma-Aldrich) in PBS overnight at 4°C, then washed 2x with ELISA wash buffer. Plates were then coated with 50 μ l/well of DNA in PBS overnight at 4°C, then washed 2x. Plates were then coated with 10 μ g/mL Histone solution overnight at 4°C, then washed 2x. Plates were then blocked for 4hrs at room temperature in blocking buffer (3% BSA, 0.1% Gelatine (Sigma Cell Culture), 3mM EDTA in PBS), then washed 2x. Samples were diluted 1:100 in buffer (2% BSA, 0.1% Gelatine, 3mM EDTA, 0.05% Tween in PBS), then washed 4x. A standard curve was generated by 1:2 serial dilution of control serum from aged MLR/LPR mice, where 1:100 dilution represents 100 reference units. After 2hrs of incubation at room temperature, plates were washed 4 times, then incubated with HRP conjugated goat-anti-mouse IgG (Southern Biotech) diluted at 1:20,000 for 2hrs at room temperature. Plates were washed 4 times, then developed with OptEIA reagent (BD Biosciences) for 10 minutes, and stopped with 1M H₃PO₄. Plates were read at 450nm.

CD4+ T cell transfers to Rag^{-/-}, TCR α ^{-/-} and WT mice. CD4+ T cells were purified as described above, from 2D2 TCR Tg mice and in some cases from CD48^{-/-} 2D2 TCR Tg mice. CD4+ T cells were resuspended in PBS, and 3-10⁶ CD4+ T cells were injected intravenously (i.v.) or i.p., as indicated in figure legends. In some cases, WT and CD48^{-/-} CD4+ T cells were mixed prior to injection. Rag^{-/-} and TCR α ^{-/-} recipients were rested for 2 weeks, to allow for homeostatic proliferation, before immunization. WT mice were immunized the same day or one day after cell transfer.

Mixed bone marrow chimeras. Bone marrow was isolated from Thy1.1/1.2 WT mice and from Thy1.1 CD48^{-/-} mice, mechanically dissociated with a syringe and then filtered to generate single cell suspensions. Red blood cells were lysed with ACK, then bone marrow cells were resuspended in PBS, and mixed at a ~1:1

ratio. Recipient Thy1.2 WT mice received two doses of 600 Rads, separated by 4 hours, and were then given 7×10^6 bone marrow cells i.v. Mice were rested for two months before further manipulation.

MOG[35-55] immunizations: Mice were injected subcutaneously with 50 μ g of MOG[35-55] (UCLA Biopolymers Facility) in 100 μ l of PBS emulsified 1:1 with 100 μ l of a mixture of Complete Freund's Adjuvant (Sigma) supplemented with 400 μ g of Mycobacterium tuberculosis H37RA (Sigma). To prepare emulsions, aqueous solutions were drawn up in one syringe, oil solutions were pulled up in a separate syringe, and the two were connected with a 3-way stopcock. Solutions were mixed in the syringes until a stiff emulsion formed, which would not dissolve in PBS. Mice were shaved on the rump, and received two 100 μ l injections such that the primary draining lymph nodes would be the inguinal lymph nodes.

Experimental autoimmune encephalomyelitis induction with MOG immunization. Mice were immunized as described above. 100ng of pertussis toxin (List Biological Laboratories) diluted in 200 μ l of PBS was injected i.p on the day of immunization and two days later. In some cases, where noted in figure legends, only one dose of pertussis toxin was given. Fc ϵ r1 γ ^{-/-} mice were given two doses of 200ng of pertussis toxin each. Mice were monitored daily for clinical scores. Scores were assigned as follows: 0.5=some tail weakness; 1.0=flaccid tail; 1.5=cannot resist being rotated supine, but can easily right itself; 2.0=cannot easily right itself from supine position; 2.2=rump drags while walking; 2.5=one hind foot paralysis; 3.0=two hind feet paralysis; 3.2=some arm weakness; 3.5=significant arm weakness; 4.0=arm paralysis; 5.0=dead.

2D2 CD4+ TH1 differentiation in vitro. CD4+ T cells from 2D2 TCR Tg mice were isolated by MACS, as described above. Feeder cells were prepared by depleting CD4+ T cells from splenocytes. CD4+ T cells were cultured at 2×10^6 /mL along with irradiated feeder cells at 10^6 /mL with IL-12 (10ng/mL, PeproTech), anti-IL-4 (20mg/mL, clone 11B11, BioXcell), and anti-CD3 (2.5 μ g/mL, clone 2C11, BioXcell). Cultures were split every two days, and supplemented with 100U/mL rhIL-2 (R&D Systems). On day 6, live cells were collected using Lymphocyte Separation Media (Mediatech, Inc), and used for either in vitro proliferation assays (described below) or restimulated to generate 2D2 TH1 CD4+ Teff for adoptive transfer EAE (described below).

In vitro proliferation of 2D2 Th1 CD4+ T cells. 2D2 CD4⁺ Th1 T cells were generated as described above, then labeled with either CFSE (1 μ M, Life Technologies) or CellTrace Violet (5 μ M, Life Technologies) in PBS at 37°C for 12 minutes. Labeled cells were washed thoroughly and cultured at 2e6/mL along with 10⁶/mL TCR α ^{-/-} or CD48^{-/-} TCR α ^{-/-} splenocytes plus 0, 1, 10 or 100 μ g/mL of MOG[35-55]. Cells were collected 3 days later for analysis of CFSE or CellTrace Violet dilution by flow cytometry.

EAE induction with 2D2 CD4+ TH1 polarized Teff. 2D2 CD4⁺ Th1 T cells were generated as described above, then restimulated for 16-24 hours on plates coated with anti-CD3 and anti-CD28 (2.5 μ g/mL each). Cells were then washed, resuspended in PBS, and injected i.v. or i.p. into recipients, as noted in figure legends. Approximately 2-6e6 live CD4⁺ T cells were injected, in each experiment.

Cytokine measurements. For measurement of antigen-specific cytokine production, total lymphocytes from spleen, lymph node or CNS were restimulated in vitro with 0, 1, 10 or 100 μ g/mL of MOG[35-55] for 3 days. Supernatants were collected and analyzed by Cytokine Bead Array (BD Biosciences) for detection of secreted cytokines. For measurement of intracellular cytokine production, total lymphocytes from spleen, lymph node or CNS were restimulated in vitro with PMA and ionomycin, in the presence of GolgiStop (BD Biosciences) at 37°C for 3-5 hours. Cells were then stained for surface markers, fixed with either 4% paraformaldehyde in PBS or Fix/Perm Buffer (Foxp3/Transcription Factor Staining Buffer Kit, eBioscience), then stained for intracellular cytokines in permeabilization buffer (Foxp3/Transcription Factor Staining Buffer Kit, Permeabilization Buffer, eBioscience), and analyzed by flow cytometry.

CNS tissue collection for flow cytometry. For collection of CNS tissue, mice were first euthanized, then perfused with 10mL of PBS through the left ventricle. Brain and spinal cord were collected, and mechanically dissociated through a nylon filter. Lymphocytes were collected using density centrifugation. Briefly, CNS tissue homogenate was resuspended in 4-5mL of 37% Percoll (GE Healthcare), and 1-3mL of 70% Percoll was carefully underlaid. Samples were centrifuged at 500g for 20 minutes with no brake. The interface was collected, washed, counted, and used for flow cytometry.

Histology. For collection of CNS tissue, mice were first euthanized, then perfused with 10mL of PBS through the left ventricle. Brain and spinal cord were collected and immediately placed in 4% PFA in PBS. Tissues were processed for histology by the Dana Farber/Harvard Cancer Center Rodent Histopathology Core. Tissues were embedded in paraffin, sliced, mounted on slides, and stained with either hematoxylin and eosin, or Luxol Fast Blue to stain myelin. Histological analysis was performed by Dr. Raymond Sobel at Stanford University.

EdU administration and staining. 800 μ g of EdU (2mg/mL, Life Technologies) in PBS was injected i.p. 12-16 hours before euthanasia. EdU incorporation was detected with the Click-iT kit EdU Alexa Flour 488 Flow Cytometry Assay Kit (Life Technologies), per the manufacturer's instructions.

In vivo antibody administration. Antibodies were given i.p. at 200 μ g per mouse, in 200 μ l PBS. Frequency of administration and number of doses is noted in figure legends. Clones used included: rat anti-mouse CD2 (RM2-1, gift of Hideo Yagita) or rat IgG isotype control (Rat IgG2a, BioXcell); mouse anti-mouse NK1.1 (PC16, Bio X Cell) or mouse IgG2a (C1.18, BioXcell); hamster anti-mouse CD48 (HM48-1, BioXcell and Biologend), or Armenian hamster isotype control (polyclonal Armenian hamster IgG, BioXcell and HTK888, Biologend); rat anti-mouse CD16/CD32 (clone 93, BioLegend) or rat IgG2a (2A3, BioXcell).

Nanostring. 2D2 Th1 CD4⁺ T effectors were generated as described above, and transferred i.p. to CD48^{-/-} recipients to induce EAE. 200 μ g of anti-CD48 or cIgG was given on day 5 after adoptive transfer, and on day 7 (prior to disease onset) spleens were collected. CD4⁺ T cells were isolated from each spleen by magnetic separation (Miltenyi), then stained for CD4, Thy1.1, Vb11, Va3.2, Thy1.2. 2D2 CD4⁺ T cells were purified as CD4⁺Thy1.1⁺Vb11⁺Va3.2⁺Thy1.2⁻ cells, counted, and frozen. Samples from eight individual mice from two independent experiments were used for RNA analysis. Cells were resuspended in RLT buffer (RNeasy Kit, Qiagen), hybridized with custom capture probesets and reporter probesets, then analyzed on the NanoString nCounter and nCounter Digital Analyzer (NanoString Technologies). The probeset examined 199 genes, including 4 housekeeping genes, plus 8 negative controls and 6 positive controls. Data was processed using the nSolver Analysis Software (NanoString Technologies), to normalize expression levels to housekeeping genes and controls. Statistics were computed in Excel using Student's t test. A p value of 0.00025 was considered

statistically significant, based on Bonferroin correction for testing 199 hypotheses with a total false discovery rate of 5%.

Statistical analysis and software. Statistical analysis was performed using Excel and Prism (GraphPad). Statistical tests used include unpaired t test and paired t test, Mann-Whitney test for non-parametric data, and Fischer's exact test for levels of incidence. Methods are noted in figure legends. Unless otherwise noted, *= $p < 0.05$, **= $p < 0.01$, ***= $p < 0.001$, ****= $p < 0.0001$.

Chapter 3: Susceptibility of CD48^{-/-} [B6] mice to spontaneous and induced lupus-like disease

ABSTRACT

CD48 has been implicated in modulating severity of a spontaneous lupus-like disease, which is mediated by epistatic interactions between a region of 129-derived DNA on chromosome 1 and the B6 genetic background. However, it is not clear to what extent CD48 provides protection against this model of lupus, nor is it clear whether CD48 can modulate the severity of disease in other models of lupus on the B6 background. Here we examine the effects of CD48 reconstitution and deficiency on immune activation and lupus-like disease in both the mixed CD48^{-/-}[B6.129] background and on a pure B6 background. We find that CD48 reconstitution does not alter immune activation in CD48^{-/-}[B6.129] mice, that CD48 deficiency does not precipitate lupus-like disease on a pure B6 genetic background, and the CD48 expression on T cells promotes disease in the BM12 graft versus host model of induced lupus.

RESULTS

Partial CD48 reconstitution does not alleviate splenomegaly in aged CD48^{-/-} [B6.129] mice

Because CD48 deficiency, as well epistatic interactions from flanking 129-derived genes, appeared to contribute to the glomerulonephritis in the CD48^{-/-} [B6.129] strain (Koh et al. 2011), we tested whether reconstituting CD48 expression in CD48^{-/-} [B6.129] mice would be sufficient to prevent lupus-like disease. To address this hypothesis, we obtained CD48^{-/-} [B6.129] mice that had been bred with transgenic mice harboring a bacterial artificial chromosome (BAC) with the B6 version of CD150 (SLAM), CD48, and CD319 (SLAMF7, CS1, CRACC) (**Figure 3.1A**). Since this was a BAC transgenic mouse, no additional promoter was included in the transgene. These mice, along with their transgene-negative littermates, were examined at 6-12 months of age for signs of glomerulonephritis. As shown in **Figure 3.1B**, CD48 reconstitution in CD48 deficient strains was not complete, as only 40-60% of lymphocytes expressed CD48. Thus, we assessed whether partial reconstitution of CD48 was sufficient to attenuate lupus-like disease in the CD48^{-/-} [129.B6] strain.

CD48 expression did not prevent splenomegaly in CD48^{-/-} [B6.129] mice (**Figure 3.1C-D**). The transgene was also not sufficient to significantly reduce the proportion of CD69⁺ cells among CD4⁺ T cells, CD8⁺ T cells, or

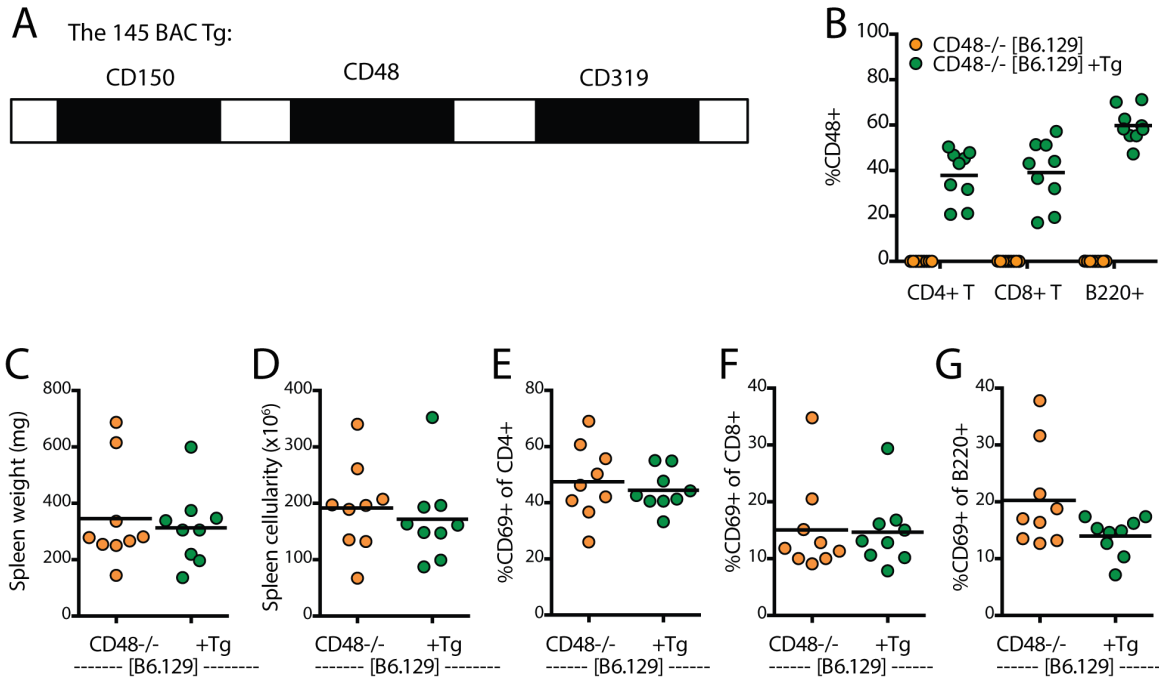


Figure 3.1. Partial CD48 reconstitution does not alleviate splenomegaly in aged CD48^{-/-} [B6.129] mice.
 A. Schematic of the 145 BAC transgene, containing the B6 alleles of CD150, CD48 and CD319. B-G BAC Tg positive and negative CD48^{-/-} [B6.129] and CD48^{-/-} [B6] mice were analyzed when 6-12 months old for signs of spontaneous autoimmunity. B. Percentage of CD4+, CD8+ and B220+ cells that stain positive for CD48 in CD48^{-/-} [B6.129] mice without and with the 145 BAC Tg. C. Spleen weight in 6-12 month old BAC Tg positive and negative CD48^{-/-} [B6.129] and CD48^{-/-} [B6] mice. D. Spleen cellularity. E. %CD69+ among CD4+ T cells in the spleen. F. %CD69+ among CD8+ T cells in the spleen. G. %CD69+ among B220+ B cells in the spleen. N= 6-10 mice per group. Representative of two independent experiments using 5-10 mice per group. Lines represent means. Statistical significance calculated using Student's t test. Data are from an experiment performed by Dr. Dan Brown in the Sharpe lab, and are included for completeness.

B220+ cells (**Figure 3.1E-G**). We conclude that partial reconstitution of CD48 in the CD48^{-/-} [B6.129] strain is insufficient to alter splenomegaly in aged mice, but can affect aspects of lymphocyte activation.

Generation of the CD48^{-/-} [B6] strain

To further investigate the role of CD48 in spontaneous autoimmunity, without confounding factors from epistatic interactions in a mixed genetic background, our laboratory generated a CD48^{-/-} on a pure B6 background. The CD48^{-/-} was created by gene targeting in the B6 embryonic stem cell line Bruce 4, and was maintained on a pure B6 background by Dr. Yvette Latchman in the Sharpe lab.

Young CD48^{-/-} [B6] have altered distribution of T cell precursors in the thymus

Because CD48 is widely expressed on hematopoietic cells, and has been implicated in hematopoietic development (Boles et al. 2011), we first examined the distribution of CD4⁺ and CD8⁺ T cells in the thymus of both young and adult mice. Thymi were collected from 26 day old male WT and CD48^{-/-} mice, stained with CD4, CD8, CD44 and CD25, and analyzed by flow cytometry. As shown in **Figure 3.2A-B**, CD48^{-/-} mice had a significant increase in the proportion of CD4SP cells among total thymocytes.

When we analyzed thymi from 11-21 week old adult mice, we saw a more skewed distribution. Thymocytes were stained for CD3, CD4, CD8 and $\gamma\delta$ TCR, and analyzed by flow cytometry. CD48^{-/-} mice had significantly increased proportions of both CD4SP and CD8SP, and a decrease in DP thymocytes (**Figure 3.2C-D**). This suggests that T cell development in CD48^{-/-} [B6] mice may be altered, compared to WT mice.

Adult CD48^{-/-} [B6] mice have altered distribution of lymphocytes in the spleen

Next we examined the distribution of lymphocytes and monocytes in the spleens of 11-21 week old mice. CD48^{-/-} mice had an increased percentage of CD4⁺ T cells and CD8⁺ T cells in the spleen, and a decreased proportion of B220⁺ B cells, compared to age matched WT mice (**Figure 3.3A**). The proportion of NK cells was not different. The percentage of CD138⁺ plasma cells was increased in the spleen of CD48^{-/-} mice (**Figure 3.3B**). Among B220⁺ B cells, there was an increase in the %CD69⁺ (**Figure 3.3C**) and %GL7⁺ cells (**Figure 3.3D**) in CD48^{-/-} mice.

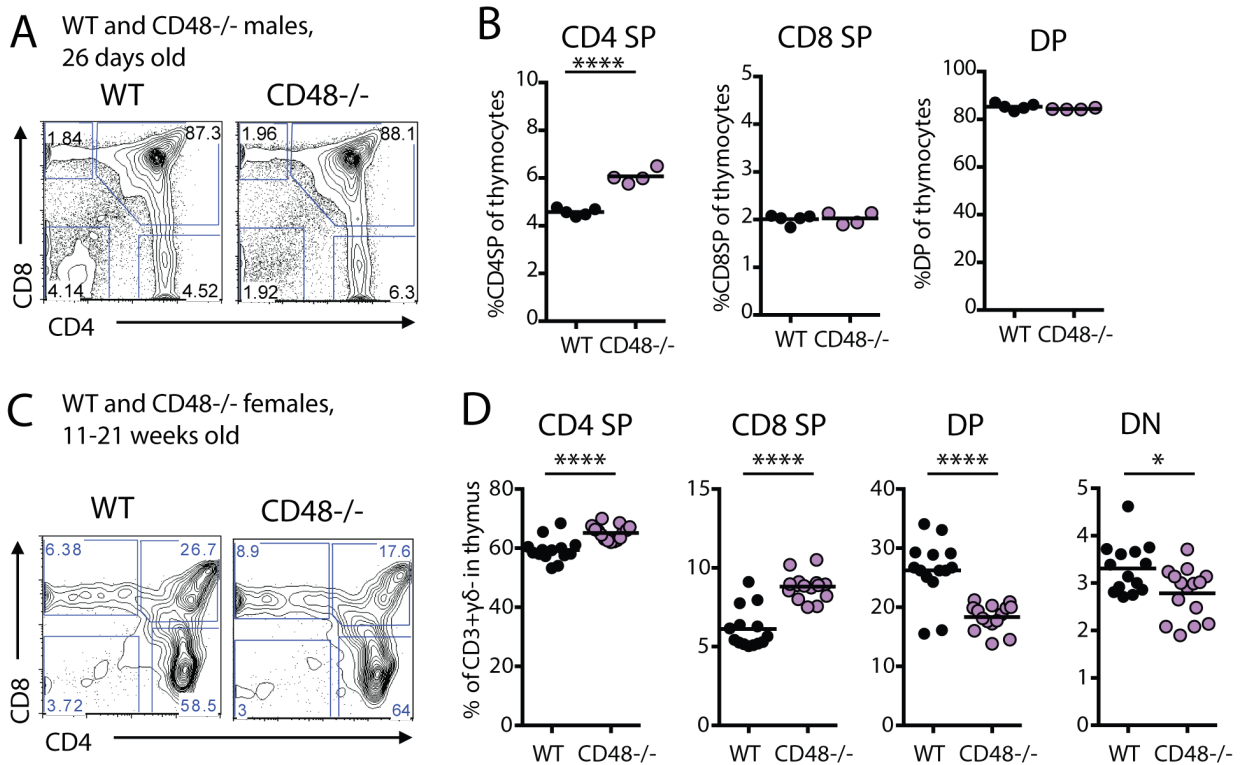


Figure 3.2. CD48^{-/-} mice have altered distribution of thymocytes. A-B Thymi were collected from 26 day old WT and CD48^{-/-} mice and stained for CD4 and CD8. A. Representative staining of thymocytes in WT and CD48^{-/-} mice. B. Percentage of CD4SP, CD8SP and DP thymocytes. C-D Thymi were collected from 6-11 week old WT and CD48^{-/-} mice and stained for CD3, CD4, CD8 and $\gamma\delta$ TCR. C. Representative staining of CD3+ $\gamma\delta$ - thymocytes in WT and CD48^{-/-} mice. D. Percentage of CD4SP, CD8SP, DP and DN thymocytes. A-B representative of a single experiment using 4 mice per group. C-D n=15 mice per group, representative of 2 independent experiments using 9-15 mice per group. Lines represent means. *p<0.05; ****p<0.0001. A-B from an experiment performed by Dr. Dan Brown. C-D from an experiment performed in collaboration with Dr. Dan Brown.

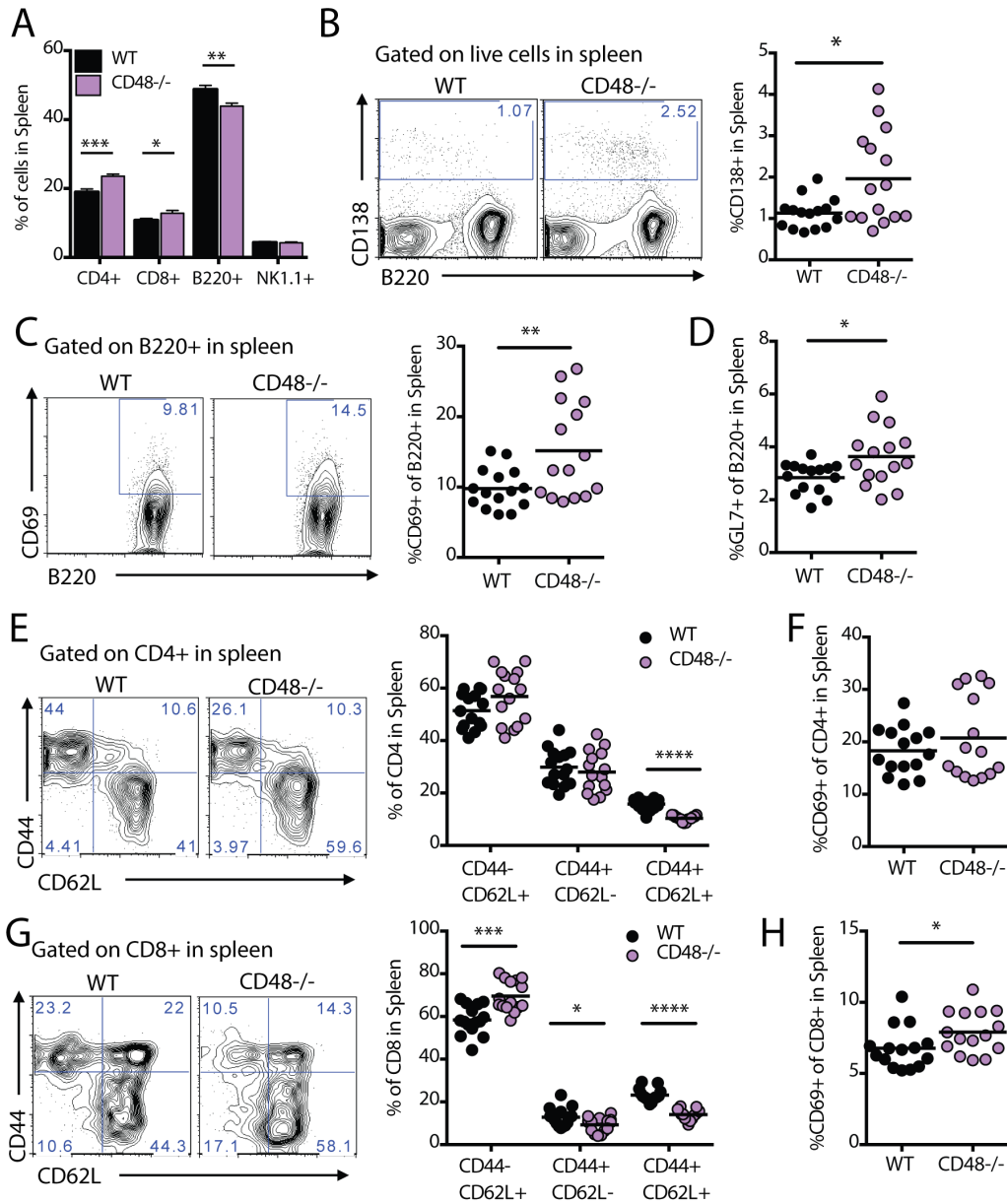


Figure 3.3: CD48^{-/-} mice have altered lymphocyte distributions in the spleen. Splenocytes from 11-21 week old WT and CD48^{-/-} mice were collected and analyzed by flow cytometry. A. Percentage of CD4⁺, CD8⁺, B220⁺ and NK1.1⁺ cells in the spleen. B-D. Splenocytes were stained for B220, CD138, GL7 and CD69. B. Representative staining for CD138 and B220 on WT and CD48^{-/-} splenocytes, and quantification of %CD138⁺ of total splenocytes in all animals. C. Representative staining of CD69 on B220⁺ cells in the spleen, and quantification of %CD69⁺ of B220⁺ cells in all animals. D. %GL7⁺ of B220⁺ cells in the spleen. E-H Splenocytes were stained for CD44, CD62L, CD69, and either CD4 or CD8. E. Representative staining of CD44 and CD62L on CD4⁺ cells in the spleen, and quantification of CD44-CD62L⁺, CD44+CD62L⁻ and CD44+CD62L⁺ CD4⁺ T cells in the spleen. F. %CD69⁺ of CD4⁺ T cells in the spleen. G. Representative staining of CD44 and CD62L on CD8⁺ cells in the spleen, and quantification of CD44-CD62L⁺, CD44+CD62L⁻ and CD44+CD62L⁺ CD8⁺ T cells in the spleen. H. %CD69⁺ of CD8⁺ T cells in the spleen. N= 15 WT and 15 CD48^{-/-} females. Representative of 3 experiments using 5-15 mice per group. Bars represent means, error bars represent SEM. Lines on dot plots represent means. *p<0.05; **p<0.01; ***p<0.001; ****p<0.0001. Data from an experiment performed in collaboration with Dr. Dan Brown.

Surface staining with CD44 and CD62L revealed that among CD4⁺ T cells, CD48^{-/-} mice had a decrease in the proportion of CD44⁺CD62L⁺ cells, but no significant difference in naïve or CD44⁺CD62L⁻ activated cells (**Figure 3.3E**). There was no significant difference in the percentage of CD69⁺ cells among CD4⁺ T cells (**Figure 3.3F**). Among CD8⁺ T cells, there was an increase in the proportion of naïve CD44⁻CD62L⁺ cells and a decrease in the proportion of both CD44⁺CD62L⁻ T cells and CD44⁺CD62L⁺ (**Figure 3.3G**). There was also an increase in the %CD69⁺ among CD8⁺ T cells (**Figure 3H**). These data suggest that the distribution of lymphocytes in CD48^{-/-} mice is not dramatically different from that in WT mice, but there are some subtle in the proportion of naïve and activated cells.

Young CD48^{-/-} [B6] mice have increased surface expression of CD2 and CD244,

Mice lacking surface receptors often have increased expression of the corresponding ligand(s). We therefore investigated whether mice lacking CD48 had altered surface expression CD2 or CD244 on T cells, B cells, NK cells, or monocytes. Splenocytes from WT and CD48^{-/-} mice were stained for CD3, CD8, CD4, $\gamma\delta$ TCR, Foxp3, B220, CD11c, CD11b and CD2 or CD244; in a separate experiment WT and CD48^{-/-} splenocytes were stained for NK1.1, CD11b and CD2 or CD244. As shown in **Figure 3.4A-B**, CD48^{-/-} mice had a significantly increased level of CD2 expression on CD4⁺ and CD8⁺ T cells and B cells, a decreased level of CD2 expression on CD11c⁺ monocytes, and no change in CD2 expression levels on CD11b⁺ monocytes or NK cells. CD48^{-/-} mice had significantly increased CD244 expression levels on $\gamma\delta$ T cells, dendritic cells and CD11b⁺CD11c⁺ monocytes (**Figure 3.4C**) as well as NK cells (**Figure 3.4D**).

Aged CD48^{-/-} [B6] mice do not develop glomerulonephritis

CD48^{-/-} [B6.129] mice develop glomerulonephritis with aging, with development of anti-dsDNA antibodies, anti-chromatin antibodies, renal pathology, and an increase in activated CD44⁺ CD4⁺ T cells (Keszei et al. 2011; Koh et al. 2011). To determine whether CD48^{-/-} [B6] mice were also susceptible to lupus-like disease, we analyzed cohorts of WT B6, CD48^{-/-} [B6], and CD48^{-/-} [B6.129] mice that were either 6-9 months old or 10-18 months old.

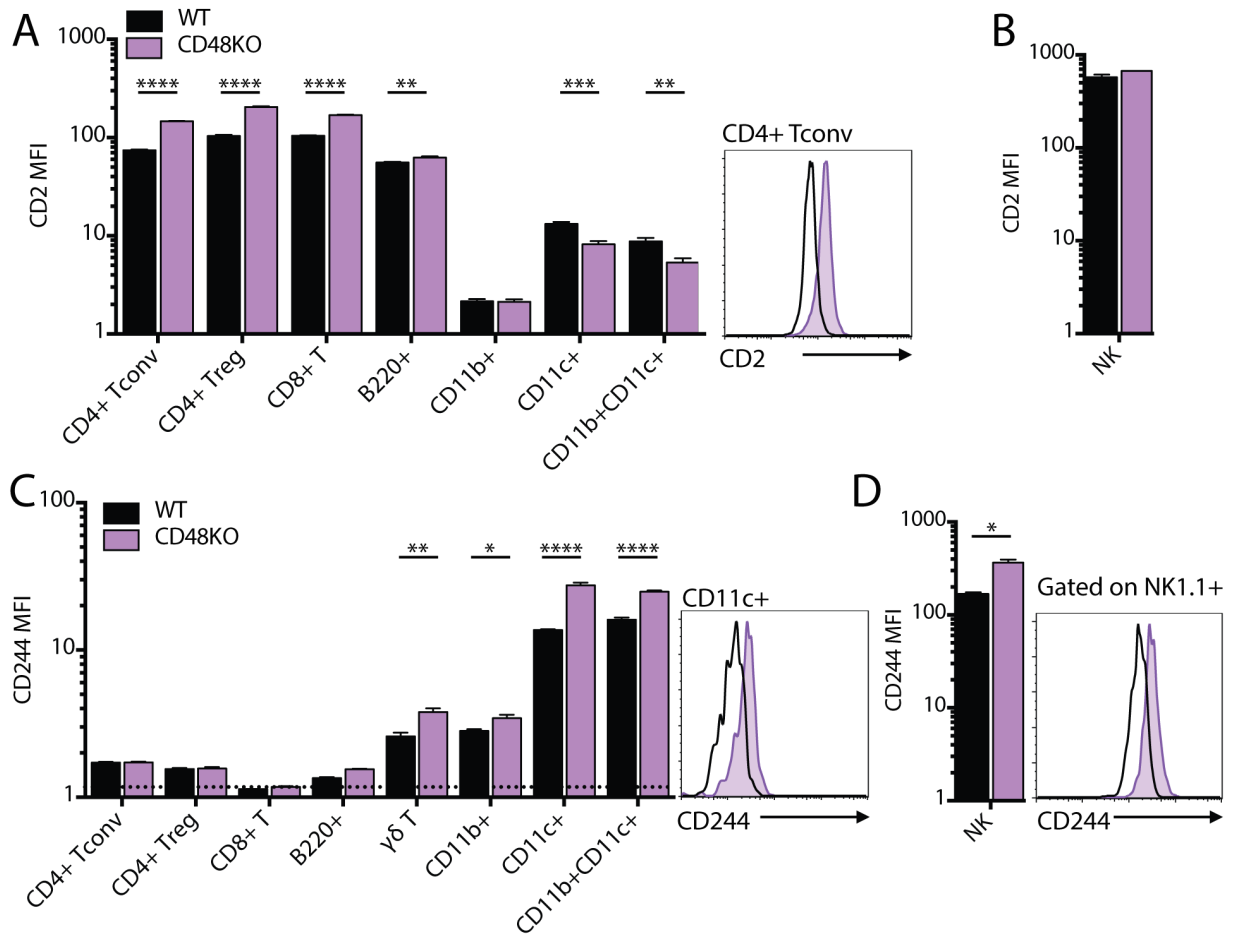


Figure 3.4: CD48^{-/-} mice have increased CD2 and CD244 MFI on select lymphocytes and monocytes. Splenocytes from 5 WT and 5 CD48^{-/-} x week old mice were collected and stained for CD3, CD4, CD8, γ δ TCR, Foxp3, B220, CD11b, CD11c, and either CD2 or CD244. In a separate experiment, splenocytes were collected and stained for NK1.1, CD11b and either CD2 or CD244. Tconv were gated as CD3+CD4+Foxp3⁻; Treg were gated as CD3+CD4+Foxp3⁺; CD8 T cells were gated as CD3+CD8+B220⁻; B cells were gated as B220+CD3⁻; gd T cells were gated as CD3+gd⁺; CD11b⁺ monocytes were gated as CD11b+CD3-B220-CD11c; CD11c+CD11b⁺ monocytes were gated as CD11c+CD11b+CD3-B220⁻; CD11c⁺ monocytes were gated as CD11c+CD3-B220-CD11b⁻. NK cells were gated as NK1.1+CD11b⁺. A. Mean MFI of CD2 on Tconv, Treg, CD8 T, B, and monocytes. A representative histogram of CD2 staining on CD3+CD4+Foxp3⁻ Tconv is shown at right. B. MFI of CD2 on NK cells. C. Mean MFI of CD244 on Tconv, Treg, CD8 T, γ δ T, B, and monocytes. A representative histogram of CD244 staining on CD11c+CD11b⁻ dendritic cells is shown at right. D. Mean MFI of CD244 on NK cells. A representative histogram of CD244 staining on NK cells is shown at right. 5 WT and 5 CD48^{-/-} mice were used for all stains except for NK cell stains; 2 WT and 2 CD48^{-/-} mice were used for NK cell stains. Bars represent means, error bars represent SEM. *p<0.05; **p<0.01; ***p<0.001; ****p<0.0001

We found that 6-9 month old CD48^{-/-} [B6] mice had a modest but significant increase in spleen weight compared to WT mice (**Figure 3.5A**), and a pronounced increase in spleen cellularity (**Figure 3.5B**), but not to the degree of CD48^{-/-} [B6.129] mice. Anti-dsDNA antibody titers in CD48^{-/-} [B6] did not differ from those in WT, while CD48^{-/-}[B6.129] had significantly higher titers than WT (**Figure 3.5C**). Two of the 14 CD48^{-/-} [B6] mice had detectable anti-chromatin IgG, in contrast to none of the WT mice and 5 of the 7 CD48^{-/-} [B6.129] mice (statistically different between B6.KO and 129.KO only, $p < 0.05$ by Fischer's exact test) (**Figure 3.5D**).

Spleens from 6-9 month old mice were also analyzed by flow cytometry, for signs of B and T cell activation. CD48^{-/-} [B6] mice did not have altered lymphocyte distribution in the spleen compared to WT mice, although CD48^{-/-} [B6.129] mice had an increased proportion of CD4⁺ T cells and a decreased proportion of CD8⁺ T cells (**Figure 3.5E**). CD48^{-/-} [B6] mice had an increase in the proportion of CD69⁺ cells among CD4⁺ T cells, but no significant increase in the %CD69⁺ among CD8⁺ T cells (**Figure 3.5F-G**). CD48^{-/-} [B6] mice had an increase in the %CD69⁺ among B220⁺ cells (**Figure 3.5H**), and also an increase in the proportion of GL7⁺ cells among B220⁺ cells (**Figure 3.5J**), but not to the degree seen in CD48^{-/-} [B6.129]. Thus, 6-9 month old CD48^{-/-} [B6] mice have a modest increase in the proportion of activated cells in the spleen, but do not display the level of lymphocyte activation seen in the CD48^{-/-} [B6.129] strain.

We also examined a small cohort of WT B6, CD48(het) [B6], CD48^{-/-} [B6] and CD48^{-/-} [B6.129] mice that were 10-18 months old, to again survey for signs of spontaneous autoimmunity. CD48^{-/-} [B6] mice had higher anti-dsDNA serum antibody levels than WT, but lower than CD48^{-/-} [B6.129] mice (**Figure 3.5K**). 3 out of the 5 CD48^{-/-} [B6] mice had anti-chromatin antibodies, compared to 1 out of 3 WT and 4 out of 4 CD48^{-/-} [B6.129] (**Figure 3.5L**). This suggests that CD48^{-/-} [B6] do not develop the robust spontaneous lupus-like disease seen in the CD48^{-/-} [B6.129] strain.

CD48^{-/-} CD4⁺ T cells fail to induce disease in the BM12 model of induced lupus nephritis

We hypothesized that lack of CD48 might make CD48^{-/-} [B6] mice more susceptible to an induced form of autoimmunity. The BM12 model of induced lupus nephritis takes advantage of a three amino acid difference in MCHII proteins between the congenic BM12 and B6 mice. Adoptive transfer of CD4⁺ T cells or total

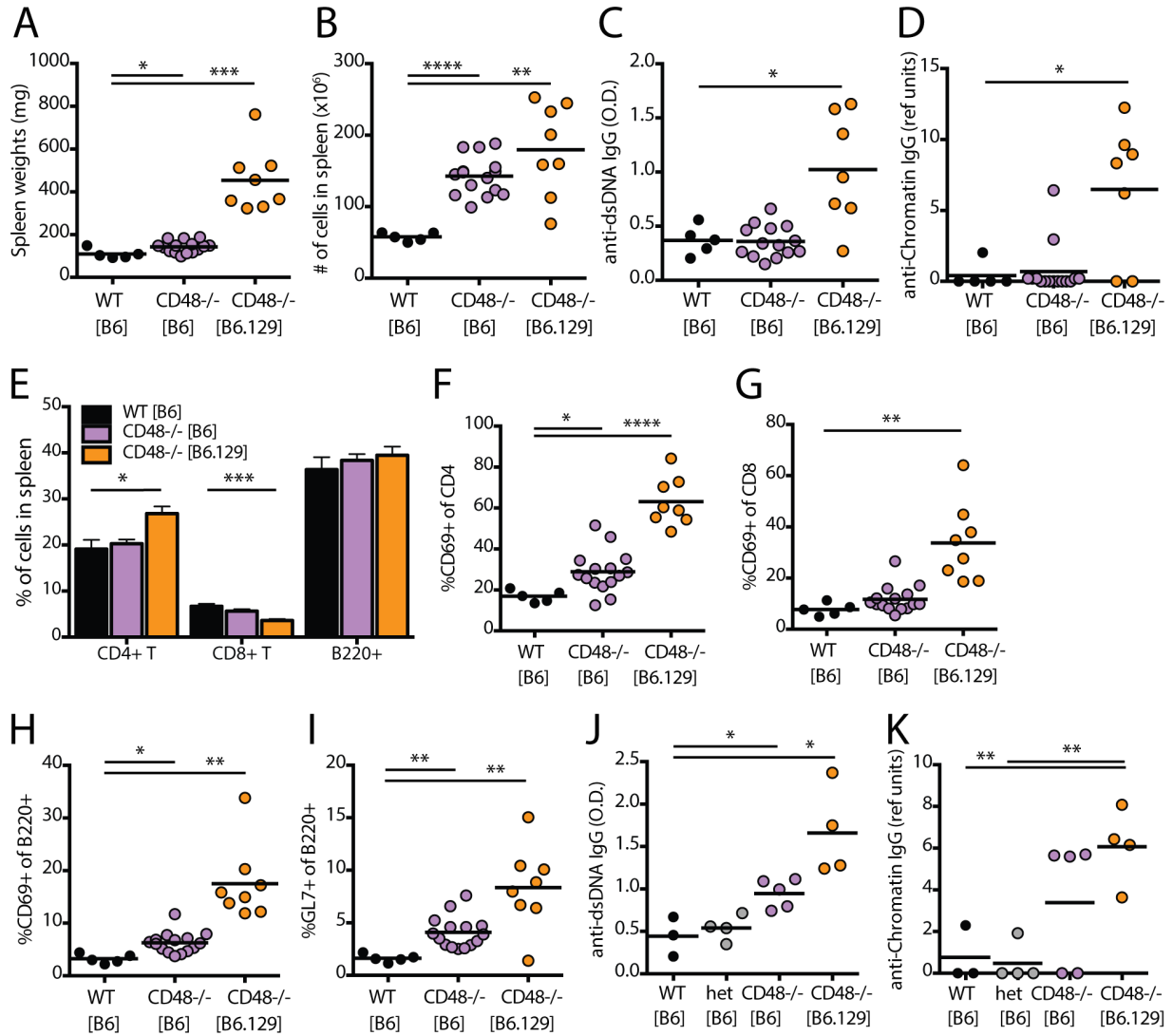


Figure 3.5. Aged CD48^{-/-} [B6] develop splenomegaly but not glomerulonephritis. A-J WT and CD48^{-/-} [B6] mice were analyzed when 6-9 months old for signs of spontaneous lupus-like disease. CD48^{-/-} [B6.129] mice were included as a positive control. A. Spleen weights. B. Splenocyte counts. C. Anti-dsDNA antibody titers from serum. D. Anti-chromatin antibody titers from serum. E-J. Splenocytes were collected and stained for CD4, CD8, B220, CD69 or GL7, then analyzed by flow cytometry. E. Distribution of lymphocytes in the spleen. F. %CD69⁺ of CD4⁺ cells. G. %CD69⁺ of CD8⁺ cells. H. %CD69⁺ of B220⁺ cells. J. %GL7⁺ of B220⁺ cells. K-L WT, CD48(het) [B6], and CD48^{-/-} [B6] mice were analyzed when 10-18 months old for signs of spontaneous lupus-like disease. CD48^{-/-} [B6.129] mice were included as a positive control. K. Anti-dsDNA antibody titers in serum. L. Anti-chromatin antibody titers in serum. A-I n=5-14 mice per group. J-K n=3-5 mice per group. Lines represent means. Significance determined using ANOVA; significance calculated using Student's t test to compare experimental groups to WT. *p<0.05; **p<0.01; ***p<0.001; ****p<0.0001. Data from an experiment performed in collaboration with Dr. Dan Brown.

splenocytes from BM12 mice into B6 mice, or visa versa, results in a CD4⁺ T cell-mediated graft-versus-host (GVH) and host-versus-graft response (Morris, Cohen, and Eisenberg 1990). Polyclonal activation of B cells ensues, with appearance of plasma cells in the spleen by day 7 after transfer and development of anti-dsDNA antibodies in the serum by day 14 after transfer. Previous work showed that CD244^{-/-} mice develop an enhanced response to BM12 transfer, including splenomegaly, donor cell expansion, plasma cell development and anti-dsDNA antibodies (Brown et al. 2011). This suggested that the CD244:CD48 pathway might be involved in susceptibility to this disease model.

We first transferred CD4⁺ T cells from BM12 donors into WT and CD48^{-/-} recipients, and examined spleens 14 days later. As shown in **Figure 3.6A,B**, we did not see a significant difference in spleen cellularity or the percentage of CD138⁺ plasma cells in the spleen. Next, we transferred CD4⁺ T cells from WT or CD48^{-/-} mice into BM12 recipients, and examined spleens 14 days later. Recipients of CD48^{-/-} CD4⁺ T cells had lower spleen cellularity than recipients of WT CD4⁺ T cells (**Figure 3.6C**), and a strikingly reduced percentage of CD138⁺ plasma cells in the spleen (**Figure 3.6D**). When we looked for donor CD4⁺ T cells in the spleens of recipients, we found that the percentage of CD48^{-/-} CD4⁺ T cells in the spleen was dramatically reduced as well (**Figure 3.6E**). Collectively, this indicated that CD48^{-/-} recipients did not have a significantly altered response to induced lupus, compared to WT mice, but CD48^{-/-} CD4⁺ T cells were not capable of inducing a lupus-like disease in this model.

We hypothesized that the absence of a persistent GVH response could be due to NK-mediated killing of CD48^{-/-} cells. NK cell target lysis can be inhibited by CD244 on NK cells binding to CD48 on target cells (Lee et al. 2004). To test this hypothesis, we administered anti-NK1.1 mAb or isotype control to BM12 mice starting one day before adoptive transfer of CD4⁺ T cells, and ever 5 days thereafter. CD4⁺ T cells from WT or CD48^{-/-} mice were transferred i.p. and spleens were analyzed 14 days later. Anti-NK1.1 did not significantly alter the number of cells in the spleen of recipients of WT or CD48^{-/-} cells (**Figure 3.6F**), nor did it affect the proportion of donor CD4⁺ T cells among total CD4⁺ T cells in recipients of either WT T cells or CD48^{-/-} T cells (**Figure 3.6G**). This suggests that NK cells do not play a critical role in regulating the number of donor T cells in the BM12 model, whether using WT or CD48^{-/-} donor cells.

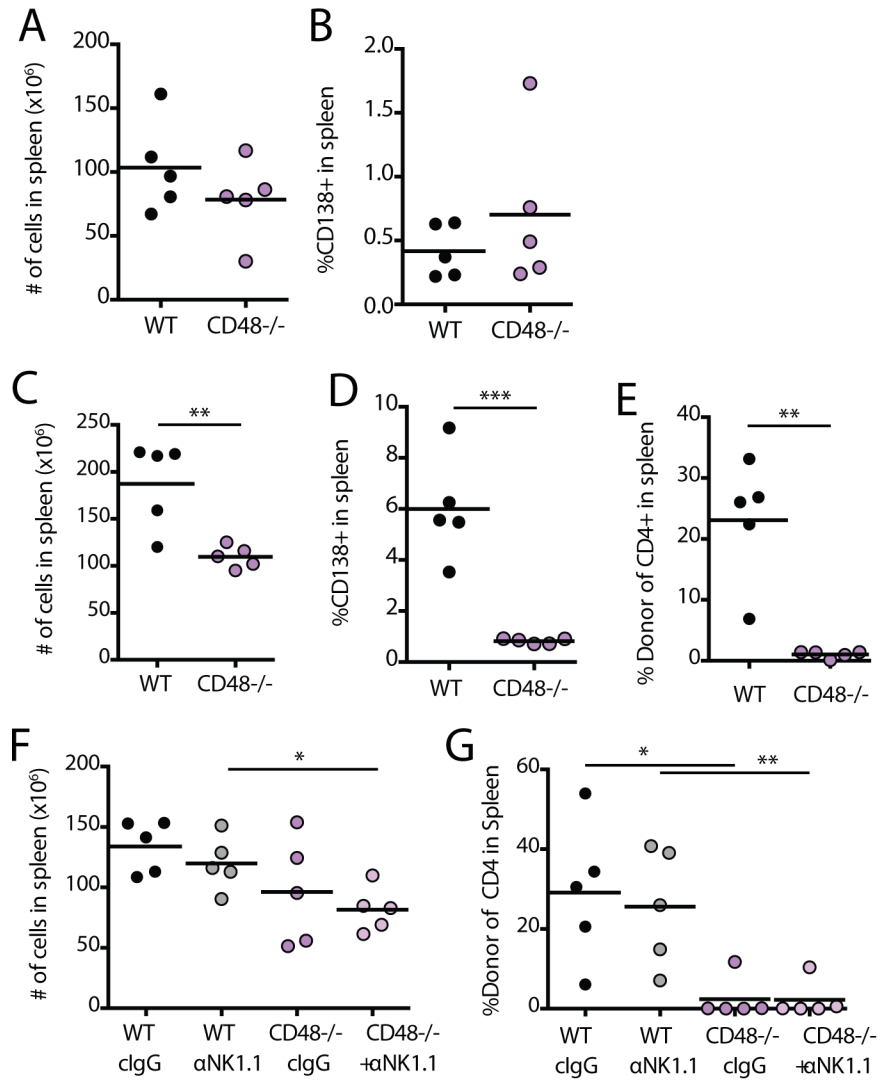


Figure 3.6. CD48^{-/-} [B6] splenocytes are not pathogenic in the BM12 model of induced lupus. A-B. CD4⁺ T cells from BM12 mice were transferred i.p. into WT or CD48^{-/-} mice to induce GVH lupus. Recipients were analyzed 14 days later. A. Spleen cellularity. B. %CD138⁺ plasma cells in spleen. C-E. CD4⁺ T cells from BM12 mice were transferred i.p. to Thy1.1 congenic WT or CD48^{-/-} mice, to induce GVH lupus. Recipients were analyzed 14 days after transfer. C. Spleen cellularity. D. %CD138⁺ plasma cells in spleen. E. %Thy1.1⁺ donor CD4⁺ T cells among total CD4⁺ T cells in spleen. F-G BM12 mice received 200 μ g of anti-NK1.1 (PK136) or isotype control (mouse IgG2a, clone CI.18) i.p. one day before transfer of CD4⁺ T cells from WT or CD48^{-/-} mice, and every 5 days thereafter. F. Spleen cellularity. G. Percentage of donor CD4⁺ T cells (Thy1.1⁺ WT or CD48^{-/-}) among total CD4⁺ T cells in the spleen. A-B representative of 2 independent experiments with 5 mice per group. C-E representative of 3 independent experiments with 5 mice per group. Lines represent means. Statistical significance calculated using Student's t-test. *p<0.05; **p<0.01; ****p<0.0001. Data are from experiments performed in collaboration with Dr. Dan Brown.

DISCUSSION

In this study, we investigated the function of CD48 in autoimmunity and tolerance. Our studies were motivated by several lines of evidence which suggested that CD48 could play a role in development of spontaneous lupus-like disease. First, CD48 is located in the lupus-susceptibility locus Sle1b, which has two common haplotypes in inbred mouse strains. Second, the CD48^{-/-} [B6.129] mouse develops spontaneous lupus-like disease with autoantibodies and glomerulonephritis. There were indications that both CD48 deficiency and epistatic interactions could contribute to the severity of disease, and it was not clear whether one of these was the primary cause or both contributed significantly (Keszei, Latchman, et al. 2011; Koh et al. 2011). The potential importance of epistatic interactions is illustrated by studies in which the haplotype 1 allele, from NZB or 129 mouse strains, was crossed on to the B6 genetic background, and precipitated lupus-like disease on the B6 genetic background but not on 129 or Balb/c backgrounds (Wandstrat et al. 2004). Thus, epistatic interactions of 129-derived genes with the B6 genetic background could contribute to development of lupus-like disease. Third, both CD48^{-/-} [B6.129] and CD48^{-/-} [Balb/c.129] mice have altered T cell and APC function as assessed by in vitro assays, suggesting that not all of the altered phenotype of CD48^{-/-} [B6.129] mice was due to epistatic interactions (Gonzalez-Cabrero et al. 1999; Keszei, Latchman, et al. 2011). Thus, we undertook this investigation to examine the role of CD48 in susceptibility to lupus-like disease on the B6 background, using three distinct approaches to overcome the limitations of these earlier studies: 1) reconstitution of CD48 in CD48^{-/-} [B6.129] mice using a BAC transgene; 2) generation and analysis of CD48^{-/-} [B6] mice, to eliminate the potential of epistatic interactions; and 3) analysis of the role of CD48 in an inducible, GVH model of lupus using CD48^{-/-} [B6] mice.

We found that reconstitution of CD48^{-/-} [B6.129] mice with a BAC transgene containing the B6 version of CD48 (haplotype 2) was insufficient to alleviate autoimmunity. In addition, 6-12 month old CD48^{-/-} [B6] mice did not develop spontaneous lupus-like disease like that seen in the CD48^{-/-} [B6.129], as assessed by splenomegaly, anti-dsDNA antibodies, anti-chromatin antibodies, and lymphocyte activation. Lastly, we found that CD4^{-/-} T cells were not potent inducers of autoimmunity in a GVH model of lupus. However, our studies revealed that CD48 deficiency led to increased B and T cell activation in both young and aged CD48^{-/-} [B6] mice, as well as altered distribution of T cell precursors in the thymus. Collectively, these data suggest that CD48 does not have

a primary role in susceptibility to lupus-like disease, but might have a critical role in lymphocyte development, homeostasis and/or activation in vivo.

In our first approach, we examined whether reconstitution of CD48 in the CD48^{-/-} [B6.129] strain with a BAC transgene could prevent the lupus-like phenotype in CD48^{-/-} [B6.129] mice. We had not anticipated that reconstitution would be incomplete. Because expression of CD48 was restored in only ~50% of all lymphocytes, the interpretation of our results is somewhat confounded. However, it appears that at least partial reconstitution of CD48 is not sufficient to alleviate splenomegaly or development of anti-nuclear antibodies in CD48^{-/-} [B6.129] mice. This suggests that either the contribution of CD48 is not dominant over the contributions of epistatic interactions between 129-derived genes and the B6 genome; that partial CD48 reconstitution is not sufficient to overcome the effects of epistatic interactions; or that the effects of CD48 are undetectable or not biologically significant in the context of autoimmunity induced by these epistatic interactions. Our interpretation was limited by the technical aspects of the experiment, and thus led us to pursue other approaches to examine the effect of CD48 deficiency on susceptibility to autoimmunity. However, the ability of epistatic interactions between 129-derived genes and the B6 genome to promote spontaneous autoimmunity remains intriguing in its own right, and suggests that other SLAM family genes may be critical in this model. For instance, it is possible that 129-derived genetic elements cause altered expression levels or regulate gene expression in this locus, possibly for other SLAM family genes.

Our second approach was to eliminate the contribution of epistatic interactions, and study the effects of CD48 deficiency on a pure genetic background. To accomplish this, we used a new CD48^{-/-} B6 mouse strain, generated in the lab by Dr. Yvette Lachtman using a B6 ES cell and maintained on the B6 background. By examining this strain, we could investigate whether there was a role for CD48 in susceptibility to lupus on the B6 background. Although the CD48^{-/-} [Balb/c.129] strain does not develop lupus-like disease, suggesting that CD48 is not critical for protection from autoimmunity, disease susceptibility can vary by genetic background. We first compared lymphocyte development and homeostasis in young WT and CD48^{-/-} B6 mice, both to generate a context in which to interpret any phenotypes in aged mice and also because studies in the CD48^{-/-} [B6.129] strain had suggested roles for CD48 in hematopoiesis, particularly B cell development and

homeostasis (Boles et al. 2011). In the thymus of 4-week old mice, we observed an increased proportion of CD4SP cells among total thymocytes. This was also described in the CD48^{-/-} [B6.129] mouse, although those studies also found a decrease in DP thymocytes, which we did not observe (Gonzalez-Cabrero et al. 1999). When we examined 6-8 week old mice, we found an altered thymocyte distribution, suggesting that T cell development may be altered in CD48^{-/-} mice. Although no publications have directly examined the role of CD48 in T cell development in the thymus, the function of CD48 as an adhesion molecule in the immune synapse between T cells and APCs might be important in thymocyte development, as well as homeostasis of mature lymphocytes.

Next we examined lymphocytes in the periphery of 6-8 week old CD48^{-/-} [B6] mice, to establish a baseline for any alterations that we might see in aged mice. Interestingly, there were some alterations in B cells in the young CD48^{-/-} [B6] mice. CD48^{-/-} [B6] mice had increased B cell activation in the spleen, including an increased percentage of CD138⁺ plasma cells, GL7⁺ germinal center B cells, and CD69⁺ activated B cells, compared to age-matched WT mice. Boles et al. had found that B cells from CD48^{-/-} [B6.129] mice had altered hematopoietic development that resulted in increased IFN γ in the bone marrow and Pak1 activation, as well as a higher incidence of B cell-type malignancies in aged mice (Boles et al. 2011). Because those studies were performed using the CD48^{-/-} [B6.129] strain, it is possible that those phenotypes are due to CD48-independent mechanisms in the mixed genetic background. However, our data suggest that B cells from CD48^{-/-} [B6] mice are more activated, as well, supporting a role for CD48 in this process. We did not explicitly look for lymphomas or tumors, nor were our aged cohorts quite as old as those analyzed by Boles et al. (6-12 months old in our studies, ~16 months old in Boles et al. studies). Thus, further investigation would be required to ascertain whether CD48^{-/-} [B6] mice also have alterations in hematopoietic development or the incidence of hematologic malignancies.

We also saw alterations in the distribution of naïve and activated T cells in the periphery of 6-8 week old mice: CD48^{-/-} [B6] mice had a reduced percentage of CD44⁺CD62L⁺ cells among both CD4⁺ and CD8⁺ T cells, as well as an increase in naïve CD44⁻CD62L⁺ CD8⁺ T cells. Considering the alterations in the thymus, this may be due to developmental alterations, or possibly due to homeostasis in the periphery. The bias towards more

naïve T cells does not explain the increase in B cell activation. Preliminary data in our lab indicate that CD48^{-/-} [B6] mice do not have altered proportions of T follicular helper or T follicular regulatory cells among total CD4⁺ T cells, suggesting that increased B cell activation may be due to cell intrinsic effects of CD48 deficiency in B cells. Additional studies would benefit from examining cytokine secretion in B cells, as well as antigen presenting functions. It is also possible that studies using immunization with either T-dependent or T-independent antigens may reveal greater differences in B cell activation, cytokine production, or antibody production. Preliminary data in our lab suggests that CD48^{-/-} [B6] mice do not have a defect in antibody production in response to either primary or secondary challenge with NP-OVA (Dan Brown, unpublished data), however addition studies could examine B cell responses to TLR agonists such as LPS.

Interestingly, when we examined the spleens of 6-12 month old CD48^{-/-} [B6] mice, we saw increased activation of B cells, as well as CD4⁺ and CD8⁺ T cells. Although these mice did not develop splenomegaly to the degree seen in 6-12 month old CD48^{-/-} [B6.129] mice, both spleen cellularity and weight were increased compared to age-matched WT animals. Although neither anti-dsDNA nor anti-chromatin antibodies were significantly elevated in CD48^{-/-} [B6] mice, compared to WT mice, the increase in spleen size and cellularity suggests some immune dysregulation. Among CD4⁺ T cells and B cells, the percentage of CD69⁺ cells was significantly increased, and a similar trend was observed in CD8⁺ T cells, although this was not statistically significant. Other measures of B cell activation, such as the percentage GL7⁺ and CD138⁺, were also increased in CD48^{-/-} [B6] mice. Thus, aged CD48^{-/-} [B6] mice had signs of increased activation of lymphocytes, compared to WT mice, but these changes did not lead to the development of the lupus-like disease seen in 6-12 month old CD48^{-/-} [B6.129] mice.

Our third approach for studying CD48 function in lupus, was to use a model of induced disease. We hypothesized that, although CD48^{-/-} [B6] mice were not susceptible to spontaneous lupus-like disease, increased B cell activation in CD48^{-/-} mice might make them more susceptible to a GVH model of lupus. To test this, we used the BM12 transfer model. We did not see any difference in plasma cell development or anti-dsDNA production when BM12 CD4⁺ T cells were transferred to WT versus CD48^{-/-} [B6] recipients. When we did the reciprocal experiment, transferring CD48^{-/-} or WT CD4⁺ T cells into BM12 recipients, we saw a

dramatic phenotype, but not of increased severity. Instead, CD48^{-/-} CD4⁺ T cells did not persist in the BM12 host. This was in stark contrast to the phenotype we had seen when transferring BM12 splenocytes into CD244^{-/-} mice, which resulted in increased spleen cellularity, plasma cell development, and anti-dsDNA antibody production (Brown et al. 2011). These results suggested that either the phenotype in CD244^{-/-} mice was not due to disruption of CD244:CD48 interactions, or that a unique factor was involved in CD48^{-/-} [B6] mice. We considered that WT NK cells might be more likely to kill CD48^{-/-} target cells, but depleting NK cells with anti-NK1.1 antibody did not restore CD48^{-/-} CD4⁺ T cell persistence. It remains possible that this phenotype is due to increased killing of CD48^{-/-} CD4⁺ T cells by CD8⁺ T cells. Additional studies are required to better understand this phenotype. Studies that could be informative include examination of the kinetics of CD48^{-/-} CD4⁺ T cell activation and number after transfer to BM12 recipients, as well as investigation of potential mechanisms such as CD8-mediated killing, reduced proliferation, increased apoptosis or altered migration. It is also possible that CD48^{-/-} CD4⁺ T cells fail to effectively compete with CD48⁺ CD4⁺ T cells in the BM12 host for access to survival signals. Thus, both cell intrinsic and extrinsic mechanisms should be assessed to understand why there is decreased persistence of CD48^{-/-} CD4⁺ T cells following transfer into BM12 recipients.

Our finding that CD48 deficiency is not solely responsible for spontaneous autoimmunity in the CD48^{-/-} [B6.129] strain, and that disease is instead likely due to epistatic interactions, suggests that other SLAM family members may be responsible for disease in the CD48^{-/-} [B6.129]. Other studies have examined the role of neighboring SLAM family genes in susceptibility to lupus-like disease. Although there are likely multiple players, Ly108 (SLAMF6) appears to play a prominent role in precipitating disease in the Sle1b.B6 strain. Keszei et al. identified a new isoform, Ly108-H1, which was present in B6 mice (SLAMF haplotype 2) but was absent in congenic lupus-prone strains with the SLAMF haplotype 1. Introduction of Ly108-H1 into Sle1b.B6 mice, using a BAC transgene, dramatically attenuated signs of lupus-like disease (Keszei, Detre, et al. 2011). Thus, there is clear evidence for roles of SLAM family genes other than CD48 in contributing to lupus in the Sle1b.B6 strain.

Notably, our observation of increased B and T cell activation in both naïve and aged mice would not be predicted by the decreased ability of CD48^{-/-} APCs to induce proliferation in vitro, or by the reduced proliferation of CD48^{-/-} T cells in vitro (Gonzalez-Cabrero et al. 1999; Keszei, Latchman, et al. 2011). This suggests that the phenotype observed in CD48^{-/-} [B6] in vivo is due to a more complex or multi-component mechanism, and raises the possibility that lack of CD48 on different cell populations may have different, opposing contributions to the whole animal. This is not too hard to imagine, considering that CD48 has been described to have functions ranging from detection and internalization of bacteria by mast cells and macrophages (Baorto et al. 1997; Malaviya et al. 1999; Moller et al. 2013), to triggering of eosinophils (Elishmereni et al. 2013; Minai-Fleminger et al. 2014), to adhesion between T cells and APCs (Latchman, McKay, and Reiser 1998; Milstein et al. 2008). Critical roles for CD48 may vary depending on the disease model used, and the key populations involved in that model, as well as the key populations involved in each phase of disease. Thus, future studies may benefit from examining the role of CD48 on specific immune cell subsets individually, with adoptive transfers of deficient cells into WT recipients, conditional knockout mice, and inducible conditional knockout mice.

In summary, the goal of these studies was to elucidate the role of CD48 in humoral autoimmunity by investigating the effects of CD48 deficiency on the B6 background, in both spontaneous and induced models of lupus. We found that 6-12 month old CD48^{-/-} [B6] mice do not develop spontaneous lupus-like disease with aging, but do display other signs of immune dysregulation such as increased plasma cells and B cell activation. Our data suggest that some prior studies of CD48 deficient cells, performed using the CD48^{-/-} [B6.129], may be worth repeating with the CD48^{-/-} [B6] mice, to clarify whether the prior observations were due to lack of CD48 or to epistatic interactions from 129-derived genes. However, our data also support prior publications describing roles for CD48 in T cell and B cell activation, and provide rationale for further studies using CD48 deficient mice to examine the role of CD48 in autoimmunity and tolerance.

Chapter 4: Susceptibility of CD48^{-/-} [B6] mice to an induced model of autoimmunity, experimental autoimmune encephalomyelitis

ABSTRACT

CD48 contributes to T cell activation via its adhesion and costimulatory properties. Our studies of CD48 in a model of induced lupus indicated that CD48 expression on CD4⁺ T cells was critical to development of disease, and suggested that this molecule might have an important role in other models of autoimmunity. A homologue of CD48 found in humans—CD58, also a ligand for CD2—was identified as a risk locus in multiple sclerosis, and suggested that the CD2 pathway may be important in regulating this autoimmune disease. Here, we investigate the role of CD48 in contributing to development of autoimmune encephalomyelitis, a mouse model of multiple sclerosis. We found that CD48^{-/-} mice have modestly attenuated EAE. Surprisingly, CD48 expression on CD4⁺ T cells did not appear to affect severity of disease. Instead, our data suggest that CD48 may have a role in modulating disease via its expression on either Tregs, CD8⁺ T cells and/or B cells.

RESULTS

CD48-deficient mice have slightly delayed and attenuated experimental autoimmune encephalomyelitis

Considering the increased development of spontaneous autoimmunity in the B6.129.CD48^{-/-} mouse, we wondered whether these animals would show increased susceptibility in an induced autoimmunity model such as experimental autoimmune encephalomyelitis (EAE). EAE can be induced by immunization with a peptide from the brain-specific protein myelin oligodendrocyte glycoprotein (MOG), emulsified in complete Freund's adjuvant (CFA). To test our hypothesis, we immunized WT B6 and CD48^{-/-} [B6.129] mice with MOG [35-55] emulsified in CFA to induce EAE. As shown in **Figure 4.1A**, CD48^{-/-} [B6.129] mice had similar disease course to WT mice up to day 17. However, resolution of disease was accelerated and enhanced in CD48^{-/-} [B6.129] mice compared to WT, as the median disease score was significantly lower on days 19 through 26. This indicated to us that the phenotype of enhanced autoimmunity in the lupus model did not carry over into the EAE model in CD48^{-/-} [B6.129] mice, and instead suggested that CD48 deficient mice might be protected in EAE.

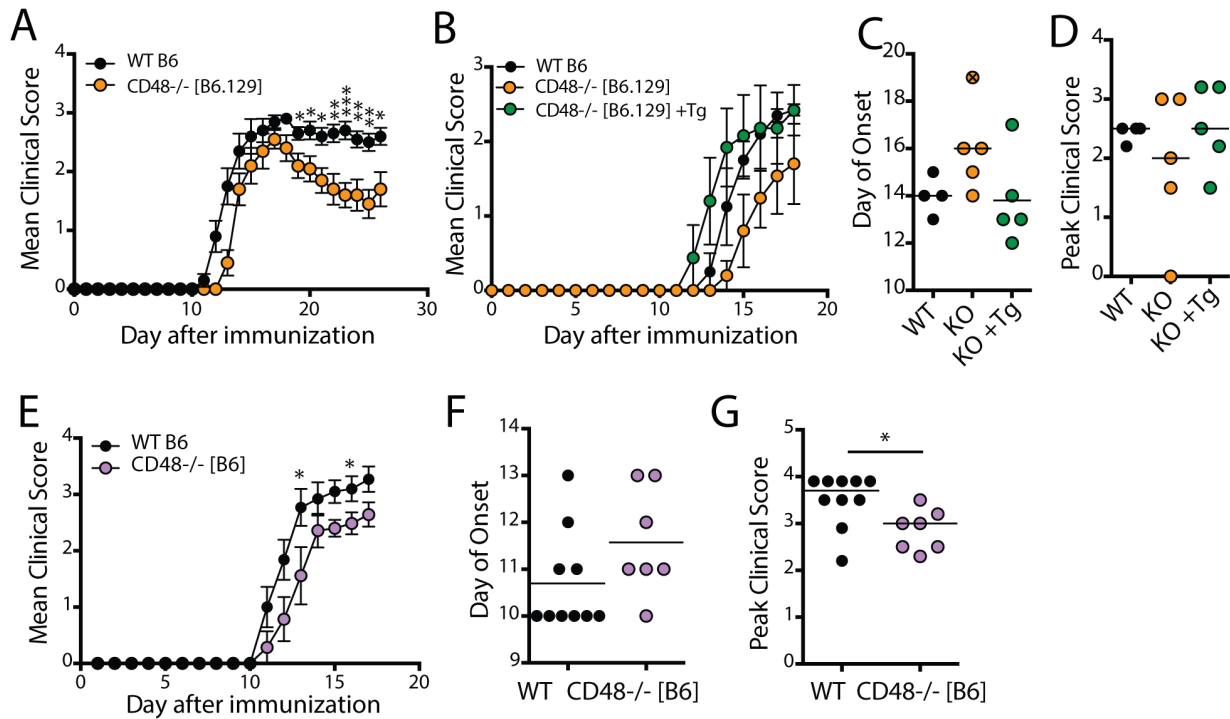


Figure 4.1 CD48^{-/-} mice have moderately attenuated EAE. Mice (8-12 week old) were immunized s.c. with 50 μ g MOG[35-55] emulsified in 100 μ l of MTb fortified CFA (400 μ g MTb), and given 100ng pertussis toxin i.p. on days 0 and 2. Mice were monitored daily for clinical disease. A. Mean clinical scores \pm SEM during EAE in WT B6 and CD48^{-/-} [B6.129] mice, which were generated from 129 ES cells and backcrossed to B6 for >10 generations. B-D. EAE in WT B6, CD48^{-/-} [B6.129] and CD48^{-/-} [B6.129] mice carrying a BAC transgene containing the B6 version of CD150, CD48, and CD319. B. Mean clinical scores, \pm SEM. C. Day of disease onset. D. Peak clinical score by day 18. E-G. EAE in WT B6 and CD48^{-/-} [B6] mice, which were generated from B6 ES cells and maintained on a B6 background. E. Mean clinical scores, \pm SEM. F. Day of disease onset. G. Peak clinical score by day 17. A, n=10 mice per group, representative of 2 experiments with 8-10 mice per group. B-D, n=4-5 mice per group. E-G, n=7-10 mice per group, representative of 3 independent experiments with 5-10 mice per group. Lines on dot plots represent mean (C, F) or median (D, G). Error bars represent SEM. Significance calculated using Mann-Whitney test (A,B,D,E,G) or Student's t test (C,F). *p<0.05, **p<0.01, ***p<0.001. Data in A-D from experiments performed in collaboration with Dr. Dan Brown.

To determine whether the lack of CD48 or flanking 129-derived genes contributed to these protective effects in EAE, we compared EAE severity in WT B6 mice, CD48^{-/-} [B6.129] mice, and CD48^{-/-} [B6.129] mice in which CD48 was reconstituted in a BAC transgene (see Figure 3.1A for transgene schematic). As shown in **Figure 4.1B**, all three groups had similar disease courses, with a slight delay in onset of disease (**Figure 4.1C**) and reduced peak disease score (**Figure 4.1D**) for CD48^{-/-} [B6.129] lacking the BAC Tg compared to those with the BAC Tg. However, this difference was not statistically significant. Due to limited availability of these strains, we only performed one experiment and did not examine the resolution phase of EAE.

To further examine the role of CD48 in EAE, we focused exclusively on the CD48^{-/-} [B6] mouse strain (hereafter referred to as “CD48^{-/-}”), in order to avoid confounding influences from flanking 129-derived genes. We

immunized a large cohort of WT B6 and CD48^{-/-} mice with MOG/CFA to induce EAE, and monitored these mice for clinical disease (**Figure 4.1E**). CD48^{-/-} mice had tended to have delayed disease onset, but this was not statistically significant (**Figure 4.1F**). However, CD48^{-/-} mice had moderately reduced peak disease score compared to WT B6 mice by day 16 after immunization, which was statistically significant (**Figure 4.1G**). This suggests that CD48 deficiency provides a degree of protection in this model of induced autoimmunity.

CD48^{-/-} mice have a reduced proportion of GM-CSF+ T cells in the CNS during EAE

To investigate a cellular mechanism for attenuated EAE severity in CD48^{-/-} mice, we examined CNS-infiltrating lymphocytes near the peak of EAE disease in WT and CD48^{-/-} mice. A representative experiment is shown in **Figure 4.2**. On day 17 after immunization, the median disease score for CD48^{-/-} mice was less than that of WT mice, but this was not statistically significant in this experiment (**Figure 4.2B**). We isolated lymphocytes from the spleen, inguinal lymph node (iLN, which drains the immunization site) and CNS of these mice, and examined the number of CD4⁺ T cells by flow cytometry. The number of CD4⁺ T cells in the CNS of CD48^{-/-} mice was less than that in WT mice, but this was not statistically significant (**Figure 4.2C**). In contrast, the number of CD4⁺ T cells in the iLN of CD48^{-/-} mice was significantly greater than that in WT mice (**Figure 4.2D**).

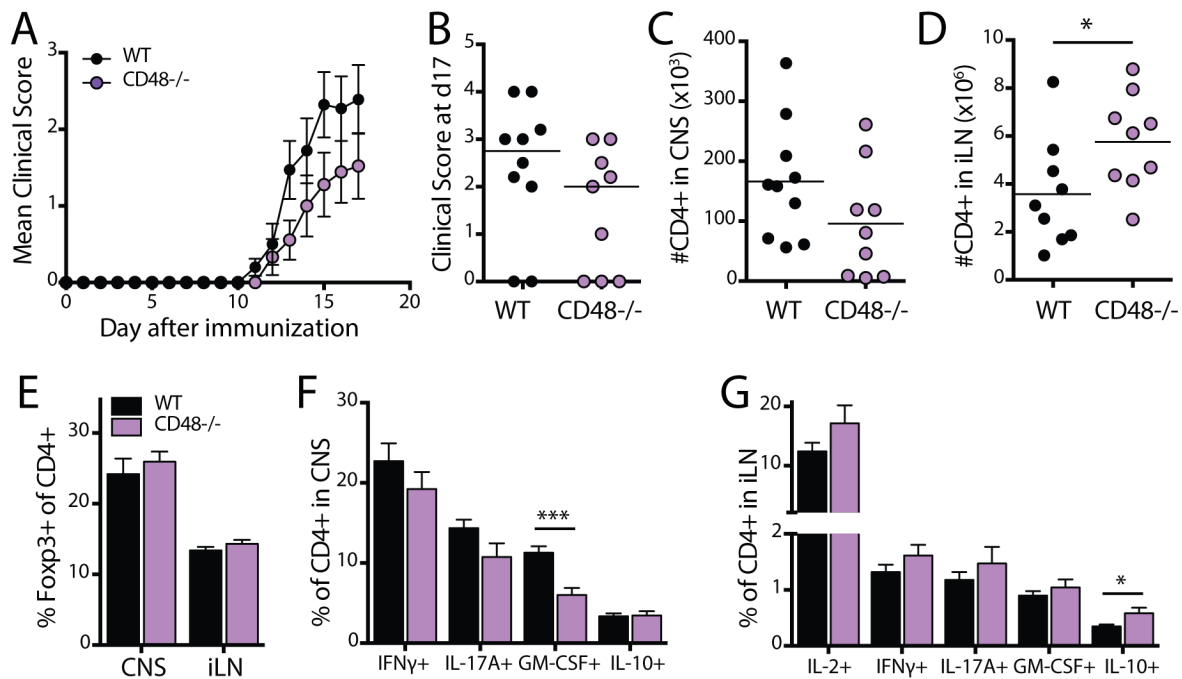


Figure 4.2 CD48^{-/-} mice have a reduced proportion of GM-CSF⁺ T cells in the CNS during EAE

WT B6 and CD48^{-/-} mice aged 8-12 weeks were immunized s.c. with 50 μ g MOG[35-55] emulsified in 100 μ l of MTb fortified CFA (400 μ g MTb), and given 100ng pertussis toxin i.p. on days 0 and 2. Mice were monitored daily for clinical disease. A. Mean clinical scores, \pm SEM. B. Clinical scores at the endpoint of the experiment. C. Number of CD4⁺ T cells isolated from the CNS of each mouse. D. Number of CD4⁺ T cells isolated from the iLNs of each mouse. E. Proportion of CD4⁺ T cells in CNS and iLN that are Foxp3⁺, as assessed by intracellular staining. F-G. Lymphocytes from CNS and iLN were restimulated for 4 hours at 37C with PMA and ionomycin in the presence of GolgiStop. Cells were then stained and fixed for flow cytometric analysis of intracellular cytokines. Percentage of CD4⁺ T cells that stain for each cytokine are shown for the CNS (F) and iLN (G). Representative of two independent experiments, with 8-10 mice per group. Bars represent means, error bars represent SEM. Significance calculated using Student's t test. *p<0.05, **p<0.01, ***p<0.001, ****p<0.0001

We hypothesized that the moderate but statistically significant attenuation of EAE in CD48^{-/-} mice might be due to altered proportions of pathogenic and regulatory cells among CD4⁺ T cells in the CNS or iLN. Foxp3⁺ Tregs in the CNS are associated with resolution of disease (McGeachy, Stephens, and Anderton 2005), while production of IFN γ , IL-17 and GM-CSF are associated with disease progression (Robinson et al. 2014). To test this, we first examined the proportion of Foxp3⁺ Tregs using intracellular Foxp3 staining and flow cytometry. As shown in **Figure 4.2E**, there was no difference in the proportion of Foxp3⁺ cells among CD4⁺ cells in the CNS or iLN. Next, we examined the proportion of cytokine-producing cells, using intracellular cytokine staining after restimulation with PMA and ionomycin. We found that CD48^{-/-} mice had a significantly lower percentage of GM-CSF⁺ cells among CD4⁺ T cells in the CNS, but no differences in the proportion of IFN γ ⁺, IL-17A⁺ or IL-10⁺ among CD4⁺ T cells in the CNS (**Figure 4.2F**). We did not observe any significant differences in intracellular cytokine expression of IL-2, IFN γ , IL-17A or GM-CSF in CD4⁺ T cells in the iLN, although there was a modest but significant increase in the percentage of IL-10⁺ CD4⁺ T cells (**Figure 4.2G**). Together, these data suggest that CD48^{-/-} mice have a slight deficit in GM-CSF production in the CNS during EAE.

CD48^{-/-} and WT mice have similar CD4⁺ T cell numbers and activation states at an early time point in EAE

We hypothesized that differences in CD4⁺ T cell activation, entry, accumulation or survival in the CNS might be more apparent at earlier time points during EAE in CD48^{-/-} mice. To address this possibility, we examined lymphocytes from the CNS and iLN of WT and CD48^{-/-} mice on day 12 after immunization for EAE, around the time of disease onset. As shown in **Figure 4.3A**, both WT and CD48^{-/-} mice were beginning to show clinical signs of disease by day 12. The incidence of disease was identical in WT and CD48^{-/-} mice at this time (70% for each), and there was no significant difference in the median clinical score at this time (**Figure 4.3B**). When we examined the CD4⁺ T cells in the CNS, we again saw trend towards fewer CD4⁺ T cells in the CNS, but this was not statistically significant (**Figure 4.3C**). There was no significant difference in the proportion of CD4⁺ T cells from the CNS that stained for intracellular IFN γ , IL-17A or GM-CSF after restimulation with PMA and ionomycin (**Figure 4.3D**), nor was there a difference in the percentage of Foxp3⁺ CD4⁺ T cells in the CNS (**Figure 4.3E**). Restimulation of CNS cells with 100 μ g/mL of MOG[35-55] peptide for three days also

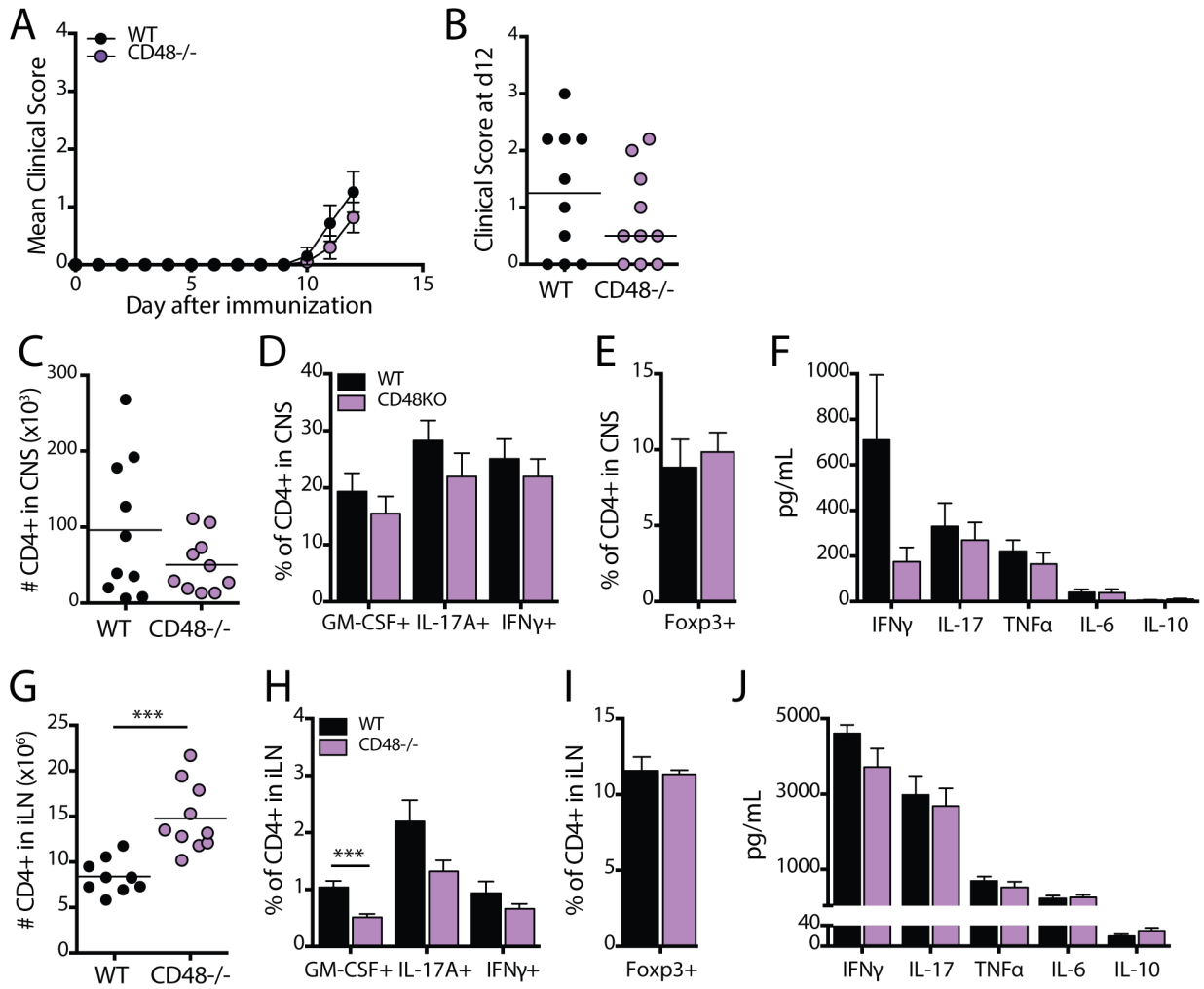


Figure 4.3 WT and CD48^{-/-} mice have similar CD4⁺ T cell infiltrates in the CNS near the onset of EAE. WT B6 and CD48^{-/-} mice (8-12 weeks old) were immunized s.c. with 50 μ g MOG[35-55] emulsified in 100 μ l of MTb fortified CFA (4004g MTb) to induce EAE, and given 100ng pertussis toxin i.p. on days 0 and 2. Mice were monitored daily for clinical disease score. A. Mean clinical scores, \pm SEM. B. Clinical scores at the termination of the experiment. C. Number of CD4⁺ T cells isolated from the CNS of each mouse. D. Intracellular cytokine expressing T cells in the CNS, after restimulation with PMA and ionomycin in the presence of GolgiStop. E. Percentage of Foxp3⁺ of CD4⁺ in CNS. F. Antigen specific cytokine secretion by CNS lymphocytes after restimulation with MOG peptide for 3 days. G. Number of CD4⁺ T cells isolated from the iLN of each mouse in A. H. Intracellular cytokine expressing T cells in the iLN after restimulation with PMA and ionomycin in the presence of GolgiStop. I. Percentage of Foxp3⁺ of CD4⁺ in iLN. J. Antigen-specific cytokine secretion by iLN lymphocytes after restimulation with MOG peptide for 3 days. N=10 mice per group. Bars represent means, error bars represent SEM. Significance calculated using Mann Whitney test (A-B) or Student's t test (C-J). ***p<0.001.

revealed no significant difference in the amount of IFN γ , IL-17, TNF α , IL-6 or IL-10 secreted in response to antigen (**Figure 4.3F**).

To assess the ongoing priming of CD4 $^{+}$ T cells in the periphery, we also examined cells from the iLN at this time point. CD48 $^{-/-}$ mice had significantly increased cellularity in the iLN (30×10^6 in WT, 45.5×10^6 in KO, $p < 0.01$, data not shown), and significantly increased numbers of CD4 $^{+}$ T cells (**Figure 4.3G**). There was no significant difference in production of IFN γ or IL-17 as measured by intracellular cytokine staining after restimulation of iLN cells with PMA and ionomycin. However, there was a lower percentage of GM-CSF $^{+}$ CD4 $^{+}$ T cells in CD48 $^{-/-}$ mice (**Figure 4.3H**). There was no difference in the percentage of Foxp3 $^{+}$ CD4 $^{+}$ T cells in the iLN (**Figure 4.3I**). There was no significant difference in the secretion of IFN γ , IL-17, TNF α , IL-6 or IL-10 after restimulation with MOG peptide for 3 days (**Figure 4.3J**). Together these data indicate that at an early time point in EAE, CD48 $^{-/-}$ mice had similar numbers of CD4 $^{+}$ T cells in the CNS and no differences in cytokine production in the CNS. However, the number of CD4 $^{+}$ T cells in the iLN was increased, while the %GM-CSF $^{+}$ of CD4 $^{+}$ T cells was decreased.

CD48 $^{-/-}$ and WT mice have similar CD4 $^{+}$ T cell activation on day 7 after MOG immunization

We next investigated whether the reduced proportion of GM-CSF $^{+}$ CD4 $^{+}$ T cells in CD48 $^{-/-}$ CNS at the peak of disease was due to a defect in CD4 $^{+}$ T cell priming earlier after immunization. To test this, we immunized WT and CD48 $^{-/-}$ mice with MOG/CFA, and examined CD4 $^{+}$ T cells from the iLN seven days later. WT and CD48 $^{-/-}$ mice had similar numbers of CD4 $^{+}$ T cells in the iLN (**Figure 4.4A**), but an increased number of CD4 $^{+}$ T cells in the spleen (**Figure 4.4B**). When we stained for intracellular Foxp3, we found no significant difference in the proportion of Foxp3 $^{+}$ Tregs among CD4 $^{+}$ T cells in the iLN or spleen (**Figures 4.4C-D**). To assess cytokine production by CD4 $^{+}$ T cells, we restimulated iLN and spleen with PMA and ionomycin, and then stained for intracellular cytokine production. As shown in **Figure 4.4E**, there was no difference in the %GM-CSF $^{+}$ in the iLN, but CD48 $^{-/-}$ mice had a significantly decreased percentages of IL-17A $^{+}$ and IFN γ $^{+}$ CD4 $^{+}$ T cells. In the spleen, production of GM-CSF, IL-17A and IFN γ was extremely low, but the percentage of GM-CSF $^{+}$ CD4 $^{+}$ T cells was significantly lower in CD48 $^{-/-}$ mice (**Figure 4.4F**). To assess antigen-specific cytokine production, we restimulated iLN with 100 μ g/mL MOG peptide for 3 days; we observed no significant

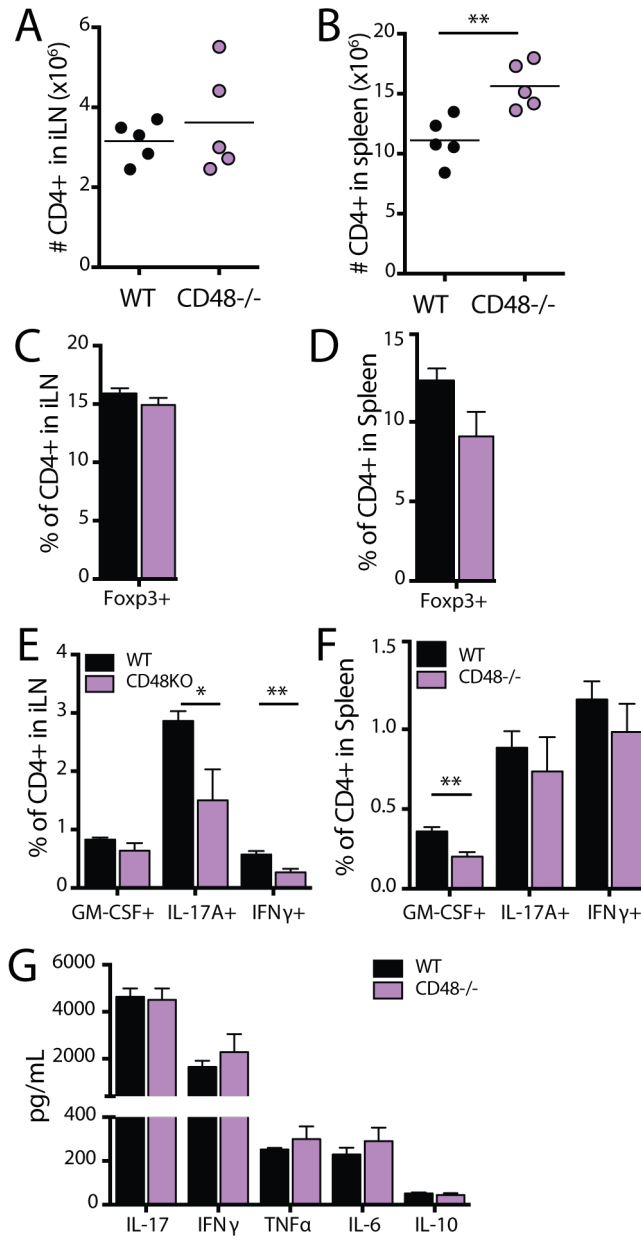


Figure 4.4 WT and CD48^{-/-} mice have similar CD4⁺ T cell activation on day 7 after MOG immunization.

WT and CD48^{-/-} mice (8-12 weeks old) were immunized s.c. with 50µg MOG[35-55] emulsified in 100µl of MTb fortified CFA (400µg MTb). Spleen and iLN were collected for analysis seven days later. A-B. Number of CD4⁺ T cells in A. iLN and B. Spleen. C-D. Intracellular cytokine production by CD4⁺ T cells, after restimulation with PMA and ionomycin in the presence of GolgiStop, in the C. iLN and D. Spleen. E-F. Proportion of Foxp3⁺ CD4⁺ T cells in the E. iLN and F. Spleen. G. Antigen-specific cytokine secretion by iLN lymphocytes after restimulation with MOG peptide for 3 days. A-F, n=5 mice per group, representative of 3 independent experiments with 4-5 mice per group. G, n= 5 mice per group, representative of 2 independent experiments with 5 mice per group. Lines on dot plots indicate mean. Bars represent means, error bars represent SEM. Significance calculated using Student's t test. *p<0.05, **p<0.01.

differences in the amount of cytokines secreted by WT or CD48^{-/-} lymphocytes (**Figure 4.4G**). These data suggest that CD48^{-/-} mice might have a slight defect in CD4⁺ T cell cytokine production by day seven after immunization, but no dramatic defect in CD4⁺ T cell priming.

Rag^{-/-} and CD48^{-/-} Rag^{-/-} mice are susceptible to EAE mediated by WT 2D2 CD4⁺ T cells

Because CD48 is widely expressed on hematopoietic cells, we considered the possibility that the absence of CD48 on different cell populations could lead to opposing phenotypes that cancelled each other out in the CD48^{-/-} mice. During our characterization of the phenotype of naïve CD48^{-/-} mice, our lab had observed that CD48^{-/-} APCs have a reduced capacity to stimulate the initial activation of naïve CD4⁺ T cells compared to WT APCs (Dr. Dan Brown, unpublished data). To evaluate the role of host cells other than lymphocytes in regulating EAE induced by WT CD4⁺ T cells, we used Rag^{-/-} and CD48^{-/-} Rag^{-/-} mice as adoptive transfer recipients. We sorted CD4⁺ T cells from 2D2 TCR Tg mice using flow cytometry and adoptively transferred these into Rag^{-/-} and CD48^{-/-} Rag^{-/-} recipients, waited two weeks for homeostatic proliferation, then immunized with MOG/CFA to induce EAE. As shown in **Figure 4.5A**, the course of disease was not significantly different for recipients of WT or CD48^{-/-} 2D2 CD4⁺ T cells. There was a slight delay in onset of EAE, but this was not statistically significant (**Figure 4.5B**). There was no difference in the incidence of disease (all mice developed EAE), and there was no significant difference in the severity of disease as assessed by the peak disease score reached by each animal (**Figure 4.5C**). This suggests that CD48 on APCs is not critical for development of EAE in this model.

CD48^{-/-} mice have attenuated EAE induced by adoptive transfer of TH1-polarized 2D2 CD4⁺ T cells

Adoptive transfer of primed, MOG-specific CD4⁺ Teff into recipient mice provides a method to specifically examine the effector phase of disease, while controlling the conditions of activation. We generated TH1-polarized Teff using CD4⁺ T cells from 2D2 mice, which have a transgenic TCR specific for MOG[35-55] in the context of IA^b MHCII molecules (Bettelli et al. 2003). By generating WT 2D2 TH1-polarized Teff in vitro, we could ensure that the priming phase is identical for all recipients, and then evaluate the role of CD48 expressed on the APC during the effector phase in CD48^{-/-} recipients.

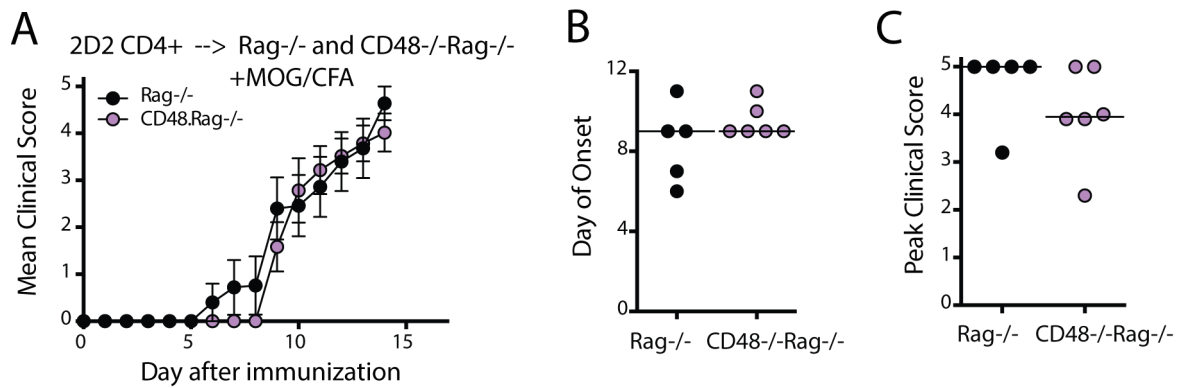


Figure 4.5 Rag-/- and CD48-/- Rag-/- mice are susceptible to EAE mediated by WT 2D2 CD4+ T cells. CD4+ T cells from 2D2 TCR Tg mice were purified by FACS and transferred i.v. to Rag-/- and CD48-/-Rag-/- recipients. Two weeks later, mice were immunized s.c. with 50 μ g MOG[35-55] emulsified in 100 μ l of MTb fortified CFA (400 μ g MTb) to induce EAE. 100ng of pertussis toxin was given i.p. on day 0 only. Mice were monitored daily for clinical disease. A. Mean clinical scores, \pm SEM. B. Day of onset of disease. C. Peak clinical score by day 15. N=4-5 mice per group, representative of 4 independent experiments with 1-6 mice per group. Lines on dot plots represent mean (B), or median (C). Statistical significance calculated using Mann-Whitney test (A, C) or Student's t test (B). *p<0.05, **p<0.01, ***p<0.001, ****p<0.0001.

First we compared the capacity of WT and CD48^{-/-} APCs to stimulate TH1-polarized 2D2 CD4⁺ T cells in vitro. 2D2 CD4⁺ T cells were cultured in vitro under TH1 polarizing conditions for 6 days. Live cells were collected and labeled with CFSE, then cultured with MOG peptide and either TCR α ^{-/-} or CD48^{-/-} TCR α ^{-/-} splenocytes for 3 days. Cell division was assessed by CFSE dilution. As shown in **Figure 4.6A**, 2D2 CD4⁺ TH1 cells divided less with CD48^{-/-} APCs than with WT APCs. This suggests that CD48 on the APC contributes to proliferation of previously activated Teff.

Based on this result, we hypothesized that CD48^{-/-} mice would have attenuated EAE induced by transfer of WT 2D2 TH1 CD4⁺ T cells, compared to WT recipients. To test this, we again cultured 2D2 CD4⁺ T cells in vitro under TH1-polarizing conditions for 6 days, then collected live cells and restimulated them for 24 hours on anti-CD3/anti-CD28-coated plates to generate Teff. These reactivated cells were then transferred into WT and CD48^{-/-} mice, and we compared the course of disease. As shown in **Figure 4.6B**, CD48^{-/-} mice had attenuated EAE compared to WT mice. There was a slight delay in onset of disease, but this was not statistically significant (**Figure 4.6C**), while the peak clinical score was significantly lower for CD48^{-/-} than for WT recipients (**Figure 4.6D**).

We hypothesized that reduced severity of EAE in CD48^{-/-} mice following transfer of TH1 polarized 2D2 cells could be due to reduced accumulation of 2D2 cells in the CNS—potentially due to altered migration, survival or proliferation in the CNS. The number of 2D2 cells in the CNS of CD48^{-/-} mice was slightly reduced compared to WT mice at day 16 post transfer, but this was not statistically significant (**Figure 4.6E**). We next compared the proportion of 2D2 cells in the CNS and spleen that produced IFN γ , GM-CSF, IL-17A and IL-10 after restimulation ex vivo with PMA and ionomycin, but did not observe any differences (**Figure 4.6F-G**).

We considered that differences in EAE severity as induced by the 2D2 cells could be amplified by altered recruitment of regulatory or pathogenic host CD4⁺ T cells in WT versus CD48^{-/-} recipients. However, we did not see a decrease in the number of host CD4⁺ T cells recovered from the CNS (data not shown), or the proportion of these that were IFN γ ⁺ or GM-CSF⁺; in fact, the percentage of host CD4⁺ IL-17A⁺ was slightly

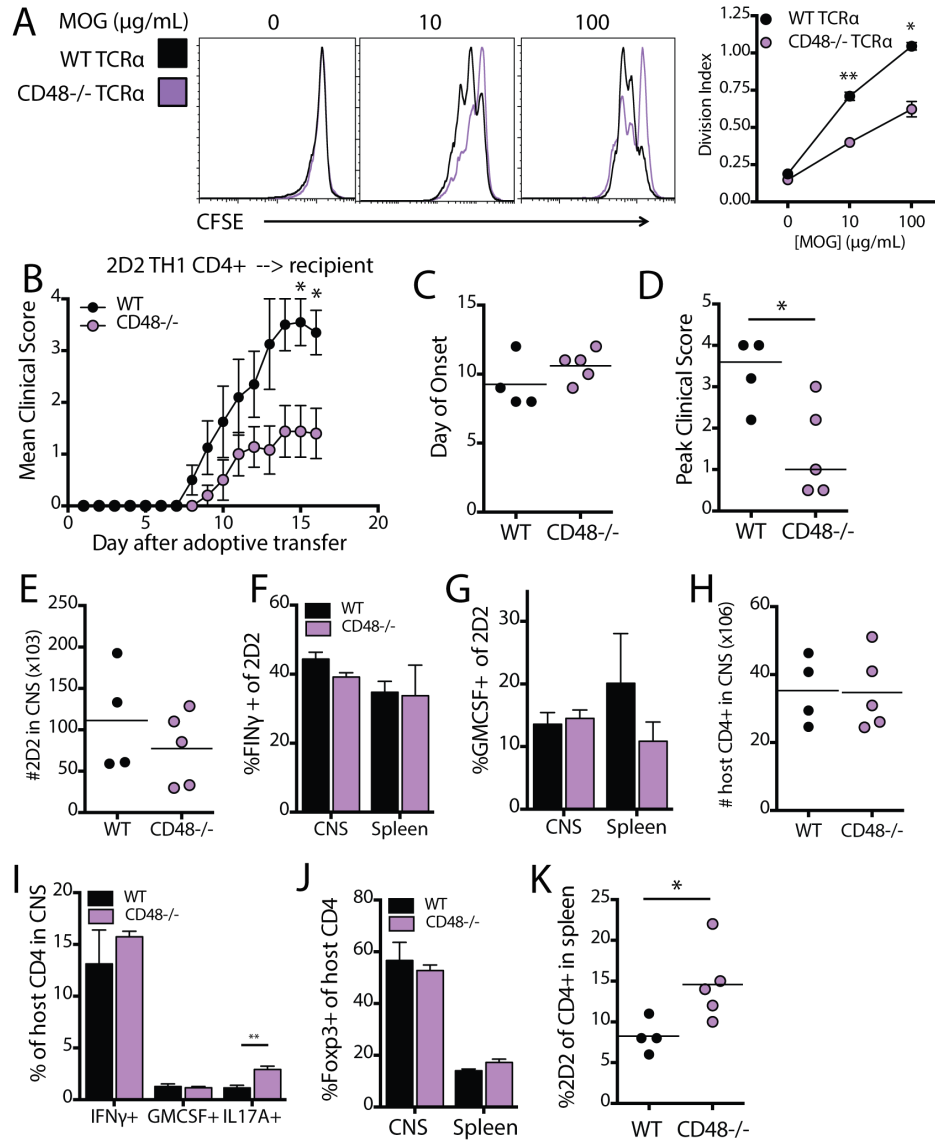


Figure 4.6 CD48 $^{-/-}$ mice have attenuated EAE induced with TH1-polarized 2D2 TCR Tg CD4 $^{+}$ T cells. CD4 $^{+}$ T cells were MACS purified from Thy1.1 congenic 2D2 TCR Tg mice, and cultured in vitro with IL-12, anti-IL4, anti-CD3 and irradiated WT splenocytes to generate TH1-polarized 2D2 CD4 $^{+}$ T cells. A. On day 6 of culture, live cells were collected with lymphocyte separation media, labeled with CFSE, and restimulated in vitro for 3 days with WT or CD48 $^{-/-}$ TCR α $^{-/-}$ splenocytes plus MOG peptide (0, 10 or 100 $\mu\text{g/mL}$). CFSE dilution was assessed by flow cytometry and division index was calculated with FlowJo. B-H. TH1-polarized cells were restimulated on anti-CD3/anti-CD28-coated plates for 24hrs, then transferred to WT and CD48 $^{-/-}$ recipients. B. Mean clinical scores, \pm SEM. C. Day of onset of EAE. D. Clinical scores at experiment endpoint. E. Number of 2D2 CD4 $^{+}$ T cells in the CNS. F-G, CNS and spleen lymphocytes were restimulated with PMA and ionomycin in the presence of GolgiStop, then stained and fixed for detection of intracellular cytokines in 2D2 CD4 $^{+}$ T cells. F. %IFN γ +. G. %GM-CSF+. H. Number of host CD4 $^{+}$ T cells in CNS. I. Proportion of host CD4 $^{+}$ T cells expressing each indicated cytokine after restimulation with PMA and ionomycin in the presence of GolgiStop. J. Proportion of Foxp3 $^{+}$ host CD4 $^{+}$ T cells in CNS and spleen. K. Proportion of 2D2 CD4 $^{+}$ T cells among total CD4 $^{+}$ T cells in the spleen. Representative experiment with n=4-5 mice per group, representative of 3 independent experiments with 4-5 mice per group. Lines on dot plots represent mean (C, E, H, K) or median (D). Bars represent mean, error bars represent SEM. * $p < 0.05$, ** $p < 0.01$, *** $p < 0.001$, **** $p < 0.0001$. Statistical significance calculated using Mann Whitney test (B, D) or Student's t test (C, E-K).

increased in CD48^{-/-} recipients (**Figure 4.6H**). There was no significant difference in the proportion of host CD4⁺ T cells in the spleen or CNS that were Foxp3⁺ (**Figure 4.6I**).

Although we did not obtain absolute cell counts in the spleen, CD48^{-/-} mice had an increased proportion of 2D2 cells in the spleen compared to WT mice (**Figure 4.6J**). Collectively, these data suggest that CD48^{-/-} mice may have a reduced ability to support the activation or pathogenicity of previously activated WT CD4⁺ T cells, although we did not examine these directly.

CD48^{-/-} CD4⁺ T cells are readily detectable in the CNS and lymphoid organs during EAE in mice with mixed WT and CD48^{-/-} CD4⁺ T cells

We next investigated whether the attenuated EAE in CD48^{-/-} mice was due to a defect in CD48^{-/-} CD4⁺ T cells. To test this hypothesis, we isolated CD4⁺ T cells from congenic Thy1.1 WT and Thy1.1/1.2 CD48^{-/-} 2D2 TCR Tg mice, mixed them at a ~1:1 ratio, and adoptively transferred these into Rag^{-/-} recipients. After allowing two weeks for homeostatic proliferation, mice were immunized with MOG/CFA to induce EAE and monitored for disease (**Figure 4.7A**). Near the peak of disease, lymphocytes from the CNS, spleen and blood were collected for analysis (lymph nodes in Rag^{-/-} recipients had very few cells). As shown in **Figure 4.7B**, we found that WT CD4⁺ T cells were more abundant than CD48^{-/-} CD4⁺ T cells in all compartments examined (~70% WT, 30% CD48^{-/-}), but there was no significant difference in the %WT of total CD4⁺ T cells in the CNS compared to the blood or spleen. There was no significant difference in activation between WT and CD48^{-/-} CD4⁺ T cells, as measured by Ki67 expression (**Figure 4.7C**), expression of the CNS-homing molecule VLA-4 (**Figure 4.7D**), or production of the effector cytokines IFN γ or GM-CSF after restimulation with PMA and ionomycin (**Figure 4.7E-F**). We concluded that in a WT host, CD48^{-/-} CD4⁺ T cells are capable of contributing to EAE, and do not display a defect in proliferation, cytokine production or expression of CNS-homing molecules by our measurements.

As an alternative approach to compare WT and CD48^{-/-} CD4⁺ T cells in the same host, we generated mixed bone marrow chimeras using congenically marked WT and CD48^{-/-} bone marrow transplanted into lethally irradiated WT recipients. After waiting two months for reconstitution of the immune system, we immunized

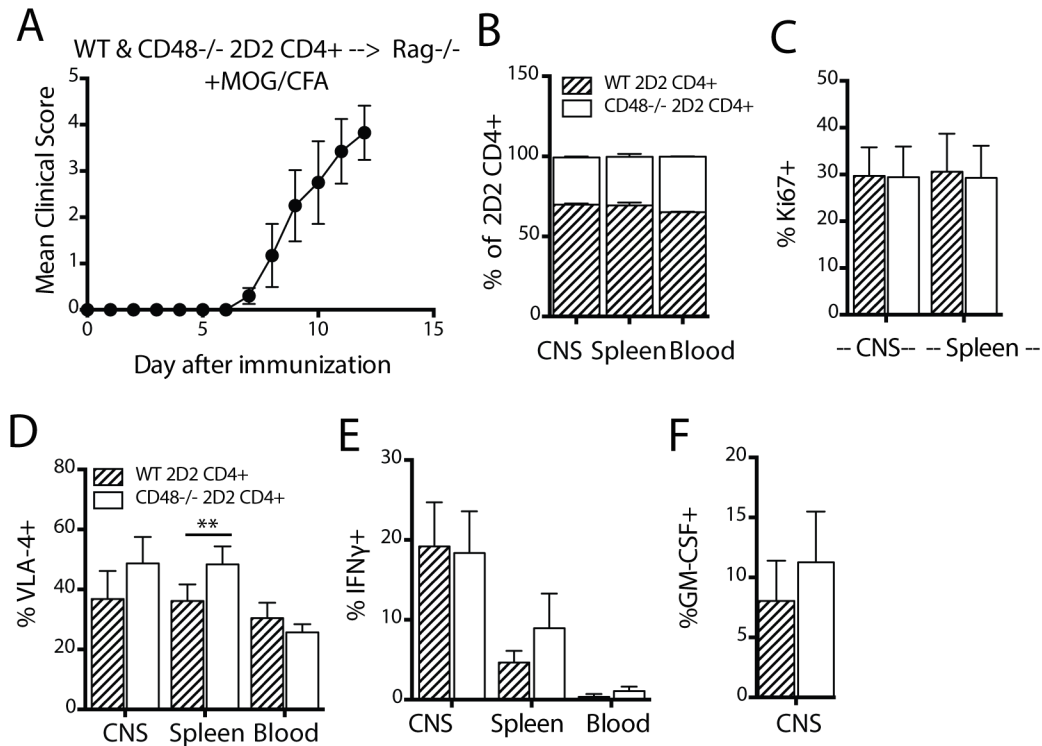


Figure 4.7. CD48^{-/-} T cells are readily detectable in the CNS and lymphoid organs during EAE in Rag^{-/-} mice reconstituted with a mix of WT and CD48^{-/-} 2D2 CD4⁺ T cells. CD4⁺ T cells were isolated from Thy1.1 congenic 2D2 TCR Tg mice and Thy1.1/1.2 CD48^{-/-} 2D2 TCR Tg mice, mixed at 1:1 ratio and transferred into Rag^{-/-} recipients. Two weeks later, mice were immunized s.c. with 50 μ g MOG[35-55] emulsified in 100 μ l of MTb fortified CFA (400 μ g MTb) to induce EAE. 100ng of pertussis toxin was given i.p. on d0 only. Mice were monitored daily for clinical disease. **A.** Mean clinical scores, \pm SEM. N=4 mice. **B.** Proportion of WT and CD48^{-/-} cells among CD4⁺ T cells in the CNS, spleen and blood. **C.** Proportion of Ki67⁺ cells among WT CD4⁺ or CD48^{-/-} CD4⁺ T cells, in the CNS and spleen. **D.** Proportion of VLA-4⁺ cells among WT CD4⁺ or CD48^{-/-} CD4⁺ T cells in the CNS, spleen and blood ex vivo. **E-F** Lymphocytes from CNS, spleen and blood were restimulated in vitro with PMA and ionomycin in the presence of GolgiStop for 4hrs at 37C, then stained and fixed for detection of intracellular IFN γ (**E**) or GM-CSF (**F**) by flow cytometry. N=4 mice, representative of 3 independent experiments with 3-4 mice per experiment. Bars represent means, error bars represent SEM. Statistical significance calculated using ANOVA (**B**) or paired t tests (**C-F**).

mice with MOG/CFA to induce EAE (**Figure 4.8A**) and then compared WT and CD48^{-/-} CD4⁺ T cells in various compartments at the peak of disease. As shown in **Figure 4.8**, CD48^{-/-} cells were more highly represented than WT among donor CD4⁺ T cells, and this was similar in all organs examined (**Figure 4.8B-C**). We looked for differences in pathogenic and regulatory cells by examining the proportion of IFN γ ⁺, IL-17A⁺ and Foxp3⁺ CD4⁺ T cells in the CNS and spleen. There were no significant differences in the percentage of IFN γ ⁺ or IL-17A⁺ CD4⁺ T cells in the CNS or spleen (**Figure 4.8D-E**). We did not observe any significant differences in the percentage of Foxp3⁺ CD4⁺ T cells in the CNS, but a lower percentage of CD48^{-/-} CD4⁺ T cells in the spleen were Foxp3⁺, compared to the %Foxp3⁺ of WTCD4⁺ T cells (**Figure 4.8F-G**). Collectively, these data indicate that CD48^{-/-} CD4⁺ T cells are capable of contributing to EAE in a WT host, and are not underrepresented among CD4⁺ T cells in the CNS compared to other lymphoid organs.

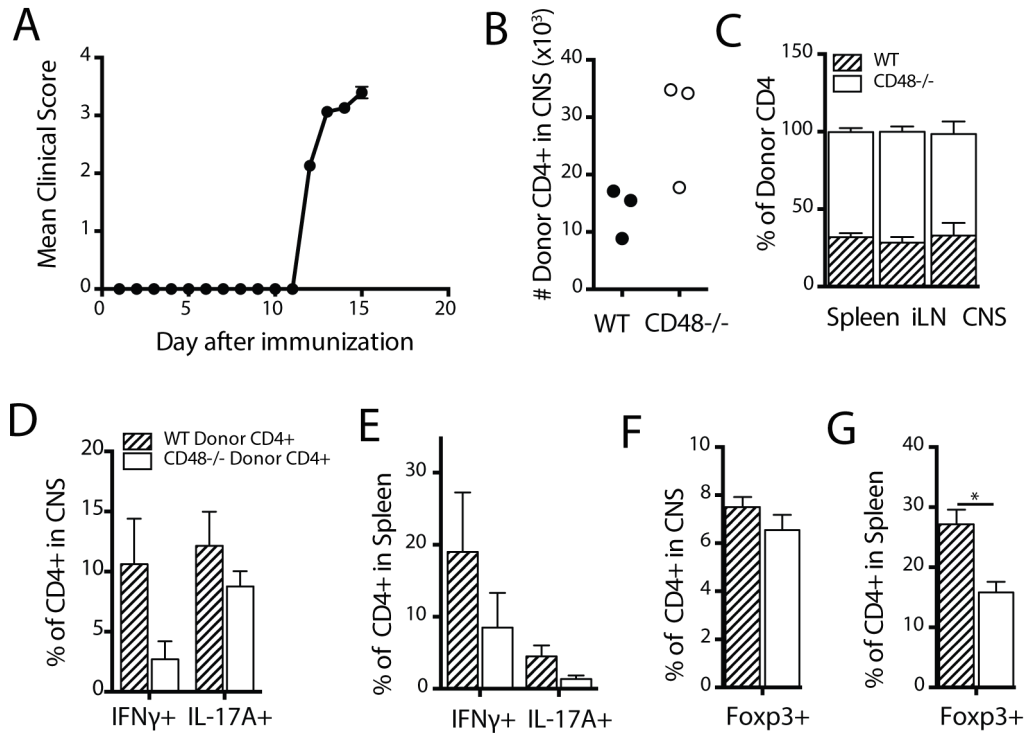


Figure 4.8. CD48^{-/-} CD4⁺ T cells are readily detectable in the CNS and lymphoid organs during EAE in mixed bone marrow chimeras. Bone marrow was isolated from Thy1.1/1.2 congenic WT mice and Thy1.1 congenic CD48^{-/-} mice, mixed at a 1:1 ratio and adoptively transferred into Thy1.2 congenic, lethally irradiated WT recipients. Two months later, mice were immunized s.c. with 50 μ g MOG[35-55] emulsified in 100 μ l of MTb fortified CFA (400 μ g MTb) to induce EAE, and given 100ng of pertussis toxin i.p. on d0 and d2. Mice were monitored daily for clinical disease. **A.** Mean clinical scores, \pm SEM. N=3 mice. **B.** Number of WT and CD48^{-/-} CD4⁺ T cells in the CNS of each mouse in **A.** Mean 13.81 $\times 10^3$ WT, 28.9 $\times 10^3$ CD48^{-/-}. **C.** Proportion of WT and CD48^{-/-} cells among CD4⁺ T cells in the spleen, iLN and CNS. **D-E.** CNS and spleen were restimulated in vitro with PMA and ionomycin in the presence of GolgiStop for 4hrs at 37C, then stained and fixed for detection of intracellular cytokines by flow cytometry. Proportion of cytokine⁺ cells among WT CD4⁺ or CD48^{-/-} CD4⁺ T cells are shown for CNS (**D**), Spleen, (**E**). **F-G.** Percentage of WT and CD48^{-/-} cells in the CNS (**F**) and spleen (**G**) that stain for intracellular Foxp3. Data are mean \pm SEM. Representative of two independent experiments with 3 mice each. Statistical significance calculated using paired t tests. *p<0.05

DISCUSSION

The goal of these studies was to investigate the role of CD48 in regulating T cell-mediated autoimmunity, by investigating how CD48 deficiency affects the pathogenesis of EAE. These studies were motivated by a number of independent factors. First, our studies of the CD48^{-/-} [B6.129] and CD48^{-/-} [B6] strains suggested a role for CD48 in lymphocyte development, homeostasis and activation, but did not demonstrate a role for CD48 in development of spontaneous humoral autoimmunity. We were interested in evaluating the role of CD48 in other autoimmune contexts, besides lupus. Second, the initial characterizations of the CD48^{-/-} [B6.129] and CD48^{-/-} [Balb/c.129] strains suggested a role for CD48 in T cell activation and proliferation *in vitro*, from both the T cell and APC sides (Gonzalez-Cabrero et al. 1999; Abadia-Molina et al. 2006; Keszei et al. 2011). *In vitro* studies with anti-CD48 antibodies also supported a role for CD48 in T:APC interactions, as did studies of human cell lines (Kato et al. 1992; Milstein et al. 2008; Muhammad et al. 2009). Third, a homologue of CD48 that exists in humans but not in mice, CD58, was found to be linked to susceptibility to multiple sclerosis, and initial functional studies suggested a role for CD58 on Tregs during autoimmune disease (De Jager et al. 2009). Fourth, costimulatory and adhesion molecules have been extensively studied in EAE, for their varied roles in priming, differentiation, and trafficking of effector cells. However, no prior studies have examined the role of CD48 in EAE, despite its demonstrated role in T cell adhesion and activation. Thus, we were interested in investigating the role of CD48 in EAE, particularly with regard to its contribution to T cell activation and its roles on the T cell and the APC.

To this end, we used the CD48^{-/-} [B6] strain, combined with EAE adoptive transfer models, to evaluate the role of CD48 in development of an induced, CD4⁺ T cell-mediated autoimmune disease. We approached this in three ways: 1) by examining cytokine production and T cell activation at various time points after immunization of WT and CD48^{-/-} mice with MOG[35-55] emulsified in CFA, both prior to and during clinical disease; 2) by evaluating the contribution of CD48 in the host using adoptive transfer of WT CD4⁺ T cells into CD48^{-/-} recipients; and 3) by examining the contribution of CD48 on CD4⁺ T cells during EAE in mice with a mix of WT and CD48^{-/-} CD4⁺ T cells.

We found that CD48^{-/-} [B6] mice had attenuated EAE, particularly during the resolution phase of disease, which was modest but statistically significant. At the peak of disease, fewer CD4⁺ T cells in the CNS of CD48^{-/-} mice produced GM-CSF than did CD4⁺ T cells in WT mice. Although we did not observe striking differences in T cell priming or cytokine production at early time points after immunization (pre-clinical or near disease onset), we did find that CD48^{-/-} mice were dramatically protected in an adoptive transfer model of EAE using WT Th1-primed 2D2 CD4⁺ T cells, when compared to WT recipients. In contrast, CD48^{-/-} CD4⁺ T cells behaved very much like WT CD4⁺ T cells during EAE, when the two populations were mixed in vivo in WT hosts. Our results suggest that CD48 may play a role in T cell activation and pathogenicity during EAE, particularly during the effector phase of disease, which is likely mediated by CD48 expression on APCs, B cells, CD8⁺ T cells or Tregs.

In our first approach, we examined how CD48 deficiency affected susceptibility to and severity of EAE, by comparing the course of EAE in WT and CD48^{-/-} mice immunized with MOG/CFA. Preliminary experiments in CD48^{-/-} [B6.129] mice indicated that CD48 deficiency might result in protection in EAE, particularly during the resolution phase of disease. In CD48^{-/-} [B6.129] mice reconstituted with a CD48-containing BAC transgene, this protection was lost, supporting a role for CD48 in mediating the severity of EAE. When we replicated these experiments in CD48^{-/-} [B6] mice, disease severity was again slightly attenuated, but this did not always reach statistical significance. In some experiments the day of onset and peak disease were identical, while in other experiments we observed a slight delay or reduced peak disease score in CD48^{-/-} [B6] mice. However, we never observed CD48^{-/-} [B6] mice to develop a more severe disease than WT mice; these observations suggest that there is a modest but significant protection from EAE in CD48^{-/-} mice.

This protection from EAE would not have been predicted by the increased B and T cell activation seen in naïve CD48^{-/-} mice, but it is consistent with the reduced T cell proliferation observed with CD48^{-/-} [B6.129] and CD48^{-/-} [Balb/c.129] T cells and APCs (Gonzalez-Cabrero et al. 1999; Keszei et al. 2011). We first looked for a cellular mechanism for this protection, by examining lymphocytes in the CNS and periphery of mice at the peak of disease. The only significant differences we consistently observed were increased numbers of CD4⁺ T cells in the iLN, and decreased numbers of GM-CSF⁺ CD4⁺ T cells in the CNS of CD48^{-/-} mice. Increased

numbers of iLN CD4⁺ T cells were present before the peak of disease, as well, suggesting that progression of CD4⁺ T cells from the iLN to the CNS might be delayed in CD48^{-/-} mice. We also saw a decrease in the %GM-CSF⁺ of CD4⁺ T cells in the iLN at day 12, suggesting that development of pathogenic CD4⁺ T cells might be reduced or delayed in the periphery, even prior to entry in the CNS. At an even earlier time point, on day 7 after immunization, we saw an increase in spleen cellularity but a decrease in the %GM-CSF⁺ CD4⁺ T cells in the spleen, while the iLN had no difference in the number of CD4⁺ T cells but a decrease in the %IFN γ and %IL-17A⁺ CD4⁺ T cells. The percentage of cytokine-producing CD4⁺ T cells in the periphery was quite low at day 7, making it difficult to ascertain whether a statistically significant, 50% reduction in cytokine-producing cells from 3% to 1.5% is biologically relevant. When we restimulated cells with MOG[35-55] and measured secreted cytokines, we did not observe any significant differences between WT and CD48^{-/-} mice at any time point. However, GM-CSF was not included in the analysis of secreted cytokines.

Collectively, our data suggest that decreased severity of EAE in CD48^{-/-} mice is due to a delay in entry of CD4⁺ Teff into the CNS, and/or reduced pathogenicity and recruitment due to decreased GM-CSF production. GM-CSF is a critical effector cytokine in EAE, allowing CD4⁺ Teff to activate monocytes in the CNS, which then secrete IL-23 to stabilize Th17 cells, thus creating a positive feedback loop that promotes neuroinflammation (El-Behi et al. 2011). Antibody blockade of GM-CSF in vivo during EAE attenuates disease (El-Behi et al. 2011), so it is possible that the reduction in GM-CSF⁺CD4⁺ T cells in the CNS of CD48^{-/-} mice is sufficient to result in attenuated disease.

Additional studies are needed to identify a molecular mechanism for the reduced GM-CSF production in CD48^{-/-} mice. It was recently shown that IL-7 activated STAT5 can promote GM-CSF production, and further promotes a Th differentiation state distinct from Th1 and Th17 (Sheng et al. 2014). It is possible that CD48^{-/-} CD4⁺ T cells are intrinsically resistant to this differentiation state, for example due to altered expression of cytokine receptors like IL-7R or IL-23R. Alternatively, extrinsic factors might influence CD4⁺ T cell differentiation, such as cytokines production by APC populations. Additional cellular and molecular characterization of both CD48^{-/-} T cells and APCs will be required to explain the attenuated GM-CSF production and EAE severity.

While we focused our attention on the early phases of disease in the CD48^{-/-} [B6] strain, additional studies are needed to examine later time points during the resolution phase. During the resolution phase of EAE, there is an increase in the ratio of Treg:Teff in the CNS (McGeachy, Stephens, and Anderton 2005). Although we did not see differences in the proportion of Tregs or Teff at early time points, it is possible that these differ at later phases of disease. Also, it is possible that reduced GM-CSF may limit the extent of inflammation and promote earlier recovery from disease.

In our second approach to study CD48 in EAE, we examined the role of CD48 on cells other than CD4⁺ Teff, such as APCs. To accomplish this, we used an adoptive transfer system such that CD48 was expressed only on CD4⁺ T cells. When WT 2D2 CD4⁺ T cells (unstimulated) were transferred to Rag^{-/-} and CD48^{-/-}Rag^{-/-} mice, and immunized with MOG/CFA to induce EAE, we saw no difference in incidence or severity of disease in CD48 deficient recipients. This was surprising, since WT T cells have been shown to proliferate less in response to CD48^{-/-} APCs, compared to WT APCs, in vitro. Although these data suggest that CD48 expression on host cells, such as APCs, is not critical for EAE, there are limitations to this interpretation. First of all, disease in this model is accelerated and severe, making it difficult to resolve slight differences in time of onset or rate of progression. It is possible that with an attenuated protocol or a different model, a difference in severity may become apparent in mice lacking CD48^{-/-} on host cells. Second, cell types other than APCs in Rag^{-/-} mice, such as NK cells, may counter any effect of reduced costimulation by CD48^{-/-} APCs, resulting in the apparent lack of difference in EAE severity. NK cells have been shown to influence EAE both in the priming phase and in the effector phase, and have been reported to have both protective and pathogenic roles (Zhang et al. 1997; Shi et al. 2000; Martin-Fontecha et al. 2004; Laouar et al. 2005; Huang et al. 2006; Winkler-Pickett et al. 2008; Hao et al. 2010; Dungan et al. 2014). Although the precise roles of NK cells in EAE are still controversial, it is possible that CD48^{-/-} NK cells are less effective at limiting CNS inflammation mediated by WT T cells, compared to the ability of WT NK cells to limit activation of WT T cells. One way to eliminate any contribution from NK cells is to generate NK cell deficient CD48^{-/-} mice, for example by crossing CD48^{-/-} with Il2r γ ^{-/-} Rag^{-/-} mice. We could then assess EAE induced by WT T cells in Il2r γ ^{-/-} Rag^{-/-} and CD48^{-/-} Il2r γ ^{-/-} Rag^{-/-} mice. Another way would be to generate conditional CD48^{-/-} mice, in order to specifically

examine the role of CD48 on APCs, versus other cell types. Thus, while our data suggest that CD48 on APCs might not be critical for EAE mediated by WT T cells, it is not yet clear whether this is the case.

As an alternative approach to examine the role of CD48 on non-CD4⁺ Teff, we used a model of adoptive transfer of primed WT Teff. This model uses *in vitro* polarized Th1 Teff, and thus allows analysis of the role of CD48 on host cells during the effector phase of disease, only. In striking contrast to our results with CD48^{-/-} Rag^{-/-} mice, we found that CD48^{-/-} mice had significantly attenuated disease induced by WT 2D2 TH1 Teff, compared to that in WT recipients. Although this observation is more consistent with the described costimulatory role for CD48 on APCs, as well as our own comparison of WT versus CD48^{-/-} APCs in stimulating WT Teff, this did not match our observations in the Rag^{-/-} model. We considered that this could be due to altered recruitment of WT versus CD48^{-/-} host CD4⁺ T cells to the periphery. However, there was no difference in the number of host CD4⁺ T cells in the CNS in WT and CD48^{-/-} recipients, nor did CD48^{-/-} mice have reduced cytokine production or increased proportions of Tregs. This suggested to us three alternative possibilities: 1) that EAE in the Rag^{-/-} model was too rapid to distinguish the contribution from CD48 on T cell costimulation; 2) that CD48 had a unique role in the effector phase of disease mediated by Th1 Teff; or 3) that the difference in EAE severity in the Th1 adoptive transfer model was due to CD48 expression on a host cell type not present in Rag^{-/-} mice, such as B cells, CD8⁺ T cells, or Foxp3⁺ Tregs. Additional studies are required to distinguish among these possibilities. Although we did not observe any difference in the proportion of Foxp3⁺ Tregs in the Th1 adoptive transfers, it remains possible that CD48^{-/-} Tregs have altered function compared to WT Tregs. This could be evaluated using *in vitro* and *in vivo* suppression assays, as well as adoptive transfers of WT or CD48^{-/-} Foxp3⁺ Tregs to mice with EAE (Kohm et al. 2002). B cells and CD8⁺ T cells are also candidates to explain the difference in these two models, and could be examined by co-transferring WT or CD48^{-/-} B cells or CD8⁺ T cells along with CD4⁺ T cells into Rag^{-/-} and CD48^{-/-} Rag^{-/-} mice. To examine the role of CD48 during the effector phase of disease, in the absence of B cells and CD8⁺ T cells, the 2D2 TH1 adoptive transfer model could be used with Rag^{-/-} and CD48^{-/-} Rag^{-/-} recipients. Collectively, these experiments could help to characterize the role of CD48 on various cell types, in the development, severity, and resolution of EAE.

For our third approach, we focused on the role of CD48 on CD4⁺ T cells during EAE, by comparing WT and CD48^{-/-} CD4⁺ T cells during EAE in CD48⁺ hosts. First, we transferred a ~1:1 mix of WT and CD48^{-/-} 2D2 CD4⁺ T cells into Rag^{-/-} recipients, waited for homeostatic proliferation, and then immunized for EAE with MOG/CFA. By mixing WT and CD48^{-/-} CD4⁺ T cells in the same host, we limited experimental variability (since these T cells were in the same host responding to the same stimuli), and performed pairwise comparisons between WT and CD48^{-/-} CD4⁺ T cells. We consistently found that WT CD4⁺ T cells were more highly represented in all organs examined. Although this could be due to lack of precision in preparing the 1:1 mix used for cell transfers, our results suggest that WT T cells might have an advantage in homeostatic proliferation, or might proliferate more in response to MOG/CFA immunization. Although additional studies are needed to discriminate amongst these possibilities, we did notice a difference in the percentage of naïve cells in the starting populations which could explain the skewed ratio: CD48^{-/-} CD4⁺ T cells had an increased percentage of CD44⁺CD62L⁻ and decreased percentage of CD44⁻CD62L⁺ CD4⁺ T cells. These differences in the starting population could influence their ability to expand *in vivo*. Future studies could use purified naïve CD4⁺ T cells to determine whether CD48^{-/-} T cells have a disadvantage in homeostatic proliferation. We did not choose this approach for our EAE model, because naïve CD4⁺ T cells transferred to lymphopenic mice can induce colitis (Powrie et al. 1993). Alternatively, the ratio of WT:CD48^{-/-} CD4⁺ T cells in the blood could be measured prior to immunization, to establish the starting ratio. Importantly, the ratio of WT:CD48^{-/-} CD4⁺ T cells was the same in the CNS as in the periphery, suggesting that CD48^{-/-} CD4⁺ T cells were not at a disadvantage for reaching the CNS. We saw no differences in cytokine production between WT and CD48^{-/-} T cells, further suggesting that both types were similarly pathogenic. These data suggest that CD48^{-/-} CD4⁺ T cells expand less than WT cells when mixed *in vivo*, but do not have a defect in reaching the CNS or producing inflammatory cytokines.

A defect in T cell expansion is consistent with *in vitro* studies using T cells from the CD48^{-/-} [B6.129] strain: CD48^{-/-} CD4⁺ T cells had reduced proliferation *in vitro* when stimulated with anti-CD3, and CD48^{-/-} total T cells had reduced proliferation in an allo-mixed lymphocyte reaction with Balb/c stimulators (Gonzalez-Cabrero et al. 1999). However, CD4⁺ T cells from CD48^{-/-} [Balb/c.129] mice were *not* found to have a defect in proliferation in a recall response *in vitro* after priming *in vivo*. Keszei et al. transferred CD48^{-/-} DO11.10

CD4⁺ T cells into CD48^{-/-} mice, immunized recipients with OVA/CFA, and three days later restimulated lymph node cells *ex vivo* with OVA. In this case, CD48^{-/-} DO11.10 cells did not have a defect in proliferation or secretion of IL-2 or IFN γ *in vitro* (Keszei et al. 2011). Preliminary work in our lab also shows that CD4⁺ T cells from CD48^{-/-} [B6] mice do not have a defect in response to antigen restimulation after *in vivo* priming (Dr. Dan Brown, unpublished data). Additional studies are needed to determine how CD48^{-/-} CD4⁺ T cell proliferation *in vivo* correlates with proliferation *in vitro*, and whether this is affected by CD48 expression on APCs or CD4⁺ T cells.

To further study CD48^{-/-} CD4⁺ T cells in EAE, we generated mixed bone marrow chimeras in WT recipients. In contrast to the Rag^{-/-} model above, donor CD48^{-/-} CD4⁺ T cells were more abundant than donor WT CD4⁺ T cells in mixed bone marrow chimeras during EAE, and this was true in all organs examined. The group size in these experiments was small (only 3 mice each in two independent experiments) so it is difficult to draw firm conclusions. However, we did not observe a significant defect in the ability of CD48^{-/-} CD4⁺ T cells to contribute to EAE: CD48^{-/-} CD4⁺ T cells were equally represented in the CNS as in the spleen, and there was no significant decrease in the percentage of CD48^{-/-} CD4⁺ T cells in the CNS or spleen that produced IL-17A or IFN γ after restimulation with PMA and ionomycin. Combined with our experiments in the Rag^{-/-} model, these data suggest that CD48^{-/-} CD4⁺ T cells do not have a significant defect in contributing to EAE.

In addition to comparing WT and CD48^{-/-} CD4⁺ T cells side by side, the mixed bone marrow chimera also provided a CD48-replete environment in which both CD48⁺ and CD48^{-/-} hematopoietic cells could develop. Thus, potential developmental differences in CD48^{-/-} CD4⁺ T cells, due to extrinsic factors, would be eliminated or reduced in the mixed chimera setting. For example, CD48^{-/-} cells have increased CD2 expression, compared to WT cells. However, WT and CD48^{-/-} CD4⁺ T cells that developed in the mixed bone marrow chimera had identical CD2 surface expression.

Based on the decreased proliferation of CD48^{-/-} cells *in vitro* (Gonzalez-Cabrero et al. 1999), we might have predicted a more dramatic phenotype of reduced EAE severity in CD48^{-/-} mice. On the other hand, increased T cell activation in CD48^{-/-} mice might have predicted a more severe EAE course when EAE was induced in

CD48 deficient mice. Our result suggests that either CD48 is not critical for activation of naïve MOG-reactive T cells in EAE, or that other mechanisms for cell adhesion and costimulation can compensate in CD48 deficient mice. In addition, we did not demonstrate a key role for CD48 on either CD4⁺ Teff or APCs, suggesting that reduced disease severity might be due to B cells, CD8⁺ T cells, or Tregs. Further studies are required to identify the key population in CD48^{-/-} mice that influence susceptibility to EAE, likely involving both conditional knockout mice and functional assays.

Our studies did reveal several interesting findings about the CD48^{-/-} [B6] strain, particularly when examined in the context of other published studies. Notably, CD48^{-/-} CD4⁺ T cells are capable of inducing EAE in a CD48^{-/-} host. This is in contrast to observations using the CD45RB^{hi} model of colitis, in which CD48 expression on either the T cell or host macrophages was sufficient for development of colitis, but lacking CD48 on both CD4⁺ T cells and on host macrophages prevented development of colitis (Abadia-Molina et al. 2006). In the colitis model, this was due to reduced efficiency of antigen uptake and processing by CD48^{-/-} peritoneal macrophages, as well as reduced costimulatory function: stimulation of CD4⁺ T cell proliferation with whole OVA was reduced by 10-fold in CD48^{-/-} peritoneal macrophages, while proliferation in response to OVA peptide was reduced by 2-fold (Abadia-Molina et al. 2006). Our EAE model did not examine antigen processing explicitly, since we immunized with the MOG[35-55] peptide. However, EAE requires de novo antigen presentation in the CNS (Tompkins et al. 2002), suggesting that progression of EAE might be limited in CD48^{-/-} mice due to reduced antigen processing in the CNS. This could be examined directly in future experiments, using WT and CD48^{-/-} CNS-derived APCs to stimulate T cells ex vivo. However, it is also possible that the function of CD48 on macrophages is distinct from that on dendritic cells and microglia in the CNS during EAE, and thus the phenotype of colitis with CD48^{-/-} cells differs from that of EAE in CD48^{-/-} mice. This highlights the benefit of examining multiple disease models during the characterization of immune receptor functions, as they may have different roles on different cell types, or under different conditions.

Our results also highlighted potential roles for CD48 in EAE, on cell types other than CD4⁺ T cells and APCs. The fact that EAE was not attenuated in Rag^{-/-} mice reconstituted with CD48^{-/-} 2D2 CD4⁺ T cells initially suggested to us that CD48 expression on the CD4⁺ T cell was the critical factor for EAE: while CD48^{-/-} mice

have attenuated EAE compared to WT mice, EAE is not attenuated in CD48^{-/-} Rag^{-/-} mice when induced with WT T cells. However, the fact that EAE *was* attenuated in CD48^{-/-} recipients of Th1-polarized 2D2 CD4⁺ T cells suggests that a non-CD4⁺ T cell mechanism is involved. It is possible that CD48 on host cells may be particularly important to sustain Th1 responses, or that CD48 is more critical during the effector phase of EAE, or that a cell type not present in Rag^{-/-} mice could attenuate EAE in CD48^{-/-} mice. Both CD8⁺ T cells and Tregs are attractive candidates to consider. CD8⁺ T cells can limit EAE severity (Lu et al. 2008; Beeston et al. 2010; Ortega et al. 2013), and have been shown to be critical for resistance to re-induction of EAE in the B10PL strain (Jiang, Zhang, and Pernis 1992). We did not rigorously examine CD8⁺ T cells in our EAE studies, nor did we examine CD8⁺ T cell function. It is possible that CD48^{-/-} CD8⁺ T cells are better than WT CD8⁺ T cells at limiting EAE severity; this would be consistent with our findings EAE is attenuated in CD48^{-/-} mice, in CD48^{-/-} recipients of WT TH1 Teff, but not in CD48^{-/-} Rag^{-/-} mice reconstituted with 2D2 CD4⁺ T cells. Alternatively, CD4⁺ Foxp3⁺ Tregs might also be involved in attenuating EAE in CD48^{-/-} mice. The initial observation of attenuated EAE in CD48^{-/-} [B6.129] mice suggested a more pronounced effect during the resolution phase of EAE, rather than during the induction phase. CNS inflammation leads to Foxp3⁺ Tregs entry and expansion in the CNS, which contributes to resolution of disease (McGeachy, Stephens, and Anderton 2005; O'Connor, Malpass, and Anderton 2007). Thus increased function of CD48^{-/-} Foxp3⁺ Tregs could explain our observations, as well.

In summary, the goal of these studies was to characterize the role of CD48 in EAE, with particular focus on its role on CD4⁺ Teff and APCs, by examining CNS infiltration and cytokine production in WT and CD48^{-/-} mice. We found that CD48^{-/-} mice have attenuated EAE, with a trend towards reduced infiltration of the CNS by CD4⁺ T cells, significantly increased numbers of CD4⁺ T cells in the periphery, and significantly reduced GM-CSF production by Teff in the CNS at the peak of disease and in the periphery prior to disease onset. Using adoptive transfers, we compared the effects of CD48 deficiency on CD4⁺ T cells and on host cells. These transfers suggested that CD48 expression on CD4⁺ Teff did not contribute significantly to severity of EAE, but that CD48 expression on other cell types was likely involved in modulating severity of disease. Future studies would benefit from examination of the resolution phase of disease, as we did not find striking differences during the priming phase of EAE and did not undertake cellular analysis beyond the peak of disease.

In addition, closer examination of other cell types such as CD8+ T cells and Tregs in the CNS is highly warranted, as we found only a few differences in CD4+ T cells at the peak of disease. Lastly, the finding of reduced GM-CSF production in CD48^{-/-} CD4+ T cells is quite tantalizing, and functional studies examining Th polarization and cytokine production in CD48^{-/-} mice may help determine whether this is a likely cause or result of attenuated EAE in CD48^{-/-} mice.

Chapter 5: Mechanisms of action of an anti-CD48 monoclonal antibody in attenuation of experimental autoimmune encephalomyelitis

ABSTRACT

CD48 is an adhesion and costimulation molecule expressed constitutively on most hematopoietic cells. We examined CD48 expression during EAE, and found that a population of CD4⁺ T cells upregulated surface CD48 expression during EAE. These CD48⁺⁺ cells were predominantly CD44⁺ and Ki67⁺, and were most prominent in the CNS. Administration of anti-CD48 mAb after induction of EAE, but before disease onset, could block or significantly attenuate clinical disease and accumulation of lymphocytes in the CNS. This treatment was similarly protective after adoptive transfer of encephalitogenic CD4⁺ T cells, and moderately protective in mice with ongoing clinical disease. At pre-clinical time points, anti-CD48 administration reduced the number of cytokine-producing CD4⁺ Teff in the spleen, but did not alter the proportion of Foxp3⁺ Tregs. The mechanism of action was dependent on FcγRs, as anti-CD48 could not limit disease in Fcεr1γ^{-/-} mice or in WT mice receiving anti-CD16/CD32 mAb. Similarly, anti-CD48 had no effect on the number of cytokine-producing CD4⁺ Teff in anti-CD16/CD32 mAb treated WT mice. Closer analysis of cytokine-producing IL-17⁺ and GM-CSF⁺ CD4⁺ Teff during EAE revealed that these pathogenic cells are a subset of the CD48⁺⁺ population. Our data suggest that this anti-CD48 antibody can both limit CD4⁺ T cell proliferation and preferentially deplete pathogenic CD4⁺ T cells during EAE, thereby preventing or attenuating disease. This highlights the potential of CD48, and its human homologue CD58 (LFA-3), to be used as markers of T cell activation during study and treatment of autoimmunity in human patients.

RESULTS

CD48 expression increases on CD4⁺ T cell subsets during EAE

We examined CD48 surface expression on CD4⁺ T cells from mice at the peak of EAE disease, using flow cytometry, and compared this to CD48 expression on CD4⁺ T cells from naïve mice. As shown in a representative experiment in **Figure 5.1A**, ~4% of CD4⁺ T cells in the spleen of a naïve mouse had exceptionally high CD48 expression (CD48⁺⁺), but this increased to ~13% in mice at the peak of EAE. In the

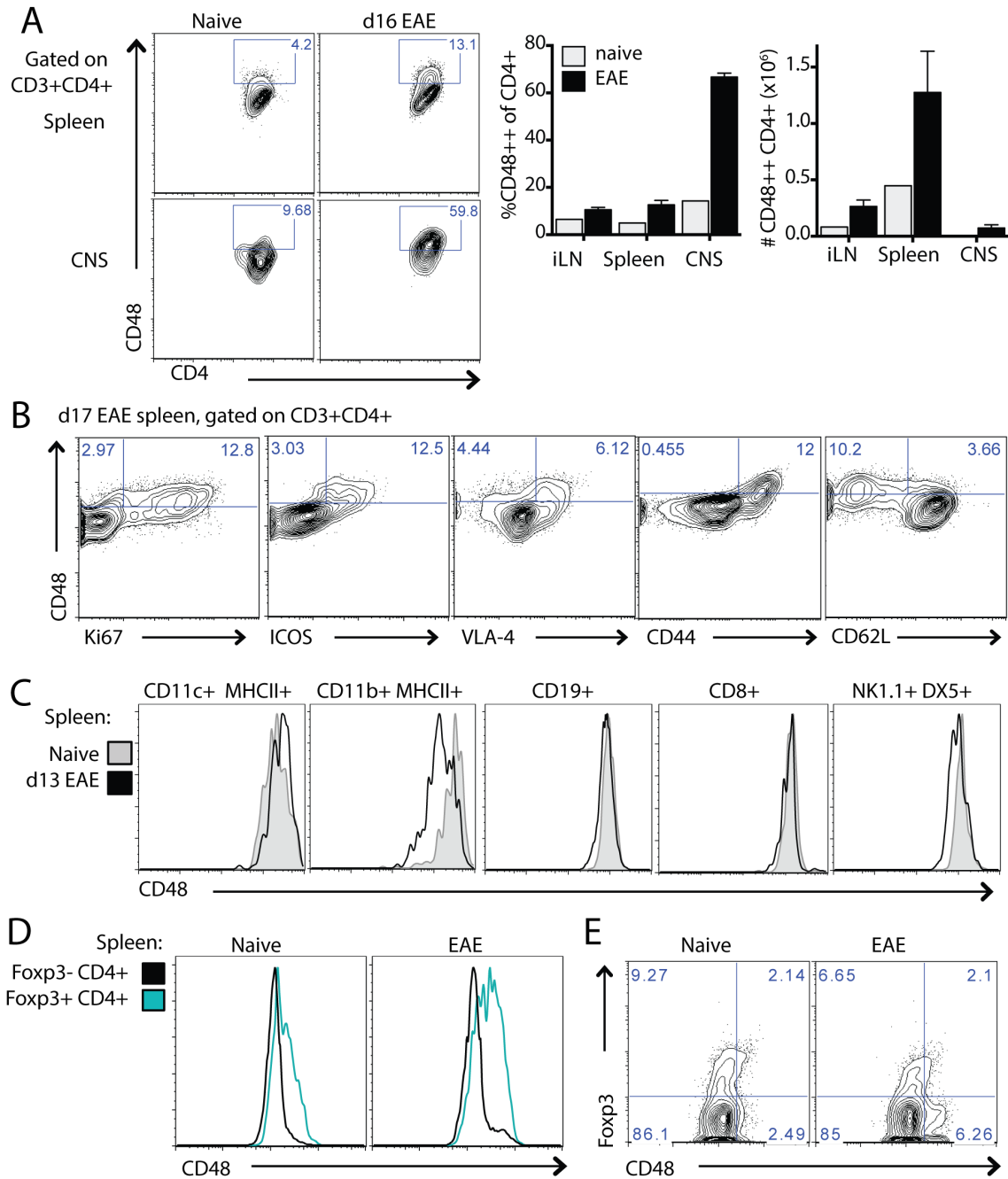


Figure 5.1 CD48 expression increases on activated CD4+ T cells during EAE. WT mice were immunized s.c. with 50 μ g of MOG[35-55] emulsified in CFA, and given 100ng of pertussis toxin i.p. on days 0 and 2. Spleen and CNS were collected from naïve and immunized mice at the peak of disease, for analysis by flow cytometry. **A.** Far left, CD48 staining on CD4+CD3+ T cells from the spleen and CNS of representative naïve and EAE mice. Quantitation of the percentage (center) and absolute number (far right) of CD48++ CD4+CD3+ T cells in the iLN, spleen and CNS. **B.** CD48 co-staining with activation markers Ki67, ICOS, VLA-4, CD44 or CD62L on CD4+CD3+ T cells from the spleen. **C.** CD48 surface staining on dendritic cells (CD11c+MHCII+), macrophages (CD11b+MHCII+), B cells (CD19+), CD8 T cells (CD8+), NK cells (NK1.1+DX5+) from the spleen. **D.** Representative CD48 staining on CD3+CD4+Foxp3+ Tregs (teal) and CD3+CD4+Foxp3- Tconv (black) from the spleen. **E.** Representative staining of CD3+CD4+ cells from the spleen, showing Foxp3 and CD48 co-staining. Data are representative of 3 independent experiments with 4-6 mice per group. One naïve control was used in **A.**

CNS of mice at the peak of EAE, ~60% of CD4⁺ T cells were CD48⁺⁺. This contrasted with approximately 10% of CD4⁺ T cells recovered from the CNS of naïve mice, although it should be noted that very few lymphocytes are found the CNS of naive mice. Although the percentage of CD48⁺⁺ cells was highest in the CNS, compared to the iLN and spleen at the peak of EAE (**Figure 5.1A, center**), the absolute number of CD48⁺⁺ CD4⁺ T cells was greater in the iLN and spleen than in the CNS (**Figure 5.1A, right**). Thus, the number of CD48⁺⁺ CD4⁺ T cells increased dramatically in all organs during EAE, but the percentage of CD48⁺⁺ cells among CD4⁺ T cells was highest in the CNS. This suggested that high CD48 surface expression might correlate with CD4⁺ T cell activation.

When we co-stained with other markers to assess cell activation, such as Ki67, ICOS, VLA4, CD44 and CD62L, we saw that CD48⁺⁺ CD4⁺ T cells were predominantly Ki67⁺, ICOS⁺, and CD44⁺, and tended to be VLA-4⁺ and CD62L⁻ (**Figure 5.1B**). To determine whether this CD48⁺⁺ population was unique to CD4⁺ T cells, or a general feature of immune cells during EAE, we examined CD48 surface expression on other lymphocytes and monocytes in the spleen of mice near the peak of EAE, and compared this with CD48 expression in naïve mice. CD48 MFI increased on CD11c⁺MHCII⁺ DCs after immunization, and decreased on CD11b⁺MCHII⁺ macrophages (**Figure 5.1C**). We did not detect a change in CD48 MFI nor %CD48⁺⁺ cells among CD19⁺ B cells, CD8⁺ T cells, or NK1.1⁺DX5⁺ NK cells in the spleen, after immunization with MOG (**Figure 5.1C** and data not shown).

We also examined CD48 expression on Foxp3⁺ versus Foxp3⁻ CD4⁺ T cells. In naïve animals, Foxp3⁺ T cells had slightly higher CD48 MFI than Foxp3⁻ CD4⁺ T cells. In mice with EAE, the CD48 MFI increased on both Foxp3⁺ T cells as well as Foxp3⁻ T cells (**Figure 5.1D**). The increase in CD48 expression was also visible when examined as the percentage of Foxp3⁺ or Foxp3⁻ cells that were CD48⁺⁺ (**Figure 5.1E**). This suggested that an increase in CD48 expression might be unique to subsets of CD4⁺ T cells and some APC populations, during EAE.

CD48 expression increases on antigen-specific 2D2 CD4⁺ T cells after activation

We hypothesized that increased CD48 expression might be a feature of antigen-activated Teff. To address this, we examined CD48 expression on cells that we knew to be antigen-specific: MOG-specific 2D2 TCR Tg

CD4⁺ T cells. We transferred purified CD4⁺ T cells from Thy1.1 congenic 2D2 mice into WT Thy1.2 recipients, and immunized recipients with MOG/CFA or left them unimmunized. Eight days later, we assessed expression of CD48 and other markers by flow cytometry on both 2D2 and host CD4⁺ T cells. In unimmunized mice, CD48 expression on naïve (CD44⁻CD62L⁺) 2D2 CD4⁺ T cells was similar to that on host naïve CD4⁺ T cells (**Figure 5.2A, left**). In immunized mice, CD48⁺⁺ cells were more prominent among 2D2 CD4⁺ T cells than among host CD4⁺ T cells. 2D2 CD4⁺ T cells also had increased percentages of CD44⁺ and Ki67⁺ cells, compared to host CD4⁺ T cells, again suggesting that high CD48 surface expression might be a feature of activated cells (**Figure 5.2A, right**).

Because the above model of MOG immunization does not guarantee that all 2D2 CD4⁺ T cells will encounter antigen and become activated, we wanted a way to examine CD48 on CD4⁺ T cells that we knew to be activated T effectors (Teff). To do this, we used CD4⁺ T cells from 2D2 mice to generate TH1-polarized Teff in vitro, and transferred these into WT recipients. Five days later, we examined expression of CD48 and other activation markers on both 2D2 TH1 and host CD4⁺ T cells, using flow cytometry. Staining from a representative experiment is shown in **Figure 5.2B**. Nearly all 2D2 cells were CD48⁺⁺ and CD44⁺, and were predominantly Ki67⁺ (approximately 88%, 100% and 74% respectively). In contrast, among host CD4⁺ T cells only 13% were CD48⁺⁺, 28% CD44⁺ and 22% Ki67⁺ (**Figure 5.2B**). We concluded that CD48 surface expression increases on activated CD4⁺ T cells after immunization or in vitro polarization and stimulation.

The anti-CD48 mAb HM48-1 causes both blocking and downmodulation of surface CD48

The expression pattern of CD48 during EAE, and its known role as an adhesion and costimulatory type molecule, led us to investigate whether this molecule could be a valuable therapeutic target to alter the course of EAE in WT animals. To first establish the effects of anti-CD48 in vivo in the absence of EAE, we administered 200µg of anti-CD48 i.p. to naïve WT mice. The antibody was detectable on the surface of CD4⁺ T cells two days after administration, using an anti-hamster IgG secondary antibody to stain cells ex vivo (**Figure 5.3A, left**), and blocked competitive staining with a fluorescently-conjugated version of the same anti-CD48 clone (HM48-1) for up to 3 days in vivo (**Figure 5. 3A, center**). Staining with purified anti-CD48 followed by anti-hamster IgG FITC was less bright in anti-CD48-treated mice, suggesting that anti-CD48 administration results

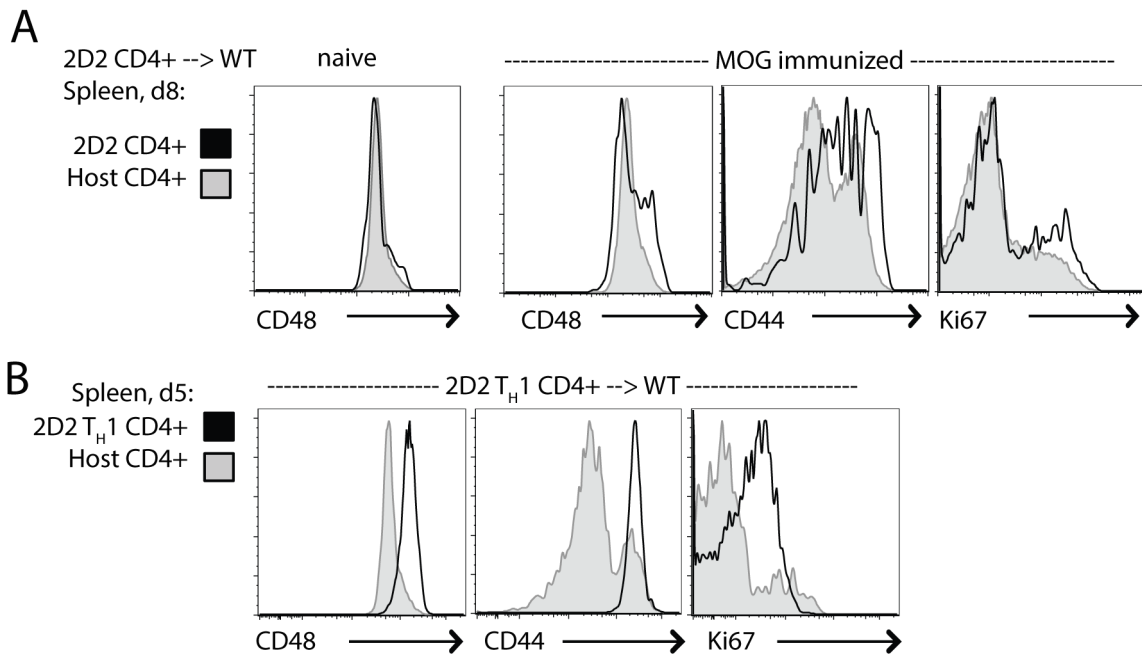


Figure 5.2 CD48 expression increases on activated antigen-specific CD4+ T cells. A. CD4+ T cells from Thy1.1 congenic 2D2 TCR Tg (MOG-specific) mice were purified by MACS and transferred into WT recipients. Mice were then immunized with MOG/CFA or left unimmunized. 8 days later, host and 2D2 donor CD4+ cells in the spleen were analyzed by flow cytometry. Left, representative CD48 staining on host (gray shaded) and 2D2 donor (black) naïve CD62L+CD44- CD4+ T cells. Right, representative staining for CD48, CD44 and Ki67 on host CD4+ and 2D2 donor CD4+ T cells. B. CD4+ T cells from Thy1.1 congenic 2D2 TCR Tg mice were purified and cultured in vitro under TH1-polarizing conditions for 6 days. Live cells were then purified and restimulated on anti-CD3/anti-CD28 coated plates for 24 hours. 2D2 TH1 Teff were collected and injected i.v. into WT recipients. 8 days later, host and donor 2D2 CD4+ T cells in the spleen were analyzed by flow cytometry. Representative CD48, CD44 and Ki67 staining on host CD4+ (gray shaded) and adoptively transferred TH1-polarized 2D2 CD4+ Teff (black lines) on day 5 after adoptive transfer is shown. Data representative of 5 independent experiments with n=3-7 mice per group (A), and 5 independent experiments with n=4-8 mice per group (B).

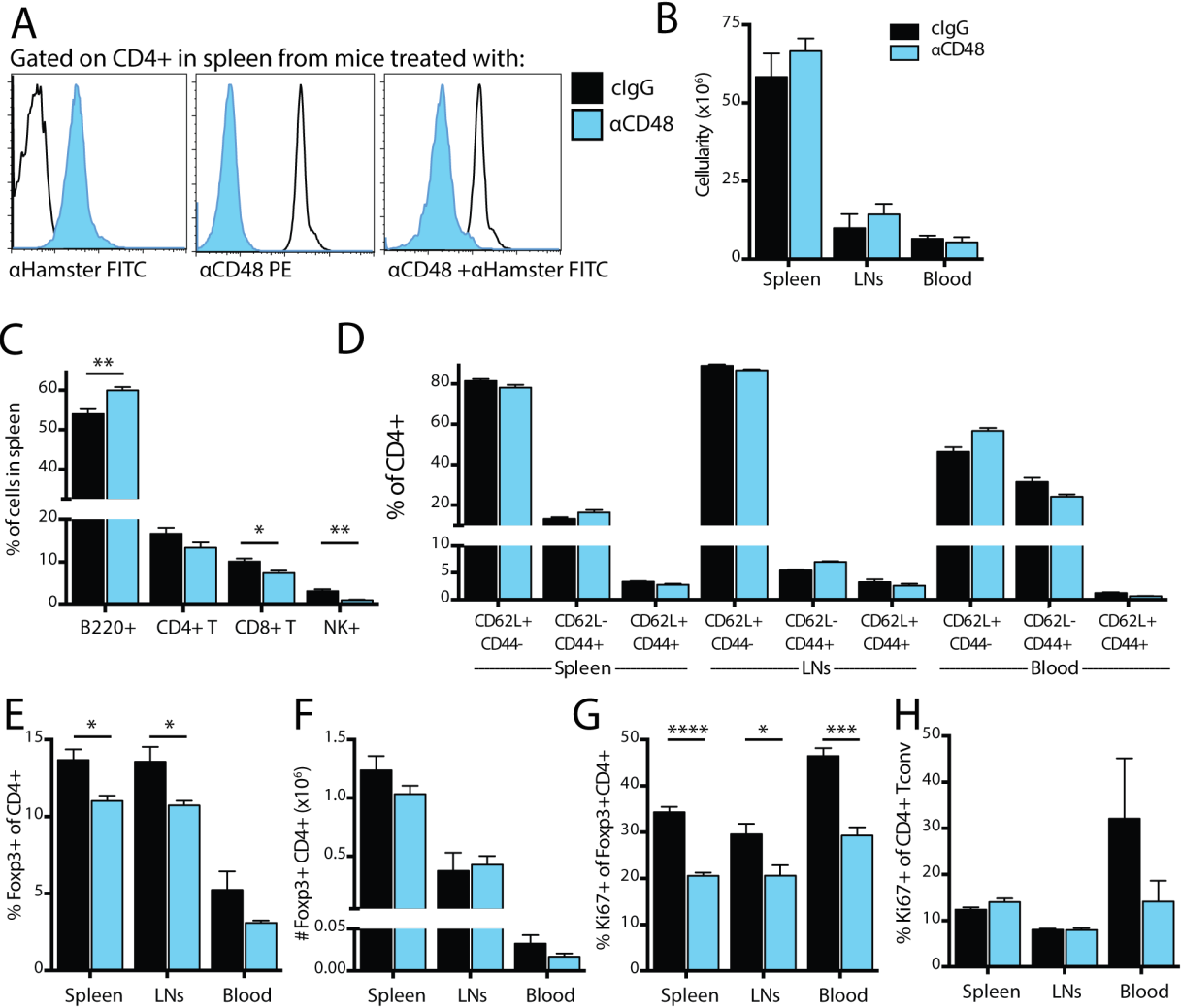


Figure 5.3 The anti-CD48 mAb HM48-1 causes both blocking and downmodulation of surface CD48. 200 μ g of anti-CD48 mAb (clone HM48-1) or control Armenian hamster IgG was given i.p. to naïve WT mice on day 0 and day 3. On day 6, spleen, skin-draining lymph nodes, and peripheral blood were collected for analysis by flow cytometry. **A**. Splenocytes were stained with CD4 and anti-Hamster IgG FITC (Left) to detect surface-bound anti-CD48 from in vivo administration; anti-CD48 PE (Center) was used to detect CD48 not bound by anti-CD48 from in vivo administration; or purified anti-CD48 plus anti-Hamster IgG FITC (Right) was used to measure total surface CD48 in mice given anti-CD48 in vivo. **B**. Cellularity in spleen, iLN and blood. **C**. Quantitation of the %B220+, %CD4+, %CD8+ and %NK1.1+ in the spleen. **D**. Distribution of naïve, activated and memory CD4+ T cells in the spleen, iLN and blood. **E**. %Foxp3+ of CD4+ T cells. **F**. Absolute number of Foxp3+ CD4+ T cells. **G**. %Ki67+ Foxp3+ CD4+ Tregs. **H**. %Ki67+ of Foxp3- CD4+ Tconv. N=4 mice per group, representative of 2 independent experiments with 3-4 mice per group. Bars represent mean \pm SEM *p<0.05, **p<0.01, ***p<0.001, ****p<0.0001. Statistical significance calculated using Student's t test.

in some down-regulation of surface CD48 after antibody treatment as well as some retention of CD48-anti-CD48 complexes on the cell surface (**Figure 5.3A, right**). This was true on all lymphocytes examined, including CD4⁺ T cells, CD8⁺ T cells, and B cells (data not shown).

This antibody clone has been reported to be non-depleting, but to alter distribution of lymphocytes (Chavin et al. 1994; Blazar et al. 1998; Munitz et al. 2007). To confirm this, we tested the effects of 200µg anti-CD48 every three days, two doses total, in naïve mice. We did not observe a decrease in cellularity in the spleen, skin-draining lymph nodes or blood (**Figure 5.3B**). We also examined the distribution of lymphocyte subsets in the spleen, lymph nodes and blood. Mice treated with anti-CD48 had an increased proportion of B cells in the spleen, decreased proportion of CD8⁺ T cells, and a decrease in the percentage of NK cells (**Figure 5.3C**). Similar trends were observed in the iLN, and there were no differences in lymphocyte distribution in the blood (data not shown).

Because we had observed that CD48 expression is higher on activated cells and Tregs, we also examined the proportion of activated CD4⁺ T cells in anti-CD48 treated mice. There was a slight increase in the proportion of naïve CD44-CD62L⁺ CD4⁺ T cells in the blood, and decrease in CD44⁺ populations (**Figure 5.3D**). The percentage of Foxp3⁺ CD4⁺ T cells was reduced in anti-CD48 treated mice, although the absolute number was not significantly altered (**Figure 5.3E-F**). The proportion of Ki67⁺ Foxp3⁺ CD4⁺ T cells was significantly reduced in all organs (**Figure 5.3G**), although this was not true for Ki67⁺ CD4⁺ Tconv (**Figure 5.3H**). This suggested that anti-CD48 treatment in vivo resulted in slight changes to the distribution of CD4⁺ T cell subsets, particularly in the blood and particularly with respect to activated Ki67⁺ Tregs. However, we did not observe lymphopenia or widespread activation of lymphocytes, in agreement with published descriptions.

Anti-CD48 attenuates EAE in WT mice

Next we examined the effect of anti-CD48 during EAE, using the MOG[35-55] immunization model. Starting on day 6 after immunization with MOG/CFA, mice received 200µg of anti-CD48 or control IgG (Armenian hamster IgG) every 3 days for a total of 3 doses. As shown in a representative experiment in **Figure 5.4A**, anti-CD48 treatment dramatically altered the course of EAE: anti-CD48 reduced the incidence of EAE (5/5 mice

receiving cIgG, 3/5 mice receiving anti-CD48) (**Figure 5.4B**), delayed the onset, and limited the severity of disease as assessed by the peak clinical score (**Figure 5.4C**). Indeed, disease was completely blocked for as long as the antibody was detectable in vivo (day 15, **Figure 5.4A**). A summary of data pooled from 5 experiments is shown in **Table 5.1**.

Histological analysis of brain and spinal cord sections at day 12 (onset of disease) and day 15 (peak of disease) after immunization revealed minimal leukocyte infiltration or lesions in anti-CD48 treated mice, compared to control mice (**Figure 5.4D-E**, **Table 5.2**, histological scoring performed by Dr. Ray Sobel). Cellular analysis of the CNS by flow cytometry similarly revealed reduced accumulation of lymphocytes in the CNS by day 17 after immunization, when control mice were near the peak of disease (**Figure 5.4F**). The number of total CD45+ cells in the CNS was reduced, but did not reach statistical significance, while the number of CD4+ T cells in the CNS of anti-CD48 treated mice was significantly reduced (**Figure 5.4G-H**). Anti-CD48 treated mice had a reduced percentage of Foxp3+ CD4+ T cells in the CNS, but no difference in the %Foxp3+ CD4+ T cells in the spleen (**Figure 5.4I**). This indicated that anti-CD48 treatment blocked EAE as assessed by clinical score, histology, and cellular analysis.

To confirm that anti-CD48 did not have off-target effects in EAE, we administered anti-CD48 in the same way to CD48^{-/-} mice immunized for EAE. We did not observe any effect of anti-CD48 on the clinical course of EAE in CD48^{-/-} mice (**Figure 5.4J**).

B cells and CD8 T cells are not required for anti-CD48-mediated attenuation of EAE

Because CD48 is widely expressed on hematopoietic cells, it was possible the mechanism of anti-CD48-mediated attenuation of EAE might involve multiple immune cell types. We wanted to identify the minimum components required for anti-CD48 to exert its protective effects. EAE in the MOG[35-55] immunization model is dependent on CD4+ T cells and MHCII antigen presentation. Although B cells and CD8 T cells are not required for this model of EAE, they have but have been shown to play modulatory roles in disease (Pistoia 1997; Fillatreau et al. 2002; Magliozzi et al. 2004; Matsushita et al. 2008; Ford and Evavold 2005; Lu et al. 2008; Ortega et al. 2013). To test whether B cells and CD8+ T cells were dispensable for anti-CD48-mediated

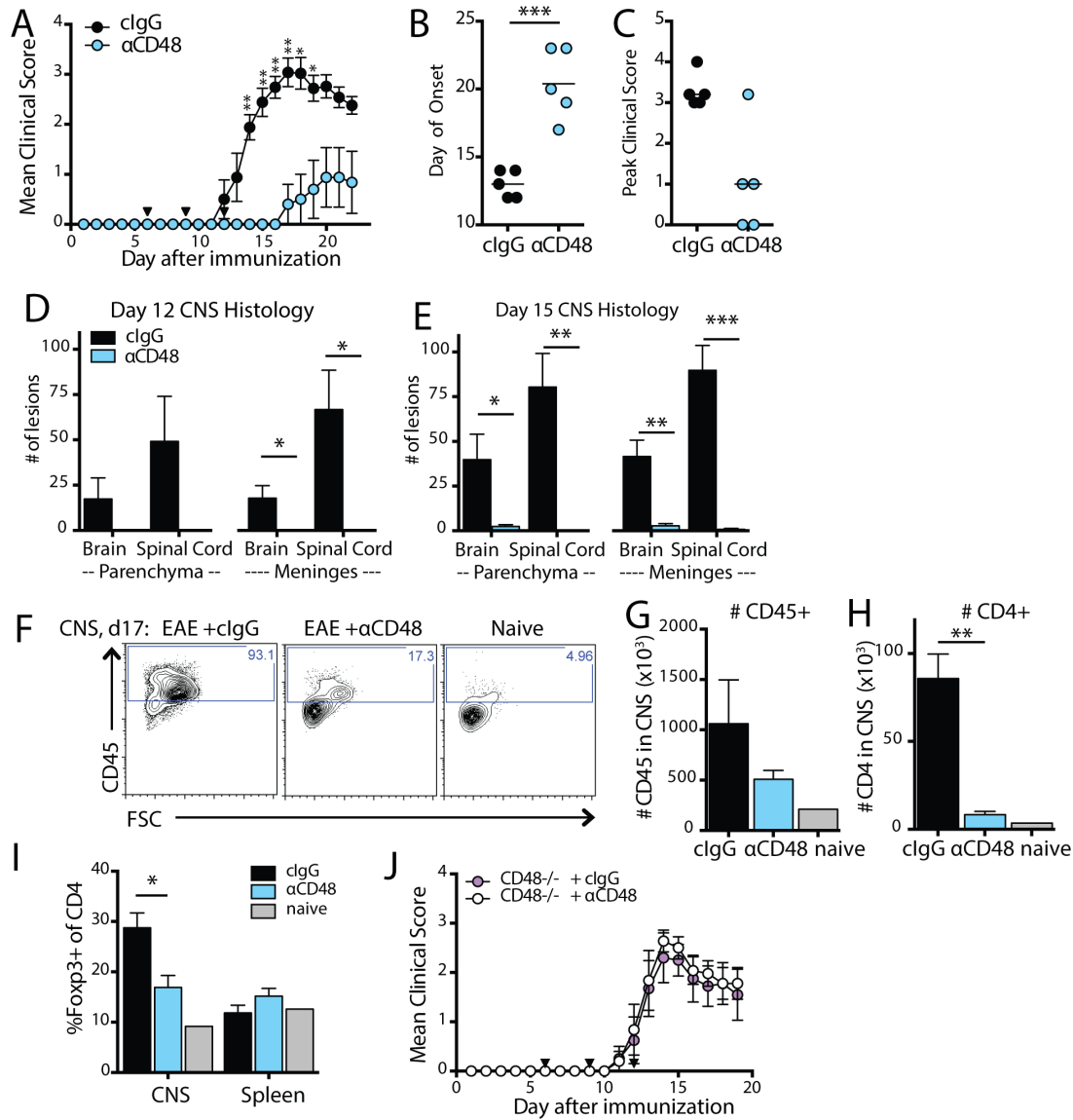


Figure 5.4 Anti-CD48 antibody in vivo attenuates clinical, histological and cellular indications of EAE in WT mice. A-I WT mice were immunized s.c. with 50 μ g MOG[35-55] in CFA to induce EAE, and given 100ng of pertussis toxin on days 0 and 2. 200 μ g of anti-CD48 or cIgG was given on days 6, 9 and 12 after immunization (black triangles). A. Mean clinical scores, \pm SEM. B. Day of onset. C. Peak clinical scores. D-E. Histological analysis of CNS lesions in WT mice near the onset of EAE (D, day 12 after immunization), or near the peak of EAE (E, day 15). CNS tissue was fixed in 4% PFA, embedded in paraffin, sectioned and mounted on slides. Sections were stained with H&E or Luxol fast blue and lesions were enumerated by Dr. Raymond Sobel. F-I. Flow cytometric analysis of CD45 $^{+}$ and CD4 $^{+}$ infiltration of the CNS in WT mice on day 17 after immunization for EAE with MOG/CFA, receiving cIgG or anti-CD48 on days 8, 11 and 14. cIgG-treated mice were at the peak of disease, anti-CD48-treated mice had no clinical disease. H. Representative FACS plots from the CNS, showing relative leukocyte (CD45 hi) accumulation. I. Absolute number of CD45 $^{+}$ cells in the CNS. J. Absolute number of CD4 $^{+}$ T cells in the CNS. K. Proportion of Fxp3 $^{+}$ CD3 $^{+}$ CD4 $^{+}$ T cells in the CNS and spleen. L. CD48 $^{-/-}$ mice were immunized for EAE and treated with anti-CD48 during EAE, as described above for WT mice. Mean clinical scores, \pm SEM. A-C, n=5 mice per group, representative of 6 independent experiments with 4-6 mice per group. D-E, n=5 mice per group. F-I, n=4-5 mice per group, representative of 3 independent experiments. J, n=5 mice per group. Bars represent mean \pm SEM. *p<0.05, **p<0.01, ***p<0.001, ****p<0.0001. Statistical significance calculated with Mann-Whitney test (A, C) or Student's t test (B, D, F, J-L).

Table 5.1 Anti-CD48 limits incidence and severity of EAE in WT mice

Treatment	Incidence of EAE		Median peak score		Mean day of onset*
	By day 15	By day 25	By day 15	By day 25	
cIgG	14 / 15	10 / 10	3	3	12.3 ± 0.3
αCD48	0/15	4 / 10	0	0	18.8 ± 0.6

WT mice were immunized for EAE with MOG/CFA as described. 200µg of anti-CD48 or cIgG was given i.p. on days 6, 9 and 12 after immunization. Clinical score was monitored for 15 or 25 days. Data are mean ± SEM. *For mice who developed disease, only.

Table 5.2 Anti-CD48 limits parenchymal and meningeal lesions in the brain and spinal cord during EAE

Treatment	Lesions in Brain		Lesions in Spinal Cord		Day of onset	Maximum clinical score
	Parenchyma	Meninges	Parenchyma	Meninges		
cIgG	39.8 ± 14.2	41.6 ± 9.1	80.4 ± 18.9	89.9 ± 14	13.4 ± 0.2	2 ± 0.4
αCD48	2.4 ± 1.0	2.8 ± 1.1	0 ± 0	0.8 ± 0.5	> 15	0

WT mice were immunized for EAE with MOG/CFA as described. 200µg of anti-CD48 or cIgG was given i.p. on days 6, 9 and 12 after immunization. Mice were sacrificed on day 15, brain and spinal cord were collected and fixed in 4% PFA, and then embedded in paraffin. Sections were collected for histology, stained with Luxol fast blue or H&E, and scored blindly for parenchymal and meningeal lesions in the brain and spinal cord. Data are mean ± SEM. Histological analysis performed by Dr. Ray Sobel at Stanford University.

attenuation of EAE, we transferred purified CD4⁺ T cells from 2D2 mice into Rag^{-/-} recipients. Two weeks later, we immunized mice with MOG/CFA. This model of EAE has accelerated disease onset compared to that in intact WT animals. To replicate the regimen in which anti-CD48 treatment starts before the onset of disease, we gave antibody on days 4, 7 and 10 after immunization. Anti-CD48 was protective in this model, significantly attenuating disease (**Figure 5.5A**), and delaying the day of onset (**Figure 5.5B**). This suggests that CD8 T cells and B cells are not required for anti-CD48-mediated attenuation of EAE.

NK cells are not required for anti-CD48-mediated attenuation of EAE

NK cells are reported to modulate EAE (Zhang et al. 1997; Huang et al. 2006; Winkler-Pickett et al. 2008; Hao et al. 2010; Garcia et al. 2013; Dungan et al. 2014). NK cells can lyse activated T cells during an immune response (Lu et al. 2007), while CD48 on target cells can limit NK-mediated lysis by binding to CD244 on the NK cell (Mooney et al. 2004). We hypothesized that blocking CD48 during EAE might allow un-checked killing of activated CD4⁺ T cells by NK cells, and thus reduce the size of the Teff pool such that mice do not develop EAE. To test this hypothesis, we eliminated NK cells in two different ways. First, we depleted NK cells in WT mice with the anti-NK1.1 mAb PK136. Anti-NK1.1 was administered one day before MOG/CFA immunization, and every 5-6 days thereafter. Anti-CD48 was administered on days 6, 9 and 12 after immunization. As shown in **Figure 5.5C**, mice receiving anti-NK1.1 plus anti-CD48 were significantly protected from EAE compared to mice receiving anti-NK1.1 only. Among all anti-NK1.1 treated mice, anti-CD48 significantly reduced disease incidence, day of onset (**Figure 5.5D**), and peak score compared to mice receiving anti-NK1.1 plus cIgG (**Figure 5.5E**).

As a second method to examine the role of NK cells, we transferred purified CD4⁺ T cells from 2D2 mice into Il2rcy^{-/-}Rag2^{-/-} recipients, which lack NK, B and T cells. After allowing 2 weeks for homeostatic proliferation, mice were immunized with MOG/CFA. EAE in this model was accelerated and severe. A representative experiment is shown in **Figure 5.5F**. Anti-CD48 administration on days 4 and 7 significantly delayed disease onset (**Figure 5.5G**) and reduced the severity of disease on days 8 and 9 (**Figure 5.5F**), but did not significantly reduce the median peak disease score (**Figure 5.5H**) or the number of 2D2 CD4⁺ T cells in the CNS (**Figure 5.5I**). These data suggest that NK cells may contribute to the mechanism of anti-CD48-mediated attenuation of

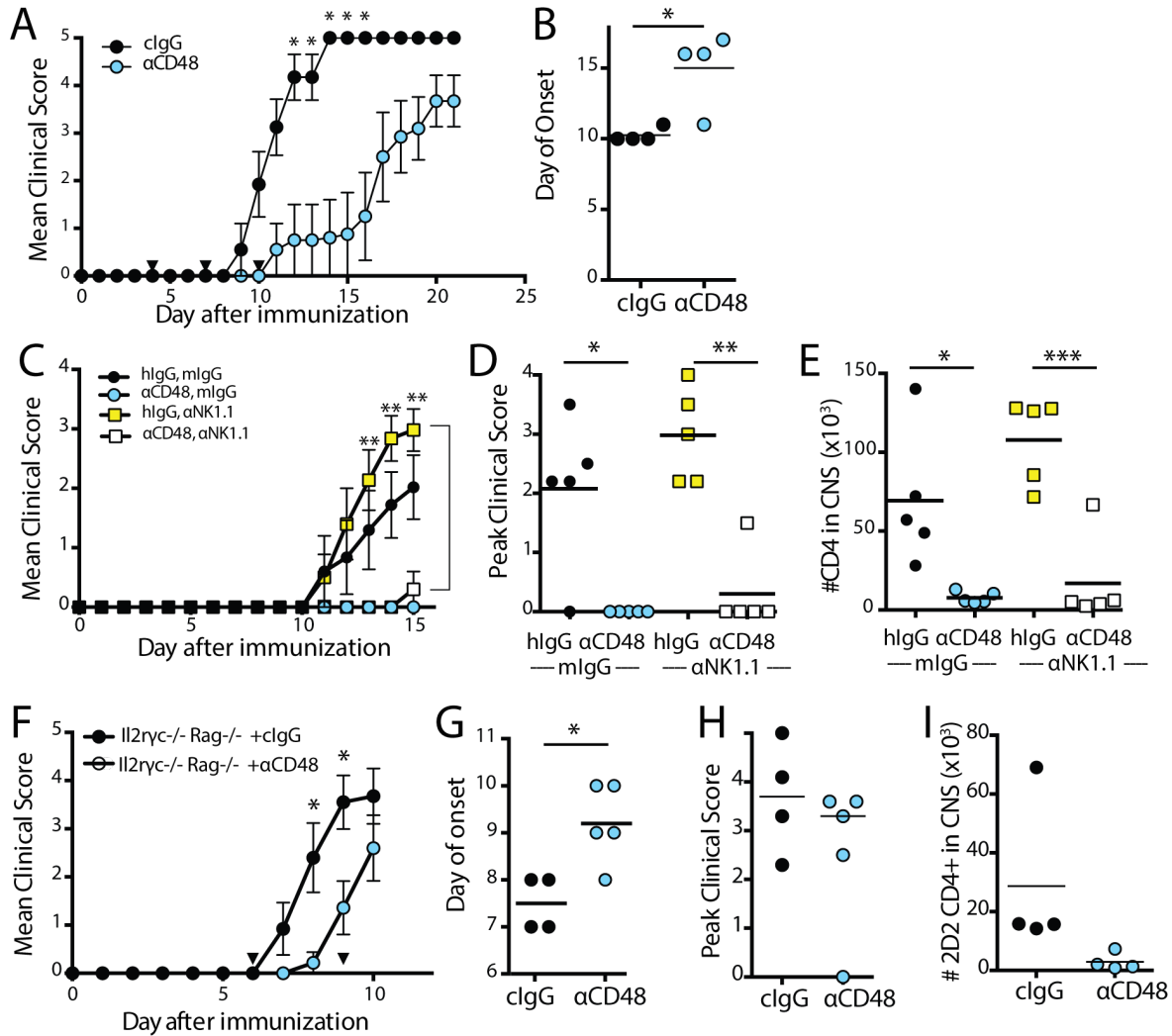


Figure 5.5 B cells, CD8+ T and NK cells are not required for anti-CD48-mediated attenuation of EAE.

A-B. CD4⁺ T cells from 2D2 TCR Tg mice were purified by flow cytometry and injected i.v. into Rag^{-/-} recipients. Two weeks later, after homeostatic proliferation, mice were immunized s.c. with 50μg MOG[35-55] in CFA to induce EAE, and given 100ng of pertussis toxin on day 0 and 2 after immunization. 200μg of anti-CD48 or cIgG was given on days 4, 7 and 10 after immunization (black triangles), and mice were monitored daily for clinical disease. A. Mean clinical scores, ±SEM. B. Day of disease onset. C-E WT mice were immunized for EAE as described above. 200μg of anti-NK1.1 or isotype control (mouse IgG1) was given one day before immunization and every 5 days thereafter to deplete NK cells. 200μg of anti-CD48 or isotype control (Armenian hamster IgG) was given on days 6, 9 and 12 after immunization (black triangles). C. Mean clinical scores, ±SEM. D. Peak clinical score. E. Number of CD4⁺ T cells recovered from the CNS of mice on day 15 after immunization. F-J. CD4⁺ T cells from 2D2 TCR Tg mice were purified by MACS and injected into Il2Ryc^{-/-}Rag^{-/-} mice, which lack T, B and NK cells. Two weeks later, after homeostatic proliferation, mice were immunized s.c. with 50μg MOG[35-55] in CFA to induce EAE, and given 100ng pertussis toxin on day 0 only. 200μg of anti-CD48 or cIgG was given on days 4 and 7 after immunization (black triangles). F. Mean clinical scores, ±SEM. G. Day of onset. H. Peak clinical score. J. Number of CD4⁺ T cells recovered from the CNS on day 10. A-B, n=4 mice per group, representative of 3 independent experiments with 4-6 mice per group. C-E, n=5 mice per group, representative of 4 independent experiments with 5 mice per group. F-G n=4-5 mice per group, representative of 3 independent experiments with 4-5 mice per group. Lines in dot plots represent mean. *p<0.05, **p<0.01, ***p<0.001, ****p<0.0001. Statistical significance calculated with Mann-Whitney test (A, C, D, F, H) or Student's t test (B, E, G, J).

EAE, but that NK cells do not appear to be solely responsible, as anti-CD48 was still capable of attenuating disease in mice lacking NK cells.

CD244 is not required for anti-CD48 to delay onset of EAE

We hypothesized that anti-CD48 treatment might block EAE by interrupting a critical interaction between CD48 and one of its ligands, CD2 or CD244. CD2^{-/-} mice are not commercially available, so we were unable to test the effect of anti-CD48 in CD2^{-/-} mice. As an alternative approach to examine the role of CD2:CD48 interactions in EAE, we administered the anti-CD2 mAb (RM2-1) to both WT and CD48^{-/-} mice during EAE. Anti-CD2 antibodies are reported to have a strong immunosuppressive effect (Chavin et al. 1993), and we found that a single dose of anti-CD2 was capable of delaying and attenuating EAE in WT mice (**Figure 5.6A**). However, anti-CD2 was also capable of attenuating EAE in CD48^{-/-} mice (**Figure 5.6B**), suggesting that the mechanism of action of this antibody was independent of CD48. Because this did not aid our investigation of the role of CD48, we did not pursue this further.

To examine whether anti-CD48 interrupted a critical interaction with CD244, we used CD244^{-/-} mice. CD244^{-/-} mice were immunized with MOG/CFA, and received anti-CD48 or cIgG on days 7, 10 and 13 after immunization. A representative experiment is shown in **Figure 5.6C**, in which anti-CD48 delayed onset of EAE, but did not entirely block disease. The day of onset was significantly delayed (**Figure 5.6D**), and the median peak clinical score by day 17 was significantly reduced (**Figure 5.6E**). However, in other experiments in which we monitored mice until later time points, CD244^{-/-} mice developed severe EAE after cessation of anti-CD48 treatment. This suggests that CD244 is not required for anti-CD48 to delay onset of EAE, but might be involved in sustained attenuation of disease.

Anti-CD48 limits antigen-specific cytokine production in the spleen

Next we examined the effects of anti-CD48 at time points prior to disease onset. One of the factors important for development of EAE is differentiation and expansion of MOG-specific Teff. We hypothesized that anti-CD48 might attenuate disease by altering the initial activation of CD4⁺ Teff in the periphery. To investigate this, we examined cytokine production by peripheral Teff prior to disease onset. WT mice were immunized

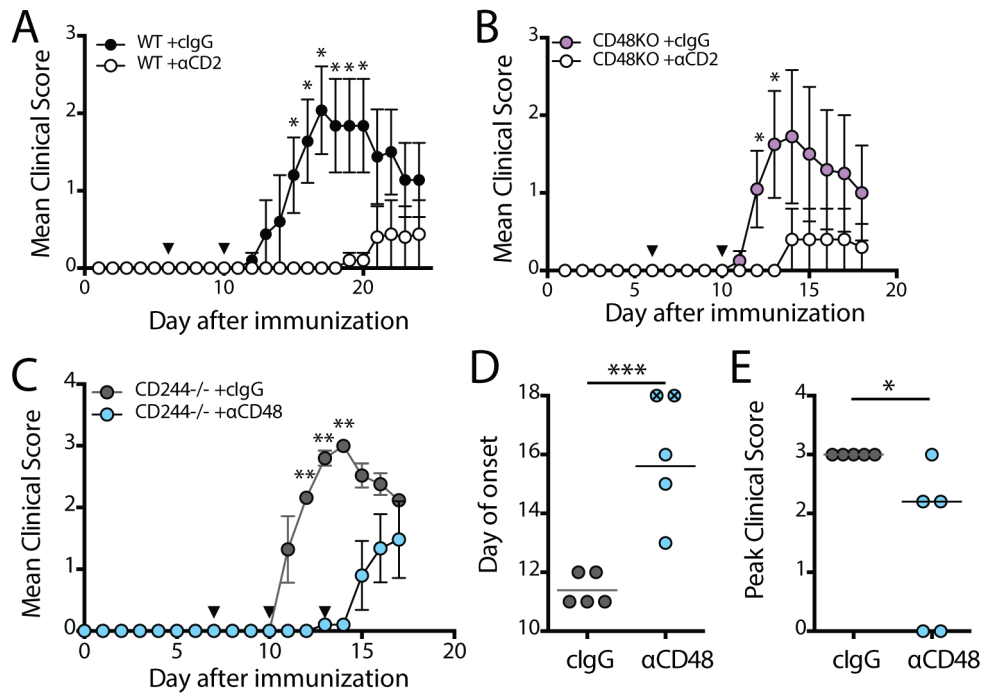


Figure 5.6 Anti-CD2 attenuates EAE independently of CD48, and anti-CD48 attenuates EAE in CD244^{-/-} mice. Mice were immunized s.c. with 50 μ g of MOG[35-55] emulsified in CFA to induce EAE, and given 100ng of pertussis toxin i.p. on days 0 and 2. A. Mean clinical scores, \pm SEM, in WT mice that received 200 μ g of anti-CD2 (RM2-1) or control IgG (rat IgG2a) on days 5 and 10 after immunization (black triangles). B. Mean clinical scores, \pm SEM, in CD48^{-/-} mice that received anti-CD2 or clgG as described in (A). C-E. CD244^{-/-} mice were immunized for EAE as described. On days 7, 10 and 13 after immunization mice received 200 μ g of anti-CD48 or cIgG (black triangles). C. Mean clinical scores, \pm SEM. D. Day of onset. E. Peak clinical scores. A, n=5 mice per group, representative of 2 independent experiments with 4-5 mice per group. B, n=4-5 mice per group. C-E, n=5 mice per group, representative of 6 independent experiments with 5-6 mice per group. Lines in dot plots represent mean. *p<0.05, **p<0.01, ***p<0.001. Statistical significance calculated with Mann-Whitney test (A-C, E) or Student's t test (D).

with MOG/CFA, and given anti-CD48 or cIgG 6 and 9 days later. On day 12, we isolated spleen and inguinal lymph nodes (iLN, draining lymph node from the immunization) and restimulated equal numbers of total cells in vitro with MOG[35-55] peptide. Three days later, we measured cytokines in the supernatants of cultures. We did not observe differences in the amount of IFN γ , TNF α , IL-17 or IL-10 produced by cells from the iLN (**Figure 5.7A, top**). However, we detected significantly less IFN γ , and TNF α in supernatants from restimulated spleen cells. IL-17 was also reduced in the spleen, but this was not statistically significant, and there was no difference in IL-10 (**Figure 5.7A, bottom**). The starting cultures had comparable proportions of CD4+ T cells (**Figure 5.7B**), suggesting that this difference was not due to decreased numbers of CD4+ T cells in the cultures. CD4+ Foxp3+ Tregs are capable of limiting T cell activation and cytokine production (Sakaguchi et al. 2009); however, we did not observe significant differences in the proportion of Foxp3+ cells among CD4+ T cells in the iLN or spleen at day 12, in anti-CD48 treated mice (**Figure 5.7C, D**).

As a second method to assess antigen-specific cytokine production, we examined intracellular cytokine production in MOG-specific 2D2 CD4+ T cells. We first transferred purified CD4+ T cells from 2D2 mice into WT recipients. Mice were then immunized with MOG/CFA, and given anti-CD48 or cIgG 4 and 7 days later. On day 8 after immunization, we collected cells from the blood, spleen and iLN of recipients, restimulated cells with PMA and ionomycin in the presence of GolgiStop, and then stained for intracellular cytokines in both host and 2D2 CD4+ T cells. A representative flow cytometry plot of 2D2 cells from the spleen is shown in **Figure 5.8A**. Mice that received anti-CD48 had a significantly reduced percentage of IFN γ + and IL-17A+ cells among 2D2 cells in the blood and spleen, and a reduced proportion of GM-CSF+ cells in the spleen; there were no differences in the iLN (**Figure 5.8B**). We did not observe differences in the %IL-2+ (data not shown), and observed very few IL-10+ 2D2 CD4+ T cells. The proportion of host CD4+ cells producing effector cytokines was not significantly altered, although there was a statistically significant decrease in the percentage of GM-CSF+ cells among host CD4+ T cells in the iLN (**Figure 5.8C**). Thus, anti-CD48 treatment has a significant effect on antigen-specific cytokine production in the spleen and blood, but minimal effect on antigen-specific cytokine production in the iLN or on non-antigen-specific cytokine production by host CD4+ T cells.

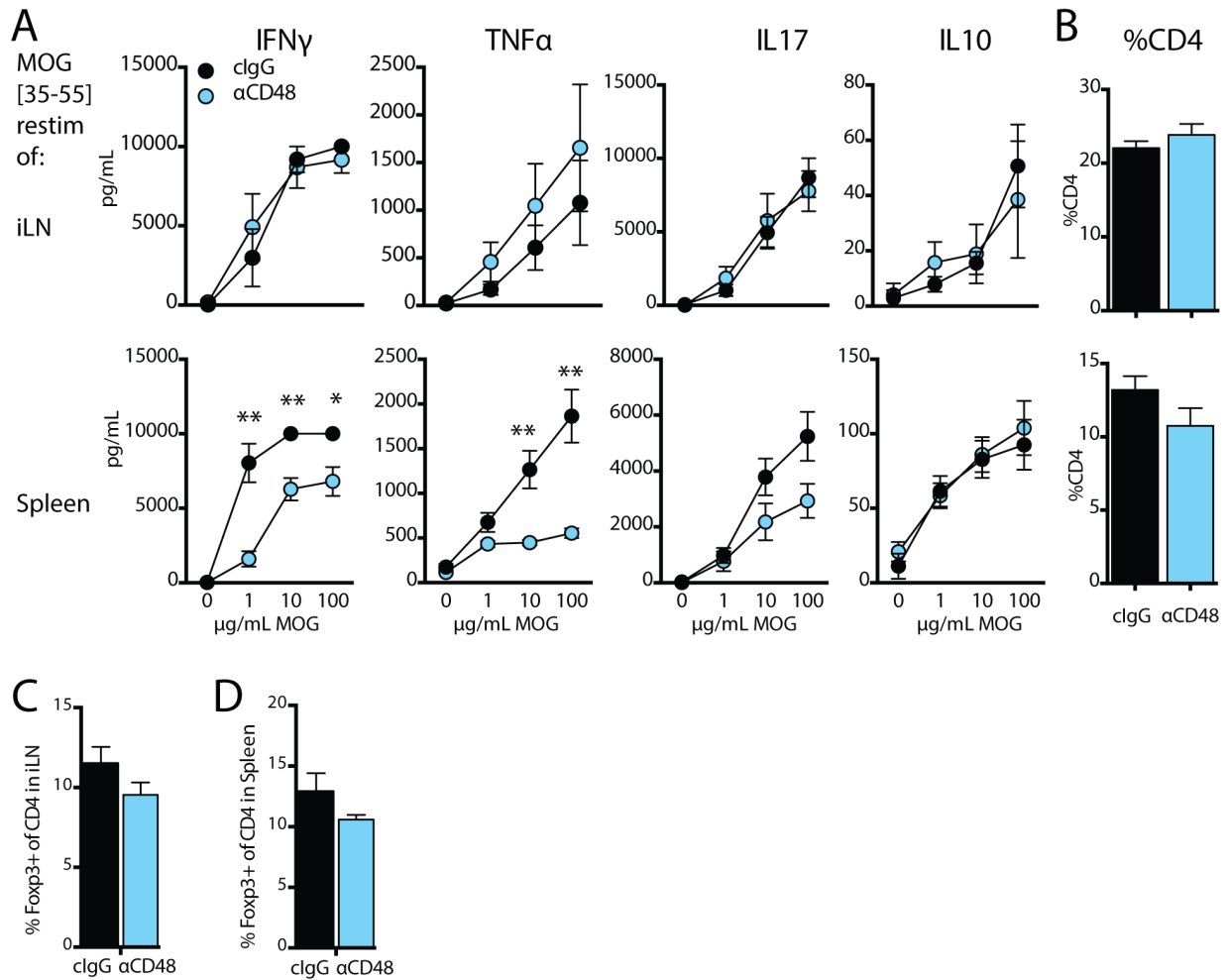


Figure 5.7 Anti-CD48 reduces antigen-specific cytokine production in the spleen but not in the iLN. WT mice were immunized s.c. with 50 μ g of MOG[35-55] emulsified in CFA, and given 100ng of pertussis toxin i.p. on days 0 and 2. 200 μ g of anti-CD48 or cIgG was given i.p. on days 6 and 9. On day 12, spleen and iLN were collected for analysis. **A.** Equal numbers of cells from spleen and iLN were restimulated in vitro with 0, 1, 10 or 100 μ g/mL of MOG[35-55] peptide for 3 days at 37 $^{\circ}$ C. Supernatants were collected and the indicated cytokines were analyzed by cytokine bead array. Top, iLN. Bottom, spleen. **B.** %CD4⁺ of lymphocytes in iLN (top) or spleen (bottom) of samples in A, at the start of culture. **C-D.** In a separate but identical experiment to that in A, iLN and spleen were collected and stained for analysis by flow cytometry. **C.** %Foxp3⁺ of CD4⁺ T cells in the iLN. **D.** %Foxp3⁺ of CD4⁺ T cells in the spleen. A-B, n=5 mice per group, representative of 2 independent experiments with 5 mice per group. C-D, n=5 mice per group, representative of 2 independent experiments with 5 mice per group. Data shown as mean \pm SEM. *p<0.05, **p<0.01. Statistical significance calculated using Student's t test.

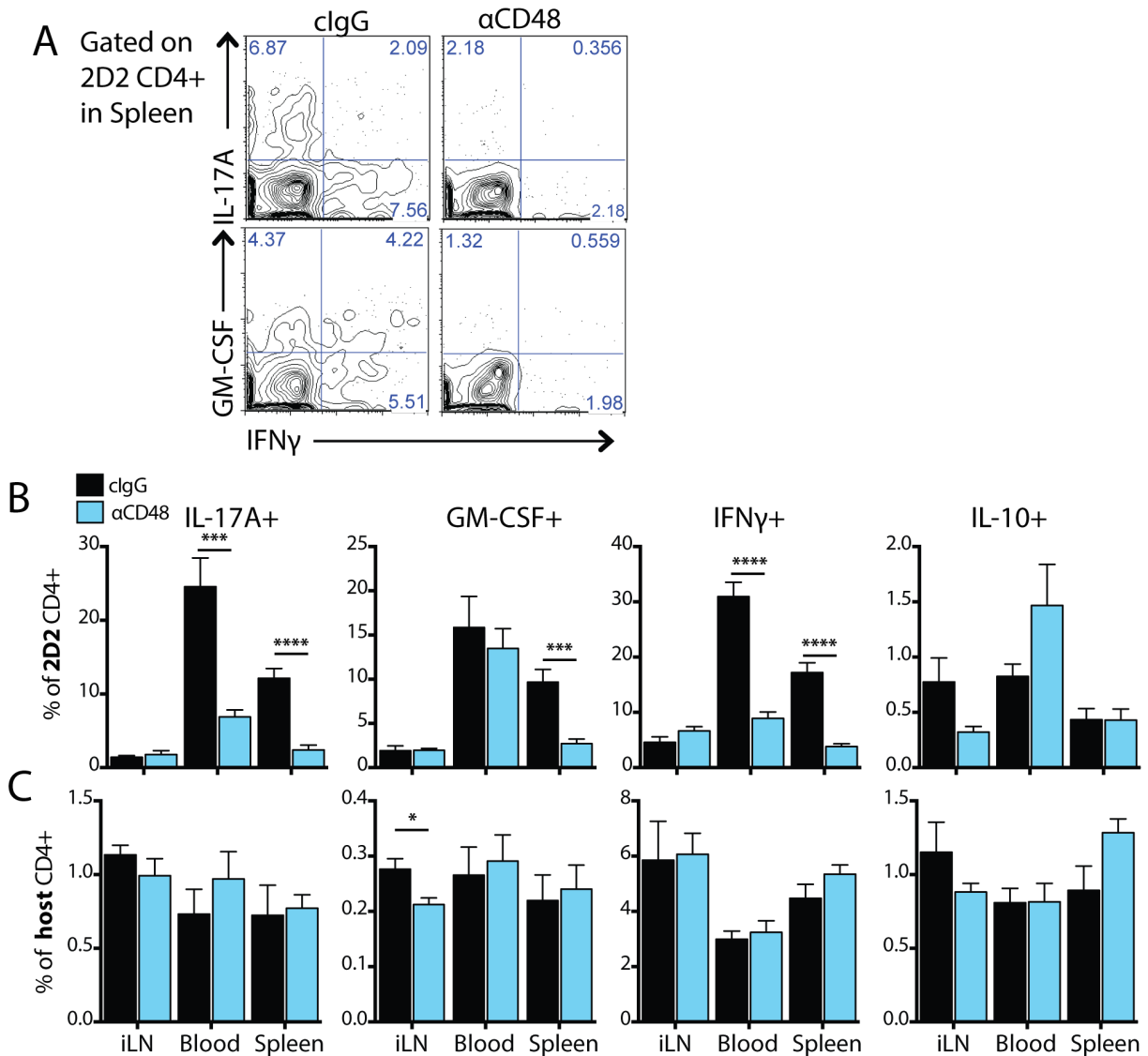


Figure 5.8 Anti-CD48 reduces cytokine production in antigen-specific CD4⁺ T cells, but not bulk CD4⁺ T cells. CD4⁺ T cells from Thy1.1 congenic 2D2 TCR Tg mice were purified by MACS and transferred into Thy1.2 WT recipients i.v. One day later, recipients were immunized with MOG/CFA, but were not given pertussis toxin, and on day 6 mice received anti-CD48 or clgG. On day 8, spleen, iLN and peripheral blood were collected, and lymphocytes were restimulated in vitro with PMA and ionomycin in the presence of GolgiStop. Cells were stained for intracellular cytokine production, and analyzed by flow cytometry. A. Representative flow cytometry plots of intracellular cytokine staining in Thy1.1+ 2D2 CD4⁺ T cells. B. Quantitation of the percentage of IL-17A⁺, IFNγ⁺, GM-CSF⁺ and IL-10⁺ 2D2 CD4⁺ T cells in the spleen, iLN and blood. C. Quantitation of the percentage of IL-17A⁺, IFNγ⁺, GM-CSF⁺ and IL-10⁺ host CD4⁺ T cells. N=7 mice per group, representative of 4 independent experiments with 3-7 mice per group. Bars represent means, error bars represent SEM. *p<0.05, **p<0.01, ***p<0.001, ****p<0.0001. Statistical significance calculated using Student's t test.

Anti-CD48 can attenuate EAE during the effector phase of disease

Since anti-CD48 was effective in blocking EAE prior to disease onset, we next investigated whether it would also be able to attenuate disease in mice that had already developed clinical symptoms. We first tested this by initiating treatment at the first sign of clinical disease: WT mice were immunized with MOG/CFA, and given anti-CD48 on days 0, 3 and 6 after disease onset in each animal. Anti-CD48 was able to limit the severity of disease in this model, significantly reducing the median clinical throughout the course of treatment (**Figure 5.9A**), and significantly reducing the median peak clinical score (**Figure 5.9B**).

As a second approach, we started anti-CD48 treatment after substantial disease progression but before the anticipated 'peak' of disease. A representative experiment is shown in **Figure 5.9C**. In this model anti-CD48 had a slight effect, reducing severity after the peak of disease. The median score was significantly lower for anti-CD48 treated mice on days 18 and 20, but anti-CD48 did not significantly reduce the median peak clinical score (**Figure 5.9D**).

Based on the time frame in which anti-CD48 could significantly attenuate EAE, we hypothesized that this method might be effective after differentiation of encephalitogenic CD4⁺ T_H1, but prior to disease onset. To test this hypothesis, we used an adoptive transfer model of EAE using TH1-polarized CD4⁺ T cells from 2D2 mice. Administration of anti-CD48 on days 6, 9 and 12 after adoptive transfer was able to delay onset, reduce incidence, and limit severity of disease in this model of EAE. A representative experiment is shown in **Figure 5.9E**, in which anti-CD48 completely prevented clinical disease (**Figure 5.9F**). CD4⁺ T cell infiltration of the CNS was significantly reduced, but 2D2 cells were readily detectable in the periphery of anti-CD48 treated mice and were in fact more abundant than in control mice (**Figure 5.9G**). We did not observe any increase in the percentage of Foxp3⁺ cells among CD4⁺ T cells in the CNS, spleen or blood; in fact, the percentage of Foxp3⁺ cells in the CNS was significantly lower in anti-CD48 treated mice (**Figure 5.9H**), similar to our observations with the MOG immunization model (**Figure 5.4I**).

Collectively, these data indicate that anti-CD48 treatment inhibits both the initiation and effector phase of EAE. Anti-CD48 treatment can have a profound effect on clinical disease when initiated prior to disease onset, a

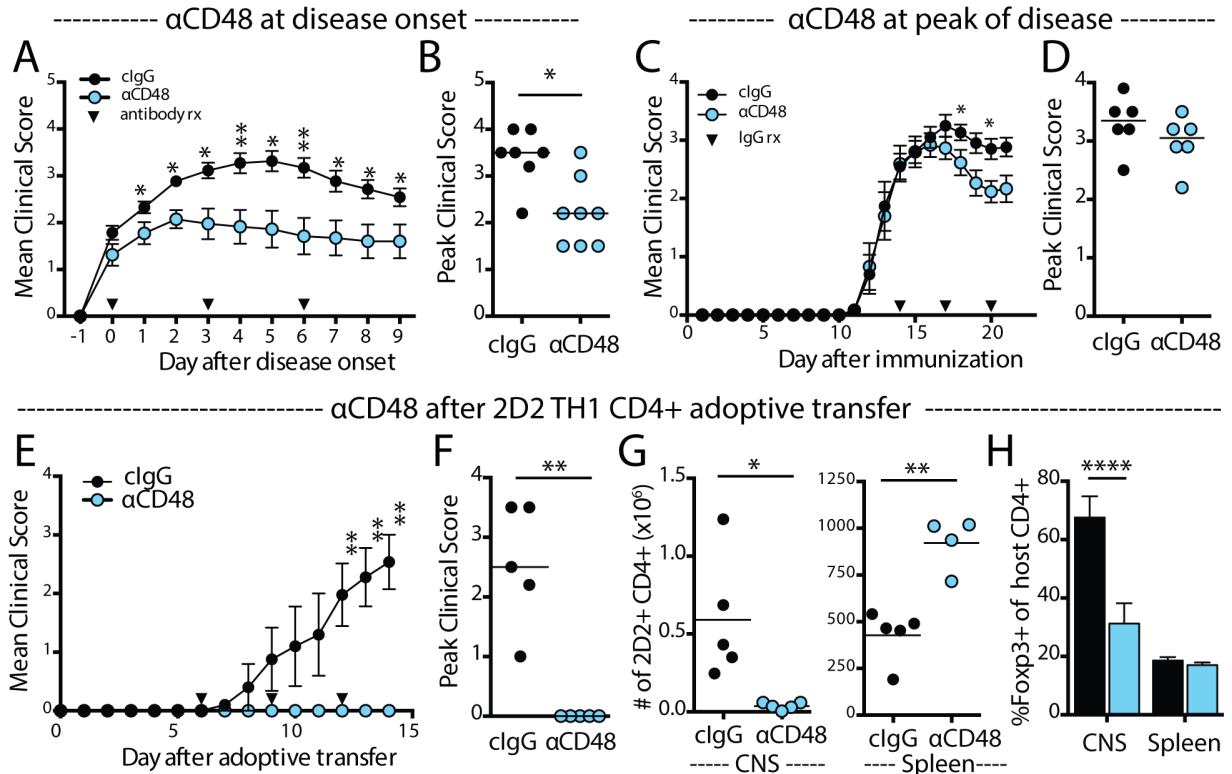


Figure 5.9 Anti-CD48 attenuates EAE during the effector phase of disease. A-B. WT mice were immunized s.c. with 50 μ g MOG[35-55] emulsified in CFA to induce EAE, and given 100ng of pertussis toxin on days 0 and 2. Starting on the first day of clinical disease, mice were then given 200 μ g of cIgG or anti-CD48 every 3 days, 3 doses total (black triangles). A. Mean clinical score \pm SEM, relative to the day of onset of disease. B. Peak clinical scores. C-D. WT mice were immunized with MOG/CFA to induced EAE as described. At day 14, mice were divided into two groups with equal median disease scores, and given 200 μ g of anti-CD48 or cIgG on days 14, 17 and 20 (black triangles). C. Mean clinical scores \pm SEM. D. Peak clinical scores. E-H. CD4⁺ T cells were isolated from 2D2 TCR Tg mice, and then activated in vitro to generate TH1-polarized 2D2 CD4⁺ T cells, as described in materials and methods. WT mice received 3-6 \times 10⁶ 2D2 CD4⁺ T cells i.p. on day 0, followed by 200 μ g of anti-CD48 or cIgG on days 6, 9 and 12 (black triangles). CNS and spleen were collected on day 14 for analysis by flow cytometry. E. Mean clinical scores \pm SEM. F. Peak clinical score. G. Absolute number of 2D2 CD4⁺ T cells in the CNS. H. Absolute number of 2D2 CD4⁺ T cells in the spleen. I. %Foxp3⁺ of host CD4⁺ T cells in CNS, spleen and blood. A-B, n=5 mice per group, representative of 3 independent experiments with 4-8 mice per group. C-D, n=6 mice per group, representative of 2 independent experiments with 5-6 mice per group. E-H, n=5 mice per group, representative of 3 independent experiments with 5-6 mice per group. Bars represent means, error bars represent SEM. Lines in dot plots indicate means. *p<0.05, **p<0.01, ***p<0.001, ****p<0.0001. Statistical significance calculated using Mann-Whitney (A-F) or Student's t test (G-I)

modest but statistically significant effect when initiated at the time of disease onset, and modest effect when initiated after substantial disease progression. Furthermore, anti-CD48 can attenuate EAE mediated by in vitro polarized MOG-specific TH1 CD4⁺ Teff if administered prior to disease onset. Thus, anti-CD48 does not need to be present during differentiation of CD4⁺ Teff in order to have its clinical effects.

Anti-CD48 mAb limits CD4⁺ Teff numbers and proliferation in vivo

The effectiveness of anti-CD48 in limiting EAE even after CD4⁺ Teff differentiation, but prior to disease onset, led us to further investigate the effect of anti-CD48 in the 2D2 TH1 adoptive transfer model of EAE. Because there are few 2D2 CD4⁺ T cells in the CNS of anti-CD48 treated mice (and also to avoid confounding factors of comparing a sick mouse to a healthy mouse), we focused our investigation on cells in the periphery at pre-clinical time points.

To investigate the effect of anti-CD48 on Teff in vivo, we examined 2D2 TH1 cells on day 5 after adoptive transfer. Anti-CD48 treatment on day 3 significantly reduced the absolute number of 2D2 CD4⁺ T cells in the spleen, blood and lymph nodes (**Figure 5.10A**). Anti-CD48 did not alter the proportion of IFN γ ⁺ 2D2 cells in the spleen or lymph nodes, although there was a modest but significant decrease in the percentage of IFN γ ⁺ 2D2 cells in the blood (**Figure 5.10B,C**).

However, the absolute number of IFN γ ⁺ 2D2 Teff cells was dramatically reduced in spleen, blood and iLN (**Figure 5.10D**). This contrasted with our observations using 2D2 cells transferred into WT mice followed by MOG immunization, in which we saw a decrease in the percentage of cytokine-producing 2D2 cells in all compartments examined (**Figure 5.8B, top**). Notably, anti-CD48 did not affect the absolute number of host CD4⁺ T cells (**Figure 5.10E**) or reduce the percentage of Foxp3⁺ host CD4⁺ T cells (**Figure 5.10F**). In fact, there was a modest but significant increase in Foxp3⁺ host CD4⁺ T cells in the spleen only (**Figure 5.10F**). Thus anti-CD48 seemed to selectively reduce the number of 2D2 CD4⁺ Teff, but not host CD4⁺ Treg or Tconv.

We considered that the decrease in 2D2 Teff cell number could be due to reduced proliferation or survival. To investigate the effect of anti-CD48 on proliferation of Teff, we first examined Ki67 expression. Anti-CD48

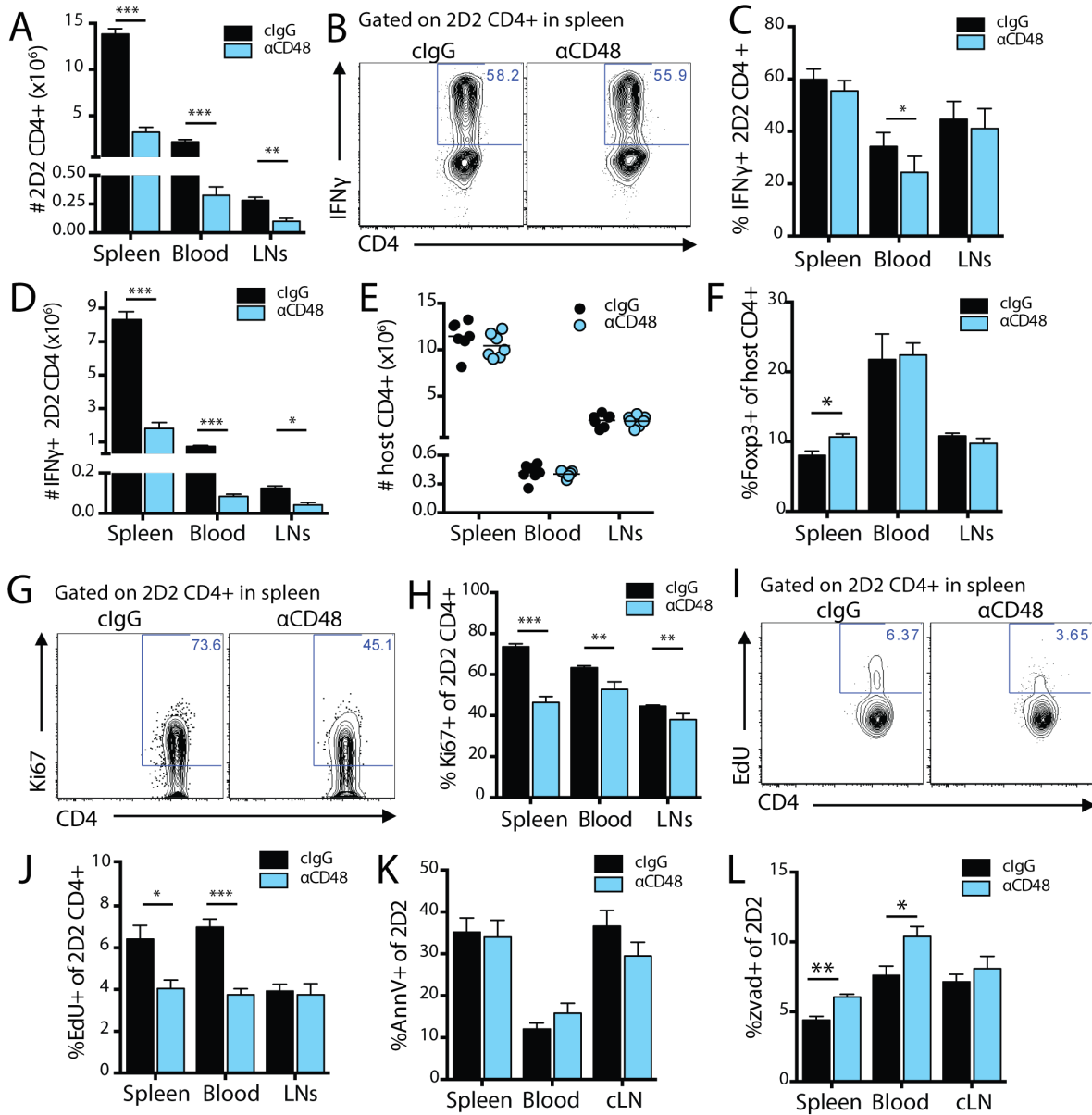


Figure 5.10 Anti-CD48 limits CD4⁺ T cell number and proliferation in vivo. CD4⁺ T cells from 2D2 TCR Tg mice were purified by MACS, polarized in vitro under TH1 conditions for 6 days, restimulated on anti-CD3/anti-CD28-coated plates for 24 hrs, then adoptively transferred to WT recipients. Mice received 200 μ g of anti-CD48 or clgG on day 3, and 800 μ g of EdU i.p. on day 4. On day 5 spleen, blood and skin-draining lymph nodes (LN) were collected for analysis. A. The absolute number of 2D2 CD4⁺ T cells in spleen, LNs and blood. B-D. Cells were restimulated in vitro with PMA and ionomycin in the presence of GolgiStop to assess intracellular cytokine production. B. Representative staining of IFN γ on Thy1.1+CD4⁺ 2D2 cells from the spleen. C. Quantitation of the %IFN γ 2D2 CD4⁺ T cells. D. Absolute number of IFN γ + 2D2 CD4⁺ T cells. E. Absolute number of host CD4⁺ T cells. F. %Foxp3⁺ of host CD4⁺ T cells. G. Representative Ki67 staining in 2D2 CD4⁺ T cells from the spleen. H. Quantitation of the %Ki67+2D2 CD4⁺ T cells. I. Representative EdU staining in 2D2 CD4⁺ T cells from the spleen. J. Quantitation of %EdU+ 2D2 CD4⁺ T cells. K-L In an identical, independent experiment, apoptosis was analyzed. K. Cells were incubated with ZVAD-FMK-fluorescein for 30 minutes at 37 $^{\circ}$ C, to label active caspases, then analyzed by flow cytometry. Quantitation of %ZVAD+ of 2D2 CD4⁺ T cells. L. %AnnV+ of 7AAD- 2D2 CD4⁺ T cells. Bars represent means, error bars represent SEM. *p<0.05, **p<0.01, ***p<0.001, ****p<0.0001. Statistical significance calculated using Student's t test.

treated mice had a significantly lower percentage of Ki67+ 2D2 cells, in both the spleen and blood but not in the lymph nodes (**Figure 5.10G-H**). In some experiments we also gave a single i.p. injection of EdU 14 hours before euthanasia, to label cells that were actively dividing. The percentage of EdU+ 2D2 CD4+ T cells was also significantly reduced in the spleen and blood of anti-CD48 treated mice, but not in the iLN (**Figure 5.10I-J**).

To investigate whether anti-CD48 might also limit 2D2 CD4+ Teff cell number by increasing cell death, we examined the proportion of apoptotic cells among 2D2 CD4+ T cells. We did not see a significant increase in the percentage of AnnV+7AAD- among CD4+ 2D2 cells from mice treated with anti-CD48 (**Figure 5.10K**). As another measure of apoptosis, we incubated cells ex vivo with FITC-ZVAD-FMK to label cells with active caspases. We saw a significant increase in the percentage of ZVAD+ 2D2 CD4+ T cells in the spleen and blood, but not in the iLN (**Figure 5.10L**). This suggests that anti-CD48 might increase Teff propensity for apoptosis.

Anti-CD48 limits proliferation of WT Teff restimulated with WT APCs, and to a lesser extent with CD48^{-/-} APCs

We next asked whether anti-CD48 mediated its effect on proliferation by interacting with CD48 on CD4+ T cells, APCs, or both. We first investigated this in vitro, by comparing the effect of anti-CD48 on proliferation of 2D2 CD4+ Teff restimulated with MOG plus WT or CD48^{-/-} APCs. We generated TH1-polarized T cells using a similar protocol for generating TH1 Teff. CD4+ T cells from 2D2 mice were cultured with IL-12, anti-IL4, anti-CD3, and irradiated splenocytes. After 6 days of culture, we collected live cells, labeled cells with CellTrace Violet, and restimulated them with MOG[35-55] and splenocytes from either TCR α ^{-/-} or CD48^{-/-} TCR α ^{-/-} mice. Anti-CD48 or cIgG was added at a final concentration of 5 μ g/mL. On day 4 of culture we assessed CellTrace Violet dilution by flow cytometry. Representative histograms are shown in **Figure 5.11**. We found that at intermediate doses of MOG, anti-CD48 could limit proliferation of T cells cultured with WT APCs, as assessed by CellTrace Violet dilution (**Figure 5.11, top**). Proliferation with CD48^{-/-} APCs was less than with WT APCs; although anti-CD48 could still limit proliferation, this effect was less pronounced with

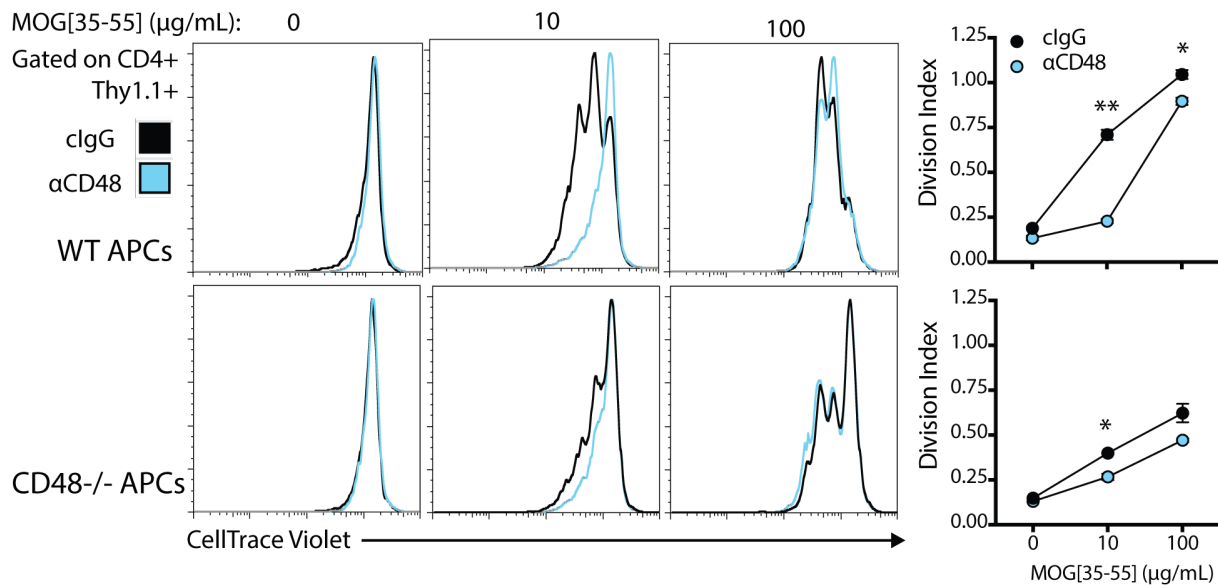


Figure 5.11 Anti-CD48 limits proliferation of WT Teff when stimulated with WT APCs, and to a lesser extent when stimulated with CD48^{-/-} APCs. CD4⁺ T cells were purified by MACs from 2D2 TCR Tg mice, and polarized in vitro under TH1 conditions for 6 days. Live cells were purified, labeled with CellTrace Violet, and restimulated in vitro with TCR $\alpha^{-/-}$ splenocytes (top) or CD48^{-/-}TCR $\alpha^{-/-}$ splenocytes (bottom) and MOG peptide in the presence of cIgG (black) or anti-CD48 (gray). After 3 days, proliferation was assessed by flow cytometry, and division index was calculated as the average number of divisions per cell, for all cells in culture (FlowJo). Data are from duplicate wells, representative of 5 independent experiments. *p<0.05, **p<0.01. Statistical significance calculated using Student's t test.

CD48^{-/-} APCs (**Figure 5.11, bottom**). This indicated that anti-CD48 was capable of limiting Teff proliferation in vitro, and suggested that this effect was partially dependent on CD48 expression on APCs.

Anti-CD48 reduces the number of WT CD4⁺ 2D2 Teff in CD48^{-/-} hosts without reducing proliferation

Because anti-CD48 had only a limited effect on proliferation of 2D2 CD4⁺ Teff in vitro when stimulated with CD48^{-/-} APCs, we next adapted this to an in vivo model in order to further assess the effects of anti-CD48 on Teff. We generated WT 2D2 TH1 CD4⁺ Teff as described in materials and methods, and adoptively transferred these to CD48^{-/-} recipients. Anti-CD48 or cIgG was given on day 5 after adoptive transfer and on day 7 we analyzed cells from the spleen by flow cytometry. In some cases, EdU was given i.p. 16 hours before harvest. As shown in a representative flow cytometry plot in **Figure 5.12A**, anti-CD48 treatment resulted in an ~10-fold decrease in the percentage of 2D2 CD4⁺ Teff in the spleen of CD48^{-/-} mice. This reduction was also present in the lymph nodes and the blood (**Figure 5.12B**). In contrast to our observations in WT recipients, anti-CD48 also reduced the percentage of IFN γ ⁺ 2D2 CD4⁺ Teff in the lymph nodes and spleen as well as the blood (**Figure 5.12C**). This reduction in cell abundance did not appear to be due to decreased proliferation, as neither the percentage of Ki67⁺ nor the percentage of EdU⁺ 2D2 Teff was significantly reduced (**Figure 5.12D, E**). We did observe an increase in the percentage of ZVAD⁺ 2D2 Teff, which was statistically significant in the blood and spleen (**Figure 5.12F**).

These results suggested that anti-CD48 could have cell intrinsic effects on CD4⁺ Teff that affected cell survival. To further investigate cell intrinsic effects of CD48 on T cells, we performed transcriptional analysis on Teff from anti-CD48-treated and control mice. We used the same protocol described above, transferring WT 2D2 TH1 Teff to CD48^{-/-} recipients on day 0, administering anti-CD48 or cIgG on day 6, and harvesting cells on day 7. 2D2 Teff were purified from the spleen as CD4⁺Thy1.1+V β 11+V α 3.2⁺ cells, using flow cytometry, then counted and frozen for storage. We analyzed cells from 8 individual mice (4 treated, 4 controls) taken from 2 independent experiments. Cells were lysed and mRNA expression was examined using a custom NanoString probe set (generously provided by Youjin Lee in the lab of Dr. Vijay Kuchroo at BWH and HMS) and the nCounter analysis system. Data was analyzed using the nSolver Analysis Software. The probe set

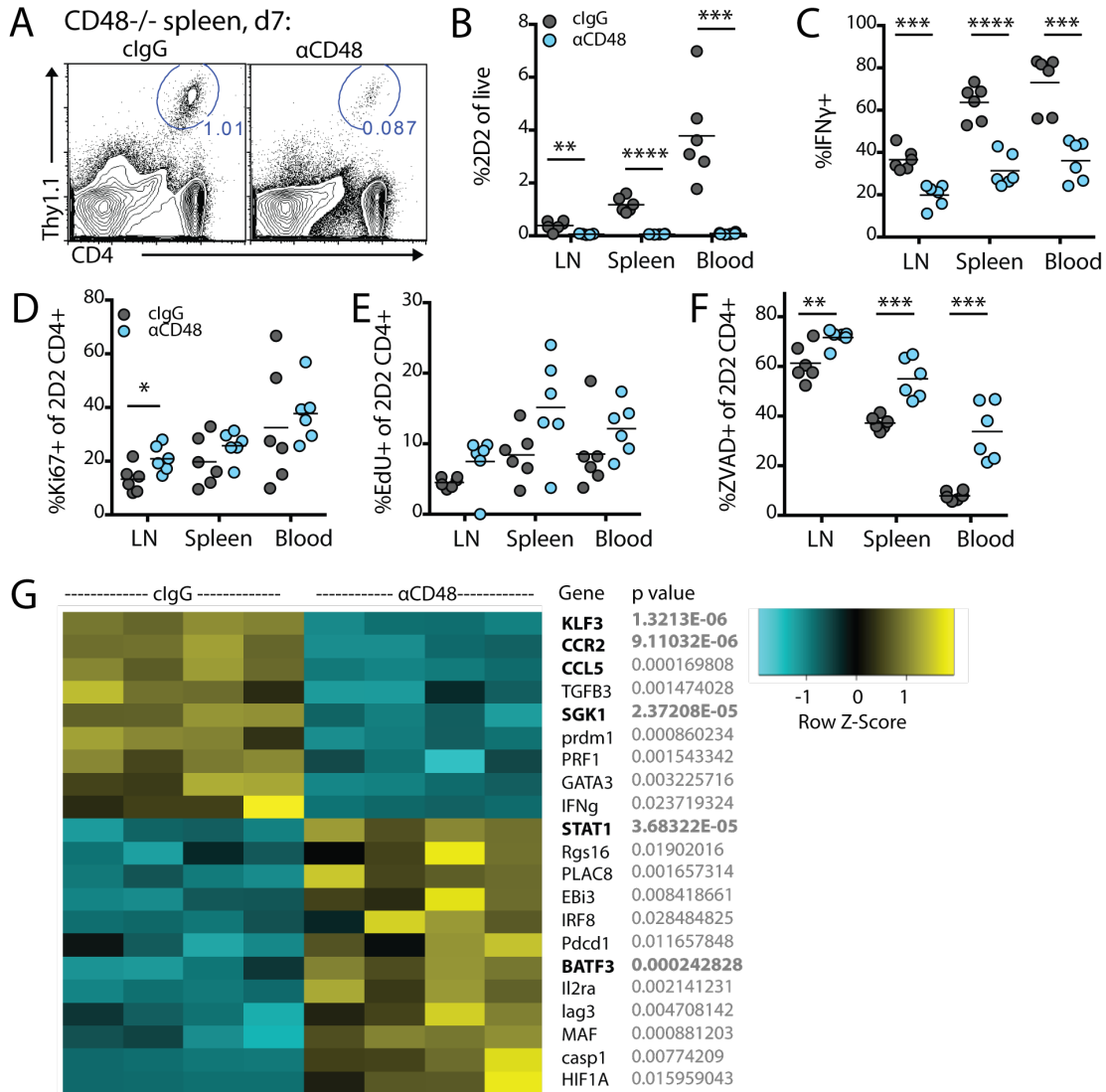


Figure 5.12 Anti-CD48 limits WT CD4⁺ 2D2 Teff cell number in CD48^{-/-} hosts without affecting proliferation. CD4⁺ T cells were isolated from 2D2 TCR Tg mice, and activated in vitro under TH1-polarizing conditions as described in materials and methods, to generate 2D2 TH1 CD4⁺ Teff cells. $3\text{-}6 \times 10^6$ 2D2 CD4⁺ Teff were adoptively transferred to CD48^{-/-} recipients. Mice received 200 μ g of anti-CD48 or cIgG on day 5, followed by 800 μ g of EdU i.p. on day 6. On day 7 spleen, blood and skin-draining lymph nodes (LN) were collected for analysis. **A.** Representative flow cytometry plot of the percentage of Thy1.1+ donor 2D2 cells among total splenocytes. **B.** Quantification of the percentage of donor 2D2 CD4⁺ T cells among total cells collected from LN, spleen and blood. **C.** Cells were restimulated in vitro with PMA and ionomycin in the presence of GolgiStop, to assess intracellular cytokine production. %IFN γ + of 2D2 CD4⁺ T cells in the LNs, spleen and blood. **D.** %Ki67+ of 2D2 CD4⁺ T cells. **E.** %EdU+ of 2D2 CD4⁺ T cells. **F.** Cells were incubated with FMK-ZVAD-fluorescein for 30 minutes at 37°C to measure active caspases. %ZVAD+ of 2D2 CD4⁺ T cells. **G.** 2D2 cells (Thy1.1+CD4+VB11+Va3.2+ Thy1.2-) were sorted from spleens on day 7 and frozen for mRNA analysis by NanoString. Heatmap shows the relative increase (yellow) or decrease (cyan) in expression for 22 genes that were most differentially expressed between cIgG and anti-CD48-treated mice, as determined using the nSolver analysis software. A-F, n=6 mice per group, representative of 3 independent experiments using 5-6 mice per group. G, n=4 mice per group, from two independent cell transfer experiments. A-F, *p<0.05, **p<0.01, ***p<0.001, ****p<0.0001. Statistical significance calculated using Student's t test. G, bold indicates p<0.00025 (Bonferroni correction for testing 199 genes, with 0.05 total FDR). NanoString experiment performed under the guidance of Youjin Lee, in the lab of Dr. Vijay Kuchroo at BWH and HMS.

examined 199 genes, including 4 housekeeping genes (beta actin, GAPDH, Tubb5, HPRT). We found that 122 genes were expressed above the level of detection, 48 genes had an average fold change of 1.5 or greater, and 14 genes had an average fold change 2.5 or greater. We found that 6 genes had a fold change greater than 2 and a p value less than 0.00025 (Bonferroni correction for 199 genes queried). The expression data are summarized in **Figure 5.12G**. Using flow cytometry, we validated some of the transcriptional changes: anti-CD48 treatment resulted in decreased %IFN γ +, no difference or increased %CCR2+, increased %CD25+ or CD25 MFI, decreased %GM-CSF+, and increased ZVAD-FMK-fluorescein staining (data not shown). We observed very low PD1 and Lag3 expression in both groups (data not shown). This suggests that anti-CD48 treatment might have an effect on the pathogenicity or survival of 2D2 CD4+ Teff, independent of any effects on APCs.

An Fc receptor blocking antibody limits the effects of anti-CD48 on 2D2 CD4+ Teff numbers in vivo

Although the effects of anti-CD48 on CD4+ Teff proliferation and/or survival might account for the reduced cell number, we considered that anti-CD48 treatment might also exert its effects, at least in part, by depleting CD4+ Teff—particularly since we had observed that activated cells have high CD48 surface expression. NK cells and macrophages can mediate antibody-dependent cellular cytotoxicity via Fc receptors, and complement factors can also bind to antibody Fc regions to promote phagocytosis via complement receptors. To investigate whether the effects of anti-CD48 involved FcR-mediated mechanisms, we co-administered anti-CD16/CD32 antibody (clone 93, anti-Fc γ RII/III) along with anti-CD48 or cIgG, to block FcRs. 2D2 TH1 CD4+ Teff were adoptively transferred to WT mice on d0, 200 μ g of each antibody was given i.p. on day 3 (pre-mixed prior to injection), and spleen and blood were collected for analysis on day 5. Although anti-CD48 dramatically reduced the number of 2D2 Teff in the periphery, when compared to mice receiving cIgG only, anti-CD48 plus anti-CD16/CD32 did not significantly reduce the number of 2D2 Teff compared to mice receiving anti-CD16/CD32 only (**Figure 5.13A**). Interestingly, mice that received anti-CD48 plus anti-CD16/CD32 still had reduced %Ki67+ 2D2 CD4+ T cells, compared to mice receiving anti-CD16/CD32 only (**Figure 5.13B**). The percentage of IFN γ + was modestly increased in mice receiving anti-CD16/CD32+anti-CD48, compared to mice receiving anti-CD16/CD32 alone (**Figure 5.13C**), and anti-CD48 did not reduce the absolute number of IFN γ + 2D2 CD4+ Teff in mice receiving anti-CD16/CD32 (**Figure 5.13D**). In contrast, other effects of anti-CD48 on 2D2 CD4+ Teff persisted with co-administration of anti-CD16/CD32, such as reduced VLA-4 MFI (**Figure**

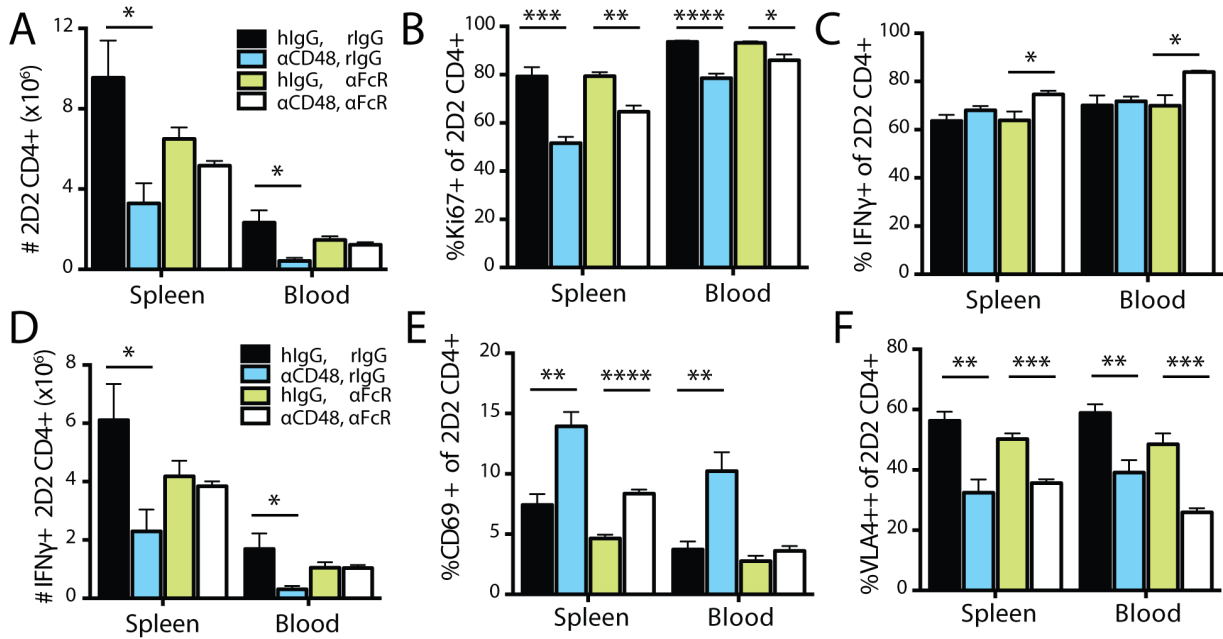


Figure 5.13 FcγRII/III are required for anti-CD48 mediated reduction of 2D2 CD4+ Teff numbers.

CD4+ T cells were isolated from 2D2 TCR Tg mice and activated under TH1-polarizing conditions as described in materials and methods. $3-6 \times 10^6$ 2D2 CD4+ Teff were adoptively transferred to WT recipients. 200μg of anti-CD48 or cigG, pre-mixed with 200μg of either anti-CD16/CD32 or isotype control (rat IgG2a), was given i.p. on day 3 after cell transfer. On day 5, spleen and blood were collected for analysis by flow cytometry. A. Number of 2D2 CD4+ Teff in the spleen and blood. B. %Ki67+ of 2D2 CD4+ Teff. C. Lymphocytes from spleen and blood were restimulated in vitro with PMA and ionomycin in the presence of GolgiStop to assess intracellular cytokine production. %IFNγ+ of 2D2 CD4+. D. Absolute number of IFNγ+ 2D2 CD4+ T cells. E. %CD69+ of 2D2 CD4+ T cells. F. %VLA4hi of 2D2 CD4+ T cells. Representative experiment with n=5 mice per group, representative of 2 independent experiments with 5 mice per group. Bars represent means, error bars represent SEM. *p<0.05, **p<0.01, ***p<0.001, ****p<0.0001. Statistical significance calculated using Student's t test.

5.13E) and increased percentage of CD69+ on 2D2 CD4+ T cells (**Figure 5.13F**). This suggests that part of the effect of anti-CD48 on limiting the number of Teff at early time points is due to an FcR-dependent mechanism, but other effects of anti-CD48 are not FcR-dependent.

Fc receptors contribute to anti-CD48-mediated attenuation of EAE

Because anti-CD16/CD32 abolished the effect of anti-CD48 treatment on reducing 2D2 CD4+ Teff cell numbers, we hypothesized that FcRs might also be required for anti-CD48-mediated attenuation of EAE. To test this, we co-administered anti-CD16/CD32 mAb along with anti-CD48 to WT mice on days 8, 11 and 14 after immunization with MOG/CFA. A representative experiment is shown in **Figure 5.14A**. Mice receiving anti-CD16/CD32 alone had similar disease to mice receiving control IgG only. Anti-CD48 did not significantly attenuate EAE in mice receiving anti-CD16/CD32, compared to mice receiving anti-CD16/CD32 alone, as measured by day of onset (**Figure 5.14B**) and peak clinical score (**Figure 5.14C**). In addition, the number of CD4+ T cells in the CNS was similar in mice that received anti-CD16/CD32 alone or anti-CD16/CD32 plus anti-CD48 (**Figure 5.14D**). These results suggest that an FcR-mediated mechanism contributes to the protective effects of anti-CD48 in EAE.

As a second means to test for the role of FcRs in anti-CD48 mediated attenuation of EAE, we administered anti-CD48 during EAE in *FcγR1*^{-/-} mice, which lack all FcγRs (**Figure 5.14E**). Anti-CD48-treated *FcγR1*^{-/-} mice had a similar disease course compared to those receiving cIgG. Anti-CD48 did not significantly reduce the median peak disease score (**Figure 5.14F**) or the number of CD4+ T cells in the CNS (**Figure 5.14G**). This suggests that FcRs are critical for anti-CD48-mediated attenuation of EAE, although our interpretation is limited by the small group sizes for these experiments with *FcγR1*^{-/-} mice. Combined, these data suggest that anti-CD48-mediated attenuation of EAE is partially dependent on FcRs, likely FcγRII/III, but that this is not solely responsible for protection. FcRs may contribute to anti-CD48 mediated attenuation of EAE by depleting CD48⁺⁺ cells, namely the activated Teff generated either in vitro or in vivo after immunization.

As a third means to investigate this possibility, we used a F(ab')₂ fragment generated from whole anti-CD48 IgG. We tested the ability of this F(ab')₂ to attenuate MOG/CFA induced EAE, in comparison to intact anti-

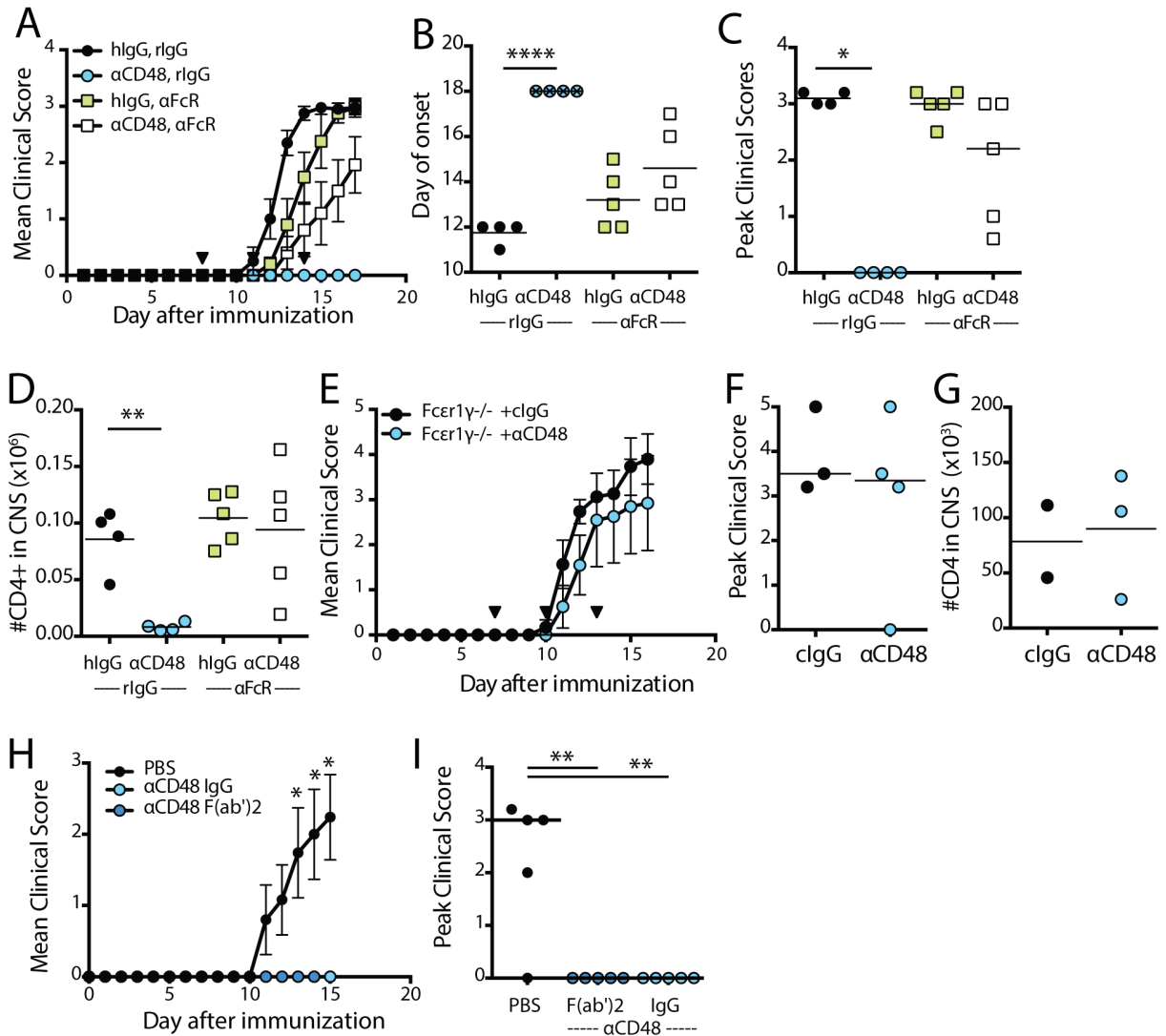


Figure 5.14 Fc γ R_s contributes to anti-CD48-mediated attenuation of EAE. A-D WT mice were immunized s.c. with 50 μ g MOG[35-55] emulsified in CFA to induce EAE, then given 100ng pertussis toxin on days 0 and 2. On days 8, 11 and 14 after immunization, mice were given 200 μ g of cIgG or anti-CD48 pre-mixed with 200 μ g of anti-CD16/CD32 or isotype control (rat IgG2a) (black triangles). A. Mean clinical scores, \pm SEM. B. Day of onset. C. Peak clinical scores. D. Number of CD4+ T cells recovered from the CNS. E-G. Fc γ 1 γ ^{-/-} mice, which lack all Fc γ R_s, were immunized for EAE as described above, and given 200ng of pertussis toxin on days 0 and 2 after immunization. On days 7, 10 and 13 after immunization, mice were given 200 μ g of anti-CD48 or cIgG (black triangles). E. Mean clinical scores, \pm SEM. F. Peak clinical scores. G. Number of CD4+ T cells recovered from the CNS. H-I. WT mice were immunized for EAE as described for (A). Mice received PBS or anti-CD48 IgG on days 6, 9 and 12 after immunization, or anti-CD48 F(ab')₂ on days 7, 10, 12 and 14. A-D, n=4-5 mice per group, representative of 3 independent experiments with 4-5 mice per group. E-G. n=3-4 mice per group, representative of 5 independent experiments with 2-5 mice per group. H-I, n=5 mice per group. *p<0.05, **p<0.01, ***p<0.001, ****p<0.0001. Statistical significance calculated using Mann Whitney test (A, C, E, G) or Student's t test (B, D, G)

CD48 IgG. PBS-treated mice were used as a positive control for disease induction. Because we anticipated a reduced half-life in vivo, 150 μ g F(ab')₂ was given every 2 days starting on day 7 after immunization, while 200 μ g anti-CD48 IgG was given every 3 days starting on day 6. As shown in **Figure 5.14H**, F(ab')₂ completely blocked EAE in WT mice, as did anti-CD48 treatment. Due to limited supply of F(ab')₂, we were able to perform this experiment only once. It is also important to note that in this experiment, the incidence of EAE in PBS-treated mice was only 80% by day 15, suggesting that EAE induction was suboptimal. When considered alongside our data using anti-FcR antibodies and Fc γ 1^{-/-}, this suggests that in a situation of mild EAE, anti-CD48 is able to mediate protection independent of Fc-mediated effects.

Anti-CD48 mAb cannot attenuate EAE mediated by CD48^{-/-} CD4⁺ T cell

We hypothesized that CD48 expression on CD4⁺ Teff would be critical for anti-CD48-mediated attenuation of EAE in a WT host—that is, that anti-CD48 would be unable to attenuate EAE induced with CD48^{-/-} CD4⁺ T cells in a WT recipient. We tested this hypothesis in two EAE models. First, we transferred CD4⁺ T cells from CD48^{-/-} 2D2 mice into Rag^{-/-} recipients, waited 2 weeks for homeostatic proliferation, and then immunized with MOG/CFA to induce EAE and administered anti-CD48. As shown in a representative experiment in **Figure 5.15A**, anti-CD48 treatment on days 6, 9 and 12 after immunization did not significantly affect the day of onset (**Figure 5.15B**), incidence, or median peak disease score (**Figure 5.15C**). Anti-CD48 also had no significant effect on the number of 2D2 CD4⁺ T cells in the CNS (**Figure 5.15D**) by day 13 after immunization.

As a second means to test the importance of CD48 on CD4⁺ T cells for anti-CD48 mediated attenuation of EAE, we transferred CD48^{-/-} 2D2 TH1 CD4⁺ Teff cells into WT recipients and administered anti-CD48 or cIgG on days 6, 9 and 12 after adoptive transfer (**Figure 5.15E**). Anti-CD48 did not delay the day of onset of EAE (**Figure 5.15F**), but anti-CD48 treatment did result in a modest but statistically significant effect on peak disease score (**Figure 5.15G**). Notably, mice treated with anti-CD48 had dramatically reduced numbers of host WT CD4⁺ T cells in the CNS, but increased numbers of CD48^{-/-} 2D2 Teff in the CNS, compared to mice treated with cIgG (**Figure 5.15H**).

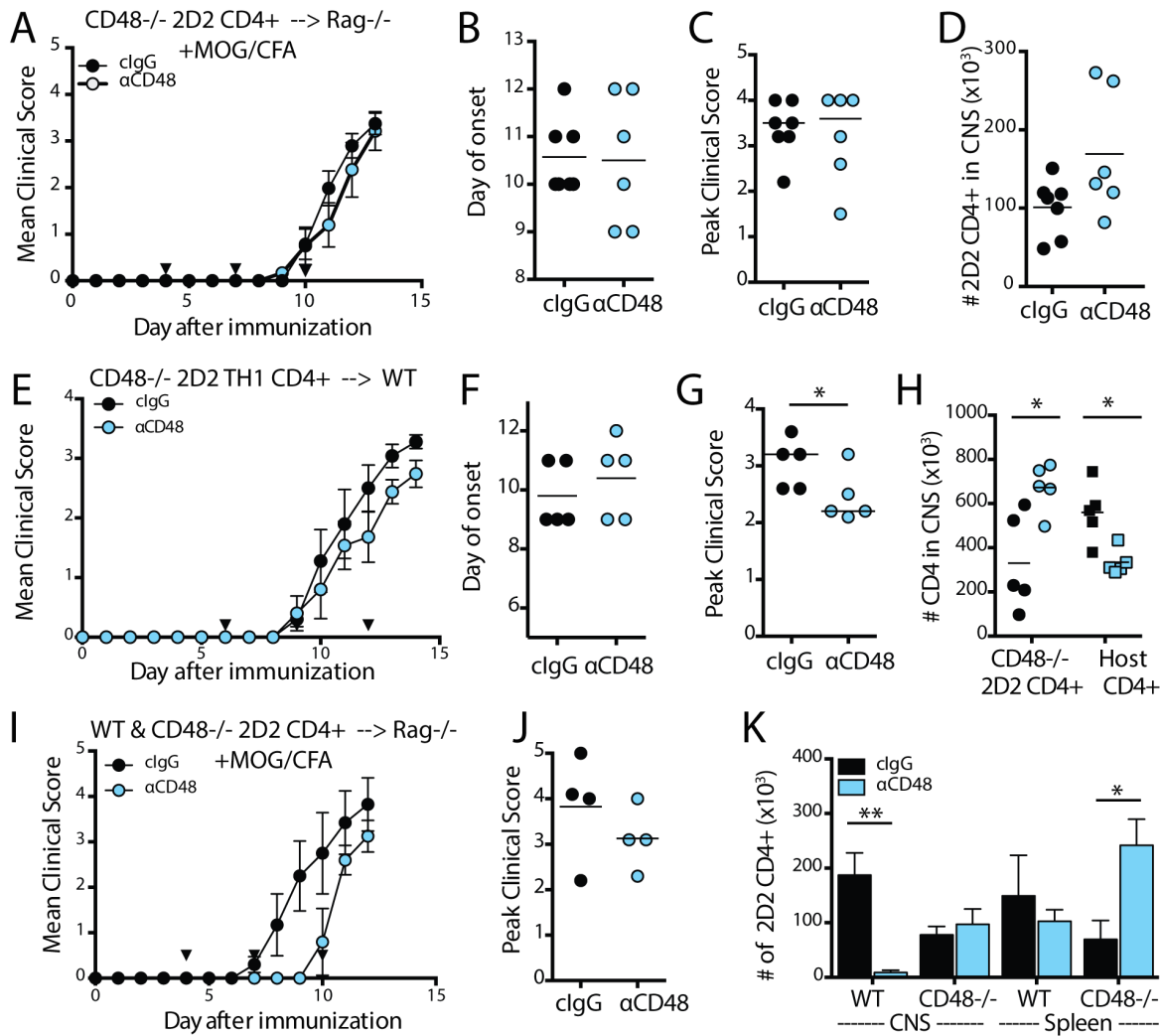


Figure 5.15 Anti-CD48 cannot attenuate EAE induced by CD48^{-/-} CD4⁺ T cells in WT recipients. A-D CD4⁺ T cells were isolated from CD48^{-/-} 2D2 TCR Tg mice, and adoptively transferred to Rag^{-/-} recipients. Two weeks later, after homeostatic proliferation, mice were immunized s.c. with 50μg MOG[35-55] emulsified in CFA to induce EAE, and given 100ng of PT i.p. on days 0 and 2. On days 4, 7 and 10 after immunization 200μg of anti-CD48 or cIgG was given i.p. (black triangles). A. Mean clinical scores, ±SEM. B. Day of onset. C. Peak clinical scores. D. Number of CD48^{-/-} 2D2 CD4⁺ T cells recovered from the CNS. E-H. CD4⁺ T cells were isolated from Thy1.1 CD48^{-/-} 2D2 TCR Tg mice, and activated in vitro under TH1-polarizing conditions as described in materials and methods to generate 2D2 TH1 CD4⁺ Teff. 3-6x10⁶ 2D2 TH1 CD4⁺ Teff were adoptive transferred to Thy1.2 WT recipients, and 200μg of anti-CD48 or cIgG was given i.p. on days 6, 9 and 12 after transfer (black triangles). E. Mean clinical scores, ±SEM. F. Day of onset. G. Peak clinical score. H. Number of CD48^{-/-} 2D2 CD4⁺ T cells (circles) and WT host CD4⁺ T cells (squares) recovered from the CNS. I-K CD4⁺ T cells were isolated from Thy1.1 2D2 TCR Tg mice and also from Thy1.1/1.2 CD48^{-/-} 2D2 TCR Tg mice, then mixed at a ~1:1 ratio and adoptively transferred into Rag^{-/-} recipients. Two weeks later, mice were immunized for EAE as described for (A). 200μg of anti-CD48 or cIgG was given on days 4, 7 and 10 after immunization (black triangles). I. Mean clinical scores, ±SEM. J. Peak clinical scores. K. Number of WT and CD48^{-/-} 2D2 CD4⁺ T cells recovered from the CNS and spleen. A-D, n=6-7 mice per group, representative of 5 independent experiments with 4-7 mice per group. E-H, n=5 mice per group, representative of 2 independent experiments with 4-5 mice per group. J-L, n=4 mice per group, representative of 4 independent experiments with 4-5 mice per group. Line on dot plots represents mean. Bars represent mean, error bars represent SEM. *p<0.05, **p<0.01, ***p<0.001, ****p<0.0001. Statistical significance calculated using Mann Whitney test (A, C, E, G, J, K) or Student's t test (B, D, F, H, L).

This suggested to us that anti-CD48 could have a targeted effect on WT CD4⁺ T cells during EAE, without limiting the pathogenicity of CD48^{-/-} T cells. To examine this further, we reconstituted Rag^{-/-} mice with a mixture of WT and CD48^{-/-} 2D2 CD4⁺ T cells, and immunized for EAE with MOG/CFA 2 weeks later. Anti-CD48 or cIgG was given on days 4, 7 and 10 after immunization (**Figure 5.15I**). There was no difference in the peak disease score (**Figure 5.15J**). Mice treated with anti-CD48 had significantly reduced WT 2D2 CD4⁺ T cells in the CNS, but no change in the number of CD48^{-/-} 2D2 CD4⁺ T cells in the CNS, and an increase in the number of CD48^{-/-} 2D2 CD4⁺ T cells in the spleen (**Figure 5.15K**). Collectively, these data suggest that anti-CD48-mediated attenuation of EAE is highly dependent on and specific to CD48-expressing CD4⁺ T cells. Furthermore, anti-CD48 can prevent CD48⁺ CD4⁺ T cells from accumulating in the CNS even in the midst of ongoing CNS inflammation mediated by CD48^{-/-} T cells.

Anti-CD48 mAb can attenuate EAE when CD4⁺ T cells are the only cells expressing CD48

The requirement for CD48 expression on CD4⁺ T cells led us to ask whether anti-CD48 could mediate its protective effects if CD4⁺ T cells were the *only* CD48-expressing cells. To test this, we purified CD4⁺ T cells from 2D2 mice, adoptively transferred these into CD48^{-/-}Rag^{-/-} recipients, waited 2 weeks for homeostatic proliferation, then immunized for EAE with MOG/CFA. In this model, anti-CD48 prevented any signs of clinical disease (**Figure 5.16A-C**). We detected very few CD4⁺ T cells in the CNS of anti-CD48 treated mice (**Figure 5.16D**), and the number of CD4⁺ T cells in the spleen was strikingly reduced as well (**Figure 5.16D**). This was also the case when we adoptively transferred WT 2D2 TH1 CD4⁺ Teff cells into CD48^{-/-} recipients: anti-CD48 completely blocked EAE (**Figure 5.16E**), prevented accumulation of 2D2 CD4⁺ T cells in the CNS, and also reduced the number of 2D2 CD4⁺ T cells in the spleen (**Figure 5.16F**).

Anti-CD48 rapidly eliminates activated CD48⁺ CD4⁺ T cells from the blood in CD48^{-/-} mice

We suspected that in the above model, where the only CD48 in the host was on a few million CD4⁺ T cells, this dose of antibody had the potential to have a strong depleting effect. We were interested in testing this hypothesis for two reasons: 1) to support our prior observations that that this antibody has the potential to cause elimination of CD4⁺ Teff under certain conditions, and 2) to determine whether our in-depth study of the

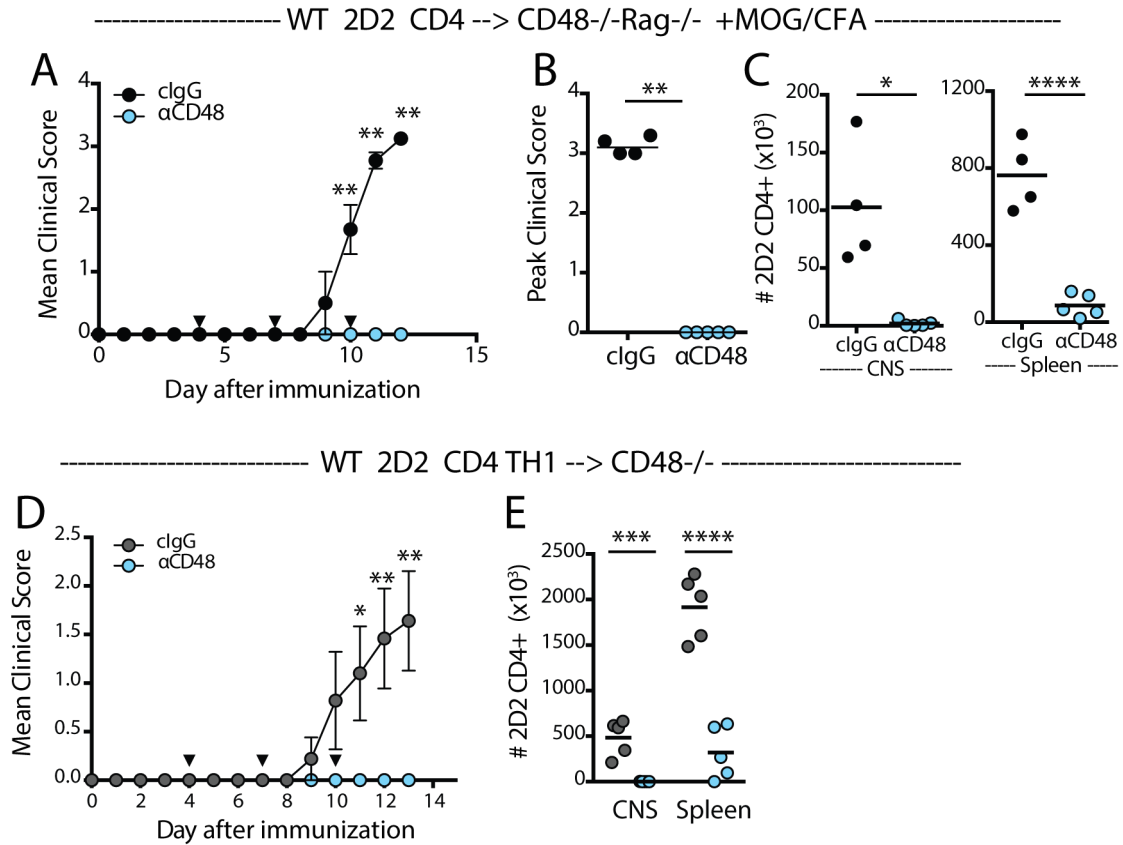


Figure 5.16 Anti-CD48 can attenuate EAE when CD4⁺ T cells are the only CD48⁺ cells. A-D. CD4⁺ T cells were isolated from 2D2 TCR Tg mice and adoptively transferred to CD48^{-/-}Rag^{-/-} recipients. Two weeks later, mice were immunized s.c. with 50 μ g MOG[35-55] emulsified in CFA to induce EAE, and given 100ng of pertussis toxin on days 0 and 2 after immunization. On days 4, 7 and 10 after immunization, mice were given 200 μ g of anti-CD48 or cIgG i.p (black triangles). A. Mean clinical scores \pm SEM. B. Day of onset. C. Peak clinical score. D. Number of CD4⁺ T cells in the CNS (left) and spleen (right). E-F. CD4⁺ T cells were isolated from Thy1.1 2D2 TCR Tg mice and activated in vitro under TH1-polarizing conditions as described in materials and methods to generate 2D2 TH1 CD4⁺ Teff. 3-6 \times 10⁶ 2D2 CD4⁺ Teff were adoptively transferred to Thy1.2 CD48^{-/-} recipients. 200 μ g of anti-CD48 or cIgG was given on days 4, 7 and 10 after adoptive transfer (black triangles). E. Mean clinical scores, \pm SEM. F. Number of donor 2D2 CD4⁺ T cells in the CNS and spleen. A-D, n=4 mice per group, representative of 4 independent experiments with 3-5 mice per group. E-F, n=5 mice per group, representative of 2 independent experiments with 4-5 mice per group. Lines on dot plots represent means. *p<0.05, **p<0.01, ***p<0.001, ****p<0.0001. Statistical significance calculated using Mann Whitney test (A, C, E) or Student's t test (B, D, F).

intrinsic effect of anti-CD48 on WT T cells in CD48^{-/-} hosts was likely to be confounded by effects of CD4⁺ T cell elimination. We tested this hypothesis in two ways. First, we examined the kinetics of disappearance of WT cells from the blood, spleen and inguinal lymph nodes in CD48^{-/-} hosts, by looking at 4 and 24 hours after anti-CD48 administration. CD48^{-/-}TCR α ^{-/-} mice were given an ~1:1 mix of WT and CD48^{-/-} 2D2 CD4⁺ T cells, and one week later recipients were immunized with MOG/CFA. 6 days after immunization, anti-CD48 or cIgG was administered, and mice were analyzed 4 hours or 24 hours later. By 4 hours, anti-CD48 significantly reduced the percentage of WT 2D2 cells in blood but not in the spleen or iLN (**Figure 5.17A**). By 24 hours, the %WT was significantly reduced in the spleen and iLN as well (**Figure 5.17B**). The kinetics of this effect suggest that the antibody causes elimination of WT cells, or relocalization of WT cells such that they are not detectable in the blood, spleen, or lymph nodes.

To further test our hypothesis that anti-CD48 caused depletion of CD48⁺ cells in CD48^{-/-} recipients, we examined the role of FcRs in this process. We transferred WT 2D2 TH1 CD4⁺ Teff into CD48^{-/-} recipients, and on day 6 after transfer we co-administered anti-CD16/CD32 along with anti-CD48 or cIgG. Spleen and blood were analyzed one day later. As shown in representative flow cytometry plots in **Figure 5.17C**, anti-CD48 alone drastically reduced the percentage of 2D2 cells in the blood and spleen, while anti-CD48 plus anti-CD16/CD32 did not reduce the percentage of 2D2 cells compared to anti-CD16/CD32 alone. The absolute number of 2D2 CD4⁺ T cells was significantly reduced in the spleen, blood and lymph nodes of anti-CD48 treated mice, compared to mice receiving control IgG; however, the absolute number was not significantly reduced in anti-CD48+anti-CD16/CD23-treated mice compared to mice receiving anti-CD16/CD32 alone (**Figure 5.17D**). Notably, addition of anti-CD16/CD32 reduced the magnitude of other effects of anti-CD48 such as that on the percentage of ZVAD⁺ and GM-CSF⁺ 2D2 CD4⁺ T cells (**Figure 5.17E, F**). Collectively, these results suggests that anti-CD48 can cause FcR-mediated elimination of CD4⁺ Teff from the blood and lymphoid compartments, and further suggests that the effects of anti-CD48 on WT T cells in CD48^{-/-} hosts may not represent exclusively cell intrinsic effects of the antibody on T cells.

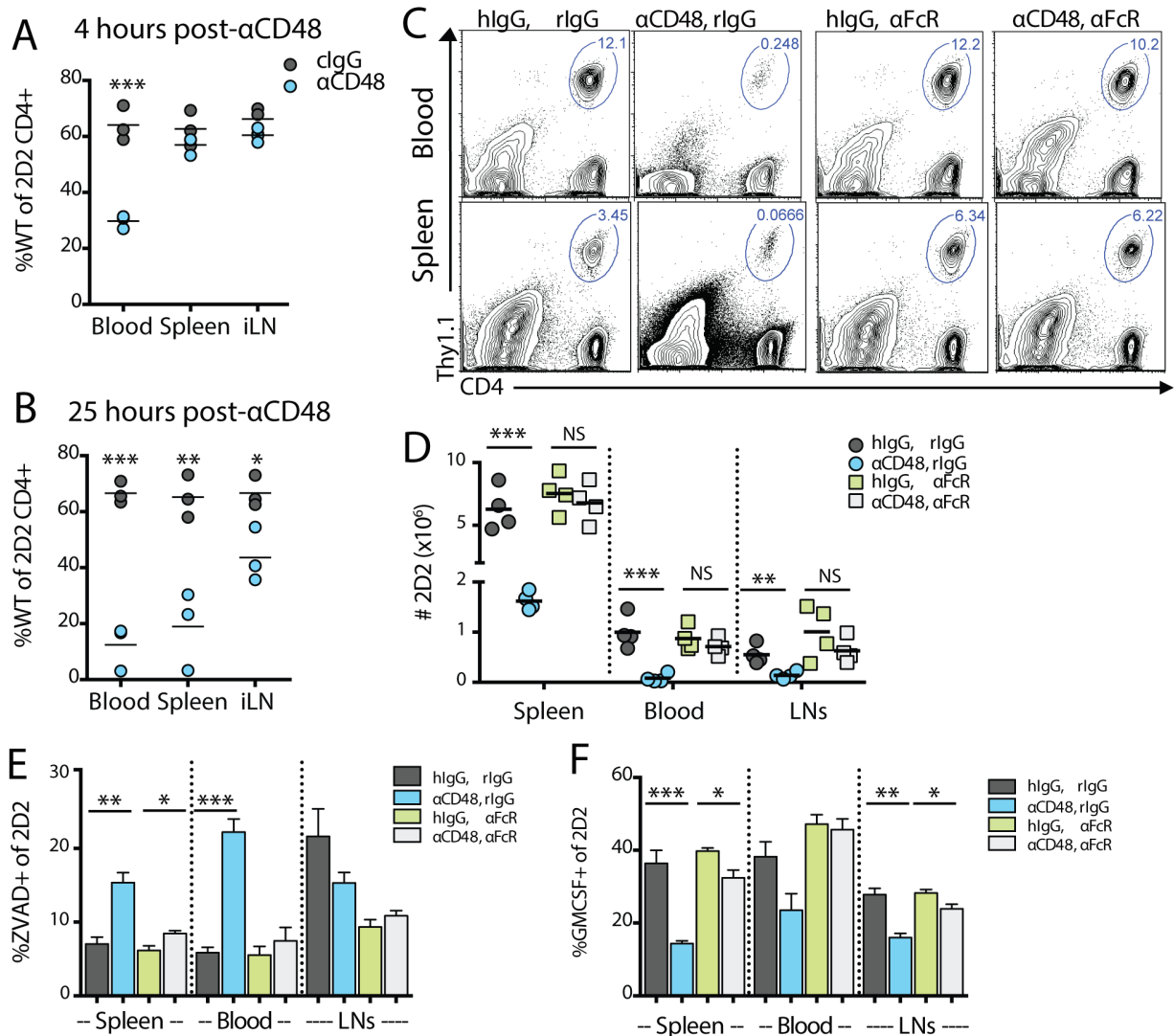


Figure 5.17 Anti-CD48 rapidly eliminates activated CD4⁺ CD4⁺ T cells from the blood in CD48^{-/-} mice.

A-B CD4⁺ T cells were isolated from Thy1.1 2D2 TCR Tg and Thy1.1/1.2 CD48^{-/-} 2D2 TCR Tg mice, mixed at a ~1:1 ratio, and adoptively transferred into CD48^{-/-}-TCR α ^{-/-} recipients. Two weeks later, mice were immunized with 50 μ g MOG[35-55] emulsified in CFA. On day 6 after immunization, 200 μ g of anti-CD48 or cIgG was given i.p. Four or 24 hours later, blood, spleen, and iLNs were collected and stained for analysis by flow cytometry. A. %WT of total CD4⁺ T cells at 4 hours after anti-CD48 administration. B. %WT of total CD4⁺ T cells at 24 hours after anti-CD48 administration. C-F CD4⁺ T cells were isolated from Thy1.1 2D2 TCR Tg mice and activated in vitro under TH1-polarizing conditions to generate 2D2 TH1 CD4⁺ Teff, as described in materials and methods. 3-6x10⁶ 2D2 TH1 CD4⁺ Teff were adoptively transferred into Thy1.2 CD48^{-/-} recipients. 200 μ g of anti-CD48 or cIgG pre-mixed with either anti-CD16/CD32 or isotype control (rat IgG2a) was given i.p. on day 4 after adoptive transfer, and spleen, blood and skin-draining lymph nodes were collected on day 6. C. Representative flow cytometry plots of live cells in the spleen and blood stained for CD4 and Thy1.1 to reveal the percentage of donor CD4⁺ T cells among lymphocytes. D. Quantification of the number of donor 2D2 CD4⁺ T cells in the spleen, blood and lymph nodes. E. Cells were incubated for 30 minutes at 37 $^{\circ}$ C with ZVAD-FMK-fluorescein to label active caspases, then analyzed by flow cytometry. F. Cells were restimulated in vitro with PMA and ionomycin in the presence of GolgiStop, then stained for intracellular cytokine production. Quantification of the %GM-CSF⁺ of 2D2 CD4⁺ T cells. A-B, n=3 mice per group, representative of 2 independent experiments with 1-3 mice per group. C-F n=4 mice per group. Lines in dot plots represent means. Bars represent mean, error bars represent SEM. *p<0.05, **p<0.01, ***p<0.001, ****p<0.0001. Statistical significance calculated using Student's t test.

Cytokine-producing cells are enriched in the CD48⁺⁺ population of CD4⁺ T cells

The effect of anti-CD48 on EAE in WT mice, and the expression pattern of CD48 on activated cells, led us to more closely examine CD48 expression on CD4⁺ T cells. Because CD4⁺ T cells infiltrating the CNS have higher CD48 than those in the periphery, we speculated that CD48⁺⁺ might be an indicator of the most potent T cells. Specifically, we hypothesized that CD48⁺⁺ cells were enriched for cytokine-producing cells. To address this, we immunized WT mice with MOG/CFA to induce EAE, then isolated cells from the CNS, iLN and spleen at the peak of disease. We then stimulated cells with PMA and ionomycin in the presence of GolgiStop, and analyzed intracellular cytokine production along with surface CD48 expression using flow cytometry. Representative flow cytometry plots are shown in **Figure 5.18A**, gated on CD4⁺CD3⁺Foxp⁻ cells in the spleen and CNS. In the spleen, GM-CSF⁺, IFN γ ⁺ and IL-17A⁺ CD4⁺ T cells had increased CD48 expression, while IL-2⁺ cells were primarily *not* CD48⁺⁺. In the CNS, all GM-CSF⁺, IFN γ ⁺, IL-17A⁺ and IL-2⁺ cells were primarily CD48⁺⁺, although this was less pronounced for IL-2⁺ cells.

We considered that CD48⁺⁺ might be a useful surrogate marker for cytokine-producing cells—that is to say, that it appeared that CD48⁺⁺ CD4⁺ T cells were enriched for some cytokine-producing cells, compared to CD48⁺ CD4⁺ T cells. Thus we calculated the percentage GM-CSF⁺, IFN γ ⁺, IL-17A⁺, IL-2⁺ and IL-10⁺ cells among CD48⁺⁺ and CD48⁺ CD4⁺ T cells in each organ. As shown in **Figure 5.18B**, CD48⁺⁺ CD4⁺ T cells were enriched for GM-CSF⁺, IFN γ ⁺ and IL-17A⁺ cells in all organs examined; enriched for IL-2⁺ cells in the CNS, but not in the iLN or spleen; and enriched for IL-10⁺ cells in the iLN and spleen but not in the CNS. This suggests that high CD48 expression might discriminate a population of CD4⁺ T cells that is enriched for cytokine-producing cells.

In a related experiment, we immunized WT mice with MOG/CFA to generate activated CD4⁺ T cells, but did not give pertussis toxin to induce EAE and instead looked at cells from the spleen and iLN at d14 after immunization (**Figure 5.18C**). In this experiment we again saw that in the spleen, CD48⁺⁺ CD4⁺ T cells were enriched for IFN γ ⁺, GM-CSF⁺, IL-17A⁺ and IL-10⁺ cells, but not for IL-2⁺ cells (**Figure 5.18D**). However, a greater portion of IFN γ ⁺ CD4⁺ T cells were CD48⁺ rather than CD48⁺⁺ (**Figure 5.18C, E**), which contrasted with our observation in mice with EAE. CD48⁺⁺ CD4⁺ T cells were still enriched for IFN γ ⁺ cells compared to

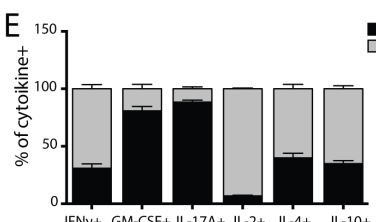
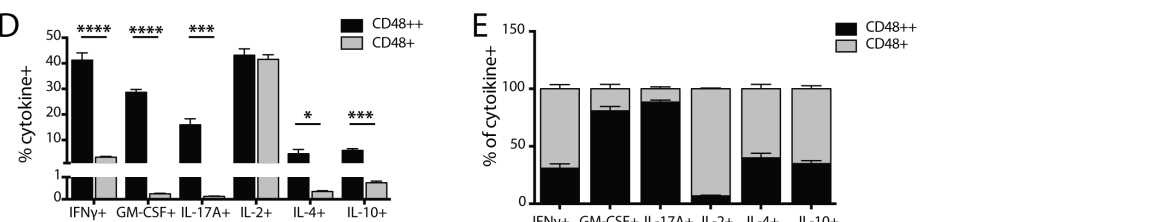
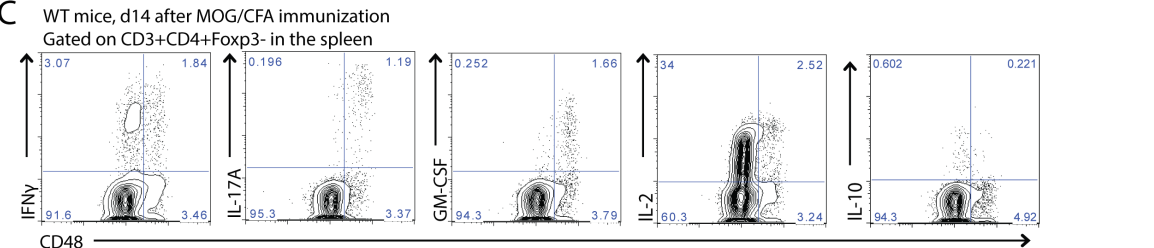
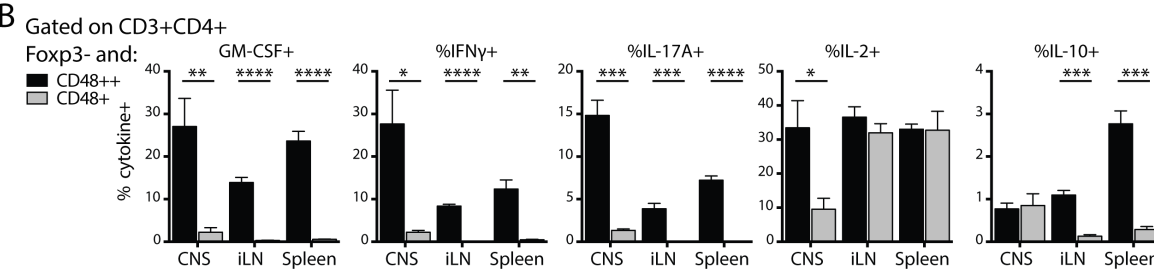
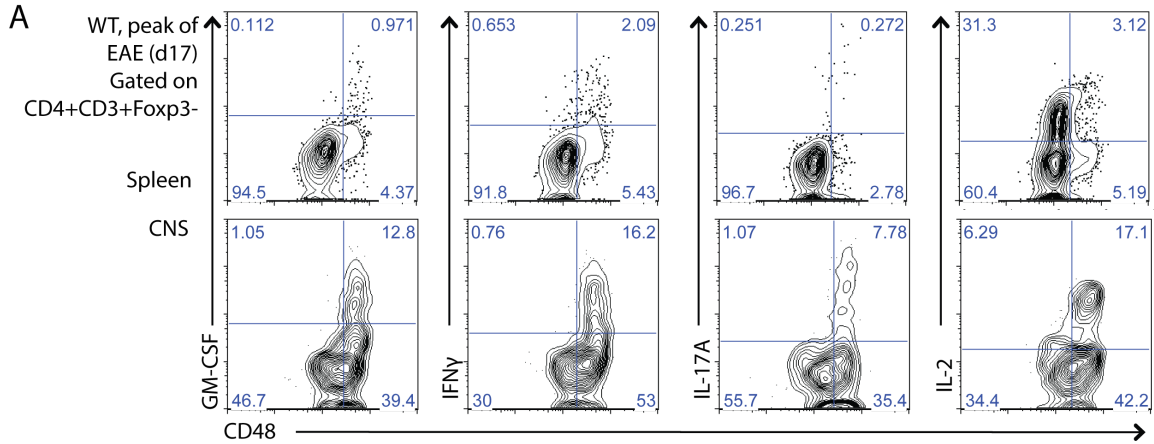


Figure 5.18 Teff cells producing pathogenic cytokines have increased CD48 surface expression. A-B. WT mice were immunized s.c. with 50µg MOG[35-55] emulsified in CFA to induce EAE, and given 100ng of pertussis toxin on days 0 and 2. On day 17, near the peak of disease, CNS, spleen and iLN were collected for analysis. Cells were restimulated with PMA and ionomycin in the presence of GolgiStop, then stained for surface CD48 and intracellular cytokines. A. Representative flow cytometry plots of CD4+ CD3+ T cells from the CNS (top) and spleen (bottom) with CD48 and cytokine co-staining. B. Based on the gates in A, %IFNγ+, %IL-17A+, %GM-CSF+ and %IL-2+ of CD48++ and CD48+ CD4+CD3+ T cells in the CNS, iLN and spleen. C-E WT mice were immunized as above, but did not receive pertussis toxin. On day 14, in the absence of EAE, spleen and iLN were collected for analysis. Cells were restimulated with PMA and ionomycin in the presence of GolgiStop, then stained for surface CD48 and intracellular cytokines. C. Representative flow cytometry plot of CD4+CD3+ T cells in the spleen with CD48 and cytokine co-staining. D. Based on the gates in C, %IFNγ+, %GM-CSF+, %IL-17A+, %IL-2+, %IL-4+ and %IL-10+ of CD48++ and CD48+ CD4+CD3+ T cells in the spleen. E. Based on the gates in C, the %CD48++ and %CD48+ of IFNγ+, GM-CSF+, IL-17A+, IL-2+, IL-4+ and IL-10+ CD4+CD3+ T cells in the spleen. A-B, n=4 mice. C-D, n=4 mice. *p<0.05, **p<0.01, ***p<0.001, ****p<0.0001. Bars represent means, error bars represent SEM. Statistical significance calculated using Student's t test.

the CD48⁺CD4⁺ population (**Figure 5.18D**), but IFN γ production was no longer so restricted to the CD48⁺⁺ population. This suggests that high CD48 expression levels might indicate a unique activation state in CD4⁺ T cells, in addition to providing a potential cell surface marker for enrichment of cytokine-producing cells.

DISCUSSION

The goal of these studies was to characterize the role of CD48 in autoimmunity and tolerance in the context of an inducible model of autoimmune disease, EAE. By using an anti-CD48 antibody, we could complement our prior studies that relied on the CD48^{-/-} [B6] strain. These studies initially were motivated by the caveats of studying germline knockout mice. We considered that CD48 deficiency might result in developmental differences in knockout mice, causing changes that were not related to lack of CD48 on mature lymphocytes. It was also possible that CD48^{-/-} mice had alterations to compensate for the absence of CD48, which could mask the roles of CD48 in WT mice. Thus, we undertook the study of CD48 function in WT mice during EAE, and administered an anti-CD48 blocking antibody to probe the pathogenic and regulatory roles of this immune receptor. Our discovery that anti-CD48 could potentially attenuate EAE led us to explore the mechanism of its action and its implications for the functions of CD48. In these studies, we: 1) characterized CD48 expression during EAE; 2) investigated the clinical, histological and cellular effects of anti-CD48 during EAE; 3) identified the cell types needed for anti-CD48 mediated attenuation of EAE; 4) analyzed the effects of anti-CD48 on proliferation, activation of and cytokine production by antigen-specific CD4⁺ T effector cells; 5) determined the cell-intrinsic effects of anti-CD48 on WT 2D2 CD4⁺ T eff in CD48^{-/-} hosts; 6) characterized the Fc-binding components required for anti-CD48 mediated attenuation of EAE; 7) identified the CD48 expression pattern required for anti-CD48 mediated attenuation of EAE; 8) characterized functional differences between CD48⁺⁺ and CD48⁺ CD4⁺ T cells from mice with EAE.

We found that CD48 expression was increased on CD4⁺ T cells during EAE, particularly those recovered from the CNS, as well antigen-specific 2D2 CD4⁺ T cells that had been activated *in vitro* or *in vivo*. High CD48 expression correlated with production of IFN γ , IL-17 and GM-CSF after restimulation *ex vivo* with MOG[35-55] or PMA and ionomycin. Administration of the anti-CD48 antibody HM48-1 to mice prior to onset of EAE was able to dramatically attenuate disease, and resulted in a reduction in the number of antigen-specific cytokine producing T eff in the periphery and CNS. CD48 expression on CD4⁺ T eff was necessary for protection, while CD48 expression on other cell types was dispensable. Our studies indicated that anti-CD48 mediated attenuation of EAE did not require B cells or CD8⁺ T cells, potentially involved NK cells, and was at least partially dependent on FcRs. Notably, anti-CD48 was effective in limiting disease during the effector

phase, and could also enhance resolution when administered near the peak of disease. Our results suggest that anti-CD48 exerts its protective effects in attenuating EAE by limiting activation/proliferation of Teff and depleting highly activated CD48⁺⁺ CD4⁺ Teff. In addition, our results suggest that high CD48 expression is correlated with production of pathogenic cytokines during EAE, and that targeting CD48⁺⁺ CD4⁺ Teff for depletion may be a useful treatment to prevent progression of autoimmunity.

First, we examined the expression of CD48 on various lymphocyte populations during EAE. We found that a subset of CD4⁺ T cells had increased CD48 expression during EAE, and that these CD48⁺⁺ CD4⁺ T cells were numerous in the spleen and represented the majority of CD4⁺ T cells in the CNS. This suggested to us that CD48⁺⁺ CD4⁺ T cells represented highly activated cells. CD48 expression is reported to increase on human B cells during EBV infection or after PHA stimulation (Yokoyama et al. 1991); on T cells, B cells and monocytes after exposure to IFN α , IFN β or IFN γ (Tissot et al. 1997); and on B cells during multiple myeloma (Hosen et al. 2012). In both cases, these cell populations are activated and highly proliferative, suggesting that CD48 expression in humans also correlates with proliferative capacity or cell cycle stage. In mice, CD48 expression is reported to increase on eosinophils during allergic inflammation (Munitz et al. 2006; Munitz et al. 2007) and on mast cells during bacterial infection (Rocha-de-Souza et al. 2008). We found that CD48 expression correlated partially with other activation markers such as CD44, ICOS, VLA-4 and Ki67. All CD48⁺⁺ cells were CD44⁺, but not all CD44⁺ cells were CD48⁺⁺, suggesting that CD48 expression levels might indicate a unique activation state of the cell. Further studies examining gene expression in CD48⁺ and CD48⁺⁺ cells may reveal whether these are distinct populations, and what upstream signaling pathways contribute to increased CD48 expression.

We also found that CD48 expression was increased on antigen-specific cells that we knew to be activated. In vitro stimulated, TH1 polarized 2D2 CD4⁺ Teff transferred into WT mice were entirely CD48⁺⁺. When we transferred 2D2 CD4⁺ T cells into WT mice and then immunized recipients with MOG/CFA, an increased percentage of 2D2 CD4⁺ T cells were CD48⁺⁺ compared to the percentage of host CD4⁺ T cells. This supported the interpretation that CD48 expression was uniquely increased on activated cells, and further suggested that CD48 expression might be increased after TCR stimulation. Additional studies are required to

determine whether TCR stimulation is critical, and what other costimulatory signals might be required, as well. In addition, future studies could identify whether other stimuli are sufficient to upregulate CD48 expression on murine T cells, such as exposure to certain cytokines or activation of certain transcription factors. Although preliminary experiments with in vitro polarization of CD4⁺ T cells did not suggest that CD48 upregulation was specific to TH1, Th2, TH17 or Tregs, further characterization is necessary to confirm this. This is of particular interest, as other costimulatory and coinhibitory molecules are associated with particular T helper functions. For instance, VLA-4 ligation during T cell priming promotes TH1 differentiation and opposes Th2 (Mittelbrunn et al. 2004).

Functional studies are also required to determine the kinetics of CD48 upregulation, and whether high CD48 expression is stable or transient. In some cases, we saw that CD48⁺⁺ cells were enriched in a population of cells with high forward scatter properties by flow cytometry, suggesting that increased CD48 MFI could be due to increased cell size. However, other surface stains were not brighter on these cells, suggesting that cell size was not the only factor influencing the brightness of CD48 staining. These larger cells may also represent large blasting cells, which would be consistent with our observation that CD48⁺⁺ cells are often Ki67⁺ as well.

We next administered anti-CD48 in vivo and assessed the effects of this antibody on cell surface expression of CD48 and proportions of lymphocyte subsets. Other publications had reported that this antibody did not cause gross depletion of lymphocytes, but did cause a change in the distribution of lymphocyte subsets (Chavin et al. 1994), and could prevent reconstitution by bone marrow in lethally irradiated mice (Blazar et al. 1998), cause downregulation of surface CD48 (Blazar et al. 1998), and augment the effects of anti-CD2 in vivo to prolong allograft survival (Qin et al. 1994). We first assessed how the antibody affected CD48 expression in naïve mice. We found that anti-CD48 administration in vivo resulted in some downregulation of total surface CD48 expression, but that much of the CD48 remained on the cell surface and was bound by anti-CD48 antibody that could be detected with a secondary antibody. Staining with directly conjugated anti-CD48 was blocked by anti-CD48 administration in vivo, but by 3-4 days after anti-CD48 antibody administration, staining with directly conjugated CD48 did not differ between cIgG and anti-CD48 treated mice. This suggests that the anti-CD48 antibody did not have a long half-life in vivo, and also that there is eventual turnover of surface CD48

molecules. We also observed a slight change in the distribution of lymphocyte subsets, most notably a decrease in the percentage of Ki67+ Foxp3+ CD4+ T cells. This was interesting to us, because in naïve mice the CD4+ T cells with highest CD48 expression levels are Ki67+ Foxp3+ CD4+ T cells. Importantly, we confirmed that anti-CD48 did not cause widespread lymphocyte depletion in our hands, but our studies suggested that the anti-CD48 antibody might have a targeted effect on CD48++ cells.

We next administered anti-CD48 to WT mice in order to evaluate the role of CD48 during EAE. When we administered anti-CD48 to mice during EAE, prior to onset of clinical disease, we found that it caused dramatic attenuation and even prevention of disease. We first hypothesized that this might be due to an inability for lymphocytes to traffic from the meninges to the CNS. For instance, during EAE in B7-1/B7-2^{-/-} mice, lymphocytes were effectively activated in the periphery, but when they reached the CNS they did not receive the necessary reactivation to then enter the parenchyma. Histologically, this was apparent as a striking accumulation of lymphocytes in the meninges of the brain and spinal cord, but very few lymphocytes in the CNS (Chang et al. 1999). When we examined the CNS histology in anti-CD48 treated mice at days 12 and 15 after immunization, times when cIgG-treated mice are at the onset and peak of disease, respectively, histological analysis revealed minimal lymphocytic infiltration in either the meninges or the parenchyma of anti-CD48 treated mice in contrast to cIgG treated mice which showed substantial infiltration. This suggested that anti-CD48 blocked pathogenesis in EAE in a different way than B7-1/B7-2 deficiency. By cellular analysis of the CNS, reduced infiltration was also apparent. The number of CD45+ lymphocytes and monocytes recovered from the CNS of anti-CD48 treated mice was significantly reduced, particularly for CD4+ T cells, but also for CD8+ T cells, CD11b+, CD11c+ and B220+ cells. This suggested to us that anti-CD48 treatment might somehow limit activation of the relevant Teff population, block migration of Teff into the CNS, reduce survival of Teff in the CNS, and/or mitigate pathogenicity of Teff such that an MOG-reactive T cell response could not be sustained in the CNS.

Adhesion and costimulatory molecules have been common targets for antibody blockade during EAE, to explore the role of immune receptors in activation and migration of CD4+ Teff. Several molecules, such as VLA-4 and LFA-1, have been found to play different roles at different phases of disease, and also to be critical to both Teff and Treg functions. Thus, the overall result of antibody treatment is sometimes difficult to

interpret. For instance, anti-VLA-4 antibody given before onset of disease limits the severity of EAE, but not incidence, likely by blocking secondary recruitment of activated T_H1 into the CNS (Brocke et al. 1999). However anti-VLA-4 given during ongoing disease exacerbates EAE, suggesting that this molecule may have multiple roles (Theien et al. 2001). Conflicting reports about the effect of anti-LFA1 during EAE also suggest that this molecule may have multiple roles, on multiple cell types, at different phases of disease (Welsh et al. 1993; Cannella, Cross, and Raine 1993; Gordon et al. 1995). Anti-CD44 was also capable of attenuating EAE during established disease (Brennan et al. 1999). Anti-CD40L antibody is also described to attenuate EAE, although the mechanism of action of this antibody was dependent on Fc receptors and thus thought to be via depletion, rather than blocking costimulation (Monk et al. 2003). Based on these published studies, it was critical to consider the many possible effects that antibodies can have in vivo—on different cell types, at different phases of disease, and potential for blocking, depleting or activating activities.

We investigated the mechanism of action of anti-CD48 in EAE by first identifying the key cellular components that were required for protection. Although CD4⁺ T cells and MHCII⁺ APCs are required to induce EAE with MOG[35-55], it was possible that anti-CD48 might act on CD8⁺ T cells, B cells or NK cells to mediate its protective effects. We found that in Rag^{-/-} mice reconstituted with 2D2 CD4⁺ T cells (thus lacking B cells and CD8⁺ T cells), anti-CD48 could still attenuate EAE. This indicated to us that neither B cells nor CD8⁺ T cells were critical for anti-CD48 to attenuate EAE. To test for the role of NK cells, we used both antibody depletion of NK cells in WT mice, and 2D2 CD4⁺ T cell transfer to Ii2R γ c^{-/-}Rag^{-/-} mice. Although EAE was more severe in mice lacking NK cells, in our hands, anti-CD48 was still able to attenuate the severity of disease. However, anti-CD48 could no longer completely block EAE in mice lacking NK cells. It is possible that anti-CD48 was having the same magnitude of effect, but the increased severity of disease in NK cell deficient mice meant that disease could not be blocked by this dose of anti-CD48. Alternatively, it is possible that the effects of anti-CD48 antibody may be partially dependent on NK cells for attenuation of disease, and in their absence the protective effects of anti-CD48 are present but reduced. To address these possibilities, future experiments could use a milder form of EAE, or an increased dose of antibody. In one preliminary experiment, we used the 2D2 TH1 adoptive transfer model to induce EAE in Ii2R γ c^{-/-} mice, rather than immunizing mice after

reconstitution with CD4⁺ T cells. Although disease was milder than in the immunization model, anti-CD48 was still only partially protective.

We can imagine several potential roles for NK cells in anti-CD48 mediated attenuation of EAE, based on the described—but controversial—roles of NK cells in EAE as well as roles of CD244 on NK cells, and the expression of Fc receptors on NK cells. NK cells can lyse activated CD4⁺ Teff, and this is enhanced in mice lacking Qa-1 (Lu et al. 2007). It is possible that anti-CD48 affects Qa-1:NKG2A interactions between CD4⁺ T cells and NK cells, respectively, and enhances NK-mediated lysis of Teff. NK cells were also suggested to limit TH17 cells in the CNS during EAE, so it is possible that anti-CD48 might augment the ability of NK cells to mediate these effects (Hao et al. 2010). In addition, CD244:CD48 interactions are described to influence NK-mediated lysis (Garni-Wagner et al. 1993; Schatzle et al. 1999; Lee et al. 2004; Vaidya et al. 2005; Chlewicki et al. 2008). Thus, anti-CD48 may limit the ability of NK cells to mediate protective, CD244-dependent effects.

We also tested the role of CD244 in anti-CD48 mediated attenuation of EAE. Considering the potential for an NK-mediated role, this was of particular interest. However, our experiments with anti-CD48 in EAE in CD244^{-/-} mice were somewhat inconsistent, and thus difficult to interpret. In some cases anti-CD48 did not attenuate EAE substantially in CD244^{-/-} mice, and in fact seemed to result in increased severity after the final dose. In other cases, anti-CD48 was just as protective as in WT mice. Additional studies would be required to determine if in fact cessation of anti-CD48 treatment results in a rebound effect, or whether there were other factors influencing the variability of EAE in this strain, in our colony. However, it did appear that anti-CD48 could be protective at least partially, during EAE in CD244^{-/-} mice. This suggested that anti-CD48 was not interrupting a critical CD48:CD244 interaction, to mediate protection, but instead blocked critical CD48:CD2 interactions and/or had cell intrinsic effects on CD48⁺ cells.

We also pursued the mechanism of action of anti-CD48 in EAE by examining the effects of anti-CD48 treatment on Teff activation, proliferation, and cytokine production prior to disease onset. We hypothesized that anti-CD48 might limit T cell activation, thus leading to delayed and attenuated EAE. To start, we

examined antigen-specific cytokine production by lymphocytes from the spleen and iLN on day 12 after immunization, in cIgG and anti-CD48 treated mice. Although we did not see any difference in production of IFN γ , TNF α , IL-17 or IL-10 in the iLN after restimulation with MOG[35-55] for 3 days, we did observe a significant decrease in the production of IFN γ and TNF α in the spleen, as well as a trend towards less IL-17 in the spleen. This was not due to a difference in the percentage of CD4 $^+$ T cells in anti-CD48 treated mice, nor to a difference in the percentage of Foxp3 $^+$ Tregs, as these were not significantly altered in anti-CD48 treated mice. This suggested that anti-CD48 did not limit T cell priming at the site of immunization, but might have an effect on the fate of these cells after leaving the lymph node. Although IFN γ is not required for development of EAE, IFN γ production by CD4 $^+$ Teff can influence CNS entry as well as the course of disease (Lees et al. 2008; O'Connor et al. 2008). Similarly, IL-17 is not required for EAE, but blocking IL-17 can attenuate disease (Park et al. 2005). Thus, we considered that the reduced production of these disease-promoting cytokines could contribute to attenuated EAE following anti-CD48 treatment.

To further examine the effects of anti-CD48 antibody on antigen-specific cytokine production by Teff, we adoptively transferred MOG-specific 2D2 CD4 $^+$ T cells to WT mice, immunized these recipients with MOG and gave anti-CD48 on day five. When we examined cytokines on day eight, we saw a striking reduction in the percentage and number of IFN γ^+ , IL-17A $^+$, and GM-CSF $^+$ 2D2 CD4 $^+$ T cells in the spleen and blood, but less of a difference in the iLN, and no differences in cytokine production by host CD4 $^+$ T cells. This again suggested that anti-CD48 had an effect on CD4 $^+$ T cells after leaving the iLN, and further suggested that this effect was specific to—or else amplified in—antigen-specific CD4 $^+$ T cells. Reduced GM-CSF production was particularly intriguing, as this cytokine has been identified as a crucial effector cytokine in EAE: GM-CSF promotes activation of dendritic cells and macrophages, and production of IL-23, which can then stabilize TH17 Teff cells (Codarri et al. 2011; El-Behi et al. 2011). Interestingly, IL-10 production by 2D2 CD4 $^+$ T cells was not reduced, nor did we see a difference in IL-2 production, suggesting that anti-CD48 had a specific effect on production of only some cytokines, or some types of cytokine-producing cells. This is particularly interesting considering that CD48 expression is highest in activated, antigen-specific cells in this model, and also in light of our subsequent findings that IFN γ , IL-17 and GM-CSF-producing cells tend to have high CD48 expression. We considered several possibilities to explain the selective effects on cytokine production. CD48:CD2

interactions are costimulatory (Kato et al. 1992; Moran and Miceli 1998; Latchman, McKay, and Reiser 1998), so it is reasonable to consider that anti-CD48 blocks a signal required for development of these highly activated, CD48⁺⁺, cytokine-producing cells. It is also possible, although not yet described, that CD48⁺⁺ cells are more dependent on CD48 signaling for their survival. It is also possible, and supported by our later findings of the dependence on FcRs for anti-CD48 to attenuate EAE, that the antibody causes selective depletion of the cells that express the highest levels of CD48. Selective depletion of high expressers has been described for other antibodies, such as anti-CTLA-4 depletion of Tregs (Simpson et al. 2013). However, these are not mutually exclusive possibilities, and further experiments would be required to identify how each might be relevant.

In complementary studies, we sought to clarify whether anti-CD48 attenuates EAE by affecting the T cell priming or effector phase. Whether anti-CD48 could affect CD4⁺ Teff that had already infiltrated the CNS was particularly interesting to us, as we considered future therapeutic implications for this work and whether anti-CD48 administration could be effective in patients with clinical disease. We found that anti-CD48 could significantly attenuate disease when treatment was initiated right at the onset of clinical symptoms, although it did not completely block progression. In contrast, when administered after substantial disease burden but prior to the peak of disease, anti-CD48 had a more modest effect; although it did increase recovery, this was not as striking as in our other administration protocols. Lastly, we found that anti-CD48 could dramatically attenuate EAE induced by adoptive transfer of TH1-polarized 2D2 CD4⁺ Teff, indicating that the antibody was capable of limiting disease independent of any effects on Th differentiation. The latter finding also suggested that anti-CD48 could act directly on activated Teff, possibly limiting their proliferation, survival or pathogenicity, rather than limiting their generation.

To further assess the effects of anti-CD48 on Teff, we examined 2D2 TH1 CD4⁺ Teff on day 5 after adoptive transfer, prior to onset of disease. We found that anti-CD48 treatment on day 3 did not alter the proportion of IFN γ ⁺ cells among the 2D2 CD4⁺ Teff, in contrast to our results using naïve 2D2 CD4⁺ T cell transfer followed by MOG immunization. This suggested that anti-CD48 did not have a direct effect on the ability of cells to product cytokine. However, the number of 2D2 CD4⁺ Teff was reduced, and thus the number of IFN γ ⁺ Teff was reduced, suggesting that anti-CD48 could keep the number of Teff below the critical threshold

required to precipitate disease. Indeed, anti-CD48 treated mice had reduced Ki67 expression in 2D2 CD4+ Teff, and also reduced EdU incorporation, suggesting that the number of Teff might be limited by reduced proliferation. Anti-CD48 was also capable of limiting 2D2 TH1 CD4+ Teff proliferation in vitro. Thus, we concluded that anti-CD48 was capable of limiting proliferation of 2D2 CD4+ Teff both in vivo and in vitro, and that anti-CD48 also reduced the number of 2D2 CD4+ Teff in vivo. This is consistent with the described role of anti-CD48 in limiting proliferation of T cell in vitro (Kato et al. 1992; Qin et al. 1994; Musgrave, Watson, and Hoskin 2003). However, these experiments did not determine whether limiting proliferation was the only, or even the critical, factor in reducing cell number.

We considered that reduced cell number might also be caused by reduced survival. To test this, we examined AnnV staining on 2D2 TH1 CD4+ Teff on day 5 after adoptive transfer, and also measured active caspases with the ZVAD-FMK-fluorescein reagent. We found an increase in the percentage of ZVAD+ 2D2 CD4+ T cells in mice that received anti-CD48 on day 3, compared to control mice, but no difference in the %AnnV+ 2D2 CD4+. This suggested that anti-CD48 treatment might result in increased apoptosis of Teff. Although the increase was modest (~30% increase) it is possible that reduced proliferation combined with reduced survival might combine to result in the dramatic decrease in cell numbers. CD2 engagement on B cells is reported to promote survival during affinity maturation, so it is possible that blocking CD48 might also prevent CD4+ T cells from receiving optimal survival signals through CD2 (Genaro et al. 1994). In addition, CD2 engagement on T cells is reported to increase IL-2 production in vitro, and blocking this with an anti-CD2 or anti-CD48 antibody results in reduced IL-2 production, decreased IL-2Ra expression, and destabilization of IL-2 mRNA (Musgrave, Watson, and Hoskin 2003; Musgrave et al. 2004). Our observations are thus consistent with other reports, in that anti-CD48 can limit both survival and proliferation signals for T cells. However, we did not observe an effect of anti-CD48 treatment on IL-2 production in 2D2 CD4+ T cells during EAE, and actually found that CD25 expression increased in anti-CD48 treated mice.

We also examined whether anti-CD48 treatment caused cell intrinsic or extrinsic effects on CD4+ Teff in vivo. Although we had observed that anti-CD48 could limit proliferation of 2D2 CD4+ Teff stimulated with WT APCs, both in vivo and in vitro, we investigated the contributions of CD48 on the T cell or APC. When we

stimulated WT Teff with CD48^{-/-} APCs in vitro, we found that CD48^{-/-} APCs were less stimulatory than WT APCs, and that the effect of anti-CD48 on proliferation was less pronounced with CD48^{-/-} APCs. This suggested that the effect of anti-CD48 on limiting proliferation was primarily by blocking CD48 on APCs. We examined this question in vivo, by transferring WT 2D2 TH1 CD4⁺ Teff into CD48^{-/-} recipients, and giving anti-CD48. Importantly, we had already established that anti-CD48 had no effect on EAE in CD48^{-/-} mice, when immunized with MOG/CFA. When we induced EAE in CD48^{-/-} mice using WT CD4⁺ T cells and administered anti-CD48 antibody, we observed a profound decrease in 2D2 CD4⁺ Teff numbers (~10-fold decrease), but minimal effect on Ki67 expression or EdU incorporation. Caspase activation was still increased. This suggested that anti-CD48 could have dramatic cell intrinsic effects on CD4⁺ Teff; we investigated this further using NanoString transcriptional analysis of 2D2 CD4⁺ Teff from the spleens of anti-CD48 and cIgG treated CD48^{-/-} recipients on day 7 after cell transfer. Our Nanostring results were in line with some of our prior observations by flow cytometry, in that anti-CD48 treatment resulted in reduced GM-CSF and IFN γ , but increased CD25 expression. However, the NanoString indicated that CCR2 expression was decreased, while flow cytometry indicated that CCR2 was unchanged or even increased. The NanoString also indicated that Lag3 was increased, although we never detected Lag3 expression by flow cytometry using the commercially available C9B7W clone. Although changes in gene expression do not always directly correlate with protein expression, our data suggest that anti-CD48 treatment in CD48^{-/-} mice can result in some cell intrinsic effects on WT 2D2 CD4⁺ T cells, including IFN γ . Further studies are required to validate the leads from the NanoString experiment, both by flow cytometry and mRNA analysis; however our later discovery suggesting profound depletion of WT CD4⁺ T cells in CD48^{-/-} hosts suggests that future experiments need to eliminate potential depletion effects, during study of cell-intrinsic effects of anti-CD48 in this model.

In further studies, we directly investigated the possibility of an Fc-mediated mechanism, such as depletion. To determine which anti-CD48 mediated effects were FcR-dependent, we first co-administered anti-CD48 with an FcR blocking antibody, anti-CD16/CD32, to WT mice that had received a 2D2 TH1 CD4⁺ Teff adoptive transfer. We found that reduction in CD4⁺ Teff cell numbers was FcR dependent. Although reduced numbers of Teff consistently correlated with attenuated disease in anti-CD48 treated mice, it was not clear whether this was required for attenuation of EAE. We also observed that some effects of anti-CD48 treatment were FcR

independent, including reduced proliferation, increased %VLA-4+ and increased %CD69+ amongst 2D2 CD4+ T_{eff}. Additional studies using other methods to ascertain the role of FcRs would be valuable, to confirm these results. For instance, we could use Fc ϵ 1 γ ^{-/-} mice as recipients, or mice lacking specific FcRs.

We also asked whether anti-CD48 attenuation of EAE was dependent on FcR interactions. Using the same anti-CD16/CD32 antibody, co-administered with anti-CD48 or cIgG, we found that anti-CD48 mediated attenuation of EAE was partially dependent on CD16/CD32. WT mice were immunized with MOG/CFA to induce EAE, and then given a mixture of anti-CD48 and/or anti-CD16/CD32, along with control antibodies. We found that mice that received anti-CD48 plus anti-CD16/CD32 developed EAE with reduced incidence and severity compared to mice that received anti-CD16/CD32 alone, while mice that received anti-CD48 alone did not develop any signs of clinical EAE. This suggests that some but not all of the effects of anti-CD48 on EAE pathogenesis required FcRs. We did not observe the course of EAE to be significantly different in mice receiving anti-CD16/CD32 alone compared to mice receiving cIgG only. This type of FcR blockade has been used by other groups to identify which FcR are involved in antibody-mediated depletion (Setiady, Coccia, and Park 2010). However, additional experiments are needed to determine if and when anti-CD48 physically interacts with CD16/CD32.

In a complementary approach to FcR blocking antibodies, we administered anti-CD48 to FcR-deficient mice during EAE (Fc ϵ 1 γ ^{-/-} mice). In these experiments, anti-CD48 treatment had almost no protective effect. This suggested that FcRs were required for anti-CD48 to attenuate EAE, although additional experiments are necessary to identify the relevant FcRs, since Fc ϵ 1 γ ^{-/-} mice lack all FcRs. In contrast to these results, however, a F(ab')₂ of anti-CD48, which should not interact with any FcRs, was also able to prevent EAE in WT mice. Although this particular experiment was only performed once, and the result would need to be confirmed, it supports the finding using anti-CD16/CD32 antibodies, that at least some of the protective effects of anti-CD48 are Fc-independent. It is possible that the dose of anti-CD48 F(ab')₂ might not have been equivalent to the dose of anti-CD48 given to Fc ϵ 1 γ ^{-/-} mice. We were not certain what the half-life of the F(ab')₂ would be *in vivo*, and so administered it every 2 days instead of every 3 days. This may have resulted in additional potency, and thus enhanced protection even in the absence of Fc-mediated effects. Collectively,

our data suggested a key role of FcRs in at least part of the mechanism of anti-CD48 mediated attenuation of EAE with clone HM48-1. Generation of new anti-CD48 antibodies, for example by immunizing CD48^{-/-} mice, could be extremely valuable for developing tools to study the effects of CD48 blockade or stimulation.

Next, we asked which CD48⁺ cells anti-CD48 acted on, to attenuate disease. To investigate this, we used various adoptive transfers of WT or CD48^{-/-} CD4⁺ T cells into WT or CD48^{-/-} recipients, to identify the CD48 expression pattern that was critical for anti-CD48 to attenuate EAE. We found that anti-CD48 could not significantly attenuate EAE mediated by CD48^{-/-} CD4⁺ T cells in a CD48⁺ host. When both WT and CD48^{-/-} CD4⁺ T cells were present in the host, anti-CD48 prevented infiltration of WT CD4⁺ T cells in the CNS, but did not prevent CD48^{-/-} CD4⁺ T cells from infiltrating the CNS. This suggested to us that expression of CD48 on CD4⁺ Teff was critical for anti-CD48 to attenuate EAE. Although we might have expected that blocking CD48 on host cells, such as APCs, could limit activation and proliferation of CD48^{-/-} CD4⁺ T cells, this is not something we have examined directly. Preliminary data from our lab indicate that CD48^{-/-} CD4⁺ T cells proliferate more in response to WT APCs, than to CD48^{-/-} APCs, *in vitro*, but additional studies are required to determine how anti-CD48 antibody affects this proliferation *in vitro* (Dan Brown, unpublished data). Our results suggest that any effect anti-CD48 might have on proliferation of CD48^{-/-} T cells in WT recipients is insufficient to alter the clinical course of EAE.

While these studies indicated that CD48 expression on CD4⁺ T cells was required for anti-CD48 to attenuate EAE, we next asked whether this was sufficient. To test this, we induced EAE with WT CD4⁺ T cells in CD48^{-/-} hosts, and administered anti-CD48. In both the MOG/CFA immunization model and the 2D2 TH1 CD4⁺ Teff adoptive transfer model, anti-CD48 completely blocked disease in CD48^{-/-} recipients. This was accompanied by a striking reduction in the number of WT CD4⁺ T cells in the spleen and lymph nodes of anti-CD48-treated mice, suggesting that anti-CD48 could act directly on CD48⁺ CD4⁺ T cells to limit proliferation or survival. Because we had observed that anti-CD48 had FcR-dependent effects in WT mice, and also that anti-CD48 might have cell intrinsic effects on WT CD4⁺ T cells in CD48^{-/-} recipients, we hypothesized that the striking reduction in cell numbers might be due to an FcR-mediated depletion mechanism.

We tested this hypothesis in two ways. First, we examined the kinetics of WT CD4⁺ T cell disappearance from blood, spleen and lymph nodes in CD48^{-/-} mice, after anti-CD48 administration. We evaluated this in MOG/CFA-immunized CD48^{-/-}TCRa^{-/-} recipients that had received a mix of WT and CD48^{-/-} 2D2 CD4⁺ T cells, and compared the proportion of CD4⁺ T cells that were WT (susceptible to anti-CD48 effects) and CD48^{-/-} (presumed to be unaffected by anti-CD48 treatment). Four hours after anti-CD48 administration, WT CD4⁺ T cells were dramatically reduced in the blood, but not in the spleen or lymph nodes. By 24 hours after anti-CD48 administration, WT CD4⁺ T cells were dramatically reduced in the spleen as well, and moderately reduced in the lymph node. The kinetics of the disappearance of WT CD4⁺ T cells from the blood, spleen, and lymph nodes were consistent with a mechanism of depletion of CD48⁺ T cells, although this could also be due to relocalization of cells in another compartment not examined. While additional experiments are required to describe the pattern of WT CD4⁺ T cell localization in other compartments after anti-CD48 treatment, these findings strongly suggested to us that anti-CD48 exerts its effects through an FcR-mediated depletion mechanism. To test for the role of FcR in anti-CD48 mediated elimination of WT CD4⁺ T cells from the blood and spleen of CD48^{-/-} mice, we co-administered anti-CD16/CD32 along with antiCD48. In CD48^{-/-} recipients of 2D2 TH1 CD4⁺ Teff, anti-CD48 treatment strikingly reduced the percentage of WT cells in the blood and spleen, while anti-CD16/CD32 plus anti-CD48 treatment was indistinguishable from anti-CD16/CD32 treatment alone. This strongly suggested that anti-CD48 treatment in CD48^{-/-} recipients could cause Fc-mediated elimination of WT CD4⁺ T cells, consistent with a mechanism of depletion. Interestingly, anti-CD16/CD32 plus anti-CD48 had little effect on apoptosis, as measured by caspase activation, whereas anti-CD48 alone increased the proportion of cells with active caspases. This suggests that increased apoptosis in anti-CD48 treated mice was also FcR-dependent. We also asked whether the effect of anti-CD48 on GM-CSF production was FcR-dependent. In mice that received anti-CD16/CD32 plus anti-CD48, the %GM-CSF⁺ of CD4⁺ T cells was modestly reduced in the spleen and lymph nodes, compared to anti-CD16/CD32 treatment alone. In contrast, anti-CD48 alone resulted in a dramatic reduction in the %GM-CSF⁺ CD4⁺ T cells compared to control mice. This suggests that some of the effects of anti-CD48 on WT CD4⁺ T cells in CD48^{-/-} hosts, which we interpreted to represent cell intrinsic effects of anti-CD48 on CD4⁺ T cells, may in fact partially be due to FcR-mediated mechanisms, as well. To better identify truly cell intrinsic effects of anti-CD48 on WT CD4⁺ T cells, studies using anti-CD16/CD32 along with anti-CD48, in CD48^{-/-} hosts, would be valuable. To

identify the specific FcRs involved in anti-CD48 mediated elimination of WT CD4⁺ T cells, future studies could use CD48^{-/-} mice that also lack specific FcRs. Similarly, to characterize the cells involved in FcR-mediated effects of anti-CD48, CD48^{-/-} mice that lack specific FcRs on specific cell types would also be valuable.

What was most striking to us, however, was the indication that an anti-CD48 antibody could dramatically limit the number of cytokine-producing WT CD4⁺ T_{eff}, in both WT and CD48^{-/-} hosts, and that this coincided with attenuated disease. It appeared that anti-CD48 might deplete CD48⁺⁺ activated cells, but also limit the generation of CD48⁺⁺ cells, resulting in fewer pathogenic CD4⁺ T cells. This led us to hypothesize that high CD48 expression might be related to production of certain cytokines. To test this, we examined CD48 expression on CD4⁺ T cells along with intracellular cytokine expression. We found that in the spleen of mice at the peak of EAE, GM-CSF⁺, IFN γ ⁺ and IL-17A⁺ CD4⁺ T cells were predominantly those that most highly expressed CD48 (CD48⁺⁺), and the percentage of cytokine-producing cells was significantly higher among CD48⁺⁺ CD4⁺ T cells, than it was among CD48^{intermediate} (int) CD4⁺ T cells. Notably, the majority of IL-2⁺ cells were CD48^{int}, rather than CD48⁺⁺, suggesting that IL-2 production is not so restricted to CD48⁺⁺ cells. In the CNS, nearly all cytokine-producing cells that we examined were CD48⁺⁺ (GM-CSF⁺, IFN γ ⁺, IL-17A⁺, IL-2⁺). It is not clear if this is because only the most activated cells enter the CNS, or because cells become more activated within the CNS. We considered that CD48⁺⁺ expression might be a result of recent antigen stimulation; thus in the CNS all cytokine-producing cells are likely responding to antigen, whereas in the periphery there may be naïve CD4⁺ T cells that produce IL-2 in response to PMA and ionomycin. Additional studies to examine CD48 expression along with cytokine production in both naïve and immunized mice may aid in understanding factors regulating CD48 expression. Additionally, we could use cell surface markers to distinguish naïve CD4⁺ T cells, such as CD62L and CD44, along with measuring intracellular cytokine production, to test the hypothesis that the spleen contains naïve, IL-2-producing, CD48^{int} CD4⁺ T cells.

Also notable was the fact that the majority of IL-10⁺ CD4⁺ T cells in the spleens of these mice were CD48^{int}, rather than CD48⁺⁺. IL-10 can attenuate inflammation in EAE, and is associated with disease resolution

(Bettelli et al. 1998; Zhang et al. 2004; McGeachy, Stephens, and Anderton 2005), and this suggested to us that CD48⁺⁺ expression might in fact be correlated with production of pathogenic cytokines during EAE. Further studies, including functional studies to compare CD48⁺⁺ and CD48^{int} CD4⁺ T cells, will be required to determine if and how this might be the case.

Our results indicate that CD48 expression tends to be higher among cytokine-producing cells during EAE, than among non-cytokine producing cells, and also that anti-CD48 treatment results in a decrease in the number of IFN γ ⁺, IL-17A⁺ and GM-CSF⁺ CD4⁺ Teff which is partially dependent on Fc γ R_s. This suggests to us a mechanism whereby anti-CD48 treatment limits the generation and survival of CD48⁺⁺, pathogenic-cytokine-producing CD4⁺ Teff during EAE, resulting in prevention or attenuation of disease. Although we cannot exclude an effect of anti-CD48 on regulatory CD4⁺ T cell populations, as well, it appears that the net effect of anti-CD48 treatment is to create a less pathogenic environment.

Our studies of CD48 using the anti-CD48 antibody were initiated to complement our study of the CD48^{-/-} mouse, in recognition of the potential developmental effects that can occur in germline knockout mice. However, the ability for anti-CD48 to dramatically attenuate EAE in WT mice instigated an investigation to study both the role of CD48 in EAE as well as the potential for this molecule as a therapeutic target in autoimmunity. Our discovery that this effect was dependent on an FcR-mediated mechanism, despite prior reports that this antibody was not depleting in other models, provides a new perspective to evaluate the role of CD48 in autoimmunity and tolerance. While CD48 can contribute to costimulation and activation of naïve T cells, its upregulation on activated cells suggests that CD48 may have a critical function on activated cells, and that it may be a valuable marker for activated cells during both immunologic studies and development of immunomodulatory therapies for disease.

Our results support a role of CD48 in costimulation, including reactivation of previously activated cells. The effect of blocking CD48 in vitro or in vivo with anti-CD48 mimicked some of the features of CD48^{-/-} cells, but not all of them. Others and we have observed that CD48^{-/-} APCs are less stimulatory to WT T cells than WT APCs (Gonzalez-Cabrero et al. 1999; Abadia-Molina et al. 2006). Similarly, addition of anti-CD48 to in vitro

cultures of WT T cells and WT APCs limited T cell proliferation, and anti-CD48 also reduced T cell proliferation in vivo. In contrast, addition of anti-CD48 to in vitro cultures of WT T cells with CD48^{-/-} APCs had only a slight effect on proliferation, suggesting that CD48 on the APC contributes more to T cell proliferation than does CD48 on the T cell. This is consistent with our in vivo findings that anti-CD48 did not effect the %Ki67⁺ or %EdU⁺ of WT T cells in CD48^{-/-} hosts.

Aside from effects on proliferation, however, anti-CD48 treatment during EAE in WT mice did not phenocopy EAE in CD48^{-/-} mice. We initially considered that the CD48^{-/-} mouse may have developmental differences that masked a role for CD48 in EAE: CD48 has been shown to affect hematopoiesis (Boles et al. 2011), and lack of a cell surface molecule can lead to increased expression of and reliance on alternative pathways. These are still possibilities in the CD48^{-/-} mouse, but our data suggest that the primary reason for the different effect of anti-CD48 treatment in EAE compared to CD48^{-/-} EAE is due to an FcR-mediated mechanism. Further studies of the effect of blocking CD48 could be performed in FcR^{-/-} animals, with F(ab')₂ and Fab', or with mutated antibodies that don't bind to FcRs, to determine whether blocking CD48 transiently has a similar effect to using CD48^{-/-} cells. Alternatively, development of a conditional or inducible CD48^{-/-} mouse would allow further study of the role of CD48 under specific conditions.

Based on our collective results, we suggest that one or more of the following models may explain the effects of anti-CD48 on EAE: 1) that anti-CD48 limits proliferation and activation such that the number of pathogenic Teff is too low to cause clinical disease; 2) that CD48⁺⁺ cells are more dependent on CD48 signaling for survival, and do not persist with anti-CD48 blockade; 3) that anti-CD48 causes selective FcR-mediated depletion of the CD48⁺⁺ CD4⁺ Teff such that the number of pathogenic Teff is too low to cause clinical disease; 4) anti-CD48 alters the migration of cells such that CD48⁺⁺ Teff are sequestered somewhere other than the spleen, blood or lymph node and they cannot migrate to induce disease in the CNS. The reduced number and percentage of Ki67⁺ Teff is consistent with both an effect on proliferation and preferential elimination of activated cells. Only the effect of anti-CD16/CD32 provides evidence against this model as the sole mechanism. Given that the %Ki67⁺ was still slightly reduced in mice that received anti-CD48 plus anti-CD16/CD32, and that clinical disease was partially attenuated in these mice, it seems likely that a combination

of models one through three contribute to the total effect of anti-CD48 on disease. We have not eliminated the possibility that Teff are sequestered in an organ such as the lung or liver or mesenteric lymph node—locations that were not routinely examined in the course of our studies. There are reports that activated cells receive further activation in the lung, so it remains possible that anti-CD48 causes cells to get stuck here (Odoardi et al. 2012).

We were initially puzzled by seemingly contradictory data regarding the effect of anti-CD48 on cytokine production in 2D2 CD4⁺ T cells transferred to WT mice. Anti-CD48 could reduce the percentage of cytokine producing cells in WT mice that had received purified 2D2 CD4⁺ T cells and then immunized with MOG, but anti-CD48 did not limit the percentage of cytokine-producing cells in WT mice that received TH1-polarized 2D2 CD4⁺ Teff. In both cases the absolute number of IFN γ ⁺ 2D2 CD4⁺ T cells was reduced; only the percentage change differed between the two experimental setups. However, this result is consistent with a mechanism whereby anti-CD48 leads to selective elimination of CD48⁺⁺ cells. In the MOG immunization model, only a portion of 2D2 CD4⁺ T cells become activated and CD48⁺⁺, and these CD48⁺⁺ cells include all of the cytokine-producing cells. Thus, if anti-CD48 treatment preferentially eliminated the CD48⁺⁺ cells, this would result in an apparent decrease in both absolute number and percent of cytokine-producing cells. In contrast, all TH1-polarized 2D2 CD4⁺ T cells are CD48⁺⁺ in vivo, regardless of whether they are IFN γ -producers. Thus, if anti-CD48 treatment preferentially eliminated CD48⁺⁺ cells, this would not affect the percentage of cytokine-producing cells, but would decrease in the absolute number. These data are also consistent with a model in which CD48⁺⁺ cells are most dependent on CD48-mediated costimulation, such that anti-CD48 treatment preferentially affects CD48⁺⁺ cells.

Depletion of high expressers has been demonstrated in other systems with in vivo antibody administration, suggesting that this mechanism is not unreasonable to consider for anti-CD48. For instance, anti-CTLA-4 mAb treatment was shown to preferentially deplete tumor-infiltrating Tregs, which have the highest CTLA-4 expression among Tconv and Treg in tumor and lymph node (Simpson et al. 2013). The anti-CD25 antibody PC61 has also been shown to have depleting effects (Setiady, Coccia, and Park 2010).

Our data are also interesting in light of the fact that Foxp3⁺ Tregs have higher CD48 expression than Tconv, at least in naïve animals, and yet anti-CD48 treatment did not result in Treg depletion and overt autoimmunity. Anti-CD48 dramatically reduced the percentage and number of inflammatory cytokine-producing Teff, but not the percentage or number of Tregs. This may be because Teff have higher CD48 expression than Tregs, making them either more susceptible to anti-CD48 mediated effects or more dependent on CD48 costimulation and thus sensitive to CD48 blockade. Although it is not always possible to predict the net effect of antibody treatment, the timing of antibody administration and preferential effects on certain cell types may determine whether EAE is exacerbated or attenuated. For instance, anti-VLA-4 treatment during EAE prior to disease onset can attenuate disease, while treatment at the peak of disease or remission in a relapsing-remitting model of EAE, can exacerbate disease (Theien et al. 2001; Mindur et al. 2014). This may be due to the combined effects of anti-VLA4 on limiting leukocyte entry to the CNS, but also affecting activation of naïve T cells (Sato et al. 1995; Mittelbrunn et al. 2004). VLA-4 is although thought to be critical for TH1 but not TH17 entry to the CNS (Rothhammer et al. 2011). Notably, lack of alpha4 integrin on TH1 Teff resulted in delayed but not attenuated EAE, suggesting that anti-VLA4 antibody treatment may mediate its critical effects via other VLA-4-expressing cells (Glatigny et al. 2011).

Recently, Glatigny et al. reported that in the absence of VLA-4, Tregs can use LFA1 to enter the CNS (Glatigny et al. 2015). This offers a potential mechanism for the effectiveness of Natalizumab (anti-VLA4 mAb) in treatment of multiple sclerosis, in that it may restrict trafficking of Teff but not Tregs to the CNS. Thus, evaluating the effect of potential therapeutic treatments on both Treg and Tconv may be beneficial to evaluating their safety or effectiveness. While we observed only a modest effect of anti-CD48 at the peak of disease, additional insights may come from administering anti-CD48 at even later time points, during the resolution phase of EAE, to see if at that time it has a more dramatic effect on Treg or Teff.

While further work is needed to understand the mechanism of action of anti-CD48 in EAE, we are particularly struck by the potential of CD48 to be a marker of highly activated cells. The expansion of the CD4⁺ CD48⁺⁺ population after immunization, the enrichment of CD48⁺⁺ cells in the target organ during EAE, and the association of cytokine production with the CD48⁺⁺ population, suggest that CD48 could be a useful marker

for activated cells in EAE and possibly other immune models as well. We have not fully explored the pattern of CD48 expression in other models of immunization or with other TCR Tg T cells, although preliminary data in our lab suggest that CD48 is highly expressed on OTII cells after OVA immunization. We are intrigued by the possibility of a pattern of cell surface expression that may be unique to antigen-activated T cells, allowing identification of these cells for study, enrichment, or depletion.

In summary, our studies of CD48 using the anti-CD48 antibody were initiated to complement our study of the CD48^{-/-} mouse, in recognition of the potential developmental effects that can occur in germline knockout mice. However, the ability of anti-CD48 to dramatically attenuate EAE in WT mice led us to study both the role of CD48 in EAE as well as the potential for this molecule to be a therapeutic target in autoimmunity. Our discovery that this effect was dependent on an FcR-mediated mechanism, despite prior reports that this antibody was not depleting in other models, suggests that cell surface molecules with expression patterns like CD48 could be valuable targets for antibody-directed therapies in human disease. The increased expression of CD48 on activated cells, particularly on cytokine-producing cells, further suggests that molecules like CD48 could be valuable as biomarkers or surrogate markers for cytokine-producing cells. In light of our observations, we believe further studies using human samples are highly warranted.

Part II

Immunologic regulation of IgG glycosylation

Chapter 6: Introduction

A link between IgG glycosylation and immune disease

Antibodies are a critical component of immunity, bridging the antigen specificity of adaptive immune responses to the effector functions of innate immunity. Though often appreciated for the remarkable specificity of their antigen-binding domain, antibodies also carry critical information to the effector arm of the immune system via the Fc region. In addition to the array of isotypes and their specialized functions, modification of N-linked glycans in the Fc region can also affect binding to Fc receptors and downstream immunologic function. IgA and IgE have numerous glycosylation sites, while IgG has a single site in the constant region of the heavy chain. Modification of IgG glycosylation has been shown to impact the effector functions of IgG, with alternate glycoforms having enhanced pathogenicity or anti-inflammatory effects (Banda et al. 2008; White, Cummings, and Waxman 1997; Nose and Wigzell 1983; Malhotra et al. 1995; Mimura et al. 2000; Shields et al. 2002; Albert et al. 2008). However, the immune mechanisms regulating alternative glycosylation of IgG are undefined. We are particularly interested in immune regulation of *galactosylation* of IgG—the presence of galactose in the glycan structure (**Figure 6.1A**). The IgG glycoform that lacks terminal galactose and sialic acid (agalactosyl IgG, abbreviated as G0-IgG) is significantly increased in patients with rheumatoid arthritis (RA) (Parekh et al. 1985). Despite this long-standing observation and the established influence of glycan structure on IgG effector functions, the relationship between pathology in RA and the altered IgG glycoform has remained correlative.

IgG has a conserved glycosylation site in the CH2 domain of the Fc region, at Asn297, which can carry one of 32 complex bi-antennary glycans (**Figure 6.1A**). X-ray crystallography indicates that the complex glycan is buried within the fully folded protein, and electron density mapping suggests that the oligosaccharide makes 85 contacts with 14 amino acids in the CH2 chain (Deisenhofer 1981). Deglycosylation of IgG1 significantly reduces thermal stability of the Fc region, indicating that these glycans are critical to the structural integrity of this domain (Mimura et al. 2000).

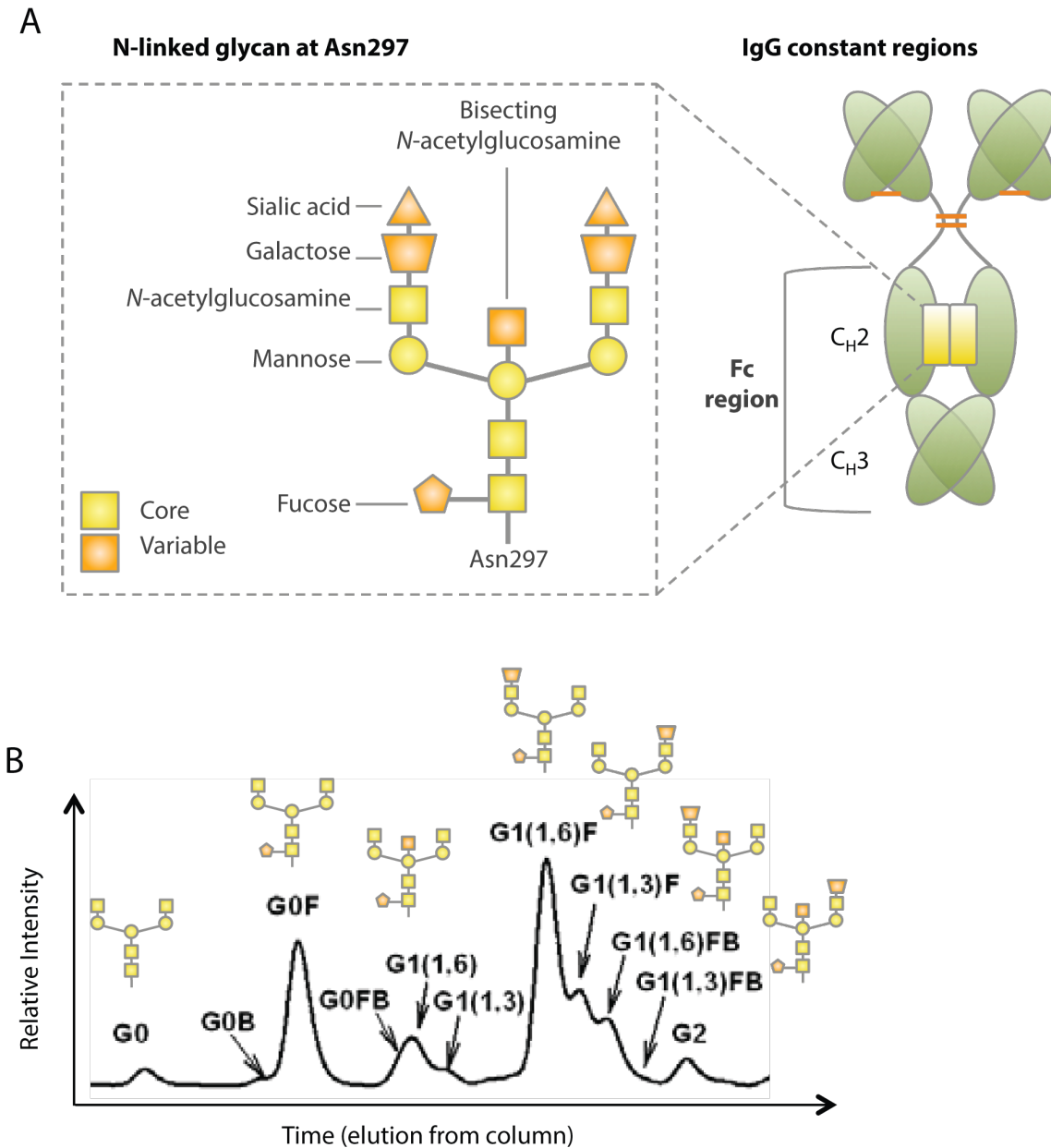


Figure 6.1. IgG has a single conserved glycosylation site in the heavy chain constant region, which can be described by glycan analysis methods. A. The Fc region of IgG, which includes the CH₂ and CH₃ regions of the heavy chain, has one conserved glycosylation site at asparagine 297 (Asn297). This sugar has 7 core residues (yellow), but may also contain variable residues (orange) such as fucose, bisecting N-acetylglucosamine, galactose on one (G1) or both (G2) arms, and sialic acid on one or both galactose. B. N-linked glycans can be released from IgG heavy chains, and analyzed by HPLC based on the characteristic elution time for each unique structure. A representative trace is shown, illustrating the elution pattern for several G0 and G1 glycoforms. The area under each elution curve represents the relative quantity of that glycan structure among the mixture of glycan structures released from the sample of IgG heavy chains. B modified from Mimura et al., 2008.

The influence of N-linked glycans on IgG structure and effector functions

Altered glycoforms of IgG vary in the efficacy of their Fc-mediated effector functions, as demonstrated by experiments both in vitro and in vivo. Deglycosylated IgG1 is unable to stimulate complement-mediated lysis, and shows a 70% reduction in stimulating superoxide production by monocytes (Mimura et al. 2000).

Activation of the alternative and classical complement pathways is enhanced by G0-IgG relative to native IgG, in a model of anti-collagen II antibody induced arthritis (Banda et al. 2008). Terminal sialic acid is thought to confer the anti-inflammatory activity of therapeutic intravenous immunoglobulin (IVIg) and to reduce antibody-dependent cell-mediated cytotoxicity (ADCC) activity (Kaneko, Nimmerjahn, and Ravetch 2006; Anthony et al. 2008; Nimmerjahn, Anthony, and Ravetch 2007). The presence of a core fucose residue was also shown to impact ADCC (Shinkawa et al. 2003; Peipp et al. 2008) by altering binding to Fc γ R2 (Shields et al. 2002). In a passive transfer model of acute synovitis, removal of terminal galactose enhanced the pathogenicity of IgG containing anti-collagen autoantibodies (Rademacher, Williams, and Dwek 1994). More recently, it was shown that removal of all but one core N-acetylglucosamine significantly reduced the pathogenicity of K/BxN IgG in serum transfer arthritis, and reduced effective platelet clearance by IgG1 and IgG2a anti-platelet antibodies (Albert et al. 2008). Collectively, these reports have indicated that Fc region glycosylation significantly influences the immunologic functions of IgG.

Agalactosyl IgG and Rheumatoid Arthritis

The relative proportion of G0-IgG in human and mouse serum increases gradually with normal ageing. However, abnormally high levels of G0-IgG are associated with a select subset of immune diseases: RA, juvenile onset chronic arthritis, Crohn's disease, a subset of Sjogren's syndrome, and tuberculosis (Parekh et al. 1989; Parekh et al. 1985; Bond et al. 1997). Notably, it is not associated with other autoimmune or rheumatologic diseases such as systemic lupus erythematosus, multiple sclerosis, or osteoarthritis (Parekh et al. 1989). During remission of disease, G0-IgG levels are observed to decrease to normal levels, for example during pregnancy in patients with RA (Rook et al. 1991). Studies in our lab indicate that G0-IgG levels rise in individuals prior to disease onset (Ercean et al. 2010). However, the functional relationship between altered glycosylation and disease etiology or progression has not been defined.

One group has sought to correlate the IgG glycan phenotype with expression of β 1,4-galactosyltransferases (GalTase), the Golgi-resident enzymes responsible for adding terminal galactose to oligosaccharides. Knock down and overexpression of GalTase-I in B cells is capable of reducing and increasing galactosylation of IgG, respectively (Keusch 1998b). It is also reported that B cells from RA patients have reduced GalTase activity but normal GalTase-I protein levels (Keusch 1998a). However, there are six other GalTases, whose relevance to B cells and IgG has yet to be defined (Amado et al. 1999). Thus, while it is clear that there are cellular factors capable of altering IgG galactosylation, there are no definitions of which are responsible for the changes observed in instances of pathology such as RA.

IgG glycosylation in B cells

A few studies have investigated an immune related regulation of IgG glycosylation. One study in autoimmune MLR-Irp/lpr mice concluded that the predominance of G0-IgG in these animals was not due to excessive IgG production or reduced Golgi transit time in plasma cells (Jeddi et al. 1999). This suggests that altered glycosylation of IgG is a regulated process, rather than a result of an overdriven secretory protein pathway. Another group examined how glycosylation varies among IgG subclasses, by comparing the profile of IgG paraproteins from several multiple myeloma patients. The authors found that the distribution of glycoforms in paraprotein IgG samples did not mirror that observed in polyclonal IgG from healthy donors. Instead, each sample was dominated by one or two glycoforms. The presence of terminal galactose was found to vary even within each IgG subclass (Jefferis et al. 1990). Their results suggest that different B cells can have a bias towards production of a unique set of IgG glycoforms, though the regulation of this bias in a cancer cell may be different than that in a normal plasma cell.

Several cytokines were shown to influence the amount of galactosylation, bisecting N-acetylglutamine, or sialylation of IgG produced by human B cells in vitro. In particular, IL-21 increased galactosylation and sialylation, while all-trans retinoic acid decreased galactosylation. This change was not observed on total cellular N-glycans, suggesting that the changes in glycosylation were specific to IgG (Wang et al. 2011). This indicates that antibody-secreting cells can be influenced to alter IgG glycosylation, and begs the question of how such influences could be active in vivo.

Arthritis in the K/BxN mouse.

The K/BxN model of arthritis is a useful system in for our investigations, as disease in these animals involves a strong antibody response against a defined autoantigen. K/BxN mice carry a transgenic TCR that recognizes the self-antigen glucose-6-phosphate isomerase (GPI), an intracellular metabolic protein (Matsumoto et al., 1999). These mice develop spontaneous, aggressive arthritis within a few weeks of birth, and autoantibodies from these mice are sufficient to induce arthritis in healthy recipients. The K/BxN mouse replicates many of the clinical, immunologic, and histologic features of human RA, and has been a valuable model for this disease (Kouskoff et al. 1996).

Here we describe the results of some preliminary studies of IgG galactosylation in K/BxN mice, suggesting that the G0/G1 ratio of total serum IgG is strongly correlated with the severity of disease, which in most cases also correlates with autoantibody titer. However, in mice resistant to arthritis, high titer autoantibodies did not necessitate aberrant galactosylation. We also show preliminary data in which hypogalactosylation was specific to autoantibodies in a model of K/BxN arthritis.

Chapter 7: Materials and Methods

Mice. Wild type C57BL/6J (WT B6) and B6.129S7-Rag1^{tm1Mom}/J (Rag^{-/-}) mice were purchased from the Jackson Labs (Bar Harbor, ME). KRN TCR Tg mice on the C57BL6/JxNOD background (K/BxN) and F1 C57BL6/JxNOD (BxN) mice were acquired from the Jackson Labs, through special arrangement with Drs. Christophe Benoist and Diane Mathis. Animal experiments were approved by the Institutional Animal Care and Use Committee of the Dana-Farber Cancer Institute. Mice were housed in the specific pathogen free animal facility of the Dana-Farber Cancer Institute.

Mouse serum. For endpoint collection of mouse serum, mice were euthanized with isofluorene and blood was collected by cardiac puncture. For serial collection of mouse serum, 25-100µl of blood was obtained by tail vein bleed. For generation of stock K/BxN serum, to be used for induction of arthritis in our laboratory, a cohort of arthritic male K/BxN mice were sacrificed periodically, blood was collected by cardiac puncture, serum was separated by centrifugation in the absence of heparin, and serum was pooled, aliquoted, and stored at -20 C until ready for use. As indicated in the text, we obtained mouse serum samples from several collaborators for use in our studies. Samples were stored at -20 C until ready for use.

Experimental arthritis. Serum transfer arthritis was induced by intraperitoneal injection of 75µl of arthritogenic K/BxN serum diluted in 75µl of sterile PBS on days 0 and 2 of each experiment (Korganow et al. 1999). K/BxN mice develop spontaneous arthritis beginning around 6 weeks of age. Clinical index was assigned based on a scale of 0-3 for each paw (score of 12 maximum), and by caliper measurement of ankle thickness.

Production of recombinant murine GPI. Mouse glucose-6-phosphate isomerase (GPI) is the target of autoantibodies in the K/BxN model of arthritis (Matsumoto et al. 1999). Our lab obtained the cDNA sequence for mouse GPI from the IMAGE consortium (IMAGE clone # 6394822), and cloned it into the glutathione-S-transferase (GST) containing PGEX 4T-3 bacterial expression vector (Amersham Biosciences, Amersham UK). GPI-GST was expressed in T7 E. coli (NEB, Ipswich MA), and was purified from bacterial cell lysates with a

glutathione column (GE Healthcare, UK). Concentration was computed based on absorbance at 280nm using a spectrophotometer.

Anti-GPI IgG ELISA. 96-well EIA/RIA plates (Corning) were coated with 500ng/well of GPI-GST in PBS. Serial dilutions of serum from donor mice were incubated with the plate-bound GPI, washed, and the assay was developed with HRP-conjugated anti-mouse IgG followed by TMB substrate (BD Biosciences). Absorbance was read at 650nm, 3-5 minutes later. A dedicated stock of K/BxN serum was used to create a standard curve, for comparison of other samples.

Mouse IgG ELISA. 96-well EIA/RIA plates (Corning) were coated with 50 μ l of 2 μ g/mL goat anti-mouse IgG (Invitrogen), washed with PBS-Tween, and blocked with 2% BSA. Serum samples were serially diluted at 1:3 or 1:5 to generate dilution curves for each sample. The assay was developed with HRP-conjugated donkey anti-mouse IgG (Jackson Immunoresearch) followed by TMB substrate. Absorbance was read at 650nm, 3-5 minutes later.

Purification of serum IgG. Serum was diluted 1:1 in PBS and incubated with Protein G sepharose beads (GE Healthcare). Columns were washed with 10 bed volumes of PBS, then IgG was eluted with 0.5M acetic acid, pH 2.5, and neutralized with 1M Tris, pH 8. Eluates were transferred to dialysis tubing, and dialyzed against PBS before measurement of protein concentration by spectrophotometry. In some cases, samples were concentrated by transferring samples to dialysis tubing and extracting water using PEG.

Purification of anti-GPI IgG. Anti-GPI IgG was purified from serum using affinity chromatography. GPI-affinity columns were made in one of two ways, depending on the intended use for the anti-GPI IgG. In some cases, glutathione-sepharose beads with bound GPI (from bacterial cell lysates) were directly incubated with donor serum diluted 1:1 in PBS. Samples were then washed with 10 bed volumes of PBS, and total beads+GPI +anti-GPI IgG was used for isolation and analysis of anti-GPI IgG heavy chains. In other cases, a GPI-affinity column was made using GPI-GST and AminoLink beads (Pierce), according to the manufacturer's instructions.

In this case, serum was diluted 1:1 with PBS, incubated with GPI-AminoLink agarose beads, then washed with 10 bed volumes of PBS. Beads+GPI+IgG were used for isolation and analysis of anti-GPI heavy chains.

Purification of non-GPI-binding IgG. Serum from donor mice was diluted 1:1 in PBS, then incubated with GPI-AminoLink agarose beads to remove anti-GPI IgG. The flow-through from the column was saved, tested for residual GPI-reactivity by GPI ELISA, and in some cases was run over a second GPI-AminoLink column to ensure complete removal of anti-GPI IgG. This 'repertoire' IgG was then captured on Protein G sepharose beads (GE Healthcare), eluted with 0.2M glycine (pH 2.5) and neutralized with 1M Tris (pH9). IgG was dialyzed against PBS using dialysis tubing or a Slide-A-Lyzer dialysis cassette (Pierce), and used for isolation and analysis of non-GPI-binding IgG heavy chains.

Analysis of N-glycans from IgG. Whole serum, purified IgG, or affinity-purified IgG bound to sepharose beads (as described above) were used for experiments. The protocol is described in *Methods in Molecular Biology* Ch 9, "Detailed Structural Analysis of N-Glycans Released from Glycoproteins in SDS-PAGE Gel Bands Using HPLC Combined with Exoglycosidase Array Digestions" (Royle 2006). Briefly, samples were reduced with DTT at 70 C, alkylated with iodoacetamide, then run on an SDS-polyacrylamide gel next to a protein size ladder. Gels were stained with coomassie blue, and heavy chain bands were identified by their size, at 52kDa, and excised from the gel using a clean razor blade. N-linked glycans were removed from the glycoprotein using PNGase F (Prozyme, San Leandro, CA), then labeled with the fluorophore 2-aminobenzamide (2-AB) according to the manufacturer's instructions (Prozyme, San Leandro, CA). Labeled N-glycans were analyzed by HPLC using a normal phase TSK gel amide-80 column (4.6mm (ID) x 25.0 cm (L)) and an ammonium formate:acetonitrile gradient (20mM ammonium formate (35%--> 47%)(Fisher Scientific, Pittsburg, PA); acetonitrile (65%-->53%) (Sigma, St. Louis, MO) over 60 minutes). G0 and G1 peaks were identified based on elution time, relative to a 2-AB labeled Glucose Homopolymer ladder (Associates of Cape Code Inc, East Falmouth, MA). G0 and G1 values were obtained by integrating the area under each elution curve, respectively, where G0 included FA2 and FA2B structures, and F1 included FA2[6]G1, FA2[6]BG1 and FA2[3]G1 structures. See Figure 1 for more details on glycan structures and analysis by HPLC.

Statistical Analysis. Statistical significance was computed using Student's t-test. Data plotted as bar graphs represent means, error bars represent standard error of the mean.

Chapter 8: Hypogalactosylation of IgG in the K/BxN model of inflammatory arthritis

RESULTS

Hypogalactosylation of IgG in the K/BxN model of arthritis

Our lab has used the K/BxN mouse model of arthritis to gain insight into mechanisms of autoimmunity, inflammation, and how these can inform parallel studies using samples from patient cohorts. One question that had not previously been addressed in mouse models of arthritis, was whether the feature of antibody hypogalactosylation during active disease was also recapitulated by the mouse model. Drs. Melissa Hazen and Altan Ercan performed a longitudinal analysis of K/BxN clinical scores, autoantibody titers, and serum glycosylation, and observed a striking correlation between these three parameters (**Figure 8.1A-C**, data from Dr. Melissa Hazen and Dr. Altan Ercan). Clinical symptoms appear after anti-GPI titers rise, and the G0/G1 ratio rises at this same time. We considered two possible explanations for this correlation. First, that the anti-GPI IgG might be exclusively responsible for the high G0/G1 ratio observed in the total serum IgG, and that as titers increase so does the G0/G1 value for total serum. This assumes that the signal from glycans on anti-GPI IgG would gradually overwhelm the signal from glycans on non-anti-GPI IgG. This might be due to the type of cells producing anti-GPI IgG, the rate of antibody secretion, the immune influences on autoreactive B cells, or some other mechanism specific to the autoantibody-secreting B cells. In this case, we would expect the anti-GPI and repertoire IgG to have different G0/G1 profiles. Alternatively, the increase in G0/G1 might be due to increased inflammation with progressing disease, influencing the glycosylation program in all antibody secreting cells or possibly even the glycosylation of circulating IgG. In this case, we would expect all IgG in an arthritic mouse to exhibit the same G0/G1 profile.

Glycan analysis of repertoire and anti-GPI IgG in arthritic K/BxN mice

To address these possibilities, we first wanted to compare the G0/G1 profiles of anti-GPI and 'repertoire' (non-GPI-binding) IgG in K/BxN mice. We examined IgG in serum from arthritic young K/BxN, adult K/BxN, and healthy adult BxN mice. Anti-GPI IgG was first separated from serum by passage over a series of GPI-GST-Sepharose columns. The flowthrough from this process was tested by ELISA for reactivity to GPI, until significant GPI-reactivity was removed. 'Repertoire' IgG was then purified from the remaining flowthrough

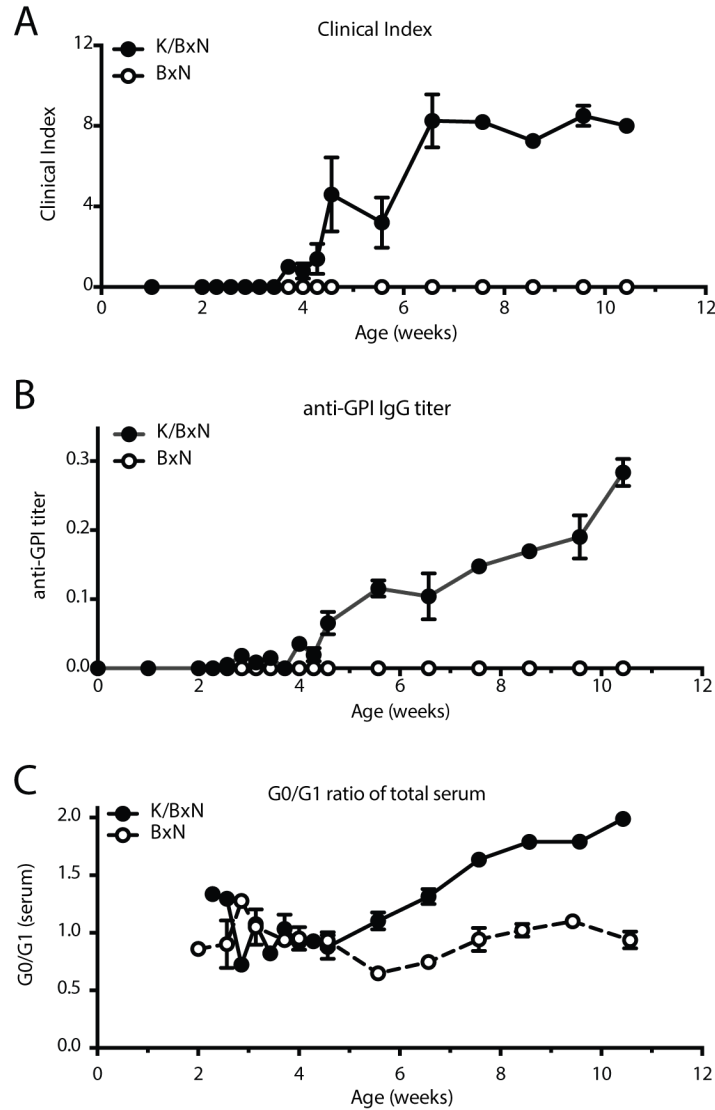


Figure 8.1. Hypogalactosylation of serum IgG in K/BxN mice increases in concert with the appearance of anti-GPI autoantibodies and the onset of clinical disease. K/BxN and BxN mice were monitored longitudinally for clinical disease, autoantibody titers, and serum glycan profiles. A. G0/G1 ratios were measured by glycan analysis of whole serum beginning at 2 weeks of age. B. Anti-GPI IgG titers in serum were measured by ELISA beginning at 1 week of age. C. Clinical index was assessed beginning at 1 week of age. Data are from experiments performed by Dr. Melissa Hazen and Dr. Altan Ercan.

using a Protein G column. As shown in **Figure 8.2A**, the GPI-reactivity of the purified ‘repertoire’ IgG was significantly reduced, compared to the starting sample. However, it was difficult to determine exactly how much anti-GPI antibodies remained, and what proportion of the IgG in this repertoire fraction was still anti-GPI IgG. Notably, K/BxN mice have extremely high titers of anti-GPI IgG, which has been measured at up to 10mg/mL (Korganow et al. 1999). Although we measured the anti-GPI and total IgG concentrations, the ‘repertoire’ fraction contained extremely low concentrations of total IgG, meaning that any residual anti-GPI IgG had the potential to represent a substantial portion of that fraction. However, we proceeded to extract glycans from the heavy chains of these two IgG populations for analysis by HPLC. Comparison of the glycan profiles in these two populations revealed that the G0/G1 ratio in repertoire IgG of arthritic K/BxN mice was not dissimilar from that of anti-GPI IgG (**Figure 8.2B**). However, we were not confident that this experiment sufficiently depleted anti-GPI IgG from the K/BxN serum, or that a ‘repertoire’ population was actually non-negligible. We performed this experiment a few times, but never felt that they provided unambiguous results.

Galactosylation of host repertoire IgG is not altered by serum transfer arthritis

Many features of K/BxN arthritis can be recapitulated in wild-type mice by transfer of K/BxN serum. We hypothesized that the systemic inflammation induced by K/BxN serum-transfer arthritis could impact the glycosylation of serum IgG in the recipient mouse. To address this possibility, we compared the G0/G1 profile of anti-GPI IgG and non-GPI-binding host repertoire IgG. WT mice received 75µl of K/BxN serum i.p. on days 0 and 2, to induce arthritis. Mice were sacrificed on days 4, 7 and 10 after the start of the experiment, and serum was collected for analysis. Anti-GPI IgG was collected using a series GPI-GST-Sepharose columns. The flowthrough from this process was tested by ELISA for reactivity to GPI, until 95-99% of GPI-reactivity was removed (**Figure 8.3A**). ‘Repertoire’ IgG was then purified from the remaining flowthrough using a Protein G column.

Glycans from the Ig heavy chains of these two populations were analyzed by HPLC. The G0/G1 profile for repertoire IgG was similar in naïve mice and arthritic mice, but was significantly lower than that of the anti-GPI

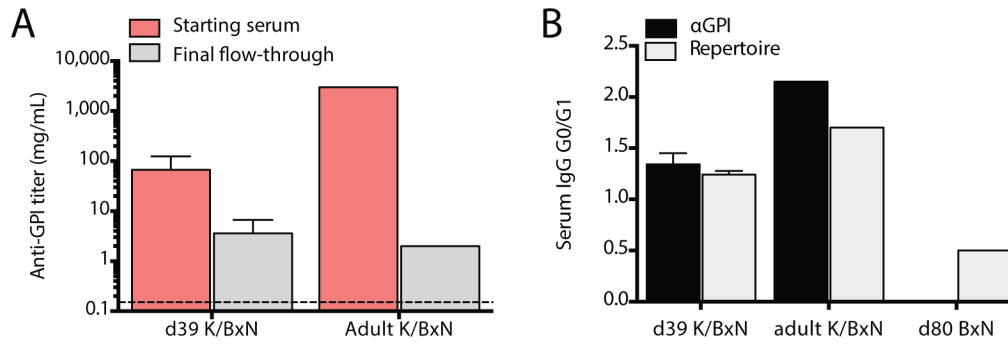


Figure 8.2. Repertoire IgG in K/BxN serum is hypogalctosylated compared to repertoire IgG in BxN serum. Serum samples were analyzed from 3 K/BxN mice that were 39 days old (mild arthritis), from pooled adult K/BxN serum (severe arthritis), and from one healthy BxN mouse that was 80 days old. Anti-GPI IgG was removed from K/BxN serum by passage over a series of GPI affinity columns, and total IgG remaining in the final flow-through was isolated with Protein G beads. A. Anti-GPI titers in the starting K/BxN serum and in the final flow-through after anti-GPI IgG removal were assessed by GPI ELISA. Anti-GPI reactivity in the flow-through was reduced to approximately 6% of the starting concentration, but not completely removed. Dashed line indicates the threshold of detection. B. IgG heavy chains were isolated from anti-GPI IgG, flow-through IgG, and BxN serum IgG. Glycans were analyzed by HPLC, and the ratio of G0/G1 glycans is shown. Data represent mean \pm SEM. N=1-3 mice per group.

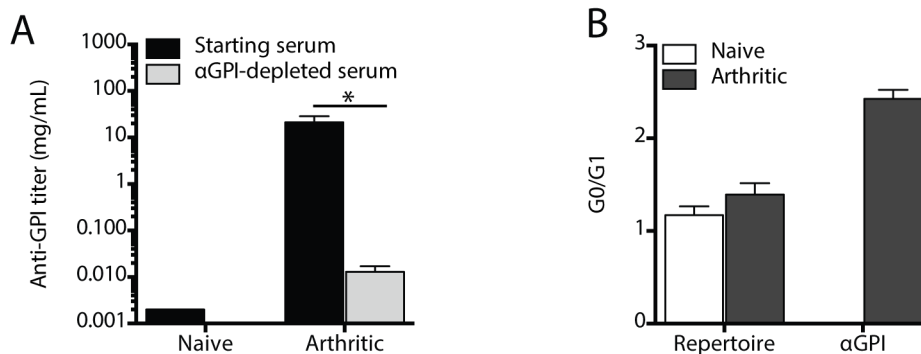


Figure 8.3. Glycosylation of host 'repertoire' IgG is not altered after serum transfer arthritis. 75 μ l of K/BxN serum was given i.p. to WT B6 mice to induce arthritis. 7 and 10 days later, serum was collected from recipients for glycan analysis of host repertoire IgG and K/BxN donor anti-GPI IgG. Anti-GPI IgG was removed from serum by passage over a series of GPI affinity columns, and total IgG remaining in the final flow-through was isolated with Protein G beads. A. To confirm removal of anti-GPI IgG from the serum of arthritic mice, GPI ELISAs were performed on the starting and anti-GPI-depleted samples. Naïve WT mouse serum was included as negative control. B. IgG heavy chain glycans from naïve mouse repertoire IgG, arthritic mouse repertoire IgG, and arthritic mouse anti-GPI IgG, were analyzed by HPLC. The ratio of G0/G1 glycans is shown. Data represent mean \pm SEM. N=3-6 mice per group. *p<0.05. Statistical significance calculated using Student's t test.

fraction in arthritic mice (**Figure 8.3B**). This indicated that serum transfer arthritis did not affect the G0/G1 profile of host IgG in circulation up to 10 days after induction of arthritis.

Hypogalactosylation is not a feature of high-titer anti-GPI in the absence of inflammation

We hypothesized that the altered G0/G1 profile of K/BxN IgG might be due to a progressive overwhelming of the secretory system in antibody secreting cells in these mice, independent of an inflammatory environment. K/BxN mice have 10-fold higher IgG concentration in serum than control WT mice (Kouskoff et al. 1996; Korganow et al. 1999). Because anti-GPI titers are tightly linked to disease progression in K/BxN mice, this system would not allow us to distinguish between the effects of inflammation versus antibody titers on IgG G0/G1 profiles. However, we learned of a model developed by Dr. Haochu Huang, in the lab of Dr. Diane Mathis and Dr. Christophe Benoist at the Joslin Diabetes Center and Harvard Medical School, which results in high titers of anti-GPI IgG in the absence of arthritis (Huang et al. 2006). These mice have knock-in BCR heavy and light chains, derived from an anti-GPI IgG1 antibody B cell clone from a K/BxN mouse. We sought out a collaboration with Dr. Huang, who by this time had established his own lab at the University of Chicago, and were able to obtain serum samples from several mice in his experiments. The BCR knock-in mice, $H^{121/+}L^{121/+}$, have low anti-GPI titers and no arthritis (**Figure 8.4A and B, far left**); serum from these mice were included as a negative control. Non-arthritic high-titer mice had been generated in two different ways. First, using co-adoptive transfers of T cells from KRN TCR Tg mice (TCR specific for the autoantigen GPI) and anti-GPI B cells sorted from $H^{121/+}L^{121/+}Rag^{+/-}$ mice into $Rag^{-/-}$ recipients. Second, by transfer of KRN Tg T cells into $H^{121/+}L^{121/+}Rag^{-/-}$ recipients. The absence of arthritis in these mice is likely due to the fact that the antibody response in these mice is monoclonal, which was previously shown to be insufficient to induce arthritis (Maccioni 2002). We compared glycosylation of total serum IgG from each of these mice, as well that that from our own K/BxN and BxN mice. We found that while anti-GPI antibody titers in adoptive transfer mice were comparable to those in arthritic K/BxN mice (**Figure 8.5A**), these disease-free mice had total IgG G0/G1 ratios like those of healthy BxN mice (**Figure 8.4B and C**). Thus, a high G0/G1 ratio was not correlated with high titer anti-GPI antibodies in this model.

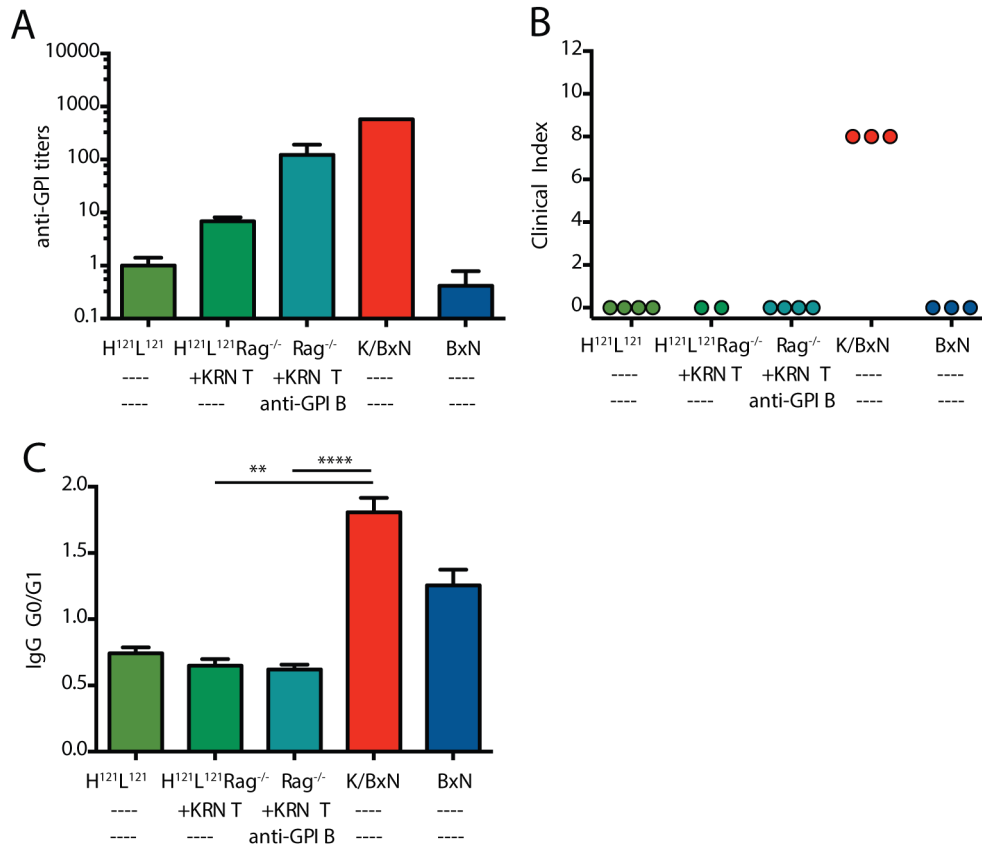


Figure 8.4. Hypogalactosylation is not a feature of high-titer anti-GPI in the absence of inflammation. Mice with KRN Tg T cells and a monoclonal anti-GPI B cell population (H¹²¹L¹²¹) have high titers of anti-GPI IgG, but no arthritis. Serum samples from these mice were provided by Dr. Haochu Huang. A. Anti-GPI titers were measured by GPI ELISA. B. Clinical index for mice in each group. C. IgG heavy chains were purified from total serum IgG, and glycans were analyzed by HPLC. The G0/G1 ratio for samples from each group is shown. Data represent mean ±SEM. N=2-3 mice per group. **p<0.01, ****p<0.0001. Statistical significance calculated using Student's t test.

IgG galactosylation in K/BxN mice with attenuated disease: FcR γ ^{-/-} and C5^{-/-} K/BxN

Next, we asked if modulating the level of inflammation in the K/BxN mouse could alter the G0/G1 profile of anti-GPI IgG, independent of autoantibody titers. We considered generating an arthritis-resistant Rag^{-/-} strain into which we could do our own transfers of KRN Tg T cells and various B cell populations to induce arthritis. Both Fc γ R deficient and C5 deficient mice are resistant to serum transfer arthritis, and we hypothesized that Rag^{-/-} mice lacking either the Fc ϵ R1 γ or C5 genes would be resistant to adoptive transfer arthritis as well. We selected the Fc γ R^{-/-}Rag^{-/-} as our preferred candidate. However, we learned in September 2009 that Dr. Bryce Binstadt, in that lab of Dr. Diane Mathis and Dr. Christophe Benoist at the Joslin Diabetes Center, had found that Fc γ R-deficient K/BxN mice are in fact not protected from arthritis, but C5-deficient K/BxN are slightly protected (Binstadt et al. 2009). They also found that K/BxN suffer from endocarditis, and that this inflammation is dependent on Fc γ R but not C5. Although we cancelled our initial plans to use Fc γ R^{-/-}Rag^{-/-} mice, we sought the opportunity to analyze IgG glycosylation in serum from Fc γ R^{-/-} and C5^{-/-} K/BxN mice.

Through a collaboration with Dr. Bryce Binstadt, who by that time had his own lab at the University of Michigan, we were able to obtain clinical scores, anti-GPI titers and serum from Fc γ R-deficient K/BxN and C5-deficient K/BxN mice. We analyzed the G0/G1 profile of total serum IgG from these mice, and looked for a correlation between the glycan profile and either clinical indices or anti-GPI titers. We found that while the C5^{-/-} mice had reduced severity of arthritis (**Figure 8.5A**), both their anti-GPI titers and G0/G1 profile were comparable to C5⁺ K/BxN (**Figure 8.5B and C**). In fact, no difference in IgG G0/G1 ratio was observed in Fc γ R⁻ or C5-deficient K/BxN mice, compared to their respective controls (Fc γ R^{+/+} K/BxN and C5^{+/-} K/BxN) (**Figure 8.5D**). G0/G1 profile did not appear to correlate with arthritis disease activity in C5-deficient mice (**Figure 8.5E**), although it is important to note that these mice all had endocarditis that is not accounted for in the arthritis score. Notably, the correlation between G0/G1 and titers remained somewhat intact (**Figure 8.5F**), even in mice with less severe disease. This would fit with a model whereby anti-GPI IgG contributes the hypogalactosyl IgG, and thus more anti-GPI results in lower G0/G1 for total serum IgG.

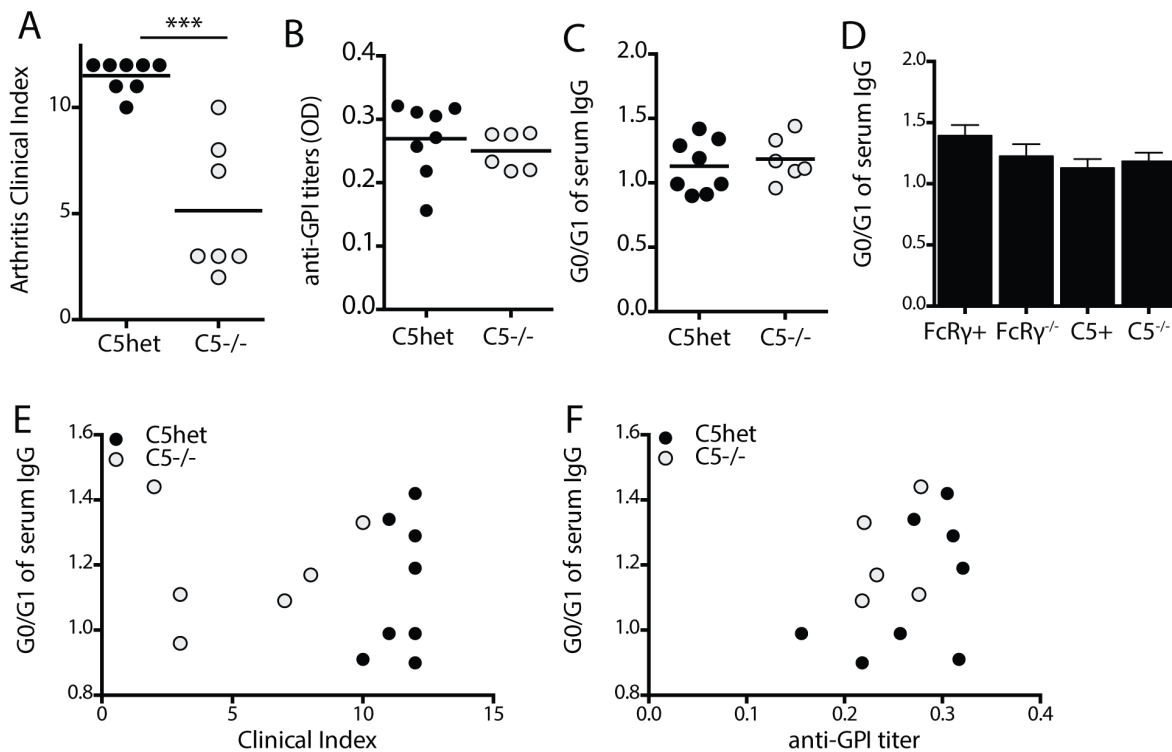


Figure 8.5. Mutant K/BxN mice with reduced arthritis or endocarditis still have hypogalactosylation of IgG. K/BxN mice lacking the Fc γ 1 chain (Fc γ R $^{-/-}$) have full arthritis, but no endocarditis. In contrast, K/BxN mice lacking the complement protein C5 have attenuated arthritis, but full endocarditis. Clinical index, titers and serum from these mice were provided by Dr. Bryce Binstadt. A. Arthritis clinical scores from C5 $^{+/-}$ and C5 $^{-/-}$ K/BxN mice. B. Anti-GPI titers from C5 $^{+/-}$ and C5 $^{-/-}$ K/BxN mice. C. IgG heavy chains were purified from total serum IgG, and glycans were analyzed by HPLC. G0/G1 ratios are shown. D. IgG heavy chains from FcR $\gamma^{-/-}$ and FcR γ^{+} mice were purified from total serum IgG, and analyzed by HPLC, as well. Summary of G0/G1 profile for all groups is shown. E. Comparison of arthritis clinical scores and G0/G1 in C5 $^{+}$ and C5 $^{-/-}$ mice. F. Comparison of anti-GPI titers with G0/G1 ratios in C5 $^{+}$ and C5 $^{-/-}$ mice. Lines on dot plots represent means. Bars represent mean, error bars represent SEM. N=6-8 mice per group. ***p<0.001. Statistical significance calculated using Student's t test.

IgG galactosylation in K/BxN mice with attenuated disease: a germ free environment

We were still interested in finding K/BxN mice with reduced disease, to see if in any case the linkage between titers and G0/G1 profiles could be broken. We learned from one of our collaborators that K/BxN mice raised in a germ free (GF) environment have delayed and attenuated arthritis, compared to their counterparts raised in specific pathogen free (SPF) environments (Wu et al. 2010). We hypothesized that if IgG glycosylation is more coupled to inflammation than to autoantibody titers, then we would expect the GF K/BxN mice to have a less dramatic IgG hypogalactosylation phenotype than their SPF counterparts. Titers, scores, and serum samples from 9.5 week old K/BxN and BxN mice raised in SPF or GF environments were kindly shared by Joyce Wu from the lab of Dr. Mathis and Dr. Benoist at Joslin Diabetes Center and HMS. Although clinical scores are reduced in 9.5 week old GF K/BxN mice compared to SPF K/BxN mice (Wu et al. 2010), this did not reach statistical significance for the groups we analyzed (**Figure 8.6A**). Anti-GPI titers in GF and SPF K/BxN mice were comparable (**Figure 8.6B**). We found that the G0/G1 ratio was slightly reduced in GF K/BxN, but this was not statistically significant (**Figure 8.6C**). However, the correlation between G0/G1 and titers remained the same in both GF and SPF mice (**Figure 8.6D**), as was the correlation between clinical score and titers (**Figure 8.6E**). This contrasts with our observation in C5^{-/-} K/BxN mice. To us, the GF K/BxN data looks like young K/BxN: lower disease, lower titers, lower G0/G1.

These results do not aid in differentiating the influences of inflammation or IgG production on IgG galactosylation, although they do support the model where anti-GPI IgG predominantly contributes to the apparent hypogalactosylation of serum IgG in arthritic mice.

Galactosylation of repertoire and anti-GPI IgG in Rituxan-treated hCD20 K/BxN mice

Although we had tried to compare repertoire and anti-GPI IgG G0/G1 profiles directly from K/BxN serum, these experiments were technically challenging and it was not clear whether a 'repertoire' population of any detectable significance was present in arthritic K/BxN mice. However, we learned from our collaborator Dr. Haochu Huang about a scenario where K/BxN mice did have a significant repertoire IgG population. We thought this could be a better system to isolate both anti-GPI and repertoire IgG from arthritic K/BxN mice. Dr. Huang had generated K/BxN mice carrying the human CD20 (hCD20) gene in a bacterial artificial chromosome, which resulted in hCD20 expression on B cells. These mice were responsive to treatment with the B cell

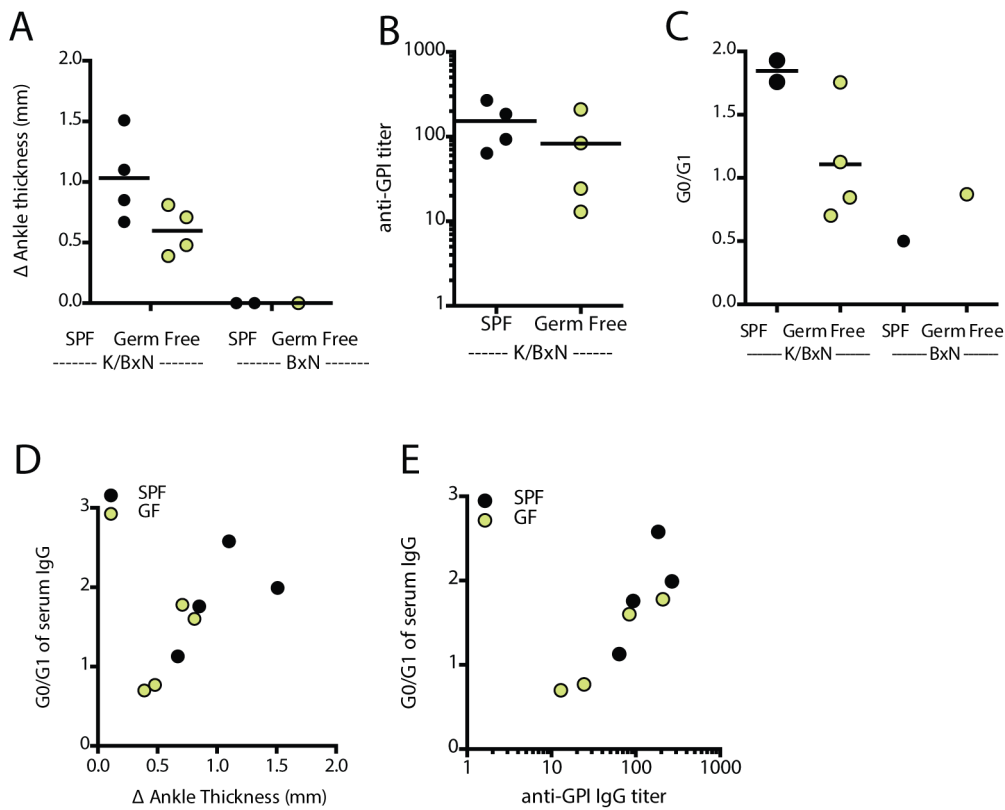


Figure 8.6. K/BxN mice raised in a germ free environment have lower G0/G1 profiles compared to SPF K/BxN mice. K/BxN and BxN mice were raised in SPF or GF environments. Clinical data, anti-GPI titers, and serum were provided by Dr. Joyce Wu from the lab of Drs. Mathis and Benoist. A. Ankle swelling as a measure of disease severity in K/BxN mice raised GF or SPF environments. B. Anti-GPI titers in K/BxN mice raised in GF or SFP environments. C. IgG heavy chains were isolated from total serum IgG, and glycans were analyzed by HPLC. G0/G1 ratios are shown for each mouse. D. Correlation of G0/G1 profile with disease burden, as measured by change in ankle thickness from baseline, in SPF and GF K/BxN mice. E. Correlation of G0/G1 profile with anti-GPI titers in SPF and GF K/BxN mice.

depleting monoclonal antibody Rituxan (anti-Human CD20) (Huang, Benoist, and Mathis 2010). Rituximab treatment in these mice reduces anti-GPI titers, depletes GPI-positive B cells, has no observable effect on clinical disease, and is accompanied by a gradual increase of ‘repertoire’ IgG (Huang, Benoist, and Mathis 2010). If hypogalactosylation of IgG in these mice was restricted to anti-GPI autoantibodies, this would suggest a change in glycosylation program specific to anti-GPI IgG-secreting B cells—possibly the splenic plasmablasts which Dr. Huang had shown to be the primary producers of anti-GPI IgG. In contrast, if hypogalactosylation was a feature of all IgG in these mice, this would point to a role for inflammatory feedback on all IgG-secreting cells.

We obtained serum samples from K/BxN and hCD20 K/BxN mice prior to and after treatment with Rituximab for different durations: 0, 4, 6, 10, 12, 14 and 17 weeks of treatment. Although the initial intent was to analyze only the post-treatment serum samples, pre-treatment samples were included as well. Serum was first depleted of the Rituxan mAb by passage over an anti-human IgG affinity column. Removal of Rituxan was confirmed by anti-human IgG ELISA. The flow-through was incubated with a series of GPI-sepharose beads to collect GPI-reactive IgG, and each flow-through was evaluated for GPI reactivity by GPI ELISA. When the reactivity was as low as that of healthy normal mouse serum, the final flow through was then incubated with protein G sepharose for purification of ‘repertoire’ IgG. As shown in **Figure 8.7A**, the repertoire IgG fraction was substantially reduced in its anti-GPI reactivity (much better than in my earlier experiments, as shown in Figure 3). Both the anti-GPI IgG and the final repertoire IgG were analyzed for their glycan profile. The repertoire IgG had a G0/G1 profile lower than that of anti-GPI IgG, both prior to and after Rituxan treatment (**Figure 8.7B and C**). Rituxan treatment did not appear to change the G0/G1 profile of either repertoire or anti-GPI IgG (**Figure 8.7D and E**). These experiments suggested that anti-GPI IgG was uniquely hypogalactosylated, and contributed to the apparent increase in G0/G1 of total serum IgG during arthritis in K/BxN mice. This data also suggests that hypogalactosylation could be specific to IgG secreted by splenic plasmablasts, since Dr. Huang had shown that anti-GPI IgG arises almost exclusively from this type of antibody secreting cell.

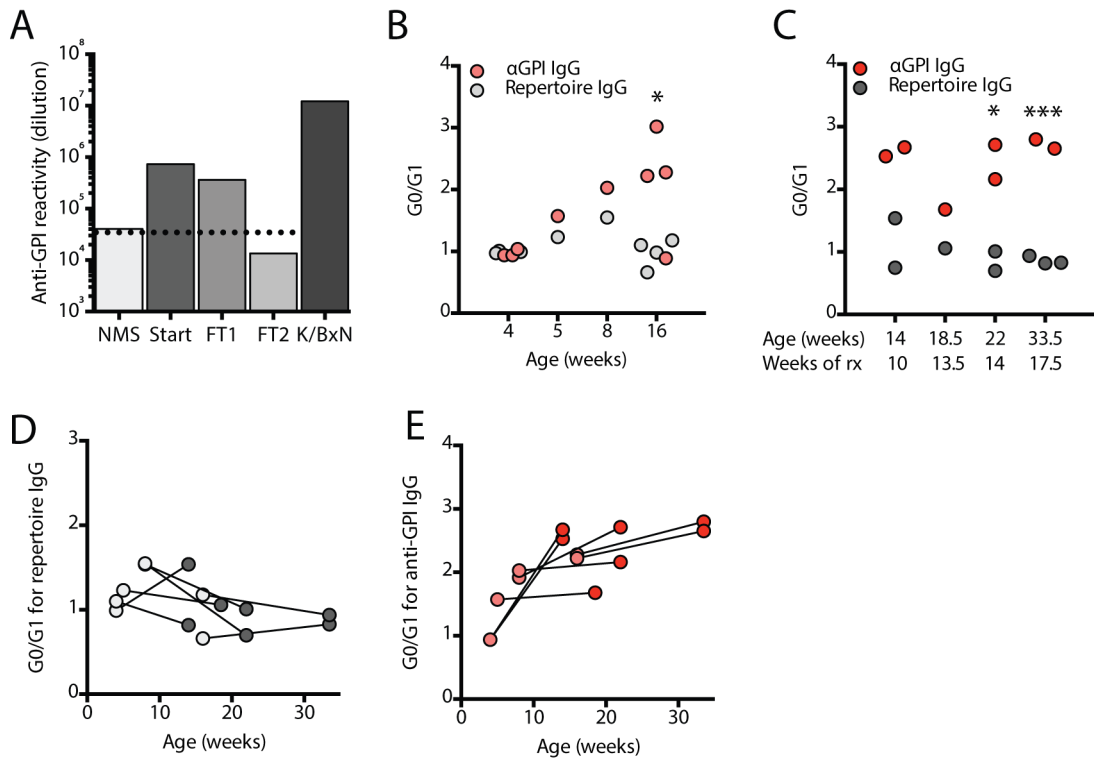


Figure 8.7. Anti-GPI IgG is hypogalactosylated compared to repertoire IgG in K/BxN mice. K/BxN mice carrying the human CD20 gene in a bacterial artificial chromosome were treated with Rituxan (anti-human CD20 mAb, human IgG1 Fc) for 10-17.5 weeks. Serum was collected prior to and at completion of Rituxan treatment. Serum was generously provided by Dr. Haochu Huang. Rituxan was first removed from serum using an anti-human IgG1 affinity column, prior to downstream analysis. Depletion of Rituxan mAb was confirmed by anti-human IgG ELISA. Anti-GPI IgG was removed from hCD20 K/BxN serum by passage over a series of GPI affinity columns. Depletion of anti-GPI IgG from the repertoire fraction was ascertained by ELISA; only when serum reached background levels of GPI-reactivity (equivalent to that of healthy normal mouse serum) was it considered ‘depleted’ of anti-GPI IgG. Total IgG remaining in the repertoire fraction was isolated with Protein G beads. IgG heavy chains were isolated from each sample and glycans were analyzed by HPLC. A. Sample GPI ELISA data, to assess depletion of anti-GPI IgG from one serum sample. NMS= normal mouse serum for negative control. Start= Rituxan-depleted serum sample. FT1= flow through from first GPI column. FT2= flow through after second GPI column. K/BxN= positive control serum for GPI reactivity. B. G0/G1 profiles for anti-GPI and repertoire IgG isolated from serum of pre-treatment mice. C. G0/G1 profiles for anti-GPI and repertoire IgG isolated from serum of mice that had been treated with Rituxan for 10, 13.5, 14 or 17.5 weeks. D. G0/G1 ratios for repertoire IgG pre- (light gray) and post- (dark gray) Rituxan treatment. E. G0/G1 ratios for anti-GPI IgG pre- (salmon) and post- (red) Rituxan treatment.

DISCUSSION

Our goals were to determine whether the K/BxN model of arthritis replicated the hypogalactosylation phenotype of RA and, if so, how this phenotype was related to disease pathology. Our lab found that the K/BxN model does in fact display a high G0/G1 profile for serum IgG, and that this increased in concert with rising autoantibody titers and clinical symptoms. We hypothesized that this G0/G1 phenotype was due to a specific hypogalactosylation on autoantibodies, and sought evidence to support or refute this. Initial experiments suggested that this hypothesis was not true, and so we instead turned our focus to determine whether hypogalactosylation was more strongly linked to disease severity (i.e. inflammation) or antibody titers. However, a more rigorous analysis of repertoire and anti-GPI IgG from a larger cohort of K/BxN mice revealed that anti-GPI IgG are in fact hypogalactosylated compared to repertoire IgG. Further studies are needed to confirm this finding, and to define the mechanism for this specificity of altered IgG glycosylation. We hypothesize that this could be due to the nature of the antibody-secreting cell producing anti-GPI IgG, or immune signals received by autoreactive B cells.

Our data is consistent with other reports in mouse models showing that hypogalactosylation or asialylation are associated with certain antigen-specific IgG species. For example, during an active immune response, sialylation decreases on total IgG, but not IgM; this decrease is enhanced on antigen-specific IgG, compared to total IgG (Kaneko et al., 2006). Another study compared the effects of tolerogenic versus immunogenic immunization on the sialylation of antigen-specific IgG: immunization with antigen plus adjuvant results in reduced sialylation of antigen-specific IgG1 compared to total IgG1, while immunization with antigen alone or in a tolerogenic manner (antigen tethered to DEC205) results in IgG1 with sialylation comparable to that of total IgG in naïve animals. Decreased sialylation of IgG correlated with decreased expression of an α -2,6 sialyltransferase (Oefner et al. 2012). Taken together, these data indicated that IgG glycosylation can be altered on an antigen-specific population of IgG during inflammatory immune response. Further studies are needed to define the precise pathways in vivo by which B cells are activated to alter IgG glycosylation.

Studies of IgG glycosylation in RA are increasingly supporting a model where altered IgG glycosylation is specific to a subset of IgG—possibly a pathogenic subset. In RA, antibodies recognizing citrullinated proteins

(anti-citrullinated protein antibodies, ACPA) are present in a subset of RA patients, and correlate with severe erosive disease (Scherer et al. 2010). Glycan analysis of ACPA from serum and synovial fluid of RA patients revealed that serum ACPA have comparable galactosylation to total serum IgG1, but tend to lack sialic acid. In contrast, synovial fluid ACPA are enriched for agalactosyl IgG compared to total synovial fluid IgG1 (Scherer et al. 2010). This further supports the idea that ACPA have a joint-specific pathological role. One study from our group using a proprietary reagent to isolate ACPA found a higher G0/G1 profile in ACPA compared to repertoire IgG, and also found that hypogalactosylation of serum IgG correlates with disease activity, and predates onset of clinical disease and diagnosis (Ercan et al. 2010). Although the precise role of anti-citrullinated protein antibodies in RA has not been demonstrated, there are numerous implications that these are pathogenic. For instance, B cells isolated from the joints of ACPA+ RA patients make more ACPAs than do B cells isolated from the joints of ACPA- RA patients, suggesting that these are joint-specific auto-antibodies (Amara et al. 2013). Collectively, these data indicate that ACPA are associated with disease in RA, but so far it has not been possible to ascertain the relative contribution of antigen specificity versus the nature of Fc glycosylation to the pathogenicity of these autoantibodies.

The studies described here show a dramatic difference in galactosylation of autoantibodies, compared to repertoire IgG, in a model of spontaneous autoimmune arthritis. Although the polyclonal anti-GPI response is critical to precipitate disease (Maccioni et al. 2002), it is likely that that the hypogalactosyl state of this abundant autoantibody also contributes to the inflammatory disease. For example, eliminating the FcR-binding ability of anti-GPI IgG in vivo (by cleaving off all IgG glycans with EndoS) significantly reduces disease severity (Albert et al. 2008). Similarly, treating arthritic K/BxN mice with IVIG can attenuate disease (Anthony et al. 2008). Although the former treatment is not suitable for patients with RA, the latter is used to alleviate numerous inflammatory diseases, and highlights the relevance of this type of work to clinical applications.

IgG glycosylation and its importance in immunology

The relevance of antibody glycosylation in immunology is multi-fold. First, for the production of therapeutic antibodies with tunable effector functions—whether neutralizing, blocking, agonistic or depleting. Although

outside the scope of this discussion, such applications are becoming increasingly important as drugs based on monoclonal antibodies emerge as successful immunotherapies (Jefferis 2012, 2009).

A second goal is to gain an understanding of how the immune system can regulate the function of IgG by modulations of N-linked glycosylation. The pro- and anti-inflammatory effects of different IgG glycoforms are well established, and linking these to the types of antibody secreting cells or the types of immune responses may help to identify mechanisms of inflammation and resolution. These could in turn lead to new targets for therapy. For example, IVIG is widely used to treat a range of inflammatory conditions, despite the lack of a definite mechanism for its mode of action—which may furthermore be varied among its different uses (Schwab and Nimmerjahn 2013). With a finer understanding, more efficient reagents could be developed to achieve the desired therapeutic effects.

On a more speculative note, the ability to link altered glycoforms to antigen-specific antibodies and specific antibody-producing cells has additional potential. This could provide a novel way to identify pathogenic antibodies in diseases of unknown etiology, which could in turn be used to identify antigenic trigger(s) or provide biomarkers to distinguish subtypes of the disease. For example, neuromyelitis optica (NMO) is a demyelinating disease of the central nervous system that was often diagnosed as multiple sclerosis (MS), prior to identification of an NMO-specific autoantibody. Although these two diseases have many overlapping symptoms, they respond quite differently to common therapies. Traditional immunomodulatory treatments for MS tend to have no effect or even a detrimental effect on patients with NMO. The ability to distinguish these two diseases has had profound effects on patients and their quality of life (Collongues and de Seze 2011). Identifying biomarkers for other diseases, based on characterization of newly-identified autoantibodies, could lead to improved selection of best treatments, and thus improved prognosis, for patients.

Part III

General Discussion

Despite the disparate nature of the studies included in this thesis, there is at least one uniting theme: investigation of inflammatory autoimmune disease for the purpose of understanding immune function and pathology, with the long term goal of developing more targeted therapies for patients. Through investigations using multiple models—including spontaneous and induced arthritis, spontaneous and induced lupus, and induced encephalomyelitis—these studies have characterized multiple pathways that contribute to autoimmune inflammation, and suggest novel approaches for future exploration.

Several challenges continue to face the development and administration of optimal treatments for autoimmune disease. Immunosuppressive drugs can lack specificity for pathogenic immune responses, and can render patients susceptible to infections or malignancies. Immunomodulatory drugs depend on our understanding of the mechanisms of pathogenesis in a particular disease or disorder, in order to tip the balance towards a protective environment. Importantly, predicting which drugs will be most beneficial for each patient is a remaining challenge, particularly in disorders with considerable heterogeneity such as multiple sclerosis. Thus, there is great impetus for developing both more targeted therapies, and also for identification of biomarkers to predict or discern how patients will respond to a given therapy.

The studies described here relate to both of these issues. In our investigation of CD48, we identified CD48⁺⁺ cells as activated cells that contributed to disease in EAE, and which could be eliminated with an anti-CD48 antibody. Furthermore, we found that CD48 expression correlated with production of certain cytokines, suggesting that CD48 might be a valuable marker to identify pathogenic T cells for further study. By analyzing the antigen specificity of these activated cells, it may be possible to identify the targets of autoimmune attack in diseases of unknown etiology. Thus, CD48 might have value as both a therapeutic target and as a biomarker. Similarly, in our preliminary studies of IgG galactosylation during arthritis in the K/BxN mouse, we examined

the value of hypogalactosylation as both an inflammatory mediator and a biomarker. We investigated whether hypogalactosylation was more likely a driver or consequence of inflammation, to guide development of future therapies that might prevent development of this inflammatory IgG. In addition, we hypothesized that hypogalactosylation might be a unique feature of antigen-specific IgG, and could thus be a valuable biomarker for identification of autoantibodies in inflammatory disease—and, by inference, of the autoantigens driving inflammatory disease. Despite the differing level of detail in which each study was investigated, both offer only preliminary suggestions for the development of clinically relevant therapies. However, each suggests unique methods for investigating the mechanisms of autoimmunity.

In our studies of CD48, using both WT and CD48 deficient strains, we learned several things about the role of this immune receptor in regulation of autoimmunity and tolerance. First, that CD48 was not critically involved in development of spontaneous lupus-like disease, and that epistatic interactions likely involving other SLAM family genes may contribute to the disease phenotype observed in CD48^{-/-} [B6.129] mice. This is important for focusing future studies on the most relevant immunologic players, for example other polymorphic SLAMF genes. In addition, our results support the view that the B6.Sle1b model of lupus is likely due to effects from multiple genetic loci. Although development of novel models using single-gene-deficient mice is useful for laboratory study, these examples of more complex, spontaneous diseases in mice may lead to improved approaches for the study of multi-gene diseases in humans. Already, polymorphisms in a neighboring SLAMF gene have been identified as contributing to disease in the B6.Sle1b model, but this was not found to be entirely responsible (Keszei et al. 2011). The methods that are used to further dissect the mechanism of action in such multi-gene diseases may be applied to investigations of human diseases, as well.

In addition, we found that different approaches for studying the function of CD48—from knockout mice to antibodies, GVH to EAE—provided unique information about the role of this molecule. Published studies using a model of colitis had identified a key role for CD48 on macrophages, in both antigen processing and costimulation of T cells (Abadia-Molina et al. 2006). Importantly, this study found that CD48 on the T cell contributed to disease development, as well, and that when CD48 was absent from both T cells and APCs, mice were completely protected from colitis. In contrast, we found that mice lacking CD48 on both APCs and T

cells were still susceptible to EAE. Whether this is due to the different cell types involved in each disease model, or other factors, remains to be determined. Collectively, this highlights the fact that immune receptors may have important roles on different cell types, during different types of immune responses and at different times. Thus, additional roles for CD48 may become apparent using alternative approaches. While we focused our studies to date on B cell activation and TH1/TH17 responses, it is possible that CD48 has a more critical role in Th2-mediated responses.

Perhaps most excitingly, these studies revealed the potential for CD48 to act as a novel activation marker on T cells, possibly allowing for identification of cytokine-producing or activated, antigen-specific T cells. Although this work is still preliminary, there are multiple potentially valuable applications for such a cell surface marker. First, as a biomarker for identification of activated cells, CD48 may be useful to identify cells that recently encountered antigen. By studying antigen specificity of CD48⁺⁺ cells, we might learn about the antigenic triggers that led to their activation. Second, by investigating the stimuli that result in CD48 upregulation, we might learn more about the mechanisms of costimulation that lead to increased T cell activation. Third, therapies that target CD48, or other molecules with similar expression patterns in humans, could be valuable for elimination of pathogenic T cells.

A monoclonal antibody targeting CD52 was recently adapted from its prior use to treat leukemia, to a new application in patients with relapsing-remitting multiple sclerosis (Willis and Robertson 2014). CD52 is expressed on most lymphocytes in humans, but has a different expression pattern in mice. However, anti-CD52 treatment in B6 mice during EAE results in reduced numbers of IFN γ -producing, MOG-specific T cells, and reduced CNS infiltration (Turner et al. 2013). This is highly reminiscent of the effects of anti-CD48. Thus, our studies of anti-CD48 may be informative about the mechanism of anti-CD52 therapy, or may suggest an alternative target. Notably, patents for anti-CD48 as a therapy for autoimmune disease already exist, suggesting that this is an area of active investigation in the pharmaceutical industry.

In summary, this thesis has described studies of multiple models of autoimmune disease, each seeking to better understand mechanisms of pathogenesis and immunoregulation. Our results collectively highlight the potential

value of biomarkers in investigation of disease, and also the relevance of antibody Fc regions to their functions in vivo. The results described here suggest multiple paths for future investigation, including the regulation of costimulatory molecule expression, and the value of such molecules as therapeutic targets. In light of the numerous antibody-mediated therapies now approved for treatment of autoimmunity and cancer, these studies have great promise for contributing to future developments of disease-modifying therapies.

Part IV: Bibliography

- Abadia-Molina, A. C., H. Ji, W. A. Faubion, A. Julien, Y. Latchman, H. Yagita, A. Sharpe, A. K. Bhan, and C. Terhorst. 2006. 'CD48 controls T-cell and antigen-presenting cell functions in experimental colitis', *Gastroenterology*, 130: 424-34.
- Abromson-Leeman, S., R. Bronson, Y. Luo, M. Berman, R. Leeman, J. Leeman, and M. Dorf. 2004. 'T-cell properties determine disease site, clinical presentation, and cellular pathology of experimental autoimmune encephalomyelitis', *Am J Pathol*, 165: 1519-33.
- Adlard, K., L. Tsaknardis, A. Beam, B. F. Bebo, Jr., A. A. Vandembark, and H. Offner. 1999. 'Immunoregulation of encephalitogenic MBP-NAc1-11-reactive T cells by CD4+ TCR-specific T cells involves IL-4, IL-10 and IFN-gamma', *Autoimmunity*, 31: 237-48.
- Albert, H., M. Collin, D. Dudziak, J. V. Ravetch, and F. Nimmerjahn. 2008. 'In vivo enzymatic modulation of IgG glycosylation inhibits autoimmune disease in an IgG subclass-dependent manner', *Proc Natl Acad Sci U S A*, 105: 15005-9.
- Aloisi, F. 2001. 'Immune function of microglia', *Glia*, 36: 165-79.
- Amado, M., R. Almeida, T. Schwientek, and H. Clausen. 1999. 'Identification and characterization of large galactosyltransferase gene families: galactosyltransferases for all functions', *Biochim Biophys Acta*, 1473: 35-53.
- Amara, K., J. Steen, F. Murray, H. Morbach, B. M. Fernandez-Rodriguez, V. Joshua, M. Engstrom, O. Snir, L. Israelsson, A. I. Catrina, H. Wardemann, D. Corti, E. Meffre, L. Klareskog, and V. Malmstrom. 2013. 'Monoclonal IgG antibodies generated from joint-derived B cells of RA patients have a strong bias toward citrullinated autoantigen recognition', *J Exp Med*, 210: 445-55.
- Ando, D. G., J. Clayton, D. Kono, J. L. Urban, and E. E. Sercarz. 1989. 'Encephalitogenic T cells in the B10.PL model of experimental allergic encephalomyelitis (EAE) are of the Th-1 lymphokine subtype', *Cell Immunol*, 124: 132-43.
- Anthony, R. M., F. Nimmerjahn, D. J. Ashline, V. N. Reinhold, J. C. Paulson, and J. V. Ravetch. 2008. 'Recapitulation of IVIG anti-inflammatory activity with a recombinant IgG Fc', *Science*, 320: 373-6.
- Arthur, A. T., P. J. Armati, C. Bye, M. S. Genetics Consortium Southern, R. N. Heard, G. J. Stewart, J. D. Pollard, and D. R. Booth. 2008. 'Genes implicated in multiple sclerosis pathogenesis from consilience of genotyping and expression profiles in relapse and remission', *BMC Med Genet*, 9: 17.
- Arulanandam, A. R., P. Moingeon, M. F. Concino, M. A. Recny, K. Kato, H. Yagita, S. Koyasu, and E. L. Reinherz. 1993. 'A soluble multimeric recombinant CD2 protein identifies CD48 as a low affinity ligand for human CD2: divergence of CD2 ligands during the evolution of humans and mice', *J Exp Med*, 177: 1439-50.
- Bai, Y., S. Fu, S. Honig, Y. Wang, L. Qin, D. Chen, and J. S. Bromberg. 2002. 'CD2 is a dominant target for allogeneic responses', *Am J Transplant*, 2: 618-26.
- Banda, N. K., A. K. Wood, K. Takahashi, B. Levitt, P. M. Rudd, L. Royle, J. L. Abrahams, G. L. Stahl, V. M. Holers, and W. P. Arend. 2008. 'Initiation of the alternative pathway of murine complement by immune complexes is dependent on N-glycans in IgG antibodies', *Arthritis Rheum*, 58: 3081-9.

- Baorto, D. M., Z. Gao, R. Malaviya, M. L. Dustin, A. van der Merwe, D. M. Lublin, and S. N. Abraham. 1997. 'Survival of FimH-expressing enterobacteria in macrophages relies on glycolipid traffic', *Nature*, 389: 636-9.
- Baron, J. L., J. A. Madri, N. H. Ruddle, G. Hashim, and C. A. Janeway, Jr. 1993. 'Surface expression of alpha 4 integrin by CD4 T cells is required for their entry into brain parenchyma', *J Exp Med*, 177: 57-68.
- Batoulis, H., M. S. Recks, K. Addicks, and S. Kuerten. 2011. 'Experimental autoimmune encephalomyelitis--achievements and prospective advances', *APMIS*, 119: 819-30.
- Becher, B., B. G. Durell, and R. J. Noelle. 2002. 'Experimental autoimmune encephalitis and inflammation in the absence of interleukin-12', *J Clin Invest*, 110: 493-7.
- — —. 2003. 'IL-23 produced by CNS-resident cells controls T cell encephalitogenicity during the effector phase of experimental autoimmune encephalomyelitis', *J Clin Invest*, 112: 1186-91.
- Becher, B., I. Bechmann, and M. Greter. 2006. 'Antigen presentation in autoimmunity and CNS inflammation: how T lymphocytes recognize the brain', *J Mol Med (Berl)*, 84: 532-43
- Beeston, T., T. R. Smith, I. Maricic, X. Tang, and V. Kumar. 2010. 'Involvement of IFN-gamma and perforin, but not Fas/FasL interactions in regulatory T cell-mediated suppression of experimental autoimmune encephalomyelitis', *J Neuroimmunol*, 229: 91-7.
- Berard, J. L., K. Wolak, S. Fournier, and S. David. 2010. 'Characterization of relapsing-remitting and chronic forms of experimental autoimmune encephalomyelitis in C57BL/6 mice', *Glia*, 58: 434-45.
- Bettelli, E., D. Baeten, A. Jager, R. A. Sobel, and V. K. Kuchroo. 2006. 'Myelin oligodendrocyte glycoprotein-specific T and B cells cooperate to induce a Devic-like disease in mice', *J Clin Invest*, 116: 2393-402.
- Bettelli, E., M. P. Das, E. D. Howard, H. L. Weiner, R. A. Sobel, and V. K. Kuchroo. 1998. 'IL-10 is critical in the regulation of autoimmune encephalomyelitis as demonstrated by studies of IL-10- and IL-4-deficient and transgenic mice', *J Immunol*, 161: 3299-306.
- Bettelli, E., M. Pagany, H. L. Weiner, C. Linington, R. A. Sobel, and V. K. Kuchroo. 2003. 'Myelin oligodendrocyte glycoprotein-specific T cell receptor transgenic mice develop spontaneous autoimmune optic neuritis', *J Exp Med*, 197: 1073-81.
- Binstadt, B. A., J. L. Hebert, A. Ortiz-Lopez, R. Bronson, C. Benoist, and D. Mathis. 2009. 'The same systemic autoimmune disease provokes arthritis and endocarditis via distinct mechanisms', *Proc Natl Acad Sci U S A*, 106: 16758-63.
- Blackburn, S. D., H. Shin, W. N. Haining, T. Zou, C. J. Workman, A. Polley, M. R. Betts, G. J. Freeman, D. A. Vignali, and E. J. Wherry. 2009. 'Coregulation of CD8+ T cell exhaustion by multiple inhibitory receptors during chronic viral infection', *Nat Immunol*, 10: 29-37.
- Blazar, B. R., P. A. Taylor, A. Panoskaltis-Mortari, H. Yagita, J. S. Bromberg, and D. A. Valleria. 1998. 'A critical role for CD48 antigen in regulating alloengraftment and lymphohematopoietic recovery after bone marrow transplantation', *Blood*, 92: 4453-63.
- Bloch-Queyrat, C., M. C. Fondaneche, R. Chen, L. Yin, F. Relouzat, A. Veillette, A. Fischer, and S. Latour. 2005. 'Regulation of natural cytotoxicity by the adaptor SAP and the Src-related kinase Fyn', *J Exp Med*, 202: 181-92.
- Boles, N. C., K. K. Lin, G. L. Lukov, T. V. Bowman, M. T. Baldrige, and M. A. Goodell. 2011. 'CD48 on hematopoietic progenitors regulates stem cells and suppresses tumor formation', *Blood*, 118: 80-7.

- Bond, A., A. Alavi, J. S. Axford, B. E. Bourke, F. E. Bruckner, M. A. Kerr, J. D. Maxwell, K. J. Tweed, M. J. Weldon, P. Youinou, and F. C. Hay. 1997. 'A detailed lectin analysis of IgG glycosylation, demonstrating disease specific changes in terminal galactose and N-acetylglucosamine', *J Autoimmun*, 10: 77-85.
- Brennan, F. R., J. K. O'Neill, S. J. Allen, C. Butter, G. Nuki, and D. Baker. 1999. 'CD44 is involved in selective leucocyte extravasation during inflammatory central nervous system disease', *Immunology*, 98: 427-35.
- Brocke, S., C. Piercy, L. Steinman, I. L. Weissman, and T. Veromaa. 1999. 'Antibodies to CD44 and integrin alpha4, but not L-selectin, prevent central nervous system inflammation and experimental encephalomyelitis by blocking secondary leukocyte recruitment', *Proc Natl Acad Sci U S A*, 96: 6896-901.
- Brown, M. H., K. Boles, P. A. van der Merwe, V. Kumar, P. A. Mathew, and A. N. Barclay. 1998. '2B4, the natural killer and T cell immunoglobulin superfamily surface protein, is a ligand for CD48', *J Exp Med*, 188: 2083-90.
- Cabrero, J. G., G. J. Freeman, and H. Reiser. 1998. 'The murine Cd48 gene: allelic polymorphism in the IgV-like region', *Eur J Immunogenet*, 25: 421-3.
- Calpe, Silvia, Ninghai Wang, Xavier Romero, Scott B. Berger, Arpad Lanyi, Pablo Engel, and Cox Terhorst. 2008. 'The SLAM and SAP Gene Families Control Innate and Adaptive Immune Responses', 97: 177-250.
- Cannella, B., A. H. Cross, and C. S. Raine. 1993. 'Anti-adhesion molecule therapy in experimental autoimmune encephalomyelitis', *J Neuroimmunol*, 46: 43-55.
- Cannons, J. L., S. G. Tangye, and P. L. Schwartzberg. 2011. 'SLAM family receptors and SAP adaptors in immunity', *Annu Rev Immunol*, 29: 665-705.
- Cao, E., U. A. Ramagopal, A. Fedorov, E. Fedorov, Q. Yan, J. W. Lary, J. L. Cole, S. G. Nathenson, and S. C. Almo. 2006. 'NTB-A receptor crystal structure: insights into homophilic interactions in the signaling lymphocytic activation molecule receptor family', *Immunity*, 25: 559-70.
- Carlucci, F., J. Cortes-Hernandez, L. Fossati-Jimack, A. E. Bygrave, M. J. Walport, T. J. Vyse, H. T. Cook, and M. Botto. 2007. 'Genetic dissection of spontaneous autoimmunity driven by 129-derived chromosome 1 Loci when expressed on C57BL/6 mice', *J Immunol*, 178: 2352-60.
- Chang, T. T., C. Jabs, R. A. Sobel, V. K. Kuchroo, and A. H. Sharpe. 1999. 'Studies in B7-deficient mice reveal a critical role for B7 costimulation in both induction and effector phases of experimental autoimmune encephalomyelitis', *J Exp Med*, 190: 733-40.
- Chavin, K. D., H. T. Lau, and J. S. Bromberg. 1992. 'Prolongation of allograft and xenograft survival in mice by anti-CD2 monoclonal antibodies', *Transplantation*, 54: 286-91.
- Chavin, K. D., L. Qin, J. Lin, J. Woodward, P. Baliga, K. Kato, H. Yagita, and J. S. Bromberg. 1994. 'Anti-CD48 (murine CD2 ligand) mAbs suppress cell mediated immunity in vivo', *Int Immunol*, 6: 701-9.
- Chavin, K. D., L. Qin, J. Lin, H. Yagita, and J. S. Bromberg. 1993. 'Combined anti-CD2 and anti-CD3 receptor monoclonal antibodies induce donor-specific tolerance in a cardiac transplant model', *J Immunol*, 151: 7249-59.
- Chen, M. L., B. S. Yan, D. Kozoriz, and H. L. Weiner. 2009. 'Novel CD8+ Treg suppress EAE by TGF-beta- and IFN-gamma-dependent mechanisms', *Eur J Immunol*, 39: 3423-35.

- Chitnis, T., N. Najafian, K. A. Abdallah, V. Dong, H. Yagita, M. H. Sayegh, and S. J. Khoury. 2001. 'CD28-independent induction of experimental autoimmune encephalomyelitis', *J Clin Invest*, 107: 575-83.
- Chlewicki, L. K., C. A. Velikovsky, V. Balakrishnan, R. A. Mariuzza, and V. Kumar. 2008. 'Molecular basis of the dual functions of 2B4 (CD244)', *J Immunol*, 180: 8159-67.
- Chu, C. Q., S. Wittmer, and D. K. Dalton. 2000. 'Failure to suppress the expansion of the activated CD4 T cell population in interferon gamma-deficient mice leads to exacerbation of experimental autoimmune encephalomyelitis', *J Exp Med*, 192: 123-8.
- Clarkson, N. G., and M. H. Brown. 2009. 'Inhibition and activation by CD244 depends on CD2 and phospholipase C-gamma1', *J Biol Chem*, 284: 24725-34.
- Codarri, L., G. Gyulveszi, V. Tosevski, L. Hesske, A. Fontana, L. Magnenat, T. Suter, and B. Becher. 2011. 'RORgammat drives production of the cytokine GM-CSF in helper T cells, which is essential for the effector phase of autoimmune neuroinflammation', *Nat Immunol*, 12: 560-7.
- Compston, A., and A. Coles. 2002. 'Multiple sclerosis', *Lancet*, 359: 1221-31.
- Collongues, N., and J. de Seze. 2011. 'Current and future treatment approaches for neuromyelitis optica', *Ther Adv Neurol Disord*, 4: 111-21.
- Crocker, B. P., G. Gilkeson, and L. Morel. 2003. 'Genetic interactions between susceptibility loci reveal epistatic pathogenic networks in murine lupus', *Genes Immun*, 4: 575-85.
- Cua, D. J., J. Sherlock, Y. Chen, C. A. Murphy, B. Joyce, B. Seymour, L. Lucian, W. To, S. Kwan, T. Churakova, S. Zurawski, M. Wiekowski, S. A. Lira, D. Gorman, R. A. Kastelein, and J. D. Sedgwick. 2003. 'Interleukin-23 rather than interleukin-12 is the critical cytokine for autoimmune inflammation of the brain', *Nature*, 421: 744-8.
- Davis, S. J., and P. A. van der Merwe. 1996. 'The structure and ligand interactions of CD2: implications for T-cell function', *Immunol Today*, 17: 177-87.
- Davis, W. C., and M. J. Hamilton. 2008. 'Use of flow cytometry to develop and characterize a set of monoclonal antibodies specific for rabbit leukocyte differentiation molecules', *J Vet Sci*, 9: 51-66.
- De Jager, P. L., C. Baecher-Allan, L. M. Maier, A. T. Arthur, L. Ottoboni, L. Barcellos, J. L. McCauley, S. Sawcer, A. Goris, J. Saarela, R. Yelensky, A. Price, V. Leppa, N. Patterson, P. I. de Bakker, D. Tran, C. Aubin, S. Pobywajlo, E. Rossin, X. Hu, C. W. Ashley, E. Choy, J. D. Rioux, M. A. Pericak-Vance, A. Ivinson, D. R. Booth, G. J. Stewart, A. Palotie, L. Peltonen, B. Dubois, J. L. Haines, H. L. Weiner, A. Compston, S. L. Hauser, M. J. Daly, D. Reich, J. R. Oksenberg, and D. A. Hafler. 2009. 'The role of the CD58 locus in multiple sclerosis', *Proc Natl Acad Sci U S A*, 106: 5264-9.
- Deisenhofer, J. 1981. 'Crystallographic refinement and atomic models of a human Fc fragment and its complex with fragment B of protein A from *Staphylococcus aureus* at 2.9- and 2.8-A resolution', *Biochemistry*, 20: 2361-70.
- Drbal, K., M. Moertelmaier, C. Holzhauser, A. Muhammad, E. Fuertbauer, S. Howorka, M. Hinterberger, H. Stockinger, and G. J. Schutz. 2007. 'Single-molecule microscopy reveals heterogeneous dynamics of lipid raft components upon TCR engagement', *Int. Immunol*, 19: 675-684.

- Dungan, L. S., N. C. McGuinness, L. Boon, M. A. Lynch, and K. H. Mills. 2014. 'Innate IFN-gamma promotes development of experimental autoimmune encephalomyelitis: a role for NK cells and M1 macrophages', *Eur J Immunol*, 44: 2903-17.
- Dustin, M. L., M. E. Sanders, S. Shaw, and T. A. Springer. 1987. 'Purified lymphocyte function-associated antigen 3 binds to CD2 and mediates T lymphocyte adhesion', *J Exp Med*, 165: 677-92.
- El-Behi, M., B. Ciric, H. Dai, Y. Yan, M. Cullimore, F. Safavi, G. X. Zhang, B. N. Dittel, and A. Rostami. 2011. 'The encephalitogenicity of T(H)17 cells is dependent on IL-1- and IL-23-induced production of the cytokine GM-CSF', *Nat Immunol*, 12: 568-75.
- Elishmereni, M., I. Bachelet, A. H. Nissim Ben-Efraim, D. Mankuta, and F. Levi-Schaffer. 2013. 'Interacting mast cells and eosinophils acquire an enhanced activation state in vitro', *Allergy*, 68: 171-9.
- Ercan, A., J. Cui, D. E. Chatterton, K. D. Deane, M. M. Hazen, W. Brintnell, C. I. O'Donnell, L. A. Derber, M. E. Weinblatt, N. A. Shadick, D. A. Bell, E. Cairns, D. H. Solomon, V. M. Holers, P. M. Rudd, and D. M. Lee. 2010. 'Aberrant IgG galactosylation precedes disease onset, correlates with disease activity, and is prevalent in autoantibodies in rheumatoid arthritis', *Arthritis Rheum*, 62: 2239-48.
- Falco, M., E. Marcenaro, E. Romeo, F. Bellora, D. Marras, F. Vely, G. Ferracci, L. Moretta, A. Moretta, and C. Bottino. 2004. 'Homophilic interaction of NTB-A, a member of the CD2 molecular family: induction of cytotoxicity and cytokine release in human NK cells', *Eur J Immunol*, 34: 1663-72.
- Fennelly, J. A., B. Tiwari, S. J. Davis, and E. J. Evans. 2001. 'CD2F-10: a new member of the CD2 subset of the immunoglobulin superfamily', *Immunogenetics*, 53: 599-602.
- Ferber, I. A., S. Brocke, C. Taylor-Edwards, W. Ridgway, C. Dinisco, L. Steinman, D. Dalton, and C. G. Fathman. 1996. 'Mice with a disrupted IFN-gamma gene are susceptible to the induction of experimental autoimmune encephalomyelitis (EAE)', *J Immunol*, 156: 5-7.
- Fillatreau, S., C. H. Sweeney, M. J. McGeachy, D. Gray, and S. M. Anderton. 2002. 'B cells regulate autoimmunity by provision of IL-10', *Nat Immunol*, 3: 944-50.
- Flaig, R. M., S. Stark, and C. Watzl. 2004. 'Cutting edge: NTB-A activates NK cells via homophilic interaction', *J Immunol*, 172: 6524-7.
- Ford, M. L., and B. D. Evavold. 2005. 'Specificity, magnitude, and kinetics of MOG-specific CD8+ T cell responses during experimental autoimmune encephalomyelitis', *Eur J Immunol*, 35: 76-85.
- Francisco, L. M., P. T. Sage, and A. H. Sharpe. 2010. 'The PD-1 pathway in tolerance and autoimmunity', *Immunol Rev*, 236: 219-42.
- Fraser, C. C., D. Howie, M. Morra, Y. Qiu, C. Murphy, Q. Shen, J. C. Gutierrez-Ramos, A. Coyle, G. A. Kingsbury, and C. Terhorst. 2002. 'Identification and characterization of SF2000 and SF2001, two new members of the immune receptor SLAM/CD2 family', *Immunogenetics*, 53: 843-50.
- Friese, M. A., and L. Fugger. 2009. 'Pathogenic CD8(+) T cells in multiple sclerosis', *Ann Neurol*, 66: 132-41.
- Fujino, M., N. Funeshima, Y. Kitazawa, H. Kimura, H. Amemiya, S. Suzuki, and X. K. Li. 2003. 'Amelioration of experimental autoimmune encephalomyelitis in Lewis rats by FTY720 treatment', *J Pharmacol Exp Ther*, 305: 70-7.
- Garcia, J. A., P. A. Pino, M. Mizutani, S. M. Cardona, I. F. Charo, R. M. Ransohoff, T. G. Forsthuber, and A. E. Cardona. 2013. 'Regulation of adaptive immunity by the fractalkine receptor during autoimmune inflammation', *J Immunol*, 191: 1063-72.

- Garni-Wagner, B. A., A. Purohit, P. A. Mathew, M. Bennett, and V. Kumar. 1993. 'A novel function-associated molecule related to non-MHC-restricted cytotoxicity mediated by activated natural killer cells and T cells', *J Immunol*, 151: 60-70.
- Genaro, A. M., J. A. Gonzalo, L. Bosca, and C. Martinez. 1994. 'CD2-CD48 interaction prevents apoptosis in murine B lymphocytes by up-regulating bcl-2 expression', *Eur J Immunol*, 24: 2515-21.
- Glatigny, S., R. Duhon, C. Arbelaez, S. Kumari, and E. Bettelli. 2015. 'Integrin alpha L controls the homing of regulatory T cells during CNS autoimmunity in the absence of integrin alpha 4', *Sci Rep*, 5: 7834.
- Glatigny, S., R. Duhon, M. Oukka, and E. Bettelli. 2011. 'Cutting edge: loss of alpha4 integrin expression differentially affects the homing of Th1 and Th17 cells', *J Immunol*, 187: 6176-9.
- Gommerman, J. L., K. Giza, S. Perper, I. Sizing, A. Ngam-Ek, C. Nickerson-Nutter, and J. L. Browning. 2003. 'A role for surface lymphotoxin in experimental autoimmune encephalomyelitis independent of LIGHT', *J Clin Invest*, 112: 755-67.
- Gonzalez-Cabrero, J., C. J. Wise, Y. Latchman, G. J. Freeman, A. H. Sharpe, and H. Reiser. 1999. 'CD48-deficient mice have a pronounced defect in CD4(+) T cell activation', *Proc Natl Acad Sci U S A*, 96: 1019-23.
- Gordon, E. J., K. J. Myers, J. P. Dougherty, H. Rosen, and Y. Ron. 1995. 'Both anti-CD11a (LFA-1) and anti-CD11b (MAC-1) therapy delay the onset and diminish the severity of experimental autoimmune encephalomyelitis', *J Neuroimmunol*, 62: 153-60.
- Gran, B., G. X. Zhang, S. Yu, J. Li, X. H. Chen, E. S. Ventura, M. Kamoun, and A. Rostami. 2002. 'IL-12p35-deficient mice are susceptible to experimental autoimmune encephalomyelitis: evidence for redundancy in the IL-12 system in the induction of central nervous system autoimmune demyelination', *J Immunol*, 169: 7104-10.
- Greer, J. M., R. A. Sobel, A. Sette, S. Southwood, M. B. Lees, and V. K. Kuchroo. 1996. 'Immunogenic and encephalitogenic epitope clusters of myelin proteolipid protein', *J Immunol*, 156: 371-9.
- Greter, M., F. L. Heppner, M. P. Lemos, B. M. Odermatt, N. Goebels, T. Laufer, R. J. Noelle, and B. Becher. 2005. 'Dendritic cells permit immune invasion of the CNS in an animal model of multiple sclerosis', *Nat Med*, 11: 328-34.
- Hao, J., R. Liu, W. Piao, Q. Zhou, T. L. Vollmer, D. I. Campagnolo, R. Xiang, A. La Cava, L. Van Kaer, and F. D. Shi. 2010. 'Central nervous system (CNS)-resident natural killer cells suppress Th17 responses and CNS autoimmune pathology', *J Exp Med*, 207: 1907-21.
- Harder, T., and K. Simons. 1997. 'Caveolae, DIGs, and the dynamics of sphingolipid-cholesterol microdomains', *Curr Opin Cell Biol*, 9: 534-42.
- Hjelmstrom, P., A. E. Juedes, J. Fjell, and N. H. Ruddle. 1998. 'B-cell-deficient mice develop experimental allergic encephalomyelitis with demyelination after myelin oligodendrocyte glycoprotein sensitization', *J Immunol*, 161: 4480-3.
- Hoffmann, J. C., C. Herklotz, H. Zeidler, B. Bayer, and J. Westermann. 1997. 'Anti-CD2 (OX34) MoAb treatment of adjuvant arthritic rats: attenuation of established arthritis, selective depletion of CD4+ T cells, and CD2 down-modulation', *Clin Exp Immunol*, 110: 63-71.
- Hosen, N., H. Ichihara, A. Mugitani, Y. Aoyama, Y. Fukuda, S. Kishida, Y. Matsuoka, H. Nakajima, M. Kawakami, T. Yamagami, S. Fuji, H. Tamaki, T. Nakao, S. Nishida, A. Tsuboi, S. Iida, M. Hino, Y.

- Oka, Y. Oji, and H. Sugiyama. 2012. 'CD48 as a novel molecular target for antibody therapy in multiple myeloma', *Br J Haematol*, 156: 213-24.
- Huang, D., F. D. Shi, S. Jung, G. C. Pien, J. Wang, T. P. Salazar-Mather, T. T. He, J. T. Weaver, H. G. Ljunggren, C. A. Biron, D. R. Littman, and R. M. Ransohoff. 2006. 'The neuronal chemokine CX3CL1/fractalkine selectively recruits NK cells that modify experimental autoimmune encephalomyelitis within the central nervous system', *FASEB J*, 20: 896-905.
- Huang, H., C. Benoist, and D. Mathis. 2010. 'Rituximab specifically depletes short-lived autoreactive plasma cells in a mouse model of inflammatory arthritis', *Proc Natl Acad Sci U S A*, 107: 4658-63.
- Huang, H., J. F. Kearney, M. J. Grusby, C. Benoist, and D. Mathis. 2006. 'Induction of tolerance in arthritogenic B cells with receptors of differing affinity for self-antigen', *Proc Natl Acad Sci U S A*, 103: 3734-9.
- Huseby, E. S., P. G. Huseby, S. Shah, R. Smith, and B. D. Stadinski. 2012. 'Pathogenic CD8 T cells in multiple sclerosis and its experimental models', *Front Immunol*, 3: 64.
- Huseby, E. S., D. Liggitt, T. Brabb, B. Schnabel, C. Ohlen, and J. Goverman. 2001. 'A pathogenic role for myelin-specific CD8(+) T cells in a model for multiple sclerosis', *J Exp Med*, 194: 669-76.
- International Multiple Sclerosis Genetics, Consortium. 2013. 'Network-based multiple sclerosis pathway analysis with GWAS data from 15,000 cases and 30,000 controls', *Am J Hum Genet*, 92: 854-65.
- International Multiple Sclerosis Genetics, Consortium, D. A. Hafler, A. Compston, S. Sawcer, E. S. Lander, M. J. Daly, P. L. De Jager, P. I. de Bakker, S. B. Gabriel, D. B. Mirel, A. J. Iverson, M. A. Pericak-Vance, S. G. Gregory, J. D. Rioux, J. L. McCauley, J. L. Haines, L. F. Barcellos, B. Cree, J. R. Oksenberg, and S. L. Hauser. 2007. 'Risk alleles for multiple sclerosis identified by a genomewide study', *N Engl J Med*, 357: 851-62.
- Jager, A., V. Dardalhon, R. A. Sobel, E. Bettelli, and V. K. Kuchroo. 2009. 'Th1, Th17, and Th9 effector cells induce experimental autoimmune encephalomyelitis with different pathological phenotypes', *J Immunol*, 183: 7169-77.
- Jeddi, P., J. Keusch, P. M. Lydyard, K. B. Bodman-Smith, M. S. Chesnutt, D. Wofsy, H. Hirota, T. Taga, and P. J. Delves. 1999. 'The effect on immunoglobulin glycosylation of altering in vivo production of immunoglobulin G', *Immunology*, 98: 475-80.
- Jefferis, R. 2009. 'Glycosylation as a strategy to improve antibody-based therapeutics', *Nat Rev Drug Discov*, 8: 226-34.
- — —. 2012. 'Isotype and glycoform selection for antibody therapeutics', *Arch Biochem Biophys*, 526: 159-66.
- Jefferis, R., J. Lund, H. Mizutani, H. Nakagawa, Y. Kawazoe, Y. Arata, and N. Takahashi. 1990. 'A comparative study of the N-linked oligosaccharide structures of human IgG subclass proteins', *Biochem J*, 268: 529-37.
- Jiang, H., S. I. Zhang, and B. Pernis. 1992. 'Role of CD8+ T cells in murine experimental allergic encephalomyelitis', *Science*, 256: 1213-5.
- Jostins, L., S. Ripke, R. K. Weersma, R. H. Duerr, D. P. McGovern, K. Y. Hui, J. C. Lee, L. P. Schumm, Y. Sharma, C. A. Anderson, J. Essers, M. Mitrovic, K. Ning, I. Cleynen, E. Theatre, S. L. Spain, S. Raychaudhuri, P. Goyette, Z. Wei, C. Abraham, J. P. Achkar, T. Ahmad, L. Amininejad, A. N. Ananthakrishnan, V. Andersen, J. M. Andrews, L. Baidoo, T. Balschun, P. A. Bampton, A. Bitton, G. Boucher, S. Brand, C. Buning, A. Cohain, S. Cichon, M. D'Amato, D. De Jong, K. L. Devaney, M.

- Dubinsky, C. Edwards, D. Ellinghaus, L. R. Ferguson, D. Franchimont, K. Fransen, R. Geary, M. Georges, C. Gieger, J. Glas, T. Haritunians, A. Hart, C. Hawkey, M. Hedl, X. Hu, T. H. Karlson, L. Kupcinkas, S. Kugathasan, A. Latiano, D. Laukens, I. C. Lawrance, C. W. Lees, E. Louis, G. Mahy, J. Mansfield, A. R. Morgan, C. Mowat, W. Newman, O. Palmieri, C. Y. Ponsioen, U. Potocnik, N. J. Prescott, M. Regueiro, J. I. Rotter, R. K. Russell, J. D. Sanderson, M. Sans, J. Satsangi, S. Schreiber, L. A. Simms, J. Sventoraityte, S. R. Targan, K. D. Taylor, M. Tremelling, H. W. Verspaget, M. De Vos, C. Wijmenga, D. C. Wilson, J. Winkelmann, R. J. Xavier, S. Zeissig, B. Zhang, C. K. Zhang, H. Zhao, I. B. D. Genetics Consortium International, M. S. Silverberg, V. Annese, H. Hakonarson, S. R. Brant, G. Radford-Smith, C. G. Mathew, J. D. Rioux, E. E. Schadt, M. J. Daly, A. Franke, M. Parkes, S. Vermeire, J. C. Barrett, and J. H. Cho. 2012. 'Host-microbe interactions have shaped the genetic architecture of inflammatory bowel disease', *Nature*, 491: 119-24
- Jung, S., K. Toyka, and H. P. Hartung. 1995. 'Suppression of experimental autoimmune encephalomyelitis in Lewis rats by antibodies against CD2', *Eur J Immunol*, 25: 1391-8.
- Kaneko, Y., F. Nimmerjahn, and J. V. Ravetch. 2006. 'Anti-inflammatory activity of immunoglobulin G resulting from Fc sialylation', *Science*, 313: 670-3.
- Kaplan, A. J., K. D. Chavin, H. Yagita, M. S. Sandrin, L. H. Qin, J. Lin, G. Lindenmayer, and J. S. Bromberg. 1993. 'Production and characterization of soluble and transmembrane murine CD2. Demonstration that CD48 is a ligand for CD2 and that CD48 adhesion is regulated by CD2', *J Immunol*, 151: 4022-32.
- Kato, K., M. Koyanagi, H. Okada, T. Takanashi, Y. W. Wong, A. F. Williams, K. Okumura, and H. Yagita. 1992. 'CD48 is a counter-receptor for mouse CD2 and is involved in T cell activation', *J Exp Med*, 176: 1241-9.
- Katsuura, M., Y. Shimizu, K. Akiba, C. Kanazawa, T. Mitsui, D. Sendo, T. Kawakami, K. Hayasaka, and S. Yokoyama. 1998. 'CD48 expression on leukocytes in infectious diseases: flow cytometric analysis of surface antigen', *Acta Paediatr Jpn*, 40: 580-5.
- Kennedy, M. K., R. J. Clatch, M. C. Dal Canto, J. L. Trotter, and S. D. Miller. 1987. 'Monoclonal antibody-induced inhibition of relapsing EAE in SJL/J mice correlates with inhibition of neuroantigen-specific cell-mediated immune responses', *J Neuroimmunol*, 16: 345-64.
- Keszei, M., Y. E. Latchman, V. K. Vanguri, D. R. Brown, C. Detre, M. Morra, C. V. Arancibia-Carcamo, E. Paul, S. Calpe, W. Castro, N. Wang, C. Terhorst, and A. H. Sharpe. 2011. 'Auto-antibody production and glomerulonephritis in congenic Slamf1^{-/-} and Slamf2^{-/-} [B6.129] but not in Slamf1^{-/-} and Slamf2^{-/-} [BALB/c.129] mice', *Int Immunol*, 23: 149-58.
- Keusch, Jeremy, Lydyard, Peter M., Berger, Eric G., Delves, Peter J. 1998a. 'B lymphocyte galactosyltransferase protein levels in normal individuals and in patients with rheumatoid arthritis', *Glycoconjugate Journal*, 15: 1093-97.
- Keusch, Jeremy, Lydyard, Peter M., Delves, Peter J. 1998b. 'The effect on IgG glycosylation of altering beta1,4-galactosyltransferase-1 activity in B cells', *Glycobiology*, 8: 1212-20.
- Khan, N. A., Y. Kim, S. Shin, and K. S. Kim. 2007. 'FimH-mediated Escherichia coli K1 invasion of human brain microvascular endothelial cells', *Cell Microbiol*, 9: 169-78.
- Kiel, M. J., O. H. Yilmaz, T. Iwashita, O. H. Yilmaz, C. Terhorst, and S. J. Morrison. 2005. 'SLAM family receptors distinguish hematopoietic stem and progenitor cells and reveal endothelial niches for stem cells', *Cell*, 121: 1109-21.
- Kim, I., S. He, O. H. Yilmaz, M. J. Kiel, and S. J. Morrison. 2006. 'Enhanced purification of fetal liver hematopoietic stem cells using SLAM family receptors', *Blood*, 108: 737-44.

- Kim, J. Y., J. S. Bae, H. J. Kim, and H. D. Shin. 2014. 'CD58 polymorphisms associated with the risk of neuromyelitis optica in a Korean population', *BMC Neurol*, 14: 57.
- Kingsbury, G. A., L. A. Feeney, Y. Nong, S. A. Calandra, C. J. Murphy, J. M. Corcoran, Y. Wang, M. R. Prabhu Das, S. J. Busfield, C. C. Fraser, and J. L. Villeval. 2001. 'Cloning, expression, and function of BLAME, a novel member of the CD2 family', *J Immunol*, 166: 5675-80.
- Kivisakk, P., B. C. Healy, V. Viglietta, F. J. Quintana, M. A. Hootstein, H. L. Weiner, and S. J. Khoury. 2009. 'Natalizumab treatment is associated with peripheral sequestration of proinflammatory T cells', *Neurology*, 72: 1922-30.
- Klaman, L. D., and D. A. Thorley-Lawson. 1995. 'Characterization of the CD48 gene demonstrates a positive element that is specific to Epstein-Barr virus-immortalized B-cell lines and contains an essential NF-kappa B site', *J Virol*, 69: 871-81.
- Koh, A. E., S. W. Njoroge, M. Feliu, A. Cook, M. K. Selig, Y. E. Latchman, A. H. Sharpe, R. B. Colvin, and E. Paul. 2011. 'The SLAM family member CD48 (Slamf2) protects lupus-prone mice from autoimmune nephritis', *J Autoimmun*, 37: 48-57.
- Kohm, A. P., P. A. Carpentier, H. A. Anger, and S. D. Miller. 2002. 'Cutting Edge: CD4+CD25+ Regulatory T Cells Suppress Antigen-Specific Autoreactive Immune Responses and Central Nervous System Inflammation During Active Experimental Autoimmune Encephalomyelitis', *The Journal of Immunology*, 169: 4712-16.
- Korganow, A. S., H. Ji, S. Mangialaio, V. Duchatelle, R. Pelanda, T. Martin, C. Degott, H. Kikutani, K. Rajewsky, J. L. Pasquali, C. Benoist, and D. Mathis. 1999. 'From systemic T cell self-reactivity to organ-specific autoimmune disease via immunoglobulins', *Immunity*, 10: 451-61.
- Kouskoff, V., A. S. Korganow, V. Duchatelle, C. Degott, C. Benoist, and D. Mathis. 1996. 'Organ-specific disease provoked by systemic autoimmunity', *Cell*, 87: 811-22.
- Krakovski, M., and T. Owens. 1996. 'Interferon-gamma confers resistance to experimental allergic encephalomyelitis', *Eur J Immunol*, 26: 1641-6.
- Kroenke, M. A., S. W. Chensue, and B. M. Segal. 2010. 'EAE mediated by a non-IFN-gamma/non-IL-17 pathway', *Eur J Immunol*, 40: 2340-8.
- Kubota, K. 2002. 'A structurally variant form of the 2B4 antigen is expressed on the cell surface of mouse mast cells', *Microbiol Immunol*, 46: 589-92.
- Kumaresan, P. R., W. C. Lai, S. S. Chuang, M. Bennett, and P. A. Mathew. 2002. 'CS1, a novel member of the CD2 family, is homophilic and regulates NK cell function', *Mol Immunol*, 39: 1-8.
- Langrish, C. L., Y. Chen, W. M. Blumenschein, J. Mattson, B. Basham, J. D. Sedgwick, T. McClanahan, R. A. Kastelein, and D. J. Cua. 2005. 'IL-23 drives a pathogenic T cell population that induces autoimmune inflammation', *J Exp Med*, 201: 233-40.
- Laouar, Y., F. S. Sutterwala, L. Gorelik, and R. A. Flavell. 2005. 'Transforming growth factor-beta controls T helper type 1 cell development through regulation of natural killer cell interferon-gamma', *Nat Immunol*, 6: 600-7.
- Larochelle, A., M. Savona, M. Wiggins, S. Anderson, B. Ichwan, K. Keyvanfar, S. J. Morrison, and C. E. Dunbar. 2011. 'Human and rhesus macaque hematopoietic stem cells cannot be purified based only on SLAM family markers', *Blood*, 117: 1550-4.

- Latchman, Y., P. F. McKay, and H. Reiser. 1998. 'Identification of the 2B4 molecule as a counter-receptor for CD48', *J Immunol*, 161: 5809-12.
- Lee, K. M., S. Bhawan, T. Majima, H. Wei, M. I. Nishimura, H. Yagita, and V. Kumar. 2003. 'Cutting edge: the NK cell receptor 2B4 augments antigen-specific T cell cytotoxicity through CD48 ligation on neighboring T cells', *J Immunol*, 170: 4881-5.
- Lee, K. M., M. E. McNerney, S. E. Stepp, P. A. Mathew, J. D. Schatzle, M. Bennett, and V. Kumar. 2004. '2B4 acts as a non-major histocompatibility complex binding inhibitory receptor on mouse natural killer cells', *J Exp Med*, 199: 1245-54.
- Lees, J. R., P. T. Golumbek, J. Sim, D. Dorsey, and J. H. Russell. 2008. 'Regional CNS responses to IFN-gamma determine lesion localization patterns during EAE pathogenesis', *J Exp Med*, 205: 2633-42.
- Li, S. C., G. Gish, D. Yang, A. J. Coffey, J. D. Forman-Kay, I. Ernberg, L. E. Kay, and T. Pawson. 1999. 'Novel mode of ligand binding by the SH2 domain of the human XLP disease gene product SAP/SH2D1A', *Curr Biol*, 9: 1355-62.
- Limaye, N., K. A. Belobrajdic, A. E. Wandstrat, F. Bonhomme, S. V. Edwards, and E. K. Wakeland. 2008. 'Prevalence and evolutionary origins of autoimmune susceptibility alleles in natural mouse populations', *Genes Immun*, 9: 61-8.
- Linington, C., M. Bradl, H. Lassmann, C. Brunner, and K. Vass. 1988. 'Augmentation of demyelination in rat acute allergic encephalomyelitis by circulating mouse monoclonal antibodies directed against a myelin/oligodendrocyte glycoprotein', *Am J Pathol*, 130: 443-54.
- Linker, R. A., E. Rott, H. H. Hofstetter, T. Hanke, K. V. Toyka, and R. Gold. 2005. 'EAE in beta-2 microglobulin-deficient mice: axonal damage is not dependent on MHC-I restricted immune responses', *Neurobiol Dis*, 19: 218-28.
- Loke, P., and J. P. Allison. 2003. 'PD-L1 and PD-L2 are differentially regulated by Th1 and Th2 cells', *Proc Natl Acad Sci U S A*, 100: 5336-41.
- Low, M. G., and A. R. Saltiel. 1988. 'Structural and functional roles of glycosyl-phosphatidylinositol in membranes', *Science*, 239: 268-75.
- Lu, L., K. Ikizawa, D. Hu, M. B. Werneck, K. W. Wucherpfennig, and H. Cantor. 2007. 'Regulation of activated CD4+ T cells by NK cells via the Qa-1-NKG2A inhibitory pathway', *Immunity*, 26: 593-604.
- Lu, L., H. J. Kim, M. B. Werneck, and H. Cantor. 2008. 'Regulation of CD8+ regulatory T cells: Interruption of the NKG2A-Qa-1 interaction allows robust suppressive activity and resolution of autoimmune disease', *Proc Natl Acad Sci U S A*, 105: 19420-5.
- Lyons, J. A., M. San, M. P. Happ, and A. H. Cross. 1999. 'B cells are critical to induction of experimental allergic encephalomyelitis by protein but not by a short encephalitogenic peptide', *Eur J Immunol*, 29: 3432-9.
- Maccioni, M., G. Zeder-Lutz, H. Huang, C. Ebel, P. Gerber, J. Hergueux, P. Marchal, V. Duchatelle, C. Degott, M. van Regenmortel, C. Benoist, and D. Mathis. 2002. 'Arthritogenic monoclonal antibodies from K/BxN mice', *J Exp Med*, 195: 1071-7.
- Magliozzi, R., S. Columba-Cabezas, B. Serafini, and F. Aloisi. 2004. 'Intracerebral expression of CXCL13 and BAFF is accompanied by formation of lymphoid follicle-like structures in the meninges of mice with relapsing experimental autoimmune encephalomyelitis', *J Neuroimmunol*, 148: 11-23.

- Malaviya, R., Z. Gao, K. Thankavel, P. A. van der Merwe, and S. N. Abraham. 1999. 'The mast cell tumor necrosis factor alpha response to FimH-expressing Escherichia coli is mediated by the glycosylphosphatidylinositol-anchored molecule CD48', *Proc Natl Acad Sci U S A*, 96: 8110-5.
- Malhotra, R., M. R. Wormald, P. M. Rudd, P. B. Fischer, R. A. Dwek, and R. B. Sim. 1995. 'Glycosylation changes of IgG associated with rheumatoid arthritis can activate complement via the mannose-binding protein', *Nat Med*, 1: 237-43.
- Martin, M., X. Romero, M. A. de la Fuente, V. Tovar, N. Zapater, E. Esplugues, P. Pizcueta, J. Bosch, and P. Engel. 2001. 'CD84 functions as a homophilic adhesion molecule and enhances IFN-gamma secretion: adhesion is mediated by Ig-like domain 1', *J Immunol*, 167: 3668-76.
- Martin-Fontecha, A., L. L. Thomsen, S. Brett, C. Gerard, M. Lipp, A. Lanzavecchia, and F. Sallusto. 2004. 'Induced recruitment of NK cells to lymph nodes provides IFN-gamma for T(H)1 priming', *Nat Immunol*, 5: 1260-5.
- Mathew, P. A., B. A. Garni-Wagner, K. Land, A. Takashima, E. Stoneman, M. Bennett, and V. Kumar. 1993. 'Cloning and characterization of the 2B4 gene encoding a molecule associated with non-MHC-restricted killing mediated by activated natural killer cells and T cells', *J Immunol*, 151: 5328-37.
- Matsumoto, I., A. Staub, C. Benoist, and D. Mathis. 1999. 'Arthritis provoked by linked T and B cell recognition of a glycolytic enzyme', *Science*, 286: 1732-5.
- Matloubian, M., C. G. Lo, G. Cinamon, M. J. Lesneski, Y. Xu, V. Brinkmann, M. L. Allende, R. L. Proia, and J. G. Cyster. 2004. 'Lymphocyte egress from thymus and peripheral lymphoid organs is dependent on S1P receptor 1', *Nature*, 427: 355-60.
- Matsushita, T., K. Yanaba, J. D. Bouaziz, M. Fujimoto, and T. F. Tedder. 2008. 'Regulatory B cells inhibit EAE initiation in mice while other B cells promote disease progression', *J Clin Invest*, 118: 3420-30.
- Mavaddat, N., D. W. Mason, P. D. Atkinson, E. J. Evans, R. J. Gilbert, D. I. Stuart, J. A. Fennelly, A. N. Barclay, S. J. Davis, and M. H. Brown. 2000. 'Signaling lymphocytic activation molecule (CDw150) is homophilic but self-associates with very low affinity', *J Biol Chem*, 275: 28100-9.
- McGeachy, M. J., L. A. Stephens, and S. M. Anderton. 2005. 'Natural recovery and protection from autoimmune encephalomyelitis: contribution of CD4+CD25+ regulatory cells within the central nervous system', *J Immunol*, 175: 3025-32.
- McLaughlin, K. A., and K. W. Wucherpfennig. 2008. 'B cells and autoantibodies in the pathogenesis of multiple sclerosis and related inflammatory demyelinating diseases', *Adv Immunol*, 98: 121-49.
- McMahon, E. J., S. L. Bailey, C. V. Castenada, H. Waldner, and S. D. Miller. 2005. 'Epitope spreading initiates in the CNS in two mouse models of multiple sclerosis', *Nat Med*, 11: 335-9.
- Meazza, R., C. Tuberosa, V. Cetica, M. Falco, F. Loiacono, S. Parolini, C. Micalizzi, A. Moretta, M. C. Mingari, L. Moretta, C. Bottino, M. Arico, and D. Pende. 2014. 'XLP1 inhibitory effect by 2B4 does not affect DNAM-1 and NKG2D activating pathways in NK cells', *Eur J Immunol*, 44: 1526-34.
- Mendel, I., N. Kerlero de Rosbo, and A. Ben-Nun. 1995. 'A myelin oligodendrocyte glycoprotein peptide induces typical chronic experimental autoimmune encephalomyelitis in H-2b mice: fine specificity and T cell receptor V beta expression of encephalitogenic T cells', *Eur J Immunol*, 25: 1951-9.
- Merrill, J. E., D. H. Kono, J. Clayton, D. G. Ando, D. R. Hinton, and F. M. Hofman. 1992. 'Inflammatory leukocytes and cytokines in the peptide-induced disease of experimental allergic encephalomyelitis in SJL and B10.PL mice', *Proc Natl Acad Sci U S A*, 89: 574-8.

- Metz, C. N., G. Brunner, N. H. Choi-Muira, H. Nguyen, J. Gabrilove, I. W. Caras, N. Altszuler, D. B. Rifkin, E. L. Wilson, and M. A. Davitz. 1994. 'Release of GPI-anchored membrane proteins by a cell-associated GPI-specific phospholipase D', *Embo j*, 13: 1741-51.
- Milstein, O., S. Y. Tseng, T. Starr, J. Llodra, A. Nans, M. Liu, M. K. Wild, P. A. van der Merwe, D. L. Stokes, Y. Reisner, and M. L. Dustin. 2008. 'Nanoscale increases in CD2-CD48-mediated intermembrane spacing decrease adhesion and reorganize the immunological synapse', *J Biol Chem*, 283: 34414-22.
- Mimura, Y., S. Church, R. Ghirlando, P. R. Ashton, S. Dong, M. Goodall, J. Lund, and R. Jefferis. 2000. 'The influence of glycosylation on the thermal stability and effector function expression of human IgG1-Fc: properties of a series of truncated glycoforms', *Mol Immunol*, 37: 697-706.
- Mimura Y, Jefferis R, Mimura-Kimura Y, Abrahams J, Rudd PM. 2008. 'Glycosylation of therapeutic IgGs', unpublished book chapter, shared by personal communication
- Minai-Fleminger, Y., R. S. Gangwar, H. Migalovich-Sheikhet, M. Seaf, V. Leibovici, N. Hollander, M. Feld, A. E. Moses, B. Homey, and F. Levi-Schaffer. 2014. 'The CD48 receptor mediates Staphylococcus aureus human and murine eosinophil activation', *Clin Exp Allergy*, 44: 1335-46.
- Mindur, J. E., N. Ito, S. Dhib-Jalbut, and K. Ito. 2014. 'Early treatment with anti-VLA-4 mAb can prevent the infiltration and/or development of pathogenic CD11b+CD4+ T cells in the CNS during progressive EAE', *PLoS One*, 9: e99068.
- Mittelbrunn, M., A. Molina, M. M. Escribese, M. Yanez-Mo, E. Escudero, A. Ursa, R. Tejedor, F. Mampaso, and F. Sanchez-Madrid. 2004. 'VLA-4 integrin concentrates at the peripheral supramolecular activation complex of the immune synapse and drives T helper 1 responses', *Proc Natl Acad Sci U S A*, 101: 11058-63.
- Mohan, C., E. Alas, L. Morel, P. Yang, and E. K. Wakeland. 1998. 'Genetic dissection of SLE pathogenesis. Sle1 on murine chromosome 1 leads to a selective loss of tolerance to H2A/H2B/DNA subnucleosomes', *J Clin Invest*, 101: 1362-72.
- Moller, J., T. Luhmann, M. Chabria, H. Hall, and V. Vogel. 2013. 'Macrophages lift off surface-bound bacteria using a filopodium-lamellipodium hook-and-shovel mechanism', *Sci Rep*, 3: 2884.
- Monk, N. J., R. E. Hargreaves, J. E. Marsh, C. A. Farrar, S. H. Sacks, M. Millrain, E. Simpson, J. Dyson, and S. Jurcevic. 2003. 'Fc-dependent depletion of activated T cells occurs through CD40L-specific antibody rather than costimulation blockade', *Nat Med*, 9: 1275-80.
- Montero, E., G. Nussbaum, J. F. Kaye, R. Perez, A. Lage, A. Ben-Nun, and I. R. Cohen. 2004. 'Regulation of experimental autoimmune encephalomyelitis by CD4+, CD25+ and CD8+ T cells: analysis using depleting antibodies', *J Autoimmun*, 23: 1-7.
- Mooney, J. M., J. Klem, C. Wulfig, L. A. Mijares, P. L. Schwartzberg, M. Bennett, and J. D. Schatzle. 2004. 'The murine NK receptor 2B4 (CD244) exhibits inhibitory function independent of signaling lymphocytic activation molecule-associated protein expression', *J Immunol*, 173: 3953-61.
- Moran, M., and M. C. Miceli. 1998. 'Engagement of GPI-linked CD48 contributes to TCR signals and cytoskeletal reorganization: a role for lipid rafts in T cell activation', *Immunity*, 9: 787-96.
- Morel, L., K. R. Blenman, B. P. Croker, and E. K. Wakeland. 2001. 'The major murine systemic lupus erythematosus susceptibility locus, Sle1, is a cluster of functionally related genes', *Proc Natl Acad Sci U S A*, 98: 1787-92.

- Morel, L., U. H. Rudofsky, J. A. Longmate, J. Schiffenbauer, and E. K. Wakeland. 1994. 'Polygenic control of susceptibility to murine systemic lupus erythematosus', *Immunity*, 1: 219-29.
- Morgan, B. P., C. W. van den Berg, E. V. Davies, M. B. Hallett, and V. Horejsi. 1993. 'Cross-linking of CD59 and of other glycosyl phosphatidylinositol-anchored molecules on neutrophils triggers cell activation via tyrosine kinase', *Eur J Immunol*, 23: 2841-50.
- Morra, M., J. Lu, F. Poy, M. Martin, J. Sayos, S. Calpe, C. Gullo, D. Howie, S. Rietdijk, A. Thompson, A. J. Coyle, C. Denny, M. B. Yaffe, P. Engel, M. J. Eck, and C. Terhorst. 2001. 'Structural basis for the interaction of the free SH2 domain EAT-2 with SLAM receptors in hematopoietic cells', *Embo j*, 20: 5840-52.
- Morris, S. C., P. L. Cohen, and R. A. Eisenberg. 1990. 'Experimental induction of systemic lupus erythematosus by recognition of foreign Ia', *Clin Immunol Immunopathol*, 57: 263-73.
- Muhammad, A., H. B. Schiller, F. Forster, P. Eckerstorfer, R. Geyeregger, V. Leksa, G. J. Zlabinger, M. Sibilja, A. Sonnleitner, W. Paster, and H. Stockinger. 2009. 'Sequential cooperation of CD2 and CD48 in the buildup of the early TCR signalosome', *J Immunol*, 182: 7672-80.
- Muller, D. M., M. P. Pender, and J. M. Greer. 2000. 'A neuropathological analysis of experimental autoimmune encephalomyelitis with predominant brain stem and cerebellar involvement and differences between active and passive induction', *Acta Neuropathol*, 100: 174-82.
- — —. 2005. 'Blood-brain barrier disruption and lesion localisation in experimental autoimmune encephalomyelitis with predominant cerebellar and brainstem involvement', *J Neuroimmunol*, 160: 162-9.
- Munitz, A., I. Bachelet, R. Eliashar, M. Khodoun, F. D. Finkelman, M. E. Rothenberg, and F. Levi-Schaffer. 2006. 'CD48 is an allergen and IL-3-induced activation molecule on eosinophils', *J Immunol*, 177: 77-83.
- Munitz, A., I. Bachelet, F. D. Finkelman, M. E. Rothenberg, and F. Levi-Schaffer. 2007. 'CD48 is critically involved in allergic eosinophilic airway inflammation', *Am J Respir Crit Care Med*, 175: 911-8.
- Munitz, A., I. Bachelet, S. Fraenkel, G. Katz, O. Mandelboim, H. U. Simon, L. Moretta, M. Colonna, and F. Levi-Schaffer. 2005. '2B4 (CD244) is expressed and functional on human eosinophils', *J Immunol*, 174: 110-8.
- Musgrave, B. L., C. L. Watson, S. M. Haeryfar, C. A. Barnes, and D. W. Hoskin. 2004. 'CD2-CD48 interactions promote interleukin-2 and interferon-gamma synthesis by stabilizing cytokine mRNA', *Cell Immunol*, 229: 1-12.
- Musgrave, B. L., C. L. Watson, and D. W. Hoskin. 2003. 'CD2-CD48 interactions promote cytotoxic T lymphocyte induction and function: anti-CD2 and anti-CD48 antibodies impair cytokine synthesis, proliferation, target recognition/adhesion, and cytotoxicity', *J Interferon Cytokine Res*, 23: 67-81.
- Nimmerjahn, F., R. M. Anthony, and J. V. Ravetch. 2007. 'Agalactosylated IgG antibodies depend on cellular Fc receptors for in vivo activity', *Proc Natl Acad Sci U S A*, 104: 8433-7.
- Nose, M., and H. Wigzell. 1983. 'Biological significance of carbohydrate chains on monoclonal antibodies', *Proc Natl Acad Sci U S A*, 80: 6632-6.
- O'Connor, R. A., C. T. Prendergast, C. A. Sabatos, C. W. Lau, M. D. Leech, D. C. Wraith, and S. M. Anderton. 2008. 'Cutting edge: Th1 cells facilitate the entry of Th17 cells to the central nervous system during experimental autoimmune encephalomyelitis', *J Immunol*, 181: 3750-4.

- O'Connor, R. A., K. H. Malpass, and S. M. Anderton. 2007. 'The Inflamed Central Nervous System Drives the Activation and Rapid Proliferation of Foxp3+ Regulatory T Cells', *The Journal of Immunology*, 179: 958-66.
- Odoardi, F., C. Sie, K. Strey, V. K. Ulaganathan, C. Schlager, D. Lodygin, K. Heckelsmiller, W. Nietfeld, J. Ellwart, W. E. Klinkert, C. Lottaz, M. Nosov, V. Brinkmann, R. Spang, H. Lehrach, M. Vingron, H. Wekerle, C. Flugel-Koch, and A. Flugel. 2012. 'T cells become licensed in the lung to enter the central nervous system', *Nature*, 488: 675-9.
- Oefner, C. M., A. Winkler, C. Hess, A. K. Lorenz, V. Holecska, M. Huxdorf, T. Schommartz, D. Petzold, J. Bitterling, A. L. Schoen, A. D. Stoehr, D. Vu Van, Y. Darcan-Nikolaisen, V. Blanchard, I. Schmutte, Y. Laumonier, H. A. Strover, A. N. Hegazy, S. Eiglmeier, C. T. Schoen, M. M. Mertes, C. Loddenkemper, M. Lohning, P. Konig, A. Petersen, E. O. Luger, M. Collin, J. Kohl, A. Hutloff, E. Hamelmann, M. Berger, H. Wardemann, and M. Ehlers. 2012. 'Tolerance induction with T cell-dependent protein antigens induces regulatory sialylated IgGs', *J Allergy Clin Immunol*, 129: 1647-55 e13.
- Ortega, S. B., V. P. Kashi, A. F. Tyler, K. Cunnusamy, J. P. Mendoza, and N. J. Karandikar. 2013. 'The disease-ameliorating function of autoregulatory CD8 T cells is mediated by targeting of encephalitogenic CD4 T cells in experimental autoimmune encephalomyelitis', *J Immunol*, 191: 117-26.
- Pacheco, Y., A. P. McLean, J. Rohrbach, F. Porichis, D. E. Kaufmann, and D. G. Kavanagh. 2013. 'Simultaneous TCR and CD244 signals induce dynamic downmodulation of CD244 on human antiviral T cells', *J Immunol*, 191: 2072-81.
- Palendira, U., C. Low, A. Chan, A. D. Hislop, E. Ho, T. G. Phan, E. Deenick, M. C. Cook, D. S. Riminton, S. Choo, R. Loh, F. Alvaro, C. Booth, H. B. Gaspar, A. Moretta, R. Khanna, A. B. Rickinson, and S. G. Tangye. 2011. 'Molecular pathogenesis of EBV susceptibility in XLP as revealed by analysis of female carriers with heterozygous expression of SAP', *PLoS Biol*, 9: e1001187.
- Parekh, R. B., R. A. Dwek, B. J. Sutton, D. L. Fernandes, A. Leung, D. Stanworth, T. W. Rademacher, T. Mizuuchi, T. Taniguchi, K. Matsuta, and et al. 1985. 'Association of rheumatoid arthritis and primary osteoarthritis with changes in the glycosylation pattern of total serum IgG', *Nature*, 316: 452-7.
- Parekh, R., D. Isenberg, G. Rook, I. Roitt, R. Dwek, and T. Rademacher. 1989. 'A comparative analysis of disease-associated changes in the galactosylation of serum IgG', *J Autoimmun*, 2: 101-14.
- Park, H., Z. Li, X. O. Yang, S. H. Chang, R. Nurieva, Y. H. Wang, Y. Wang, L. Hood, Z. Zhu, Q. Tian, and C. Dong. 2005. 'A distinct lineage of CD4 T cells regulates tissue inflammation by producing interleukin 17', *Nat Immunol*, 6: 1133-41.
- Parolini, S., C. Bottino, M. Falco, R. Augugliaro, S. Giliani, R. Franceschini, H. D. Ochs, H. Wolf, J. Y. Bonnefoy, R. Biassoni, L. Moretta, L. D. Notarangelo, and A. Moretta. 2000. 'X-linked lymphoproliferative disease. 2B4 molecules displaying inhibitory rather than activating function are responsible for the inability of natural killer cells to kill Epstein-Barr virus-infected cells', *J Exp Med*, 192: 337-46.
- Peipp, M., J. J. Lammerts van Bueren, T. Schneider-Merck, W. W. Bleeker, M. Dechant, T. Beyer, R. Repp, P. H. van Berkel, T. Vink, J. G. van de Winkel, P. W. Parren, and T. Valerius. 2008. 'Antibody fucosylation differentially impacts cytotoxicity mediated by NK and PMN effector cells', *Blood*, 112: 2390-9.
- Pistoia, V. 1997. 'Production of cytokines by human B cells in health and disease', *Immunol Today*, 18: 343-50.

- Pollinger, B., G. Krishnamoorthy, K. Berer, H. Lassmann, M. R. Bosl, R. Dunn, H. S. Domingues, A. Holz, F. C. Kurschus, and H. Wekerle. 2009. 'Spontaneous relapsing-remitting EAE in the SJL/J mouse: MOG-reactive transgenic T cells recruit endogenous MOG-specific B cells', *J Exp Med*, 206: 1303-16.
- Ponomarev, E. D., L. P. Shriver, K. Maresz, J. Pedras-Vasconcelos, D. Verthelyi, and B. N. Dittel. 2007. 'GM-CSF production by autoreactive T cells is required for the activation of microglial cells and the onset of experimental autoimmune encephalomyelitis', *J Immunol*, 178: 39-48.
- Poy, F., M. B. Yaffe, J. Sayos, K. Saxena, M. Morra, J. Sumegi, L. C. Cantley, C. Terhorst, and M. J. Eck. 1999. 'Crystal structures of the XLP protein SAP reveal a class of SH2 domains with extended, phosphotyrosine-independent sequence recognition', *Mol Cell*, 4: 555-61.
- Powrie, F., M. W. Leach, S. Mauze, L. B. Caddle, and R. L. Coffman. 1993. 'Phenotypically distinct subsets of CD4+ T cells induce or protect from chronic intestinal inflammation in C. B-17 scid mice', *Int Immunol*, 5: 1461-71.
- Punnonen, J., B. G. Cocks, J. M. Carballido, B. Bennett, D. Peterson, G. Aversa, and J. E. de Vries. 1997. 'Soluble and membrane-bound forms of signaling lymphocytic activation molecule (SLAM) induce proliferation and Ig synthesis by activated human B lymphocytes', *J Exp Med*, 185: 993-1004.
- Purtilo, D. T., C. Cassel, and J. P. Yang. 1974. 'Letter: Fatal infectious mononucleosis in familial lymphohistiocytosis', *N Engl J Med*, 291: 736.
- Qin, L., K. D. Chavin, J. Lin, H. Yagita, and J. S. Bromberg. 1994. 'Anti-CD2 receptor and anti-CD2 ligand (CD48) antibodies synergize to prolong allograft survival', *J Exp Med*, 179: 341-6.
- Rademacher, T. W., P. Williams, and R. A. Dwek. 1994. 'Agalactosyl glycoforms of IgG autoantibodies are pathogenic', *Proc Natl Acad Sci U S A*, 91: 6123-7.
- Reboldi, A., C. Coisne, D. Baumjohann, F. Benvenuto, D. Bottinelli, S. Lira, A. Uccelli, A. Lanzavecchia, B. Engelhardt, and F. Sallusto. 2009. 'C-C chemokine receptor 6-regulated entry of TH-17 cells into the CNS through the choroid plexus is required for the initiation of EAE', *Nat Immunol*, 10: 514-23.
- Robinson, A. P., C. T. Harp, A. Noronha, and S. D. Miller. 2014. 'The experimental autoimmune encephalomyelitis (EAE) model of MS: utility for understanding disease pathophysiology and treatment', *Handb Clin Neurol*, 122: 173-89.
- Rocha-de-Souza, C. M., B. Berent-Maoz, D. Mankuta, A. E. Moses, and F. Levi-Schaffer. 2008. 'Human mast cell activation by *Staphylococcus aureus*: interleukin-8 and tumor necrosis factor alpha release and the role of Toll-like receptor 2 and CD48 molecules', *Infect Immun*, 76: 4489-97.
- Romero, X., D. Benitez, S. March, R. Vilella, M. Miralpeix, and P. Engel. 2004. 'Differential expression of SAP and EAT-2-binding leukocyte cell-surface molecules CD84, CD150 (SLAM), CD229 (Ly9) and CD244 (2B4)', *Tissue Antigens*, 64: 132-44.
- Romero, X., N. Zapater, M. Calvo, S. G. Kalko, M. A. de la Fuente, V. Tovar, C. Ockeloen, P. Pizcueta, and P. Engel. 2005. 'CD229 (Ly9) lymphocyte cell surface receptor interacts homophilically through its N-terminal domain and relocates to the immunological synapse', *J Immunol*, 174: 7033-42.
- Rook, G. A., J. Steele, R. Brealey, A. Whyte, D. Isenberg, N. Sumar, J. L. Nelson, K. B. Bodman, A. Young, I. M. Roitt, and et al. 1991. 'Changes in IgG glycoform levels are associated with remission of arthritis during pregnancy', *J Autoimmun*, 4: 779-94.

- Rothhammer, V., S. Heink, F. Petermann, R. Srivastava, M. C. Claussen, B. Hemmer, and T. Korn. 2011. 'Th17 lymphocytes traffic to the central nervous system independently of alpha4 integrin expression during EAE', *J Exp Med*, 208: 2465-76.
- Rottman, J. B., T. Smith, J. R. Tonra, K. Ganley, T. Bloom, R. Silva, B. Pierce, J. C. Gutierrez-Ramos, E. Ozkaynak, and A. J. Coyle. 2001. 'The costimulatory molecule ICOS plays an important role in the immunopathogenesis of EAE', *Nat Immunol*, 2: 605-11.
- Sakaguchi, S., K. Wing, Y. Onishi, P. Prieto-Martin, and T. Yamaguchi. 2009. 'Regulatory T cells: how do they suppress immune responses?', *Int Immunol*, 21: 1105-11.
- Salama, A. D., T. Chitnis, J. Imitola, M. J. Ansari, H. Akiba, F. Tushima, M. Azuma, H. Yagita, M. H. Sayegh, and S. J. Khoury. 2003. 'Critical role of the programmed death-1 (PD-1) pathway in regulation of experimental autoimmune encephalomyelitis', *J Exp Med*, 198: 71-8.
- Sandrin, M. S., E. Mouhtouris, H. A. Vaughan, H. S. Warren, and C. R. Parish. 1993. 'CD48 is a low affinity ligand for human CD2', *J Immunol*, 151: 4606-13.
- Sato, T., K. Tachibana, Y. Nojima, N. D'Avirro, and C. Morimoto. 1995. 'Role of the VLA-4 molecule in T cell costimulation. Identification of the tyrosine phosphorylation pattern induced by the ligation of VLA-4', *J Immunol*, 155: 2938-47.
- Sayos, J., C. Wu, M. Morra, N. Wang, X. Zhang, D. Allen, S. van Schaik, L. Notarangelo, R. Geha, M. G. Roncarolo, H. Oettgen, J. E. De Vries, G. Aversa, and C. Terhorst. 1998. 'The X-linked lymphoproliferative-disease gene product SAP regulates signals induced through the co-receptor SLAM', *Nature*, 395: 462-9.
- Schatzle, J. D., S. Sheu, S. E. Stepp, P. A. Mathew, M. Bennett, and V. Kumar. 1999. 'Characterization of inhibitory and stimulatory forms of the murine natural killer cell receptor 2B4', *Proc Natl Acad Sci U S A*, 96: 3870-5.
- Scherer, H. U., D. van der Woude, A. Ioan-Facsinay, H. el Bannoudi, L. A. Trouw, J. Wang, T. Haupl, G. R. Burmester, A. M. Deelder, T. W. Huizinga, M. Wuhler, and R. E. Toes. 2010. 'Glycan profiling of anti-citrullinated protein antibodies isolated from human serum and synovial fluid', *Arthritis Rheum*, 62: 1620-9.
- Schuhmachers, G., K. Ariizumi, P. A. Mathew, M. Bennett, V. Kumar, and A. Takashima. 1995. '2B4, a new member of the immunoglobulin gene superfamily, is expressed on murine dendritic epidermal T cells and plays a functional role in their killing of skin tumors', *J Invest Dermatol*, 105: 592-6.
- Schwab, I., and F. Nimmerjahn. 2013. 'Intravenous immunoglobulin therapy: how does IgG modulate the immune system?', *Nat Rev Immunol*, 13: 176-89.
- Sedgwick, J. D., A. L. Ford, E. Foulcher, and R. Airriess. 1998. 'Central nervous system microglial cell activation and proliferation follows direct interaction with tissue-infiltrating T cell blasts', *J Immunol*, 160: 5320-30.
- Setiady, Y. Y., J. A. Coccia, and P. U. Park. 2010. 'In vivo depletion of CD4+FOXP3+ Treg cells by the PC61 anti-CD25 monoclonal antibody is mediated by FcgammaRIII+ phagocytes', *Eur J Immunol*, 40: 780-6.
- Sheng, W., F. Yang, Y. Zhou, H. Yang, P. Y. Low, D. M. Kemeny, P. Tan, A. Moh, M. H. Kaplan, Y. Zhang, and X. Y. Fu. 2014. 'STAT5 programs a distinct subset of GM-CSF-producing T helper cells that is essential for autoimmune neuroinflammation', *Cell Res*, 24: 1387-402.

- Shi, F. D., H. B. Wang, H. Li, S. Hong, M. Taniguchi, H. Link, L. Van Kaer, and H. G. Ljunggren. 2000. 'Natural killer cells determine the outcome of B cell-mediated autoimmunity', *Nat Immunol*, 1: 245-51.
- Shin, J. S., Z. Gao, and S. N. Abraham. 2000. 'Involvement of cellular caveolae in bacterial entry into mast cells', *Science*, 289: 785-8.
- Shinkawa, T., K. Nakamura, N. Yamane, E. Shoji-Hosaka, Y. Kanda, M. Sakurada, K. Uchida, H. Anazawa, M. Satoh, M. Yamasaki, N. Hanai, and K. Shitara. 2003. 'The absence of fucose but not the presence of galactose or bisecting N-acetylglucosamine of human IgG1 complex-type oligosaccharides shows the critical role of enhancing antibody-dependent cellular cytotoxicity', *J Biol Chem*, 278: 3466-73
- Shlapatska, L. M., S. V. Mikhalap, A. G. Berdova, O. M. Zelensky, T. J. Yun, K. E. Nichols, E. A. Clark, and S. P. Sidorenko. 2001. 'CD150 association with either the SH2-containing inositol phosphatase or the SH2-containing protein tyrosine phosphatase is regulated by the adaptor protein SH2D1A', *J Immunol*, 166: 5480-7.
- Sido, B., G. Otto, R. Zimmermann, P. Muller, S. C. Meuer, and T. J. Dengler. 1997. 'Modulation of the CD2 receptor and not disruption of the CD2/CD48 interaction is the principal action of CD2-mediated immunosuppression in the rat', *Cell Immunol*, 182: 57-67.
- Simpson, T. R., F. Li, W. Montalvo-Ortiz, M. A. Sepulveda, K. Bergerhoff, F. Arce, C. Roddie, J. Y. Henry, H. Yagita, J. D. Wolchok, K. S. Peggs, J. V. Ravetch, J. P. Allison, and S. A. Quezada. 2013. 'Fc-dependent depletion of tumor-infiltrating regulatory T cells co-defines the efficacy of anti-CTLA-4 therapy against melanoma', *J Exp Med*, 210: 1695-710.
- Sinha, S. K., N. Gao, Y. Guo, and D. Yuan. 2010. 'Mechanism of induction of NK activation by 2B4 (CD244) via its cognate ligand', *J Immunol*, 185: 5205-10.
- Smith, G. M., J. Biggs, B. Norris, P. Anderson-Stewart, and R. Ward. 1997. 'Detection of a soluble form of the leukocyte surface antigen CD48 in plasma and its elevation in patients with lymphoid leukemias and arthritis', *J Clin Immunol*, 17: 502-9.
- Springer, T. A., and M. L. Dustin. 2012. 'Integrin inside-out signaling and the immunological synapse', *Curr Opin Cell Biol*, 24: 107-15.
- Sriram, S., D. Solomon, R. V. Rouse, and L. Steinman. 1982. 'Identification of T cell subsets and B lymphocytes in mouse brain experimental allergic encephalitis lesions', *J Immunol*, 129: 1649-51.
- Staunton, D. E., R. C. Fisher, M. M. LeBeau, J. B. Lawrence, D. E. Barton, U. Francke, M. Dustin, and D. A. Thorley-Lawson. 1989. 'Blast-1 possesses a glycosyl-phosphatidylinositol (GPI) membrane anchor, is related to LFA-3 and OX-45, and maps to chromosome 1q21-23', *J Exp Med*, 169: 1087-99.
- Stefanova, I., and V. Horejsi. 1991. 'Association of the CD59 and CD55 cell surface glycoproteins with other membrane molecules', *J Immunol*, 147: 1587-92.
- Stefanova, I., V. Horejsi, I. J. Ansotegui, W. Knapp, and H. Stockinger. 1991. 'GPI-anchored cell-surface molecules complexed to protein tyrosine kinases', *Science*, 254: 1016-9.
- Stromnes, I. M., L. M. Cerretti, D. Liggitt, R. A. Harris, and J. M. Gorman. 2008. 'Differential regulation of central nervous system autoimmunity by T(H)1 and T(H)17 cells', *Nat Med*, 14: 337-42.
- Stulnig, T. M., M. Berger, T. Sigmund, H. Stockinger, V. Horejsi, and W. Waldhausl. 1997. 'Signal transduction via glycosyl phosphatidylinositol-anchored proteins in T cells is inhibited by lowering cellular cholesterol', *J Biol Chem*, 272: 19242-7.

- Sun, D., J. N. Whitaker, Z. Huang, D. Liu, C. Coleclough, H. Wekerle, and C. S. Raine. 2001. 'Myelin antigen-specific CD8+ T cells are encephalitogenic and produce severe disease in C57BL/6 mice', *J Immunol*, 166: 7579-87.
- Svensson, L., K. B. Abdul-Majid, J. Bauer, H. Lassmann, R. A. Harris, and R. Holmdahl. 2002. 'A comparative analysis of B cell-mediated myelin oligodendrocyte glycoprotein-experimental autoimmune encephalomyelitis pathogenesis in B cell-deficient mice reveals an effect on demyelination', *Eur J Immunol*, 32: 1939-46.
- Taniguchi, R. T., D. Guzik, and V. Kumar. 2007. '2B4 inhibits NK-cell fratricide', *Blood*, 110: 2020-3.
- Tchorsh-Yutis, D., G. Hecht, A. Aronovich, E. Shezen, Y. Klionsky, C. Rosen, R. Bitcover, S. Eventov-Friedman, H. Katchman, S. Cohen, O. Tal, O. Milstein, H. Yagita, B. R. Blazar, and Y. Reisner. 2009. 'Pig embryonic pancreatic tissue as a source for transplantation in diabetes: transient treatment with anti-LFA1, anti-CD48, and FTY720 enables long-term graft maintenance in mice with only mild ongoing immunosuppression', *Diabetes*, 58: 1585-94.
- Theien, B. E., C. L. Vanderlugt, T. N. Eagar, C. Nickerson-Nutter, R. Nazareno, V. K. Kuchroo, and S. D. Miller. 2001. 'Discordant effects of anti-VLA-4 treatment before and after onset of relapsing experimental autoimmune encephalomyelitis', *J Clin Invest*, 107: 995-1006.
- Thorley-Lawson, D. A., and C. A. Poodry. 1982. 'Identification and isolation of the main component (gp350-gp220) of Epstein-Barr virus responsible for generating neutralizing antibodies in vivo', *J Virol*, 43: 730-6.
- Tissot, C., C. Rebouissou, B. Klein, and N. Mechetti. 1997. 'Both human alpha/beta and gamma interferons upregulate the expression of CD48 cell surface molecules', *J Interferon Cytokine Res*, 17: 17-26.
- Tompkins, S. M., J. Padilla, M. C. Dal Canto, J. P. Ting, L. Van Kaer, and S. D. Miller. 2002. 'De novo central nervous system processing of myelin antigen is required for the initiation of experimental autoimmune encephalomyelitis', *J Immunol*, 168: 4173-83.
- Tuohy, V. K., Z. Lu, R. A. Sobel, R. A. Laursen, and M. B. Lees. 1989. 'Identification of an encephalitogenic determinant of myelin proteolipid protein for SJL mice', *J Immunol*, 142: 1523-7.
- Vaidya, S. V., S. E. Stepp, M. E. McNerney, J. K. Lee, M. Bennett, K. M. Lee, C. L. Stewart, V. Kumar, and P. A. Mathew. 2005. 'Targeted disruption of the 2B4 gene in mice reveals an in vivo role of 2B4 (CD244) in the rejection of B16 melanoma cells', *J Immunol*, 174: 800-7.
- Veillette, A. 2010. 'SLAM-family receptors: immune regulators with or without SAP-family adaptors', *Cold Spring Harb Perspect Biol*, 2: a002469.
- Waggoner, S. N., and V. Kumar. 2012. 'Evolving role of 2B4/CD244 in T and NK cell responses during virus infection', *Front Immunol*, 3: 377.
- Waggoner, S. N., R. T. Taniguchi, P. A. Mathew, V. Kumar, and R. M. Welsh. 2010. 'Absence of mouse 2B4 promotes NK cell-mediated killing of activated CD8+ T cells, leading to prolonged viral persistence and altered pathogenesis', *J Clin Invest*, 120: 1925-38.
- Waldner, H., M. J. Whitters, R. A. Sobel, M. Collins, and V. K. Kuchroo. 2000. 'Fulminant spontaneous autoimmunity of the central nervous system in mice transgenic for the myelin proteolipid protein-specific T cell receptor', *Proc Natl Acad Sci U S A*, 97: 3412-7.

- Wandstrat, A. E., C. Nguyen, N. Limaye, A. Y. Chan, S. Subramanian, X. H. Tian, Y. S. Yim, A. Pertsemlidis, H. R. Garner, Jr., L. Morel, and E. K. Wakeland. 2004. 'Association of extensive polymorphisms in the SLAM/CD2 gene cluster with murine lupus', *Immunity*, 21: 769-80.
- Wang, J., C. I. Balog, K. Stavenhagen, C. A. Koeleman, H. U. Scherer, M. H. Selman, A. M. Deelder, T. W. Huizinga, R. E. Toes, and M. Wuhrer. 2011. 'Fc-glycosylation of IgG1 is modulated by B-cell stimuli', *Mol Cell Proteomics*, 10: M110 004655.
- Ward, J., M. Bonaparte, J. Sacks, J. Guterman, M. Fogli, D. Mavilio, and E. Barker. 2007. 'HIV modulates the expression of ligands important in triggering natural killer cell cytotoxic responses on infected primary T-cell blasts', *Blood*, 110: 1207-14.
- Webb, M., C. S. Tham, F. F. Lin, K. Lariosa-Willingham, N. Yu, J. Hale, S. Mandala, J. Chun, and T. S. Rao. 2004. 'Sphingosine 1-phosphate receptor agonists attenuate relapsing-remitting experimental autoimmune encephalitis in SJL mice', *J Neuroimmunol*, 153: 108-21.
- Welsh, C. T., J. W. Rose, K. E. Hill, and J. J. Townsend. 1993. 'Augmentation of adoptively transferred experimental allergic encephalomyelitis by administration of a monoclonal antibody specific for LFA-1 alpha', *J Neuroimmunol*, 43: 161-7.
- West, E. E., B. Youngblood, W. G. Tan, H. T. Jin, K. Araki, G. Alexe, B. T. Konieczny, S. Calpe, G. J. Freeman, C. Terhorst, W. N. Haining, and R. Ahmed. 2011. 'Tight regulation of memory CD8(+) T cells limits their effectiveness during sustained high viral load', *Immunity*, 35: 285-98.
- White, K. D., R. D. Cummings, and F. J. Waxman. 1997. 'Ig N-glycan orientation can influence interactions with the complement system', *J Immunol*, 158: 426-35.
- Whitham, R. H., D. Wingett, J. Wineman, M. Mass, K. Wegmann, A. Vandembark, and H. Offner. 1996. 'Treatment of relapsing autoimmune encephalomyelitis with T cell receptor V beta-specific antibodies when proteolipid protein is the autoantigen', *J Neurosci Res*, 45: 104-16.
- Willenborg, D. O., S. Fordham, C. C. Bernard, W. B. Cowden, and I. A. Ramshaw. 1996. 'IFN-gamma plays a critical down-regulatory role in the induction and effector phase of myelin oligodendrocyte glycoprotein-induced autoimmune encephalomyelitis', *J Immunol*, 157: 3223-7.
- Williams, J. L., D. W. Holman, and R. S. Klein. 2014. 'Chemokines in the balance: maintenance of homeostasis and protection at CNS barriers', *Front Cell Neurosci*, 8: 154.
- Winkler-Pickett, R., H. A. Young, J. M. Cherry, J. Diehl, J. Wine, T. Back, W. E. Bere, A. T. Mason, and J. R. Ortaldo. 2008. 'In vivo regulation of experimental autoimmune encephalomyelitis by NK cells: alteration of primary adaptive responses', *J Immunol*, 180: 4495-506.
- Wolf, S. D., B. N. Dittel, F. Hardardottir, and C. A. Janeway, Jr. 1996. 'Experimental autoimmune encephalomyelitis induction in genetically B cell-deficient mice', *J Exp Med*, 184: 2271-8.
- Wong, Y. W., A. F. Williams, S. F. Kingsmore, and M. F. Seldin. 1990. 'Structure, expression, and genetic linkage of the mouse BCM1 (OX45 or Blast-1) antigen. Evidence for genetic duplication giving rise to the BCM1 region on mouse chromosome 1 and the CD2/LFA3 region on mouse chromosome 3', *J Exp Med*, 171: 2115-30.
- World Health Organization. 2008. 'Atlas: Multiple Sclerosis Resources in the World 2008.'
- Wu, H. J., Ivanov, II, J. Darce, K. Hattori, T. Shima, Y. Umesaki, D. R. Littman, C. Benoist, and D. Mathis. 2010. 'Gut-residing segmented filamentous bacteria drive autoimmune arthritis via T helper 17 cells', *Immunity*, 32: 815-27

- Yan, Q., V. N. Malashkevich, A. Fedorov, E. Fedorov, E. Cao, J. W. Lary, J. L. Cole, S. G. Nathenson, and S. C. Almo. 2007. 'Structure of CD84 provides insight into SLAM family function', *Proc Natl Acad Sci U S A*, 104: 10583-8.
- Yokoyama, S., D. Staunton, R. Fisher, M. Amiot, J. J. Fortin, and D. A. Thorley-Lawson. 1991. 'Expression of the Blast-1 activation/adhesion molecule and its identification as CD48', *J Immunol*, 146: 2192-200.
- York, N. R., J. P. Mendoza, S. B. Ortega, A. Benagh, A. F. Tyler, M. Firan, and N. J. Karandikar. 2010. 'Immune regulatory CNS-reactive CD8+T cells in experimental autoimmune encephalomyelitis', *J Autoimmun*, 35: 33-44.
- Yuan, D., Y. Guo, and S. Thet. 2013. 'Enhancement of antigen-specific immunoglobulin G responses by anti-CD48', *J Innate Immun*, 5: 174-84.
- Zhang, B., T. Yamamura, T. Kondo, M. Fujiwara, and T. Tabira. 1997. 'Regulation of experimental autoimmune encephalomyelitis by natural killer (NK) cells', *J Exp Med*, 186: 1677-87.
- Zhang, W., T. Wan, N. Li, Z. Yuan, L. He, X. Zhu, M. Yu, and X. Cao. 2001. 'Genetic approach to insight into the immunobiology of human dendritic cells and identification of CD84-H1, a novel CD84 homologue', *Clin Cancer Res*, 7: 822s-29s.